

# An Assessment of BWR Mark-II Containment Challenges, Failure Modes, and Potential Improvements in Performance

---

Prepared by D. L. Kelly, K. R. Jones, R. J. Dallman, K. C. Wagner

Idaho National Engineering Laboratory  
EG&G Idaho, Inc.

Prepared for  
U.S. Nuclear Regulatory Commission

## AVAILABILITY NOTICE

### Availability of Reference Materials Cited in NRC Publications

Most documents cited in NRC publications will be available from one of the following sources:

1. The NRC Public Document Room, 2120 L Street, NW, Lower Level, Washington, DC 20555
2. The Superintendent of Documents, U.S. Government Printing Office, P.O. Box 37082, Washington, DC 20013-7082
3. The National Technical Information Service, Springfield, VA 22161

Although the listing that follows represents the majority of documents cited in NRC publications, it is not intended to be exhaustive.

Referenced documents available for inspection and copying for a fee from the NRC Public Document Room include NRC correspondence and internal NRC memoranda; NRC Office of Inspection and Enforcement bulletins, circulars, information notices, inspection and investigation notices; Licensee Event Reports; vendor reports and correspondence; Commission papers; and applicant and licensee documents and correspondence.

The following documents in the NUREG series are available for purchase from the GPO Sales Program: formal NRC staff and contractor reports, NRC-sponsored conference proceedings, and NRC booklets and brochures. Also available are Regulatory Guides, NRC regulations in the *Code of Federal Regulations*, and *Nuclear Regulatory Commission Issuances*.

Documents available from the National Technical Information Service include NUREG series reports and technical reports prepared by other federal agencies and reports prepared by the Atomic Energy Commission, forerunner agency to the Nuclear Regulatory Commission.

Documents available from public and special technical libraries include all open literature items, such as books, journal and periodical articles, and transactions. *Federal Register* notices, federal and state legislation, and congressional reports can usually be obtained from these libraries.

Documents such as theses, dissertations, foreign reports and translations, and non-NRC conference proceedings are available for purchase from the organization sponsoring the publication cited.

Single copies of NRC draft reports are available free, to the extent of supply, upon written request to the Office of Information Resources Management, Distribution Section, U.S. Nuclear Regulatory Commission, Washington, DC 20555.

Copies of industry codes and standards used in a substantive manner in the NRC regulatory process are maintained at the NRC Library, 7920 Norfolk Avenue, Bethesda, Maryland, and are available there for reference use by the public. Codes and standards are usually copyrighted and may be purchased from the originating organization or, if they are American National Standards, from the American National Standards Institute, 1430 Broadway, New York, NY 10018.

## DISCLAIMER NOTICE

This report was prepared as an account of work sponsored by an agency of the United States Government. Neither the United States Government nor any agency thereof, or any of their employees, makes any warranty, expressed or implied, or assumes any legal liability of responsibility for any third party's use, or the results of such use, of any information, apparatus, product or process disclosed in this report, or represents that its use by such third party would not infringe privately owned rights.

---

---

# An Assessment of BWR Mark-II Containment Challenges, Failure Modes, and Potential Improvements in Performance

---

---

Manuscript Completed: July 1990  
Date Published: July 1990

Prepared by  
D. L. Kelly, K. R. Jones, R. J. Dallman, K. C. Wagner\*

Idaho National Engineering Laboratory  
Managed by the U.S. Department of Energy

EG&G Idaho, Inc.  
P.O. Box 1625  
Idaho Falls, ID 83415

\*Currently with SAIC, Albuquerque, NM

**Prepared for**  
**Division of Safety Issue Resolution**  
**Office of Nuclear Regulatory Research**  
**U.S. Nuclear Regulatory Commission**  
**Washington, DC 20555**  
**NRC FIN A6885**  
**Under DOE Contract No. DE-AC07-76ID01570**





## **ABSTRACT**

This report assesses challenges to BWR Mark II containment integrity that could potentially arise from severe accidents. Also assessed are some potential improvements that could prevent core damage or containment failure, or could mitigate the consequences of such failure by reducing the release of fission products to the environment. These challenges and improvements are analyzed via a limited quantitative risk/benefit analysis of a generic BWR/4 reactor with a Mark II containment. Point estimate frequencies of the dominant core damage sequences are obtained and simple containment event trees are constructed to evaluate the response of the containment to these severe accident sequences. The resulting containment release modes are then binned into source term release categories, which provide inputs to the consequence analysis. The output of the consequence analysis is used to construct an overall base case risk profile. Potential improvements and sensitivities are evaluated by modifying the event tree split fractions, thus generating a revised risk profile. Several important sensitivity cases are examined to evaluate the impact of phenomenological uncertainties on the final results.

## EXECUTIVE SUMMARY

In SECY-88-147, dated May 25, 1988, the NRC staff presented to the Commission its plan to evaluate potential generic severe accident containment vulnerabilities in a research effort entitled the Containment Performance Improvement (CPI) Program. This effort is predicated on the presumption that there are generic severe accident challenges to each light water reactor (LWR) containment type that should be assessed to determine whether additional regulatory guidance or requirements concerning needed containment features are warranted, and to confirm the adequacy of the existing Commission policy. These assessments are needed because of the uncertainty in the ability of LWR containments to successfully survive some severe accident challenges, as indicated by the NUREG-1150 results. All LWR containment types are to be assessed in the CPI Program, beginning with the boiling water reactors (BWRs) with Mark I containments. The potential improvements for BWRs with Mark I containments were documented in NUREG/CR-5225 (including Addendum 1) and SECY-89-017, dated January 23, 1989. This effort is integrated closely with the Individual Plant Examination (IPE) Program and is intended to focus on hardware and procedural issues related to potential generic containment challenges.

The results of work performed under NRC sponsorship are presented here. This work is related to severe accident challenges and potential enhancements that could improve containment performance in plants with a BWR Mark II containment design. An additional report is to be published in the future providing more information on BWR Mark II accident response. The purpose of these reports is to provide BWR Mark II owners with information they may find useful in assessing their plants as part of the IPE. This report contains no requirements and is being provided for information only. The present report concentrates on identifying potential challenges to containment integrity that could arise from a severe accident and potential improvements that could reduce the frequency of a severe accident or mitigate the offsite consequences of a release. The impact of these improvements upon core damage frequency and risk is examined both qualitatively and quantitatively.

As a result of the limited analysis done for phenomenological uncertainties, the benefits from potential improvements contained in this report should be viewed as tentative. Similarly, the estimated costs for selected improvements were taken from previously

published information and should not be interpreted as firm estimates.

Severe accident sequences at the Mark II plants can be grouped into two general categories: one where containment integrity is challenged before core degradation, the other where core damage precedes any threat to containment integrity. In the first category, which includes loss of long-term containment heat removal with reactor scram (TW) and anticipated transient without scram (ATWS) sequences, the challenge to containment is from overpressurization due to inadequate containment heat removal. In the second category, which includes station blackout (SBO) and other transients where reactor scram occurs, the challenge can be from either overpressurization at or near the time of reactor vessel failure or overpressure or over-temperature failure several hours after vessel failure. These later challenges are generally a result of core-concrete interaction (CCI) in the containment, but also may be associated with core-concrete-water interactions, especially in the case of the Shoreham Nuclear Power Station and Nine Mile Point Unit 2 reactor pedestal designs.

Potential improvements addressing the first category of containment challenges include containment pressure control. Examples could include venting from the wetwell through a hardened vent pipe, and containment pressure control and fission product scrubbing, such as the use of containment sprays with a backup water supply. A hardened vent line would allow excess energy in the containment to be rejected to the environment, while avoiding concerns associated with venting through existing "soft" heating, ventilating, and air conditioning (HVAC) ductwork. However, with the high estimated probability of suppression pool bypass in the base case via failure of in-pedestal drain lines shortly after vessel breach, the vent systems would need an external filter, such as the Swedish multi-venturi scrubbing system, to prevent a severe offsite release of fission products. Containment sprays could be used to condense steam in the containment, thus delaying overpressurization failure. Use of a backup water supply for the sprays would avoid any problems associated with pumping saturated water from the suppression pool. One utility has shown that the reactor water cleanup system is capable of removing sufficient decay heat from the reactor to eliminate the need for containment venting in the TW sequence.

For the second category of containment challenges (core melt before containment failure), potential improvements include: (a) containment pressure control,

such as a hardened vent from the wetwell, (b) improved means of depressurizing the reactor, such as enhancements to the automatic depressurization system (ADS) and the safety/relief valves (SRVs), (c) containment temperature control and fission product scrubbing, such as containment sprays with a backup water supply and external cooling of the drywell head, and (d) mitigation of the fission product releases, such as the use of reactor building fire protection sprays to enhance fission product retention in the secondary containment. The hardened vent line (with or without an external filter) could be used to mitigate late overpressurization challenges. Enhancements to the ADS and to the SRVs would lower the probability of vessel failure at high pressure, thus reducing the contribution of high pressure sequences to core damage frequency (such as TQUX, which is a loss of feed with the loss of all high pressure injection capability and failure to depressurize the reactor). These enhancements would also allow diesel fire pumps, which operate at low pressure, to be used for vessel injection in those sequences, such as long-term SBO, where loss of DC power would normally cause the SRVs to reclose, preventing injection from low pressure systems. Containment sprays have the potential to mitigate both late

overpressure and thermal challenges. However, a backup water supply would be needed. In addition, the minimum spray flow rate required for successful mitigation of overpressurization has not yet been identified. External cooling of the drywell head by flooding it with water has the potential to mitigate late thermal challenges, as well as to scrub any fission products released through leakage in the drywell head seal. Leakage past the drywell head seal might be considered to be an alternative method of containment pressure control, thus allowing the containment atmosphere to “burp” into the flooded refueling water cavity could provide some scrubbing. Finally, some plants may have the ability to spray large areas of the reactor building with the installed fire protection sprays. In the event of primary containment failure or venting into the reactor building, these sprays could remove aerosol fission products from the secondary containment atmosphere, lessening the offsite consequences of a release.

Table ES-1 summarizes the qualitative benefits, as well as any negative aspects, of each of the potential improvements.

**Table ES-1.** Qualitative benefits and drawbacks of potential Mark II containment improvements

Potential Improvement	Potential Benefits	Potential Drawbacks
<b>1. Vent Systems</b>		
a. Filtered containment vent system <sup>a</sup>	<ul style="list-style-type: none"> <li>• Prevents overpressure failures for transients with scram</li> <li>• Delays overpressure failures for ATWS</li> <li>• Preemptive venting reduces base pressure before core damage</li> <li>• Mitigates hydrogen burns in secondary containment</li> <li>• Ensures scrubbing of aerosol releases</li> <li>• Unaffected by suppression pool bypass</li> </ul>	<ul style="list-style-type: none"> <li>• Filtra – very high cost (\$30–50M)</li> <li>• MVSS – high cost (~\$5M)</li> <li>• Minimal benefit if release is scrubbed by suppression pool</li> </ul>
b. Hard-pipe vent system with dedicated power source	<ul style="list-style-type: none"> <li>• Prevents overpressure failures for transients with scram</li> <li>• May delay overpressure failures for ATWS</li> <li>• Preemptive venting reduces base pressure before core damage</li> <li>• Mitigates hydrogen burns in secondary containment</li> </ul>	<ul style="list-style-type: none"> <li>• Moderately high cost (\$2.9M at Pilgrim)</li> <li>• No decontamination of release in secondary containment – increased risk if suppression pool is bypassed</li> </ul>
<b>2. Alternate containment heat removal systems<sup>a</sup></b>	<ul style="list-style-type: none"> <li>• Maintains suppression pool subcooled</li> <li>• Prevents overpressure failures for TW</li> <li>• May reduce pressurization rate for less severe ATWS</li> <li>• Low cost for use of RWCU blowdown</li> </ul>	<ul style="list-style-type: none"> <li>• Very high costs for ARHR (\$183M+) – other methods may be less expensive</li> </ul>

**Table ES-1.** (continued)

Potential Improvement	Potential Benefits	Potential Drawbacks
3. Enhanced reactor depressurization capability	<ul style="list-style-type: none"> <li>• Can prevent high pressure core damage and RPV failure</li> <li>• Relatively low cost (\$0.5M)</li> <li>• May reduce vacuum breaker failure</li> <li>• Can prevent core melt in long-term SBO</li> </ul>	<ul style="list-style-type: none"> <li>• None identified</li> </ul>
4. Improved hydrogen control	<ul style="list-style-type: none"> <li>• None for Mark II plants (inerted)</li> </ul>	<ul style="list-style-type: none"> <li>• Interferes with containment access for maintenance, testing, and leak identification</li> </ul>
5. Backup water supply to RPV injection and containment sprays	<ul style="list-style-type: none"> <li>• Can prevent core damage in low pressure transients with scram</li> <li>• Ex-vessel debris cooling and aerosol scrubbing</li> <li>• May mitigate thermal failure</li> <li>• Independent of RHR</li> <li>• Relatively low cost for use of fire systems</li> </ul>	<ul style="list-style-type: none"> <li>• RPV must be at low pressure for injection</li> <li>• Analysis of EPG spray initiation limit required</li> <li>• Procedures for concurrent fire if fire systems used</li> <li>• Low spray flow rate of fire systems will limit pressure reduction capability</li> <li>• Requires many operator actions and additional piping</li> <li>• May increase potential for ex-vessel steam explosions</li> </ul>
6. Core debris control		
a. Eliminating in-pedestal downcomers	<ul style="list-style-type: none"> <li>• Decreases probability of suppression pool bypass after RPV failure</li> <li>• Decreases probability of steam explosion or rapid steam spike</li> </ul>	<ul style="list-style-type: none"> <li>• Benefits uncertain due to FCI uncertainties</li> <li>• Increases probability of CCI and ex-vessel fission product release</li> <li>• Requires reanalysis of containment pressure suppression capability</li> </ul>
b. Adding in-pedestal downcomers	<ul style="list-style-type: none"> <li>• Increases probability of quenching core debris ex-vessel</li> <li>• Reduces need for containment sprays and venting</li> </ul>	<ul style="list-style-type: none"> <li>• Increases probability of steam explosion/steam spike</li> </ul>

**Table ES-1.** (continued)

Potential Improvement	Potential Benefits	Potential Drawbacks
6. (continued)		
b. (continued)		<ul style="list-style-type: none"> <li>• Increases probability of suppression pool bypass after RPV failure</li> <li>• May be very expensive</li> </ul>
c. Strengthening ex-pedestal downcomers <sup>a</sup>	<ul style="list-style-type: none"> <li>• Decreases probability of suppression pool bypass after RPV failure</li> </ul>	<ul style="list-style-type: none"> <li>• Few suitable materials available (high cost)</li> <li>• Increases probability of CCI</li> <li>• Does not reduce ablation of drywell floor</li> </ul>
d. Plug in-pedestal cavity penetrations	<ul style="list-style-type: none"> <li>• Decreases probability of suppression pool bypass after RPV failure</li> <li>• Decreases probability of steam explosion/steam spike</li> </ul>	<ul style="list-style-type: none"> <li>• Requires system modifications</li> <li>• May increase probability of steam explosion in deep cavity</li> <li>• Requires seismic reanalysis of primary containment</li> </ul>
7. External cooling of drywell head	<ul style="list-style-type: none"> <li>• Mitigates or prevents drywell head seal failure</li> <li>• Leakage scrubbed by overlying water pool</li> <li>• Low cost</li> </ul>	<ul style="list-style-type: none"> <li>• Must be manually initiated early in the accident</li> <li>• Benefits uncertain</li> <li>• Does not prevent leakage of other isolation valves or penetrations</li> </ul>
8. Use of fire protection sprays in the reactor building <sup>a</sup>	<ul style="list-style-type: none"> <li>• May scrub aerosol fission products released from primary containment</li> <li>• Hardware already in place at some plants</li> </ul>	<ul style="list-style-type: none"> <li>• Limited spray coverage</li> <li>• May provide greater benefit as alternate containment spray or RPV injection system</li> </ul>

a. These improvements are not quantitatively analyzed in this report.

A limited quantitative risk analysis was performed. A base case risk profile for a generic BWR Mark II plant was established to evaluate the effects of several potential plant improvements to reduce the offsite consequences of a severe accident. The first step in the analysis was the construction of accident sequence event trees to model the dominant core damage sequences. The dominant sequences were selected based on a review of past probabilistic risk assessments (PRAs) of BWR Mark II plants and do not include sequences initiated by external events (earthquake, fire, flood, etc.) or plant-specific special initiators. The sequences chosen for modeling are SBO (both short- and long-term), ATWS at full power with the reactor isolated from the main condenser (isolation ATWS), and transient-initiated sequences with successful shutdown of the reactor by the reactor protection system.

A simplified approach was taken in constructing these generic front-end event trees. First, the scope is narrower than in a typical Level 1 PRA. For example, there are undoubtedly areas where support system interdependencies have been neglected. These interdependencies would be important in an analysis with the goal to rigorously determine the core damage frequency for a specific plant. Here, however, the goal is to determine the *change* in the core damage frequency effected for a generic BWR Mark II plant by a change in hardware or operating procedure. Component failure rates, human error probabilities, and system unavailabilities were obtained largely from studies previously performed for similar plants.

The result of the accident sequence analysis is a point estimate profile of the core damage frequency for a generic BWR Mark II plant. This profile is shown in Table ES-2.

**Table ES-2.** Base case core damage frequencies for a generic BWR Mark II plant

Accident Sequence	Frequency (per year)
Long-term SBO	3.75E-06
TQUX	3.54E-06
Short-term SBO	1.57E-06
ATWS (CM < CF)	2.30E-06
ATWS (CF < CM)	1.27E-06
TW	3.47E-07
Total	1.28E-05

The next step in the analysis was the construction of base case simple containment event trees (SCETs) to model the containment response to the dominant core damage sequences. SCETs were constructed for all of the above sequences, except TW. Containment response to the TW sequence was not modeled, because its low frequency of occurrence ( $<1 \times 10^{-6}/y$ ) and long duration ( $>20$  h) make it a small contributor to risk. Each SCET has approximately 15 top events, rather than the 100 or more in the BWR accident progression event trees developed for NUREG-1150. The current uncertainties (both stochastic and due to lack of knowledge) in many important phenomenological issues tend to offset attempts to include a great amount of detail in the containment event trees. Even in the SCETs used here, the quantification of several important events remains indeterminate because of a lack of data, both calculational and experimental, and because some events can only be precisely and accurately quantified on a plant-specific basis.

Analysis of the SCETs produces a set of containment release modes for each core damage sequence. These release modes are then binned into 10 release categories, which provide the source term inputs for the calculation of offsite consequences. The offsite consequences were calculated under the assumption that the generic BWR Mark II plant is located at the Peach Bottom site. This assumption allowed the NUREG-1150 MACCS input deck for Peach Bottom to be used in the consequence calculations. Other sites with different population distributions, emergency response plans, etc., will have consequences that vary from those in this report. This should be taken into account if the results of this report are to be applied to a specific plant.

The dominant containment failures at the generic BWR Mark II plant were found to be the result of early containment overpressurization with suppression pool bypass due to failure of in-pedestal drain lines or drain plate covers shortly after vessel breach. There also is a significant probability of late containment failure, with the drywell head seal being the likely failure location; this type of failure also produces an unscrubbed release. If the assumption of early suppression pool bypass due to drain line failure is removed, these late unscrubbed releases dominate risk (as measured by the offsite dose). Table ES-3 shows the conditional containment failure probabilities as calculated from the SCETs. These probabilities are a frequency-weighted average over all plant damage states. A brief description of each failure mode is provided below for reference.

Containment Failure Mode	Characteristics	Containment Failure Mode	Characteristics
REC-IV	Core melt recovered in-vessel, noble gas release or no containment failure.	LCF-OP-nSP	Late overpressure containment failure, release bypasses the suppression pool.
REC-EV	Core melt recovered ex-vessel, noble gas release or no containment failure.	LCF-OT	Late overtemperature containment failure, release bypasses the suppression pool.
REC-TOTAL	Sum of in-vessel and ex-vessel recovery.	<p>Table ES-3 shows that, given a severe core damage accident, there is a 55% chance of recovering the sequence in-vessel, with no significant release from containment. Should the sequence progress to vessel failure, there still is a 24.9% chance of establishing a coolable debris bed inside containment, again with no significant release to the environment. However, there is an 11.8% chance that a severe core damage sequence will lead to early overpressure containment failure. Of these early failures, ~90% will involve suppression pool bypass, because of either in-pedestal drain line failure or a failure location in the drywell. Should the containment survive the early challenge to its integrity, there still is a significant late challenge. By far the most significant late challenge is failure of the drywell head seal, primarily due to high temperature accompanied by elevated pressure.</p>	
ECF-OP-SP	Early overpressure containment failure, release scrubbed through the suppression pool.		
ECF-OP-nSP	Early overpressure containment failure, release bypasses the suppression pool.		
LV-SP	Late vented release through the suppression pool.		
LV-nSP	Late vented release bypassing the suppression pool.		
LCF-OP-SP	Late overpressure containment failure, release scrubbed through the suppression pool.		

**Table ES-3.** Summary of Mark II conditional containment failure probabilities

Containment Failure Mode	Base Case	Hardened Vent	Alternate Water Supply and Enhanced Depressurization	Blackstart Gas Turbine <sup>a</sup>	Drywell Head Flooding	No Drain Line or Downcomer Failure
REC-IV	5.50E-01	5.50E-01	4.76E-01	4.71E-01	5.50E-01	5.50E-01
REC-EV	2.49E-01	2.49E-01	3.47E-01	3.23E-01	2.50E-01	2.49E-01
REC-TOTAL	7.99E-01	7.99E-01	8.23E-01	7.94E-01	8.00E-01	7.99E-01
ECF-OP-SP	1.18E-02	1.16E-02	1.62E-02	1.64E-02	1.18E-02	6.51E-02
ECF-OP-nSP	1.06E-01	1.04E-01	1.45E-01	1.47E-01	1.06E-01	5.28E-02
LV-SP	5.40E-08	3.07E-05	3.75E-08	7.52E-08	5.40E-08	2.72E-06
LV-nSP	5.24E-04	3.56E-03	3.60E-04	7.30E-04	5.24E-04	5.20E-04
LCF-OP-SP	1.94E-05	1.94E-05	5.82E-06	9.92E-06	7.08E-04	9.71E-04
LCF-OP-nSP	1.93E-03	1.93E-03	5.77E-04	9.82E-04	7.02E-02	9.71E-04
LCF-OT	7.55E-02	7.55E-02	1.49E-02	4.09E-02	5.32E-03	7.55E-02

a. Blackstart gas turbine improves containment response by reducing SBO core damage frequency.

Each of the suggested improvements will alter some or all of these conditional failure mode probabilities. The primary effect of the alternate water supply (with enhanced depressurization capability) is to decrease the conditional probability of late containment failure. Note that the conditional probability of recovering the sequence in-vessel decreases, with this decrease being more than offset by the increase in the conditional probability of ex-vessel recovery. Because the only effect of the blackstart combustion turbine is to reduce the SBO core damage frequency, a slight decrease in the late challenge to containment is seen. Flooding the drywell head during SBO changes all late thermal failures to late overpressure failures or to end states with ex-vessel recovery. With no early failure of the in-pedestal drain lines, the probability of an early unscrubbed release decreases by approximately 50%, while the probability of a late unscrubbed release decreases by only about 1%. This very significant latter result is due to the high probability of a late unscrubbed release, given a long-term SBO plant damage state.

The calculated offsite consequences are conditional upon the occurrence of core damage and a release of fission products from containment. To obtain the absolute risk per year, these conditional consequences are combined with the conditional containment release probabilities from the SCETs and with the core damage sequence (plant damage state) frequency from the accident sequence analysis. The resulting consequences per year, for each of the three risk

measures selected for use in this report, are shown in Table ES-4.

This table shows that the risk (as measured by the population dose per year) associated with the generic BWR Mark II plant at the Peach Bottom site is quite low. A majority of this risk is due to early overpressure containment failures, with a release of fission products that bypasses the suppression pool, because the in-pedestal drain lines in the generic reference plant are postulated to fail shortly after vessel breach. For plants that do not have these drain lines (the Susquehanna plants), early suppression pool bypass is expected to be considerably less likely, and the offsite risk is dominated by late containment failures. Plants with in-pedestal downcomers are expected to have a risk profile that is very similar to that of the reference plant, because the in-pedestal downcomers are also assumed to fail shortly after vessel breach.

Because the Mark II base case risk profile is dominated by early containment failure (although the absolute frequency of the early containment failure is very low), with a release that bypasses the suppression pool, hardened venting is considered not to be beneficial in reducing offsite consequences. Because a significant fraction of the offsite risk comes from late containment failures, improvements that focus on mitigating either the late challenges to the containment or the severity of the release are expected to yield the highest benefit in terms of reducing the offsite dose. Examples of such improvements are as follows. The

**Table ES-4.** Offsite consequences for the generic BWR Mark II plant (per reactor-year)

Plant Damage State	Mean Latent Fatalities	Mean Population Dose (Man-Rem) <sup>a</sup>	Mean Offsite Costs (\$)
TQUX	3.29E-05	5.98E-02	99.4
ST-SBO	2.01E-04	1.95E-01	1.09E+03
LT-SBO	2.98E-03	2.80	1.07E+04
ATWS (core melt before containment failure)	1.13E-03	1.02	6.21E+03
ATWS (core melt after containment failure)	4.60E-03	4.60	1.91E+04
Total	8.94E-03	8.67	3.72E+04

a. The population dose is calculated for the Peach Bottom site, and is that received within a 50-mi radius of the plant.



first improvement is the installation of a blackstart combustion generator. This is an AC generator with the ability to start independently of onsite or offsite sources of power. Such a generator is expected to reduce the core damage frequency due to SBO and, consequently, the frequency of late containment challenges resulting from blackout sequences. A second potential improvement is using diesel fire pumps for injection of water into the vessel during long-term SBO. This improvement needs to be used in conjunction with a dedicated source of DC power to the safety/relief valve (SRV) solenoids and the containment vent valves. These modifications would help to ensure that the vessel remains at a low enough pressure to allow the fire pumps to inject. A third potential improvement is using the diesel fire pumps to inject water into the containment after vessel failure to cool the debris. This

could mitigate late containment failure and provide some scrubbing for any release that might occur. Fourth, flooding the drywell head could mitigate late thermal failure of the drywell head seal (or other elastomeric seals in the drywell head region) and might scrub any leakage past the seal. The relative benefit of these first four improvements is greater for plants without in-pedestal drain lines or in-pedestal downcomers, because offsite risk in these plants is dominated by late containment failure, with the likely failure location being the drywell head seal. Finally, plugging in-pedestal drain lines to prevent early suppression pool bypass results in a significant decrease in all offsite consequence measures. Table ES-5 presents a summary of the calculated quantitative benefits of these potential improvements.

**Table ES-5.** Summary of quantitative benefits of potential Mark II improvements

	Hardened Vent	Alternate Water Supply and Enhanced Depressurization	Blackstart Gas Turbine <sup>a</sup>	Drywell Head Flooding	No Drain Line or Downcomer Failure
CM Frequency	↓	↓↓	↓↓	↔	↔
Latent Fatalities	↓	↓↓	↓↓	↓	↓↓
Population Dose	↑	↓↓	↓↓	↓	↓↓
Offsite Costs	↓	↓↓	↓↓	↓	↓↓

a. Blackstart gas turbine improves containment response by reducing SBO core damage frequency.

↑ = slight increase (< 5%)

↓ = slight decrease (< 5%)

↓↓ = large decrease (> 20%)

↔ = no change

# CONTENTS

ABSTRACT .....	iii
EXECUTIVE SUMMARY .....	iv
ACRONYMS .....	xix
SYMBOLGY .....	xxi
1. INTRODUCTION .....	1
2. DESCRIPTION OF MARK II PLANT FEATURES AND CONTAINMENT DESIGNS .....	3
2.1 Reactor Design .....	6
2.2 Primary Containment Design .....	6
2.3 Secondary Containment Design .....	17
3. CONTAINMENT CHALLENGED PRIOR TO CORE MELT .....	19
3.1 Definition of Sequences .....	19
3.1.1 Anticipated Transients Without Scram .....	19
3.1.2 TW, Loss of Long-Term Containment Heat Removal .....	20
3.2 Discussion of Containment Challenges and Failure Modes .....	20
3.3 Potential Improvements .....	23
3.3.1 Containment Venting .....	23
3.3.2 Containment Sprays and Backup Water Supply .....	24
3.3.3 RHR Heat Exchanger Capacity .....	25
4. CONTAINMENT CHALLENGED AFTER CORE MELT .....	28
4.1 Definition of Sequences .....	28
4.1.1 Transients with Scram .....	28
4.1.2 Station Blackout .....	28
4.2 Definition of Containment Challenges and Failure Modes .....	28
4.2.1 Challenges At or Near the Time of Vessel Failure .....	28
4.2.1.1 Overpressure Challenges .....	29
4.2.1.2 Rapid Steam Pressurizations .....	29
4.2.2 Challenges after Vessel Failure (Late Challenges) .....	31
4.2.2.1 Late Overpressure Failure .....	31
4.2.2.2 Late Thermal Failure .....	34
4.2.3 Discussion of Containment Failure Modes .....	35

4.3	Potential Improvements .....	36
4.3.1	Mitigating Transients with Scram .....	36
4.3.2	Hydrogen Control .....	38
4.3.3	Containment Sprays and Backup Water Supply .....	38
4.3.4	Containment Venting .....	39
4.3.5	Core Debris Control .....	40
4.3.5.1	Cavities With In-Pedestal Downcomers (Shoreham and NMP-2) .....	40
4.3.5.2	Deep Cavity Below Drywell Floor (WNP-2 and La Salle) .....	40
4.3.5.3	Flat Floor Cavity With No In-Pedestal Downcomers (Limerick and Susquehanna) .....	41
4.3.6	Enhanced Reactor Building Fission Product Attenuation .....	41
4.3.7	Enhanced Reactor Depressurization Capability .....	42
4.3.8	External Cooling of the Drywell Head Seal .....	42
5.	CONTAINMENT BYPASS .....	43
5.1	Definition of Challenges .....	43
5.2	Potential Improvements .....	43
6.	QUALITATIVE RISK ANALYSIS OF CONTAINMENT CHALLENGES AND IMPROVEMENTS .....	45
6.1	Core Damage Frequency .....	45
6.2	Sequence and Failure Mode Risk Significance .....	46
6.3	Summary of Potential Improvements .....	49
7.	QUANTITATIVE RISK ANALYSIS OF ANTICIPATED TRANSIENTS WITHOUT SCRAM ....	55
7.1	Accident Sequence Analysis .....	55
7.1.1	Event Tree Quantification .....	55
7.2	Containment Event Tree Analysis .....	59
7.2.1	Class IV SCET .....	60
7.2.2	Class IC SCET .....	60
7.3	Consequence Analysis .....	66
7.4	Sensitivities and Effects of Potential Improvements .....	67
8.	QUANTITATIVE RISK ANALYSIS OF STATION BLACKOUT .....	72
8.1	Accident Sequence Analysis .....	72
8.1.1	Event Tree Quantification .....	72

8.2	Containment Event Tree Analysis .....	75
8.2.1	Short-term SBO (Class IB1) .....	75
8.2.2	Long-term SBO (Class IB2) .....	78
8.3	Consequence Analysis .....	80
8.4	Sensitivities and Effects of Potential Improvements .....	80
9.	QUANTITATIVE RISK ANALYSIS OF OTHER SEQUENCES (TQUX, TQUV, and TW) .....	87
9.1	Accident Sequence Analysis .....	87
9.1.1	Event Tree Quantification .....	87
9.2	Containment Event Tree Analysis .....	89
9.3	Consequence Analysis .....	91
9.4	Sensitivities and Effects of Potential Improvements .....	92
10.	TECHNICAL FINDINGS .....	95
10.1	Core Damage Frequency Results .....	95
10.1.1	ATWS Level Control .....	95
10.1.2	Hardened Vent .....	95
10.2	Containment Failure Modes .....	97
10.3	Consequence Results .....	100
10.3.1	Decreased Probability of In-Pedestal Drain Line Failure .....	102
10.3.2	Preemptive Venting .....	103
10.3.3	Use of Diesel Fire Pumps .....	104
10.3.4	Blackstart Combustion Generator .....	104
10.3.5	In-Pedestal Downcomers .....	105
10.3.6	Drywell Head Flooding .....	106
10.3.7	Increased Probability of Early Containment Failure .....	106
10.4	Limitations and Uncertainties .....	108
11.	REFERENCES .....	111
	APPENDIX A—PRIMARY CONTAINMENT RESPONSE CALCULATIONS FOR UNMITIGATED SHORT-TERM STATION BLACKOUT AT PEACH BOTTOM .....	A-1
	APPENDIX B—ROLE OF THE BWR OWNERS GROUP EMERGENCY PROCEDURE GUIDELINES IN SEVERE ACCIDENT MANAGEMENT .....	B-1
	APPENDIX C—SOURCE TERM BINNING METHODOLOGY .....	C-1
	APPENDIX D—DETAILED INPUTS TO THE MACCS CONSEQUENCE ANALYSIS .....	D-1

## FIGURES

1.	Shoreham containment .....	7
2.	Nine Mile Point 2 containment .....	9
3.	La Salle containment .....	10
4.	WNP-2 containment .....	11
5.	Limerick containment .....	12
6.	Susquehanna containment .....	13
7.	Shoreham in-pedestal cavity .....	14
8.	Nine Mile Point 2 drywell floor .....	15
9.	Susquehanna drywell floor .....	16
10.	Postulated Mark II containment failure locations .....	22
11.	Typical leak test connection for containment isolation valves .....	44
12.	Shoreham probability of exceeding a dose of 5 rems as a function of distance .....	48
13.	Shoreham probability of exceeding a dose of 200 rems as a function of distance .....	49
14.	Base case ATWS event tree .....	56
15.	Class IV SCET .....	61
16.	Class IC SCET .....	62
17.	Base case loss of offsite power event tree .....	73
18.	Base case short-term station blackout SCET .....	76
19.	Base case long-term station blackout SCET .....	79
20.	Event tree for transient-initiated sequences .....	88
21.	Base case SCET for the TQUX plant damage state .....	90
22.	Mark II base case core damage frequency .....	96
23.	Mean latent fatalities for the reference Mark II plant .....	101
24.	Mean population dose for the reference Mark II plant .....	101
25.	Mean offsite costs for the reference Mark II plant .....	102

## TABLES

ES-1. Qualitative benefits and drawbacks of potential Mark II containment improvements .....	v
ES-2. Base case core damage frequencies for a generic BWR Mark II plant .....	viii
ES-3. Summary of Mark II conditional containment failure probabilities .....	ix
ES-4. Offsite consequences for the generic BWR Mark II plant (per reactor-year) .....	x
ES-5. Summary of quantitative benefits of potential Mark II improvements .....	xi
1. United States nuclear power plants with Mark II containments .....	3
2. Comparison of BWR Mark II reactor design characteristics .....	4
3. Comparison of BWR Mark II primary containment design characteristics .....	5
4. Comparison of BWR Mark II secondary containment design characteristics .....	17
5. Containment Performance Working Group leakage estimates for Limerick .....	21
6. RHR capacity as a percentage of plant thermal power rating .....	26
7. Temperature-dependent leakage estimates for Shoreham .....	35
8. Estimated annual core damage frequencies for BWR Mark II plants .....	45
9. Susquehanna plant damage state estimated annual frequencies (base case values) .....	46
10. Effects of containment venting on the estimated annual Shoreham core damage frequency .....	47
11. Qualitative assessment of benefits and drawbacks of potential Mark II containment improvements ..	50
12. Summary of cost estimates from previous studies .....	52
13. Conditional containment release probabilities for the Class IV plant damage state: base case .....	63
14. Conditional containment release mode probabilities for Class IC plant damage state: base case .....	66
15. Conditional consequence results of the source term release categories .....	67
16. Base case consequence results for ATWS sequences (per reactor-year) .....	67
17. Effect of RPS mechanical failure probability on ATWS core damage frequency .....	68
18. Effect of SLCS failure probability on ATWS core damage frequency .....	68
19. Effects of failure to throttle low pressure injection on ATWS core damage frequency .....	69
20. Offsite consequences for ATWS with diesel fire pump containment sprays (per reactor-year) .....	71
21. Conditional containment release mode probabilities for short-term SBO sequences .....	81

22.	Conditional containment release probabilities for long-term SBO sequences .....	81
23.	Base case consequence results for SBO sequences (per reactor-year) .....	82
24.	Effects of onsite blackstart gas turbine generator on SBO core damage frequency .....	82
25.	Consequence results for SBO sequences with blackstart gas turbine (per reactor-year) .....	82
26.	Effect of preemptive venting on the consequences of SBO (per reactor-year) .....	83
27.	Effect of venting at the PCPL on the consequences of SBO (per reactor-year) .....	83
28.	Effects of diesel fire pump on offsite consequences of SBO (per reactor-year) .....	85
29.	Offsite consequences for SBO sequences with drywell head flooding (per reactor-year) .....	85
30.	Summary of station blackout risks for the generic Mark II plant .....	86
31.	Core damage frequency for transient initiators .....	89
32.	Conditional containment release mode probabilities for TQUX sequences .....	92
33.	Base case consequence results for TQUX sequences (per reactor-year) .....	92
34.	Effects of in-pedestal downcomers on the containment release mode probabilities for TQUX sequences .....	93
35.	Effects of in-pedestal downcomers on the offsite consequences of TQUX sequences (per reactor-year) .....	93
36.	Effects of diesel fire pumps on offsite consequences of TQUX sequences (per reactor-year) .....	93
37.	Offsite consequences for TQUX sequences with no hydrogen burn (per year) .....	94
38.	Base case core damage frequencies for the generic Mark II plant .....	95
39.	ATWS core damage frequencies with no level control and an increased suppression pool temperature limit .....	96
40.	ATWS core damage frequencies with hardened venting .....	96
41.	Base case weighted-average conditional containment failure mode probabilities .....	98
42.	Effects of diesel fire pumps and enhanced depressurization capability on containment failure modes .....	98
43.	Effects of blackstart combustion generator on containment failure modes .....	98
44.	Effects of preemptive venting (during SBO) on containment failure modes .....	98
45.	Effects of increased probability of venting at the PCPL (during SBO) on containment failure modes .....	99
46.	Effects of drywell head flooding (during SBO) on containment failure modes .....	99

47.	Conditional containment failure mode probabilities with no early in-pedestal drain line failure .....	99
48.	Summary of results of conditional consequence analysis .....	100
49.	Base case consequence results for the generic Mark II plant (per reactor-year) .....	100
50.	Offsite consequences with no in-pedestal drain line failure at vessel breach (per reactor-year) .....	103
51.	Effect of preemptive venting on the consequences of SBO (per reactor-year) .....	103
52.	Offsite consequences for SBO and TQUX sequences with diesel fire pump available (per reactor-year) .....	105
53.	Effects of blackstart gas turbine on consequences of SBO (per reactor-year) .....	105
54.	Consequence results with in-pedestal downcomers and high probability of suppression pool bypass (per reactor-year) .....	106
55.	Offsite consequences for SBO sequences with drywell head flooding (per reactor-year) .....	107
56.	Offsite consequences with increased probabilities of early containment failure (per reactor-year) .....	107
57.	Offsite consequences with base case probability of early containment failure and 95% evacuation (per reactor-year) .....	108
58.	Offsite consequences for the case of increased probability of early containment failure and 95% evacuation (per reactor-year) .....	108
59.	Summary of quantitative benefits for potential Mark II improvements .....	109



## ACRONYMS

AC	Alternating Current	ESF	Engineered safety feature
ADS	Automatic depressurization system	FCI	Fuel-coolant interaction
AEOD	NRC Office for the Analysis and Evaluation of Operational Data	FSAR	Final safety analysis report
ALARA	As low as reasonably achievable	HCTL	Heat capacity temperature limit
ARHR	Alternate residual heat removal	HEP	Human error probability
ARI	Alternate rod insertion	HPCI	High pressure coolant injection
ATWS	Anticipated transient without scram	HPCS	High pressure core spray
BNL	Brookhaven National Laboratory	HPIS	High pressure injection systems
BWR	Boiling water reactor	HVAC	Heating, ventilating, and air conditioning
BWROG	BWR Owners Group	INEL	Idaho National Engineering Laboratory
CCI	Core-concrete interaction	IPE	Individual plant examination
CI	Containment isolation	LGS	Limerick Generating Station
CPI	Containment Performance Improvement Program	Lilco	Long Island Lighting Company
CPWG	Containment Performance Working Group	LPCI	Low pressure coolant injection
CRD	Control rod drive	LOCA	Loss of coolant accident
CS	Core spray	LPCS	Low pressure core spray
CST	Condensate storage tank	LPIS	Low pressure injection systems
DBA	Design basis accident	LSCS	La Salle County Station
DC	Direct current	LWR	Light water reactor
DCH	Direct containment heating	MAAP	Modular Accident Analysis Program
DF	Decontamination factor	MACCS	MELCOR Accident Consequence Code System
ECCS	Emergency core cooling systems	MOVs	Motor-operated valves
EDG	Emergency diesel generator	MSIV	Main steam isolation valve
EOP	Emergency operating procedure	MVSS	Multi-Venturi Scrubber System
EPG	Emergency procedure guideline	NMP-2	Nine Mile Point Unit 2

NPSH	Net positive suction head	SBO	Station blackout
NRR	Office of Nuclear Reactor Regulation	SCET	Simple containment event tree
ORNL	Oak Ridge National Laboratory	SCS	Supplemental containment system
PC	Personal computer	SGTS	Standby gas treatment system
PCPL	Primary containment pressure limit	SLCS	Standby liquid control system
PCS	Power conversion system	SNL	Sandia National Laboratory
PRA	Probabilistic risk assessment	SNPS	Shoreham Nuclear Power Station
PWR	Pressurized water reactor	SRV	Safety/relief valve
RBCCW	Reactor building component cooling water	SSES	Susquehanna Steam Electric Station
RBSVS	Reactor building standby ventilation system	STCP	Source term code package
RCIC	Reactor core isolation cooling	TAF	Top of active fuel
RERS	Reactor enclosure recirculation system	TBUX	High pressure short-term station blackout
RHR	Residual heat removal	TQUX	High pressure core melt
RPS	Reactor protection system	TW	Loss of long-term containment heat removal
RWCU	Reactor water cleanup	WNP-2	Washington Nuclear Plant 2

## SYMBOLOLOGY

$(X) -$	Event X. Generally refers to the lower event tree branch at event X.
$(/X) -$	The complement of event X. $P(/X) = 1 - P(X)$ . Generally refers to the upper event tree branch at event X.
$P(X) -$	The probability that event X occurs.
$P(X Y) -$	The conditional probability that event X occurs, given that event Y has occurred.
$(X \cup Y) -$	The union of events X and Y. Interpreted as X <i>or</i> Y. $P(X \cup Y) = P(X) + P(Y) - P(X \cap Y)$ . If $P(X)$ and $P(Y)$ are both $\ll 1$ , then the <i>rare event approximation</i> can be used to evaluate $P(X \cup Y)$ : $P(X \cup Y) \approx P(X) + P(Y)$ .
$(X \cap Y) -$	The intersection of events X and Y. Interpreted as X <i>and</i> Y. $P(X \cap Y) = P(X Y) * P(Y) = P(Y X) * P(X)$ . $P(X \cap Y) = P(X) * P(Y)$ if, and only if, events X and Y are stochastically independent.
$P(\text{nOSP} @ t \text{ h}) -$	The probability that offsite power is not recovered within t hours.
$\text{CF} < \text{CM} -$	Containment integrity challenged prior to core melt
$\text{CM} < \text{CF} -$	Containment integrity challenged after core melt

2000

# AN ASSESSMENT OF BWR MARK II CONTAINMENT CHALLENGES, FAILURE MODES, AND POTENTIAL IMPROVEMENTS IN PERFORMANCE

## 1. INTRODUCTION

On May 25, 1988, the NRC staff presented to the Commission its program plan to evaluate potential generic severe accident containment vulnerabilities in a research effort entitled the Containment Performance Improvement (CPI) Program.<sup>1</sup> This effort is predicated on the presumption that there may be generic severe accident challenges to each light water reactor (LWR) containment type that should be assessed to determine whether additional regulatory guidance or requirements concerning needed containment features are warranted, and to confirm the adequacy of the existing Commission policy. These assessments are needed because of the uncertainty in the ability of LWR containments to successfully survive some severe accident challenges, as indicated by NUREG-1150.<sup>1,2</sup> The present report concerns boiling water reactor (BWR) plants with a Mark II containment design. Previously, the CPI program has analyzed potential improvements for BWRs with Mark I containments.<sup>3</sup> Other studies will address BWRs with Mark III containments, pressurized water reactors (PWRs) with ice condenser containments, and PWRs with dry containments.

This report focuses on dominant severe accident challenges, as identified by current severe accident research, which can potentially threaten Mark II containment integrity. Potential improvements are evaluated as to their ability to arrest core melt progression, prevent or delay containment failure during postulated severe accidents, or mitigate the offsite health consequences of a fission product release. Accordingly, a risk analysis is performed in order to correlate containment challenges, resulting consequences, sequence frequencies, and potential improvement benefits for each containment challenge. As seen in Equation (1-1), the risk that arises from the operation of a nuclear power plant is a function of all of these factors:

$$RISK_k = \sum_{i=1}^m \sum_{j=1}^n FREQ_i * CRMP_{ij} * CONS_k(FP_{ij}) \quad (1-1)$$

where,

$RISK_k$  = the risk associated with consequence measure  $k$

$FREQ_i$  = the frequency of accident sequence  $i$

$CRMP_{ij}$  = the conditional probability of containment release mode  $j$ , given accident sequence  $i$

$FP_{ij}$  = fission product source term for containment release mode  $j$  of accident sequence  $i$

$CONS_k$  = mean magnitude of consequence  $k$ , given fission product source term ( $FP_{ij}$ ) for release mode  $j$  and sequence  $i$ .

Consequently, all factors affecting plant risk should be considered in a program to improve containment performance.

The Mark II BWR plants and their important safety design features, along with the differences and similarities among the various plants, are discussed in Section 2. In Sections 3 through 5, the important accident sequences and containment failure modes are introduced. Section 3 discusses those sequences, originating from inadequate containment heat removal, that could challenge containment integrity prior to extensive core damage. Examples of these accidents are anticipated transients without scram (ATWS) and sequences with a loss of long-term containment heat removal (TW). Section 4 discusses sequences where core damage occurs prior to a significant challenge to containment integrity. Station blackouts (SBO), loss of coolant accidents (LOCA), and transients with a loss of coolant injection are the primary constituents of this sequence class. Section 5 briefly considers primary containment bypass sequences, which result from failures of low pressure valves and piping that release reactor coolant outside containment. Section 6 qualitatively analyzes potential improvements based on the existing risk profiles of BWR Mark II containments,

as established in past probabilistic risk assessments (PRAs) of the Limerick Generating Station<sup>4</sup> and the Shoreham Nuclear Power Station,<sup>5,6</sup> and on the Individual Plant Examination (IPE) of the Susquehanna Steam Electric Station.<sup>7</sup>

A limited quantitative risk analysis of several potential improvements is presented in Sections 7 through 10. Simple event trees were used to analyze the system and containment response to selected dominant severe accident sequences. The findings of this analysis are a frequency of occurrence for each sequence (core damage frequency) and a set of containment release modes and their conditional probabilities of occurrence. The containment release modes are then binned into release categories and the source term associated with each release category is used as an input to the consequence analysis. The output of the consequence analysis is the conditional probability of occurrence associated with each of the risk measures, for example, latent fatalities and population dose.

Simple containment event trees (SCETs) were used

for the quantitative containment response analysis, with each tree having approximately 15 top events, rather than the 100 or more used in the BWR accident progression event trees developed for NUREG-1150.<sup>8</sup> The current uncertainties in many important phenomenological issues (both stochastic and due to lack of knowledge) tend to offset attempts to include a great amount of detail in the containment event trees. Even in the SCETs used here, the quantification of several important events remains indeterminate because of a lack of data, both calculational and experimental. For more details on the SCET methodology, see Reference 3.

Source terms used in the consequence analysis were not determined from original fission product transport calculations. Instead, the source terms calculated in Reference 9 were used as inputs to the MELCOR Accident Consequence Code System (MACCS),<sup>10</sup> using the NUREG-1150 MACCS deck for Peach Bottom (see Appendix D for more details). Because this report is primarily concerned with changes in offsite consequences effected by a proposed improvement, this methodology is considered to be adequate.

## 2. DESCRIPTION OF MARK II PLANT FEATURES AND CONTAINMENT DESIGNS

This section presents a general summary of design information for the U.S. BWR nuclear power plants with Mark II containments. As Table 1 indicates, there are nine Mark II nuclear power plants in the U.S., located at six sites.<sup>11</sup> All of the reactors have been licensed for operation in the 1980s. As seen in the table, many different architect engineers and construction firms were used to build the nine plants. Tables 2 and 3 present design similarities and differences. Section 2.1

discusses and compares general reactor design characteristics and the safety systems for water injection. Similarly, Sections 2.2 and 2.3 discuss the primary and secondary containment designs. When available, plant-specific design information is presented. Such information was taken from the Final Safety Analysis Reports (FSARs) for each of the plants, unless otherwise noted.<sup>12,13,14,15,16,17</sup>

**Table 2.** United States nuclear power plants with Mark II containments<sup>a</sup>

Utility/Plant	Architect Engineer	Constructor	Commercial Date
Commonwealth Edison			
La Salle 1	Sargent & Lundy	Utility	10/82
La Salle 2	Sargent & Lundy	Utility	6/84
Long Island Lighting Co.			
Shoreham	Stone & Webster	Utility	— <sup>b</sup>
Niagara Mohawk Power Corp.			
Nine Mile Point 2	Stone & Webster	Stone & Webster	4/88
Pennsylvania Power & Light Co.			
Susquehanna 1	Bechtel	Bechtel	6/83
Susquehanna 2	Bechtel	Bechtel	2/85
Philadelphia Electric Co.			
Limerick 1	Bechtel	Bechtel	2/86
Limerick 2	Bechtel	Bechtel	9/89
Washington Public Power Supply System			
WNP-2	Burns & Roe	Bechtel	12/84

a. "World List of Nuclear Power Plants," *Nuclear News*, 32, 2, American Nuclear Society, February 1989.

b. Shoreham received a full power operating license on 4/20/89. However, the future of the plant remains uncertain because of the pending agreement between Lilco and N.Y. State, which would result in the permanent closure of Shoreham.

**Table 2. Comparison of BWR Mark II reactor design characteristics**

Parameter	Limerick	Susquehanna	La Salle	Nine Mile Point 2	Shoreham	WNP-2
BWR Type	4	4	5	5	4	5
Vessel ID (in.)	251	251	251	251	218	251
Number of fuel bundles	764	764	764	764	560	764
Rated power (MWt)	3293	3293	3293	3300	2436	3293
Power density (kW/L)	48.71	48.71	50.00	50.00	49.16	49.16
Linear power density (kW/ft)	5.34	5.34	5.40	5.40	5.41	5.40
Turbine bypass capacity (%)	26	30	25	25	25	25
HPCI/HPCS gpm NPSH (ft) Design Injection Location	HPCI 6250 — Turbine Feedwater —	HPCI 5000 21 Turbine Feedwater —	HPCS 6250 12 AC motor Above core —	HPCS 6250 12 AC motor Above core —	HPCI 4250 18 Turbine Feedwater —	HPCS 6250 — AC motor Above core —
LPCS gpm NPSH (ft) Design Injection Location	6250 * 2 — AC motor Above core —	6250 * 2 9 AC motor Above core —	6250 1 AC motor Above core —	6250 14 AC motor Above core —	4625 * 2 13 AC motor Above core —	6250 — AC motor Above core —
LPCI gpm NPSH (ft) Design Injection Location	10000 * 4 5 AC motor Core shroud —	7500 * 4 9 AC motor Recirc. Lines —	7067 * 3 6 AC motor 3 places —	7400 * 3 14 AC motor Core shroud —	9650 * 2 14 AC motor Recirc. lines —	7067 * 3 — AC motor Core shroud —
RCIC gpm Design Injection Location	600 Turbine Feedwater —	600 Turbine Feedwater —	600 Turbine Feedwater —	600 Turbine Feedwater —	400 Turbine Feedwater —	600 Turbine Feedwater —



**Table 3.** Comparison of BWR Mark II primary containment design characteristics

Parameter	Limerick	Susquehanna	La Salle	Nine Mile	Shoreham	WNP-2
Total volume (ft <sup>3</sup> )	536,759	520,294	526,880	650,100	406,812	457,727
Wetwell volume (ft <sup>3</sup> )	289,100	281,500	297,000	346,800	215,400	256,400
Containment volume/power rating (ft <sup>3</sup> /MWt)	87.79	85.48	90.19	105.09	88.42	77.86
In-pedestal relative to DW floor	Same	Same	Below	Below	Same	Below
Downcomer area (ft <sup>2</sup> )	257	242	295	363	242	309
No. ex-pedestal	87	82	82	121	88	99
Height (in.)	18	18	18	3-6	6	?
No. in-pedestal	0	0	0	8	4	0
Height (in.)	n/a	n/a	n/a	?	0.5	n/a
Design pressure (psig)						
Internal	55	53	45	45	48	45
External	-5	-5	-5	-5	-5	-2
DW floor design $\Delta P$ (psid)						
Downward	30	28	25	25	30	25
Upward	10	?	5	10	10	6.4
RHR capacity (MBTU/h)	122 * 2	134 * 2	156 * 2	95 * 2	89 * 2	122 * 2
% of core thermal power	2.2	2.4	2.7	1.7	2.1	2.2
DBA Peak Response						
DW (psig)	46	44	40	40	46	34.7
WW (psig)	34	29	31	34	34	27.6
DW floor load (psid)	23	22	24	17	23	19
Design Temperature						
DW (°F)	340	340	340	340	340	340
WW (°F)	220	220	275	212	225	275

## 2.1 Reactor Design

BWR Plants with Mark II containments feature the General Electric (GE) BWR/4 and BWR/5 reactor product lines. Table 2 summarizes some of the important Mark II reactor design information. Three of the sites, Limerick, Susquehanna, and Shoreham, use BWR/4 reactors while the other sites use BWR/5 reactors. The thermal power ratings for the nine plants are very similar except for Shoreham, which has a smaller reactor vessel, a smaller number of fuel bundles, and a lower thermal power rating than the other Mark II plants.

Table 2 also includes a comparison of emergency core cooling systems (ECCS). The BWR/4 reactors feature turbine-driven high pressure coolant injection (HPCI) with DC controllers, AC-powered low pressure core spray (LPCS), and an AC-powered low pressure coolant injection (LPCI) system. As noted in Table 2, LPCI at Limerick injects into the core shroud rather than into the recirculation lines (typical BWR/4 LPCI injection location). The BWR/5 reactors use a different ECCS featuring AC-powered high pressure core sprays (HPCS) with backup power from a dedicated diesel generator, AC-powered low pressure core spray (LPCS), and an AC-powered LPCI system. Unlike the BWR/4 ECCS configuration, the HPCS and LPCI injection is over the core and into the core bypass region, respectively. It is important to note that BWR/5 plants do not use turbine-driven high pressure ECCS pumps.

Other high pressure injection systems common to both reactor models include the condensate/feedwater system, reactor core isolation cooling (RCIC) system, and control rod drive (CRD) hydraulic system. The RCIC and CRD systems are not part of the ECCS and have a lower makeup flow rate than the ECCS. However, in postulated high pressure severe accidents, these systems can become important sources of high pressure makeup flow. The RCIC makeup flow rates are included in Table 2. The turbine-driven RCIC system delivers approximately 10% of the HPCI/HPCS flow rate. A survey of plant-specific CRD flow rates was not made. At Limerick, the CRD injection rate during normal operations is a maximum of 63 gpm. However, with optimum manual valve lineup, each CRD pump could deliver more than 100 gpm to the reactor vessel.

All the Mark II plants include an automatic depressurization system (ADS) as part of the ECCS to depressurize the vessel and allow low pressure ECCS to

inject water. Upon receipt of an ADS initiation signal, the ADS opens a subset of the safety/relief valves (SRVs). Effluent leaving the vessel through the SRVs is piped to spargers near the bottom of the suppression pool. Discharging effluent from the SRVs into the bottom of the suppression pool maximizes steam condensation and the scrubbing of any non-noble gas fission products. The SRVs are grouped into banks of valves that operate in unison to protect the vessel from over-pressurization. Each SRV bank has a different pressure set point to provide graduated pressure relief with increasing reactor system pressure.

Once the vessel is depressurized, two redundant systems of low pressure injection are available from the ECCS: LPCS and LPCI. As seen in Table 2, LPCI is a high capacity injection source while LPCS has a somewhat lower injection capacity. At the BWR/5 plants and Limerick, the licensees have verified with the manufacturers that the LPCI pumps are capable of pumping saturated water without failure. Conversely, the other BWR/4 LPCI pumps are postulated to fail while pumping saturated liquid. (Alternate, or non-ECCS, injection systems are discussed in other sections of the report related to potential improvements and plant response during postulated transients.)

Reactivity control in the event of an accident is provided by two redundant systems: the CRD system and the standby liquid control system (SLCS). During conditions that call for a reactor scram, the CRD system rapidly inserts the boron carbide (B<sub>4</sub>C) control rods into the core. The alternate rod insertion (ARI) system provides a backup scram signal should the reactor protection system (RPS) signal fail. If the CRD system totally fails to control core reactivity in response to the RPS and ARI signals, several manual operator actions, including actuating the SLCS, are prescribed by the BWR Emergency Procedure Guidelines (EPGs). The SLCS injects a sodium pentaborate solution into the lower plenum just below the core plate (the Limerick SLCS injects into the core spray sparger). A more detailed discussion of reactivity control during accidents, including manual operator actions, is provided in Section 3.1.

## 2.2 Primary Containment Design

The BWR Mark II containment consists of two regions, the drywell and the wetwell (see Figure 1). The wetwell region lies directly below the drywell and is separated from it by the drywell floor. Vertical downcomers with a nominal diameter of 2 ft connect the

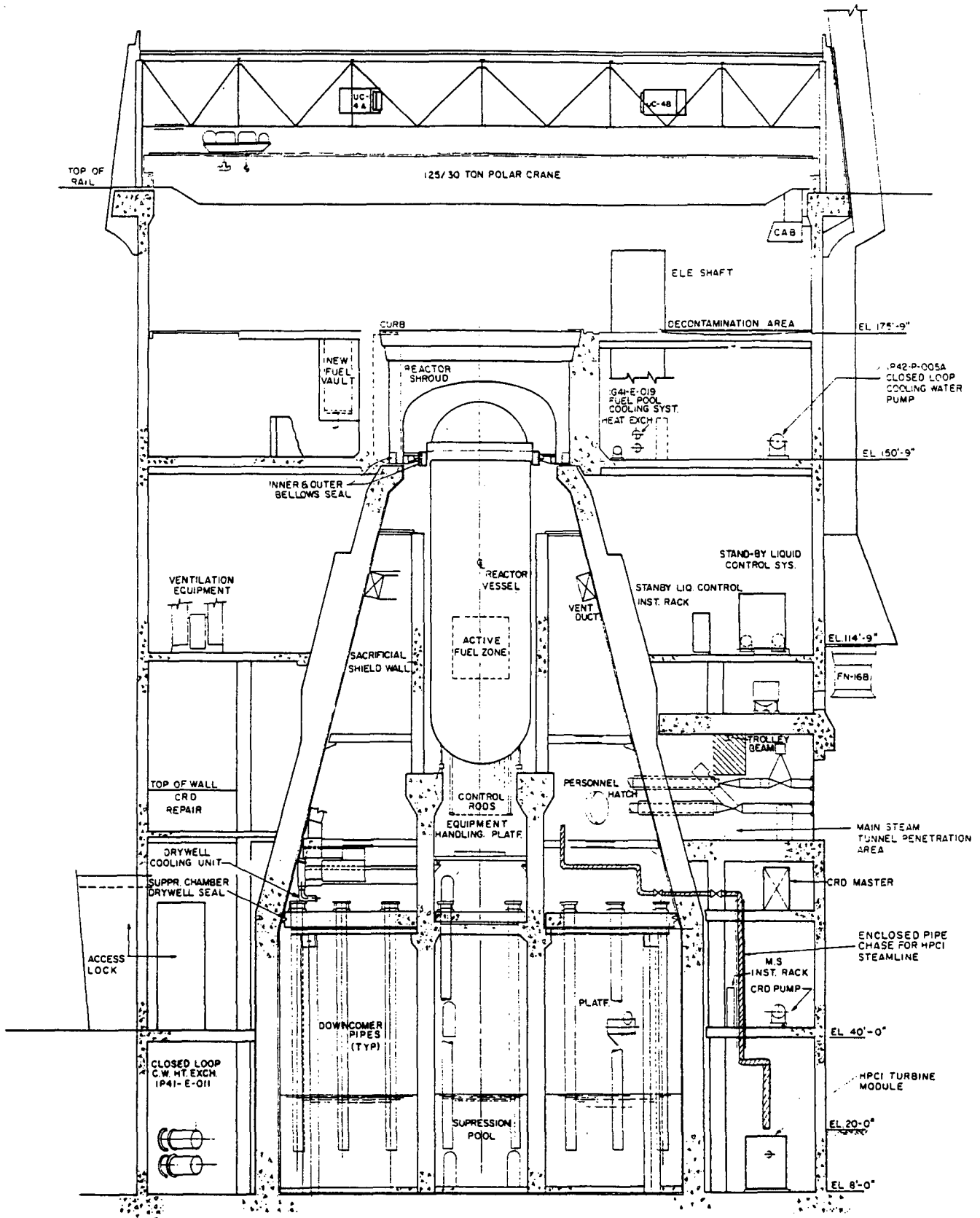


Figure 1. Shoreham containment.

drywell airspace to the suppression pool (WNP-2 employs 84 2-ft downcomers and 18 28-in. downcomers). When the drywell airspace is pressurized, gases from the drywell are forced through these downcomers into the suppression pool. Because the downcomers discharge below the water level of the pool (approximately 8 to 12 ft), all effluent entering the wetwell must pass through the suppression pool. The benefits of the suppression pool include (a) scrubbing of the non-noble gas fission products, (b) a source of water for the ECCS, and (c) a large heat sink for steam condensation. For example, a 140,000 ft<sup>3</sup> pool is capable of absorbing 100 MW-h of energy with only a 40°F temperature rise.<sup>18</sup>

Table 3 summarizes general containment design information for the six Mark II plant sites. The total free volume is approximately the same at Limerick, Susquehanna, and La Salle (within 30%). Shoreham, due to its smaller reactor thermal power rating, has a smaller primary containment. Washington Nuclear Project Number 2 (WNP-2) has the same pool volume as the larger Mark II plants, but has a smaller total containment volume. Comparison of the containment free and pool volumes to thermal power rating also illustrates that the Shoreham containment free volume appears to be sized consistently with the other plants, but the pool volume ratio is slightly lower.

The reactor pressure vessel is supported by an annular pedestal that extends to the vessel from the containment basemat through the drywell floor. The design of this in-pedestal region varies from plant to plant (see Figures 1 through 6). The Shoreham and Nine Mile Point 2 containments have downcomers inside the pedestal region (referred to as in-pedestal downcomers). At La Salle, WNP-2, and Nine Mile Point 2, the in-pedestal region is at a lower elevation than the ex-pedestal drywell floor. WNP-2 has two sumps cast into the in-pedestal floor. The design of the in-pedestal region can have a significant influence on severe accidents in which debris is discharged onto the drywell floor. The presence of downcomers in this region could allow relocation of a larger fraction of the corium debris to the suppression pool than would be likely in plants without in-pedestal downcomers (see Figures 7 and 8). This design could eliminate problems associated with core-concrete interactions (CCI) but there could be significant problems with energetic fuel-coolant interactions (FCI). Conversely, a recessed cavity would tend to retain more of the corium in the cavity. La Salle has the largest recessed cavity, which is capable of holding approximately two entire core volumes of molten debris. This design would

probably result in the maximum CCI and the minimum potential for cooling the core ex-vessel. The Limerick and Susquehanna plants have a flat in-pedestal floor at approximately the same elevation as the ex-pedestal floor. This design likely would result in significant CCI and large uncertainties associated with the timing of suppression pool bypass, but with a significant potential for ex-vessel cooling of the corium with containment sprays. However, as identified in the FSARs, all designs, except for Susquehanna, have in-pedestal drains into the wetwell. Although there is no analysis to support or refute this hypothesis, failure of these lines is postulated to result in suppression pool bypass shortly after reactor vessel failure. The containment cavity designs for the six sites are summarized in Figures 2 through 9.

The ex-pedestal downcomer pipes extend approximately 3 to 18 in. (site-specific value) above the drywell floor to prevent clogging. The ex-pedestal downcomers for all plants have a steel cover to prevent direct impingement damage and localized suppression pool heating during LOCAs. The number of downcomers varies from site to site as indicated in Table 3. Other penetrations in the drywell floor include floor drains, sumps, and SRV penetrations.

Figure 9 shows the drywell floor layout and floor penetrations at the Susquehanna Steam Electric Station. While the in-pedestal drywell floor at Susquehanna does have a thin steel liner, this liner is not considered to significantly delay initiation of CCI. At Shoreham, an inflatable boot is used to seal the gap between the drywell floor and the side of the containment. WNP-2 uses a steel "ring girder" embedded in the drywell floor and welded to a steel peripheral seal assembly, which in turn is attached to the liner of the primary containment. Failure of a drywell floor penetration, the drywell floor seal, or the floor itself (by core-concrete attack or from excessive differential pressure across the floor) would allow fission products in the drywell to bypass the suppression pool.

The wetwell airspace communicates with the drywell through normally closed check valve vacuum breakers. These vacuum breakers are designed to (a) open when there is a positive wetwell airspace-to-drywell pressure difference (valves typically begin opening between 0.25 and 0.50 psid), and (b) provide sufficient flow to maintain the pressure difference below the drywell floor upward design pressure (see Table 3). The maximum upward design pressure loading for the drywell floor ranges from 5.0 to 10.0 psid. Currently, no information is available on the drywell floor's ultimate pressure loading capability or the

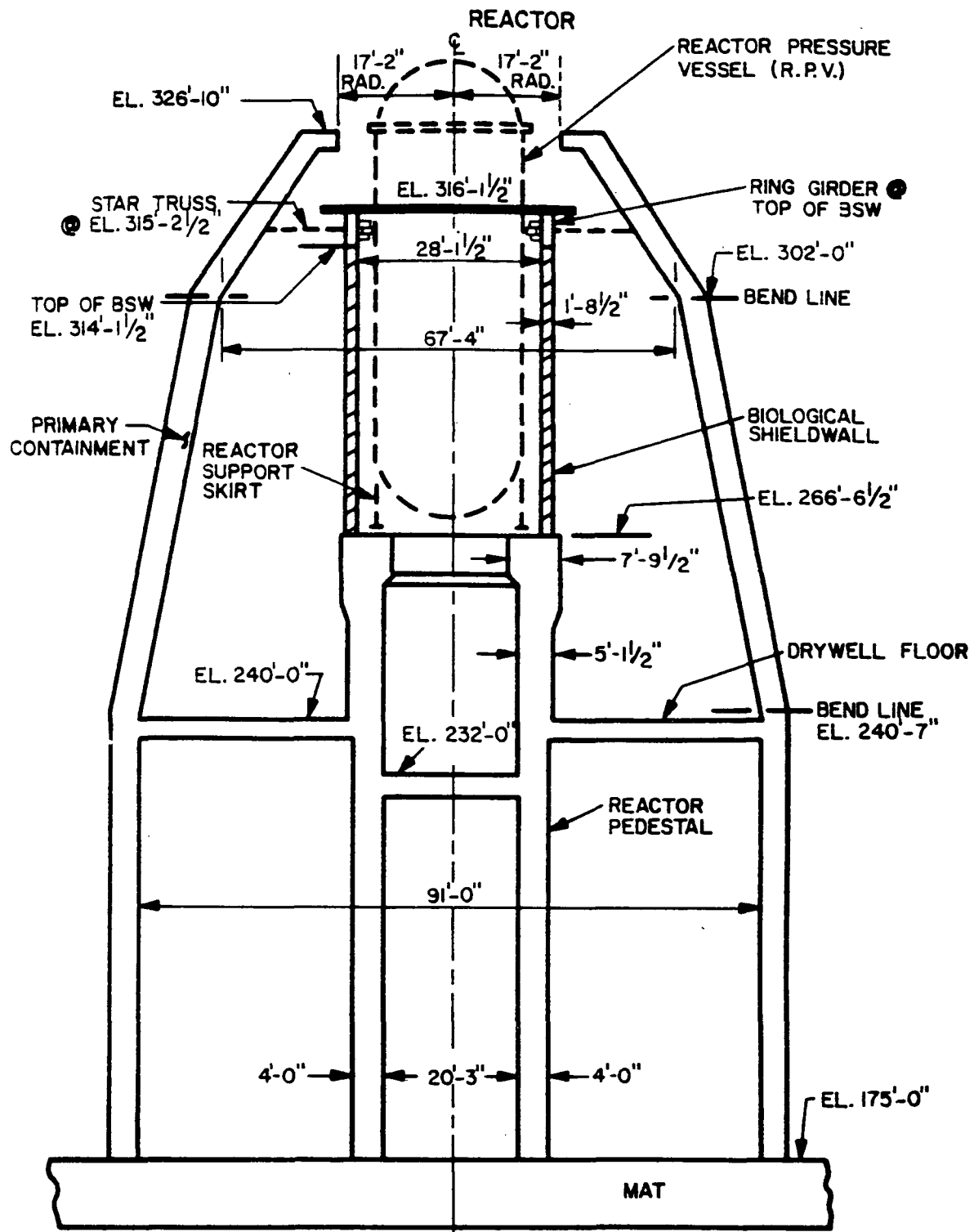
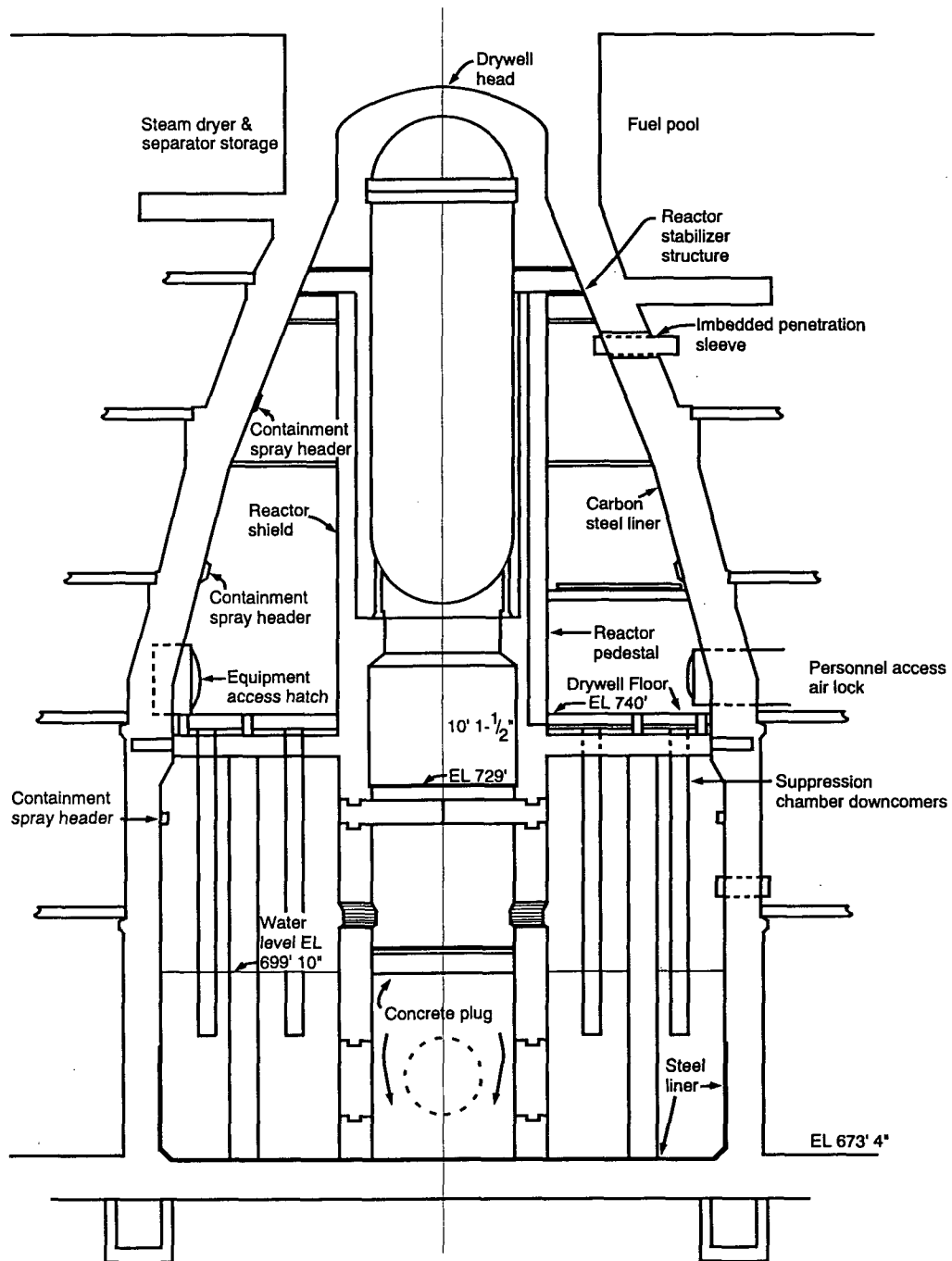
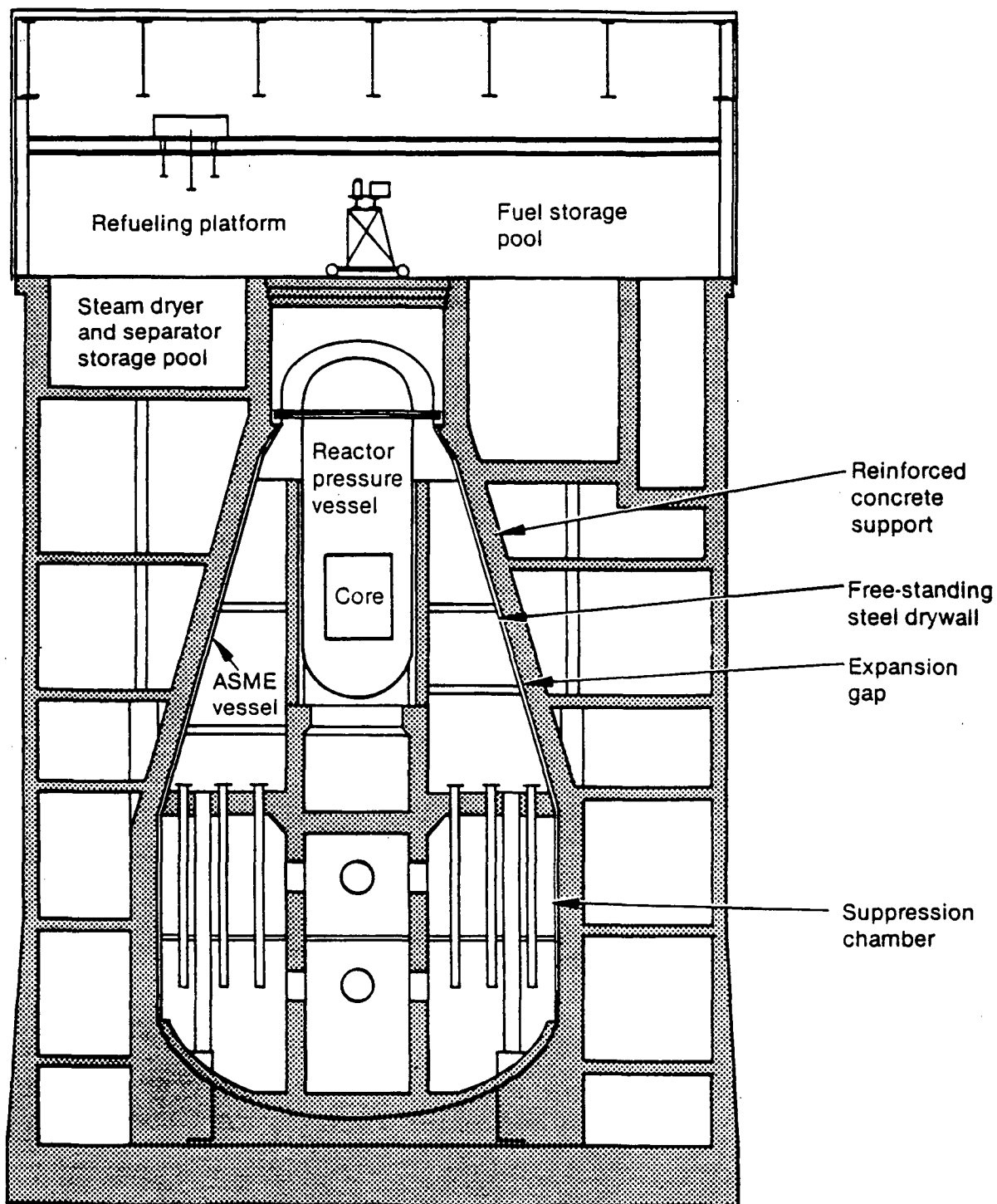


Figure 2. Nine Mile Point 2 containment.



P90 0203

**Figure 3.** La Salle containment.



7-2784

**Figure 4.** WNP-2 containment.

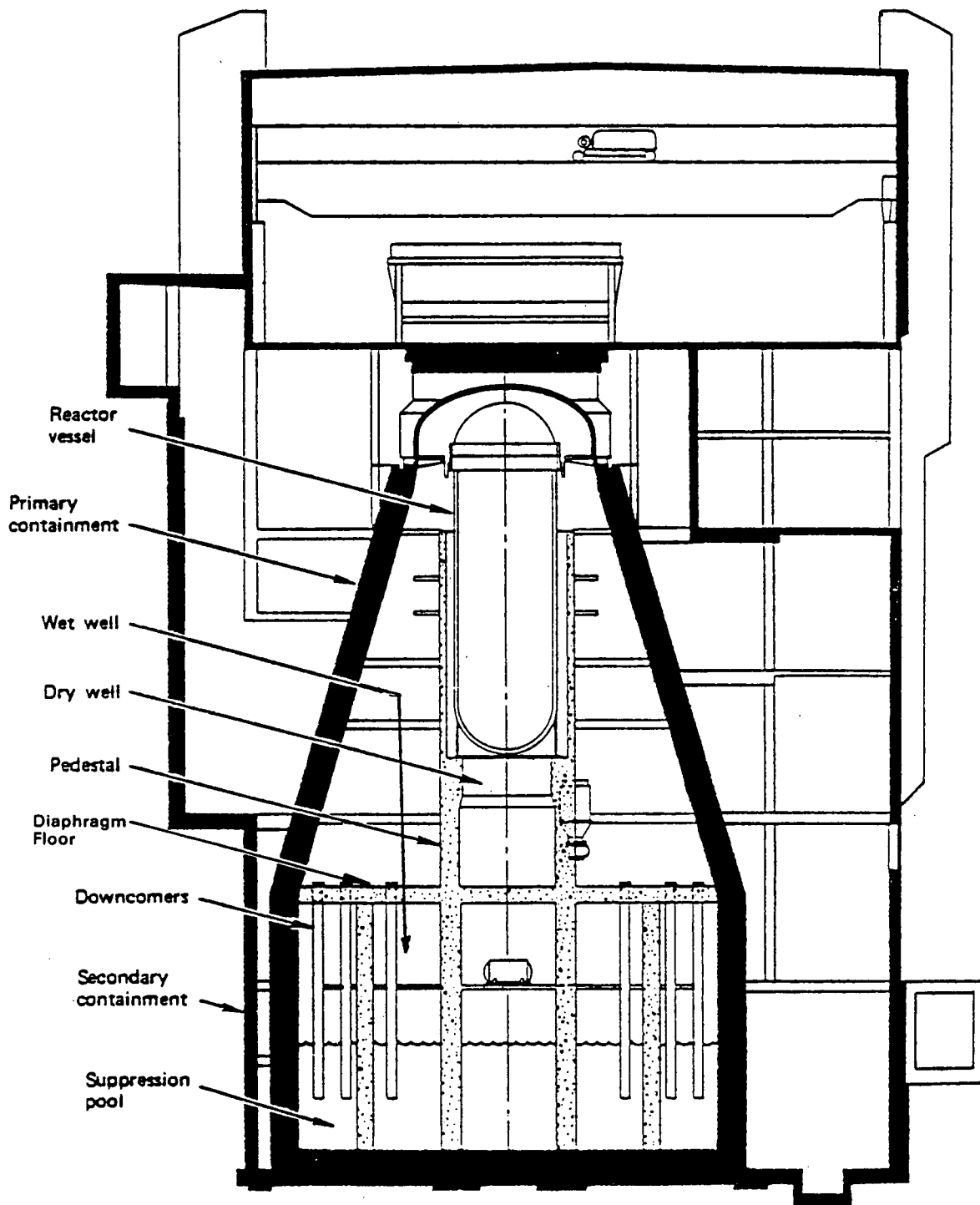
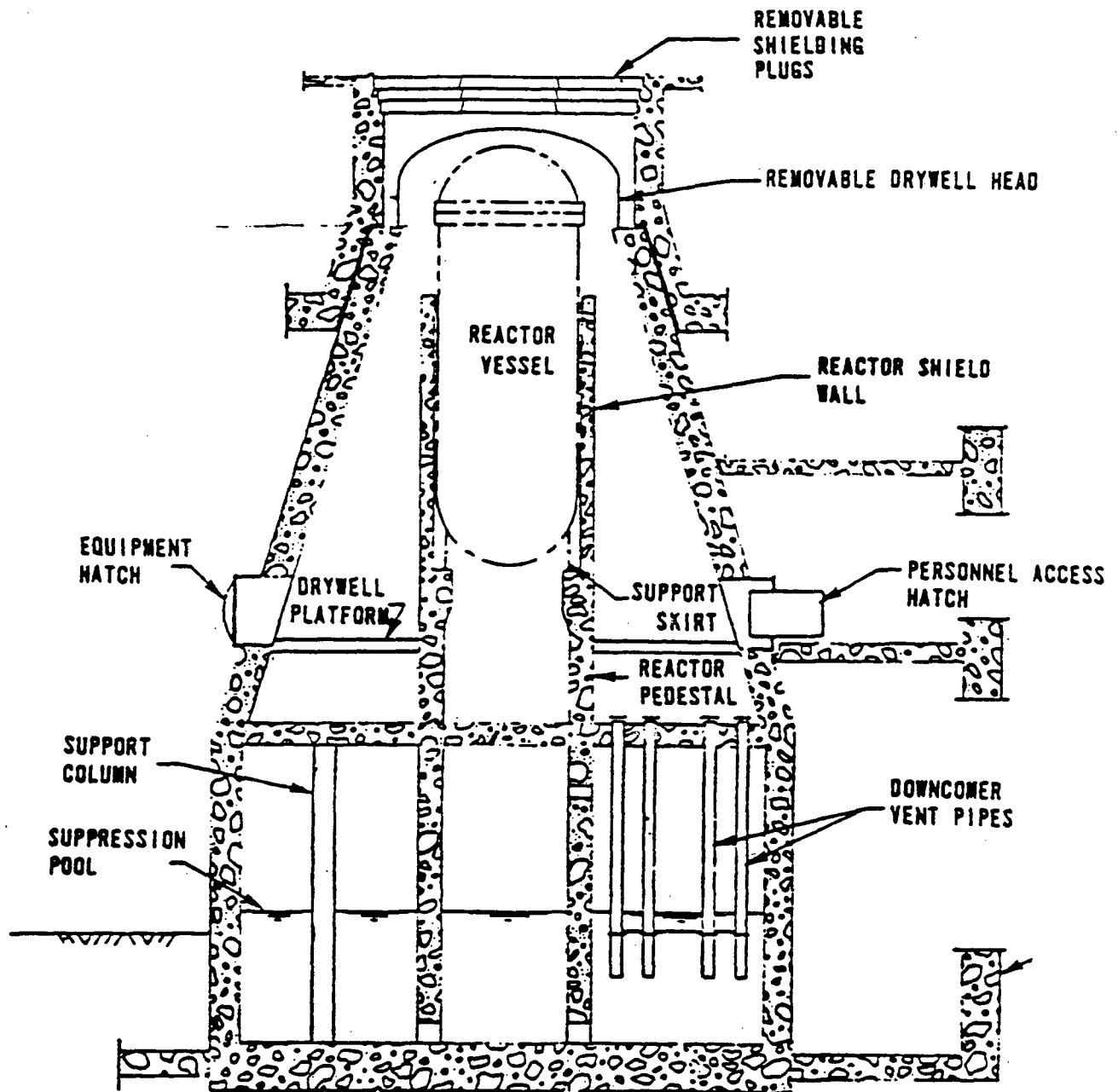


Figure 5. Limerick containment.





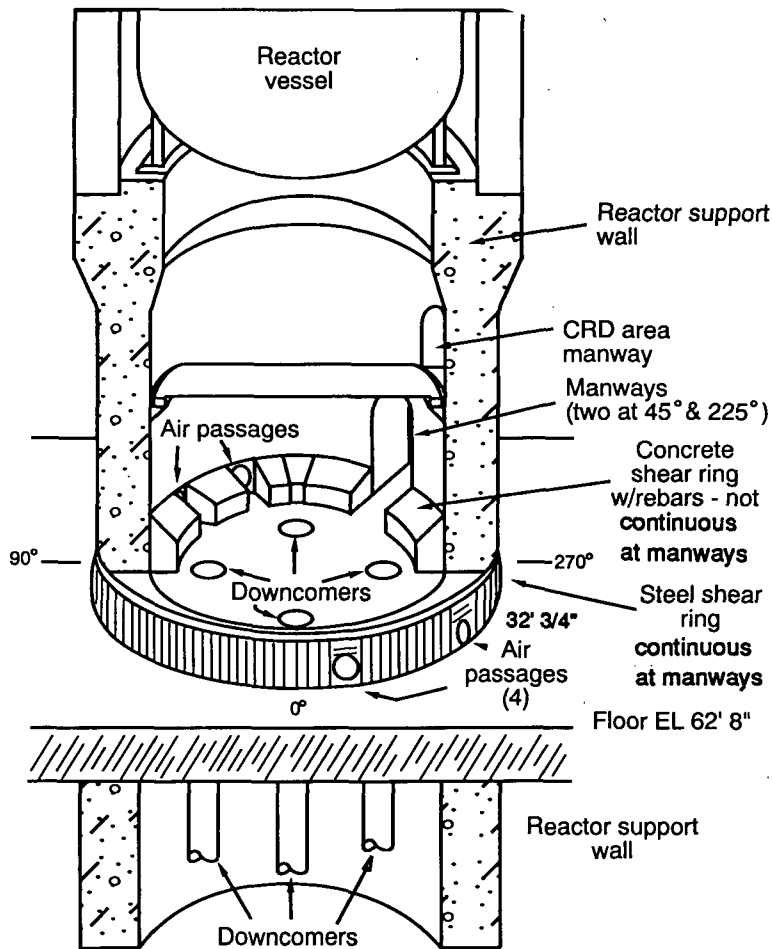
**Figure 6.** Susquehanna containment.

relationship of this capability to the loading capacity of the penetrations and floor seals.

The containment could also be damaged by a negative pressure difference between the primary containment and the reactor building. However, the BWR EPGs provide some procedural guidance for situations where rapid condensation could reduce the primary containment pressure too rapidly.<sup>19</sup> The primary containment external design pressure ranges from

-4.7 to 10.0 psig. Only WNP-2 (a steel containment), which has three 24-in. vacuum breakers connecting the reactor building to the wetwell airspace, has the ability to equilibrate a pressure differential between the primary and secondary containment.

The Mark II containments were constructed using three general methods (see Reference 18). Susquehanna 1 and 2, Limerick 1 and 2, and Nine Mile Point 2 were constructed using deformed steel bars



P90 0204

**Figure 7.** Shoreham in-pedestal cavity.

with concrete reinforcement, a flat base, a 1/4 to 3/8-in. thick steel internal liner, and a steel dome closure cap. La Salle 1 and 2 were constructed from prestressed concrete with a steel cap, steel liner, and a flat base. WNP-2 was built with steel surrounded by concrete with an ellipsoidal base.

The primary containment design pressure ranges from 45 to 56 psig. However, the ultimate containment

pressure has been estimated to be significantly higher than the design pressure. Examples of assessed ultimate Mark II containment failure pressures are as follows: 133 psig by Ames Laboratory for WNP-2, 140 psig by General Electric for Limerick, 150 psig by Sargent and Lundy (Architect Engineer for La Salle) for a standard Mark II,<sup>20</sup> and 135 psig by Stone and Webster for Shoreham (see Reference 5). In addition, the NUREG-1150 expert elicitation panel revised the La Salle failure pressure upward to 190 psig.

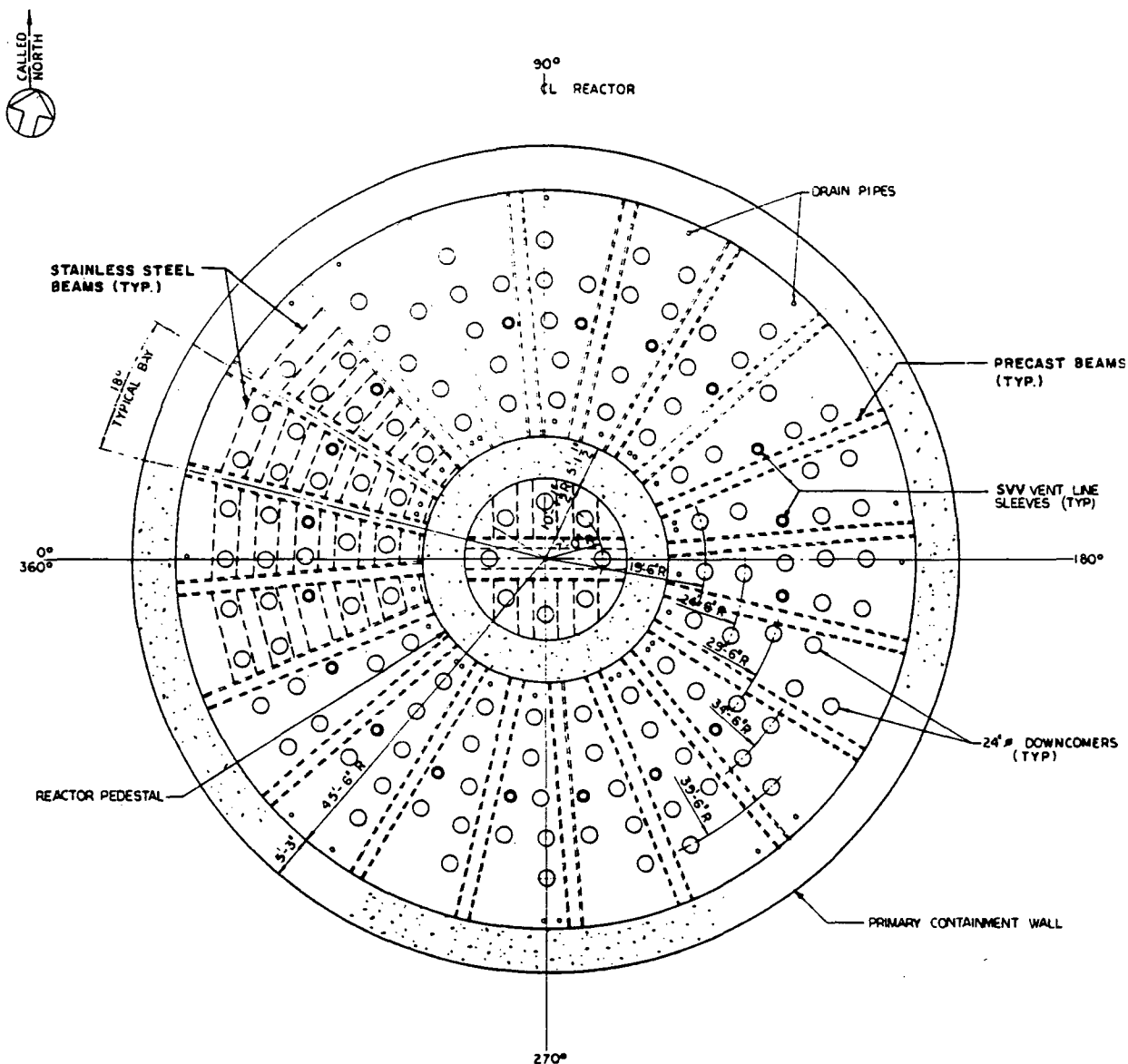


**Figure 8.** Nine Mile Point 2 drywell floor.

The most limiting containment pressure response to a set of design basis accidents (DBAs) is included in Table 3. Comparison of the DBA results with the containment design pressure and the design differential drywell floor pressure reveals various safety margins for the different plants. The calculated response is dependent upon geometric differences, core thermal power rating, and safety equipment differences. However, it is interesting to note that the larger number of downcomers at Nine Mile Point 2 reduces the drywell floor loading relative to the other plants.

The main system for removing energy from the containment during an accident is the residual heat removal (RHR) system. The RHR system is considered as

part of the ECCS and can be operated in several different modes, such as LPCI (discussed in Section 2.1). Another mode of operation is the suppression pool cooling mode, in which the RHR system takes suction from the suppression pool, cools the water in one of two redundant heat exchangers, and returns the cooler water back to the pool. The nominal ratings of the heat exchangers are provided in Table 3. In general, the referenced conditions were for a peak pool temperature near 212°F. As seen in Table 3, the RHR heat exchangers are capable of removing 1.7 to 2.7% of rated core thermal power.

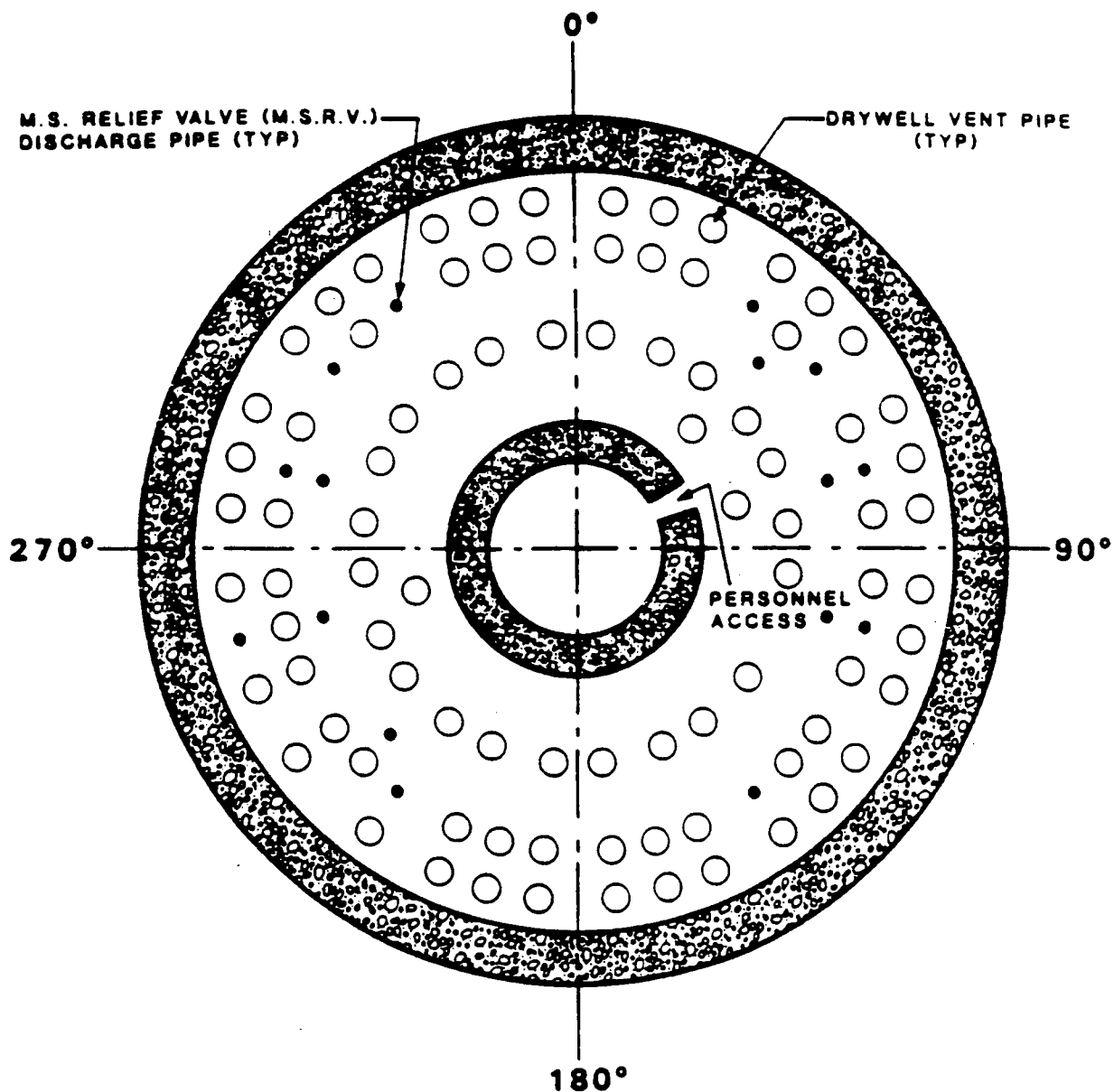


**Figure 9.** Susquehanna drywell floor.

The RHR system can also be aligned to take suction from the suppression pool, cool the water in the heat exchangers, and discharge the water through the containment spray headers in both the drywell and the wetwell. In most accidents, the peak wetwell airspace temperature is expected to be at or below saturation conditions due to the presence of the large water pool. Conversely, temperatures above saturation can be expected in the drywell, especially if molten corium is present on the floor. Most plants distribute approximately 95% of the spray flow to the drywell and only 5% to the wetwell. While the spray distribution was established to enhance DBA performance, it could also

be beneficial during severe accidents. However, use of drywell sprays is constrained by the EPG limits on drywell pressure and temperature. Drain pumps, sumps, and downcomers in the drywell floor are used to return the water to the suppression pool. Nine Mile Point 2 also has a sloped floor to direct water to the sumps.

As noted previously, the BWR/5 (and Limerick) RHR pumps are capable of pumping saturated water. If the RHR pumps are taking suction from the suppression pool, three conditions could cause the suppression pool to boil as a result of containment depressurization and fail BWR/4 RHR pumps: (a) containment

venting,<sup>21</sup> (b) rapid depressurization caused by containment spray operation (see Section 4.3), and (c) containment failure.

Three methods are provided for controlling combustible gas concentration in the primary containment following an accident. First, the primary containment is inerted with nitrogen to maintain the maximum oxygen concentration below 5%. (However, the plant Technical Specifications permit de-inerting of the containment for short periods prior to shutdown and during startup.) Second, the hydrogen concentration from long-term radiolytic generation following a DBA is maintained below 4 to 5% by use of hydrogen recombiners. The hydrogen recombiners take suction from the containment, chemically combine the oxygen and hydrogen into water, and return the effluent back to the containment. As seen in Table 3, the low capacity of the hydrogen recombiners is consistent with a slow radiolytic hydrogen generation rate. The recombiners were intended to be manually initiated several hours after a DBA was terminated and would be of little use during a severe accident and might actually compound problems by exceeding the recombiner influent composition design specifications (potential for release path). Finally, the nitrogen purge system and

the standby gas treatment system (SGTS) in the secondary containment dilute, filter, and vent gases from the primary containment. As specified in the EPG, hydrogen control via venting through the nitrogen purge system is used only if all other control measures are unsuccessful.

## 2.3 Secondary Containment Design

A secondary containment, consisting of the reactor building and refueling bay, surrounds the primary containment. The design of the secondary containment is site-specific, as determined by the architect/engineer. However, secondary containments for Mark II plants are generally similar to those for Mark I plants. General secondary containment characteristics are discussed below for completeness.

The secondary containment, in conjunction with the SGTS, serves as the final barrier to prevent or mitigate the release of fission products to the environment. As seen in Table 4, the Mark II secondary containments are large structures. At multi-unit sites, a single secondary containment is divided into separate zones, which may be isolated from one another.

**Table 4.** Comparison of BWR Mark II secondary containment design characteristics

Parameter	Limerick	Susquehanna	La Salle	Nine Mile	Shoreham	WNP-2
Secondary containment vol. (10 <sup>6</sup> ft <sup>3</sup> )						
RB #1	1.8	1.5	4.5	4.6	1.4	3.5
RB #2	1.8	1.6	4.5	n/a	n/a	n/a
RF Bay	2.2	2.7	?	?	0.7	?
Design pressure (psia)	0.25	0.25	0.25	0.25	0.25	0.25
Operating pressure (in. H <sub>2</sub> O)	-0.25	-0.25	-0.25	-0.25	-0.25	-0.25
Leakage rate (v/o per day)	100	100	100	100	100	100
Fission product Control Systems Capacity (kft <sup>3</sup> /min)	RERS + SGTS (0.5–8.4) * 2 SGTS 60 * 2 RERS	SGTS (3–10.5) * 2	SGTS 4 * 2	SGTS 4 * 2	RBSVS 1.16 * 2 (exhaust) 45 * 2 (recirculate)	SGTS 4.5 * 2

The operating pressure of the secondary containments is typically -0.25 in. of water gauge to prevent leakage to the environment. The secondary containment atmosphere recirculation and filter systems are redundant and sized to maintain the system operating pressure with 100% leakage per day. The buildings generally are protected against overpressurization by blowout panels near the top of the refueling bay. However, at Susquehanna, the blowout panels are located in the lower and middle levels of the reactor building (Shoreham has no blowout panels). If the building pressure were to exceed the design pressure, the blowout panels would open to prevent gross structural damage. The ultimate failure pressure of the secondary containments is plant-specific. However, the structures were only designed to withstand differential pressure created by the maximum anticipated external wind loadings, not large internally generated pressure loads. For example, the aboveground secondary containment design pressure rating at the Browns Ferry BWR Mark I is only 3 psid. Therefore, the secondary containment might fail as a result of hydrogen burns in a severe accident.<sup>22</sup>

Fission product control in the secondary containment is provided by different systems at the various Mark II sites. In the event of an accident, the SGTS [the reactor building standby ventilation system (RBSVS) at Shoreham] operates to filter all releases to the environment and to maintain a negative pressure inside the secondary containment. The filtered effluent is discharged to the plant stack or to an elevated release point. The SGTS, or the filtered exhaust section of the RBSVS, utilizes two filter trains to remove the non-noble gas fission products. At Limerick, Susquehanna,

and Shoreham, high capacity fans recirculate gases within the secondary containment. At Limerick, the reactor enclosure recirculation system (RERS) mixes, filters, and recirculates the effluent to the reactor building and the refueling bay. Conversely, the RBSVS at Shoreham simply takes a suction from the reactor building and discharges the effluent to the refueling bay without a significant amount of filtering (see References 16 and 22).

Oak Ridge National Laboratory has analyzed the response of BWR systems (e.g., reactor vessel, primary containment, and secondary containment) to postulated severe accidents. Preliminary review of secondary containment performance by ORNL has led to several insights (see Reference 22). First, as mentioned above, the designs of BWR secondary containments are highly plant-specific. Plant-specific parameters affecting system performance include (a) degree of secondary containment compartmentalization, (b) filtering and exhaust capacities of the secondary containment atmospheric fission product control systems, (c) mixing and filtering by reactor building ventilation systems, (d) area coverage of the fire protection spray system in the reactor building, and (e) effects of a severe reactor building environment on the systems located there. Other transient-specific insights affecting fission product retention in the secondary containment include (a) primary containment failure location, (b) availability of AC power to operate the secondary containment atmospheric fission product control systems, and (c) likelihood of secondary containment hydrogen burns capable of damaging the structure. Specific details about secondary containment performance during accident situations are provided in Sections 3 and 4.

### 3. CONTAINMENT CHALLENGED PRIOR TO CORE MELT

This section discusses severe accident sequences that challenge containment integrity prior to core melt. The primary sequences with this characteristic are ATWS and TW. In ATWS sequences, scram is not successful and the vessel steaming rate to the containment exceeds the capacity of the available containment energy removal systems. High pressure conditions in the containment can lead to containment failure and loss of vessel injection. During a TW transient, the reactor scram is successful, but without containment heat removal, the containment slowly pressurizes. If the sequence is not mitigated, the containment either fails from overpressurization or the high pressure conditions lead, directly or indirectly, to a loss of vessel injection. Section 3.1 discusses plant system response during sequences that lead to containment overpressure challenges prior to core melt. Section 3.2 discusses the containment response to the pressure loading. Section 3.3 presents a qualitative discussion of systems or actions that could potentially mitigate the consequences from these sequences.

#### 3.1 Definition of Sequences

##### 3.1.1 Anticipated Transients Without Scram.

An ATWS is, by definition, a transient where all control rods (typically 180+) fail to insert as the result of the failure of both divisions of the RPS. The alternate rod insertion (ARI) system is also assumed to fail in cases where the RPS failure was in the electrical portion of the system. The transient is assumed, for this discussion, to eliminate the feedwater system and isolate containment from the main condenser, with the control rods still at their full power rod positions.

ATWS sequences can, for convenience, be divided into two general classes, depending upon whether core melt occurs before containment integrity is challenged, or whether containment failure induces core melt (see Reference 6). In the first case, the ATWS initiating event leads to a loss of all high pressure injection and a failure to depressurize the vessel. Core melt proceeds with the reactor at high pressure and the containment intact. This sequence is more appropriately grouped with sequences in Section 4 and will not be discussed further here. In the second case, the ATWS sequence results in a high pressure condition in the containment, which leads to loss of injection systems or to containment failure and induced core melt.

Initially during the sequence, injection is provided by the high pressure systems (HPCI/HPCS, RCIC, and CRD) and energy is transferred to the suppression pool

via SRV actuation. Due to the high energy addition rate to the suppression pool during a severe ATWS sequence, the pool temperature increases rapidly. The EPGs instruct the operator to depressurize the reactor to prevent exceeding the suppression pool heat capacity temperature limit (HCTL) (see Reference 19). Initially, the HPCI/HPCS and RCIC systems take suction from the condensate storage tank (CST). Upon receipt of a high suppression pool or a low CST level signal, the HPCI/HPCS (and RCIC at some plants) suction is automatically realigned to the suppression pool (this is likely in TW and ATWS sequences). Because some of the injection water is used to cool the lube oil in the HPCS/HPCI and RCIC pumps, with high suppression pool temperature, the HPCS/HPCI injection systems may fail due to inadequate lube oil cooling (e.g., the Peach Bottom HPCI design water temperature for lube oil cooling is 140°F) (see Reference 21). However, the NUREG-1150 expert panel has concluded that the HPCS pump at La Salle is not likely to be disabled by high suppression pool water temperature. Therefore, this may not be an issue at all Mark II plants. As the containment continues to pressurize, RCIC would isolate on high exhaust back-pressure (e.g., set point of 40.0 psig at Shoreham). The CRD system would continue to inject, and with both pumps running, would provide adequate core cooling in all sequences except the most severe ATWS.<sup>23</sup> If the operator successfully depressurized the reactor when the HCTL was exceeded or after HPCI/HPCS and RCIC failed, several low pressure injection systems (LPIS) would be available. However, as the containment continued to pressurize, the SRVs could close at high containment pressure. Closure of the SRVs would repressurize the vessel and leave limited injection capability (for reasons stated previously).

The point in the sequence at which the SRVs close is dependent upon SRV design, reactor pressure/containment pressure, and control air (nitrogen) pressure. For example, two-stage Target Rock SRVs use the reactor vessel-to-drywell pressure differential and the control air-to-drywell pressure differential in tandem to reposition the pilot valve and cause the main disc to open. Increasing the reactor pressure would increase the differential pressure between the reactor and the drywell and cause the SRVs to reopen. If the reactor pressure exceeded the low pressure shutoff head of the LPIS during this pressure excursion, injection would be temporarily stopped. Reopening the SRVs would depressurize the reactor and reestablish low pressure injection (see Reference 21). However, a reactivity excursion following coolant entering the core during an

ATWS sequence could repressurize the reactor and again terminate low pressure injection.<sup>24</sup> Although this response might be self-correcting and result in adequate core cooling, there are many uncertainties in neutronic response, valve operation, and core thermal-hydraulics (potential for instabilities, density wave oscillations, and system chugging).<sup>25</sup> Further plant-specific complications may include the possibility of the plant instrument air being isolated by the containment isolation signal and decaying with time due to system leakage (see Reference 21).

If adequate vessel injection were provided but the transient were not mitigated, the containment would continue to pressurize to failure. Failure of the containment or venting to prevent containment overpressurization could lead to failure of injection systems as the result of inadequate net positive suction head (NPSH), followed by core degradation.<sup>21,26</sup>

**3.1.2 TW, Loss of Long-Term Containment Heat Removal.** A sequence with adequate coolant injection, but with a loss of long-term containment heat removal, is a slowly developing accident. After a transient initiator, the reactor is successfully scrammed and the main steam isolation valves (MSIVs) are closed. Decay heat is transferred from the reactor to the suppression pool via the SRVs. Because the RHR heat exchangers are not available in this sequence, the suppression pool will heat up slowly. Coolant injection is provided by the HPIS until the suppression pool HCTL is exceeded. At this time, the operator would be expected to depressurize the vessel and maintain vessel inventory with low pressure systems. Note: The CRD pumps, with manual valve realignment, should be capable of providing adequate core cooling within approximately 30 min after the reactor is shutdown (see References 7 and 23). As in the ATWS, there is a concern that the SRVs could eventually close on high containment pressure, causing low pressure injection to be lost. This would not affect injection by the CRD pumps. Because the containment pressurization rate is much slower and the reactor is shut down, there would be no large power spikes accompanied by rapid primary system pressurization. Continued heating of the containment would occur until (a) injection systems failed, (b) containment failed catastrophically, (c) containment leakage matched the energy addition rate, or (d) heat removal systems were recovered (see Reference 8).

Because the TW sequence is such a slowly developing accident, ample time is available to attempt to establish some means of heat removal before containment integrity is challenged. There is little or

no chance that operators would overlook the need for decay heat removal. Consequently, following a transient with successful scram (event T), loss of containment heat removal (event W) is dominated by equipment unavailability. The functionally redundant means of heat removal (see Section 3.3), along with the time available to make repairs, are generally felt to result in TW contributing very little to the overall core damage frequency. Accident sequences involving a loss of containment heat removal were not found to be a significant contributor to the total core melt frequency in the Limerick, Shoreham, and Susquehanna PRAs (see References 4, 5, 6, and 7).

A survey of a few PRAs indicated that, in those PRAs that used simplistic WASH-1400 models, and gave little or no credit for operator actions in recovering from the accident, a high TW frequency ( $10^{-3}$  –  $10^{-5}$  per reactor-year) was calculated. When detailed models were used and operator actions (including, in some instances, containment venting) were considered, the calculated TW frequency was relatively low ( $10^{-6}$  –  $10^{-8}$  per reactor-year). As a result, the Limerick, Shoreham and Susquehanna PRAs identified a low core damage frequency for TW.<sup>27</sup>

## 3.2 Discussion of Containment Challenges and Failure Modes

The principal containment challenge from TW and ATWS sequences is containment overpressurization, which can lead to core melt. As stated in Section 2.2, the ultimate containment failure pressure of the Mark II containment is much greater than the design pressure. For example, the ultimate static failure pressure for Limerick was assessed to be 140 psig versus a design pressure of 55 psig (see Reference 20). This large difference provides significant time for mitigative action. In the absence of any mitigative actions, containment overpressure failure at Limerick during the TW sequence is expected to occur in approximately 30 h versus only 40 min for the case of a full isolation ATWS sequence (see Reference 18). Further, operator actions can be very effective in changing the base case responses (see Section 3.3).

Containment leakage at high pressure conditions may also affect the containment response. The Containment Performance Working Group (CPWG) evaluated the effect of leakage from typical containment penetrations during severe accident loads.<sup>28</sup> Limerick was selected as the Mark II reference plant. The results from the study are shown in Table 5. At 75 psig, the



**Table 5.** Containment Performance Working Group leakage estimates for Limerick

Containment Pressure (psia)	Drywell Leakage (in <sup>2</sup> )	Wetwell Leakage (in <sup>2</sup> )
0	0.003	0.002
55	0.003	0.002
75	0.003	0.2 <sup>a</sup>
85	1.0 <sup>b</sup>	0.3
140	42.0	0.3

a. Wetwell personnel hatch unseats at 75 psig.

b. Drywell head unseats at 85 psig.

equipment hatch in the suppression pool unseats and causes a small increase in the wetwell leakage area. At 85 psig, the drywell head unseats, and by 140 psig, the amount of drywell leakage is substantial. Leakage during steam loading has both positive and negative implications. A simple steam critical flow calculation shows that the leakage at 140 psig (equivalent to approximately 3.5% of rated thermal power) would easily exceed decay heat removal requirements. Consequently, catastrophic failure of the containment during a TW sequence may be unlikely. On the negative side, leakage of high temperature steam into the reactor building would likely terminate repair operations and might cause failure of injection systems. However, because most of the leakage is predicted to occur at the drywell head, the injection pumps located in the lower elevations of the reactor building likely would not be affected. Flooding the reactor cavity above the drywell head might minimize the negative effects from drywell head seal leakage (see Section 4.3.8). While it may be possible to operate the containment at 140 psig without leakage, it may not be prudent to operate at that pressure or rely on containment integrity during a severe accident at a pressure so close to the anticipated ultimate failure pressure.

Temperature-induced containment leakage is also a concern. However, since the early containment challenge from sequences in this section is due only to steam loading, the temperature in both the drywell and the wetwell would be close to saturation (360°F at

140 psig). Significant seal degradation due to a high temperature environment is not expected until much higher temperatures are reached (see Section 4.2.2.2).

Research by the CPWG supports a high likelihood of large leakage rates prior to reaching the containment ultimate failure pressure (see Reference 28). However, there is a possibility that the containment leakage rates have been overestimated and catastrophic containment overpressure failure could still occur. Several probable failure locations have been identified through finite element analyses and simplified analysis methods (see Reference 20). The deformation predictions are generally regarded as reliable, assuming the containment configuration is described accurately, that is, known geometry, materials, and loads. However, actual predictions of leakage are uncertain. Consequently, the ultimate strength results should be regarded as predictions of deformation failure.

In failure analysis calculations for WNP-2, the lower circumferential unstiffened cylinder was assessed to be the most likely failure location (see Reference 20). This region encompasses the top half of the wetwell cylinder. Since the downcomers extend below this region, gross failure in this region would not necessarily lead to suppression pool bypass. If the downcomers were intact, failure above the suppression pool water line would simulate venting, except that the release would be uncontrolled and could not be isolated. This type of failure would be relatively benign, since the suppression pool would still scrub non-noble gas fission products.

The results from the Limerick failure analysis show that the yield stresses at the middle section of the cylinder and the wall-to-base junction exceed the allowable value of 150 psig (see Reference 20). Other critical sections include the diaphragm slab-to-wall junction and the removable drywell head-to-wall junction as indicated in Figure 10. Failure at the wall-to-base junction would drain the suppression pool into the reactor building. Although the suppression pool function would be lost, fission products would be retained in the containment until the pool drained. Furthermore, the release point would be low in the reactor building. However, site-specific flooding problems after lower wetwell failure and loss of a water supply could lead to more severe consequences. Failure at either of the other two critical locations, the drywell head-to-wall junction and the diaphragm slab-to-wall junction, would cause immediate suppression pool bypass and tend to increase the magnitude of the source term.

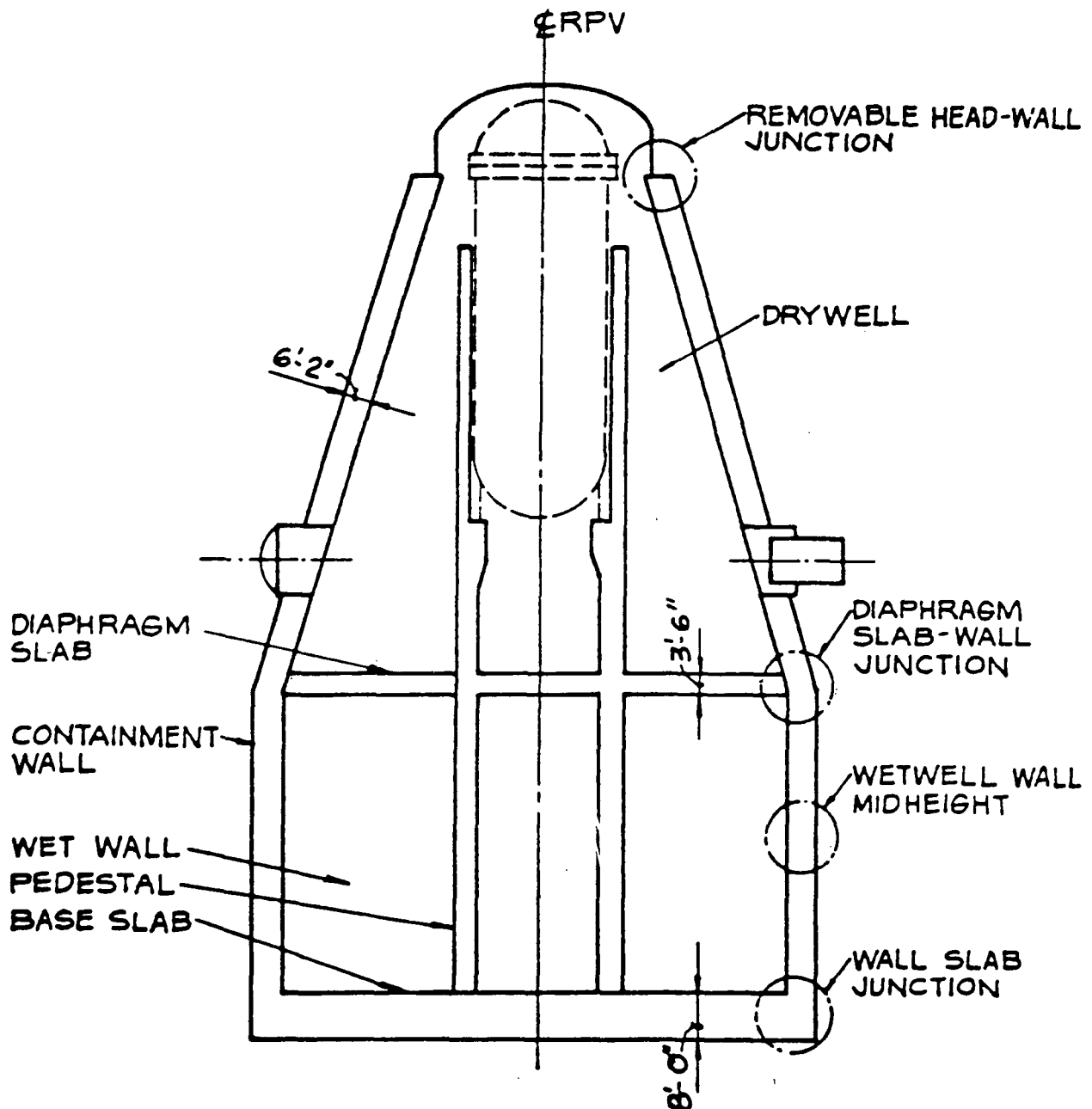


**Figure 10.** Postulated Mark II containment failure locations.

In the containment analysis performed for the 1988 Shoreham PRA,<sup>29</sup> a probabilistic analysis was done to couple the early containment failure modes to the sequence class, containment failure pressure, break size, and break location. A continuous failure probability density function was used to characterize the containment failure pressure, with failure deemed most probable between 130 and 145 psig. Subsequently, sequence-specific failure mode event trees were

constructed to quantify the distribution of the different failure modes. Slow pressurizations, such as in the TW sequence, would be more likely to lead to a small break above the wetwell water line. Conversely, in an ATWS sequence with rapid containment pressurization, small and large breaks were deemed equally probable at three different locations. Small breaks led to increased leakage and prevented further pressurization, whereas large breaks depressurized the containment rapidly.

In summary, sequences that challenge the containment prior to core degradation can lead to containment leakage or catastrophic failure. Two important leakage locations for Mark II containments are the drywell head seal and the wetwell personnel hatch. For sequences with slow containment pressurization, leakage might prevent catastrophic containment failure. However, significant leakage probably would not occur until the containment pressure was significantly higher than the containment design pressure. Temperature-dependent leakage is not considered important until after core degradation occurs. In the event of a containment pressurization rate greater than the leakage rate, gross containment failure could occur. The failure location, hole size, and containment failure pressure are both plant-specific and sequence-specific. Eliminating the drywell head flange failure, overpressurization failures are more likely to occur in the wetwell than in the drywell.

### 3.3 Potential Improvements

ATWS or TW sequences can challenge containment integrity before core damage begins. In both cases, the danger lies in (a) high containment pressure leading to an overpressure containment failure, which in turn fails injection systems and leads to core melt in a breached containment, and (b) SRV reclosure on high drywell pressure, causing the vessel to repressurize above the shutoff head of the LPIS (injection from the CRD system may be adequate to prevent core damage). Mitigation of this challenge focuses on preventing overpressurization by removing excess heat from the containment. Several suggestions have arisen as to how this might be accomplished, both in terms of using existing plant equipment and improvements that might be made to increase the probability of successful mitigation. Each improvement is discussed below.

**3.3.1 Containment Venting.** Containment venting has been touted as a means of both relieving primary containment pressure and preserving the integrity of the secondary containment.<sup>30,31</sup> Venting could reduce the likelihood of core damage from TW sequences. Venting could also delay or prevent core degradation and containment failure for some ATWS sequences. Mark II plants currently have the ability to vent via existing piping and ductwork to the reactor building HVAC systems; Revision 4 to the EPGs provides direction for when this should be done (see Reference 19). However, vent paths for some Mark IIs may be via reactor building ductwork, which is not designed to withstand the internal pressure associated with venting at the EPG primary containment pressure limit (PCPL).<sup>3,21,26,30,32</sup> Using these existing "soft"

vent systems could induce core melt (due to loss of injection).

Foremost among the concerns expressed in the above references is the effect of venting on the suppression pool and upon the reactor building environment following failure of the HVAC ductwork or the neoprene boot that typically connects the vent piping to the ductwork. Because venting at the PCPL would likely lead to saturated conditions in the suppression pool, pumps that take suction from the pool could fail due to loss of NPSH (see Reference 8). At BWR/5 plants such as La Salle, where the ECCS pumps are designed to operate with the suppression pool saturated (see Reference 13), this is less of a concern than at plants where a positive suction head is required to prevent pump cavitation damage. For these plants, operator realignment of pump suction to another water source prior to venting would eliminate this problem (assuming that another water source is available).

References 22, 32, 33, and 34 discuss in detail the calculated effects of venting upon the atmosphere in the reactor building. Based upon this work, Reference 26 assigned a very low probability to survival of reactor building equipment following venting at one plant, and a high probability to bypassing the reactor building fission product control systems during core melt. As Reference 22 points out, not all BWR secondary containments are equally vulnerable to the effects of venting. However, venting at the PCPL via existing "soft" ductwork would be expected to cause some problems at all plants, and at the very least, it would make at least some sections of the reactor building uninhabitable for personnel who might need to enter to repair equipment, align alternate injection, etc.

One solution to this problem is to install a "hardened" vent pipe, which would be designed to withstand the pressure associated with venting at the PCPL. The vent pipe would lead from the wetwell airspace to an elevated release point above the reactor building, such as the plant stack. As long as the suppression pool was not bypassed by downcomer failure, drywell floor failure, or some other means, the release would be filtered by scrubbing through the suppression pool. If the suppression pool was saturated, this would result in a decontamination factor (DF) on the order of 10 for non-noble gas fission products and 1 (no scrubbing) for noble gases. The DF for a subcooled suppression pool has been estimated to be on the order of 100 for non-noble gas fission products and 1 for noble gases.<sup>35</sup> However, all of the Mark II plants (except Susquehanna) have between two and four 4-in. drains from the in-pedestal area to the wetwell air space. No analysis has been performed to estimate the

susceptibility of these drain lines to failure by corium attack. However, the lines at La Salle were postulated to fail within 20 min after vessel breach in most sequences.<sup>a</sup> Philadelphia Electric Company has estimated that the drain plate covers at Limerick would fail within approximately 6 min after reactor vessel breach.<sup>36</sup> Thus, fission products could be released to the environment if an unfiltered vent system were used.

There are several factors that should be considered to ensure operability of the hardened vent system when it is needed (see Reference 3). First of all, the vent piping should be sized to accommodate the expected containment pressure rise for each sequence that the system is required to mitigate. The limiting sequence in this respect is a high power ATWS where the reactor may be producing 25 to 30% of rated steam flow following shutdown of the recirculation pumps. However, the lower pressurization rate associated with the TW sequence (reactor power at decay heat levels) may be accommodated at a more moderate cost. Second, the system should be able to be actuated under all conditions, including SBO. Most existing vent systems do not meet this criterion since AC control power required to open the valves typically is not supplied from an uninterruptible source. Also, interlocks would currently have to be bypassed with electrical jumpers since the isolation valves in the vent lines receive a closure signal during an accident. Therefore, even with power available, venting would require numerous operator actions. Utilities have indicated that local manual operation of the vent valves is possible; however, unless the vent valves are opened very early in the sequence, radiation levels and the post-venting steam environment in the reactor building could present an unacceptable hazard to the operators (see Reference 30). Because of this concern, a proposal has been made to open the vent lines immediately during a SBO or ATWS.<sup>37</sup> While this could be effective in preventing containment overpressurization, it could also result in an unnecessary release to the environment. This problem could be eliminated by installing an uninterruptible power supply for the vent valves. Third, the vent valves should be capable of being reclosed to isolate containment under certain conditions, such as when suppression pool bypass occurs.

Another possible modification is the construction of an external filtered vent system, such as the Supplemental Containment System (SCS) proposed by the

Long Island Lighting Company (Lilco) for Shoreham (see Reference 6). Briefly, the SCS would be a gravel-filled concrete structure separate from the reactor building, but connected to the primary containment by a high capacity hardened vent line. The system would be actuated by operator action. The gravel bed would scrub particulates and the height of the structure would provide for an elevated release, as well. Reference 26 analyzed the proposed Shoreham installation and found that reductions in both core damage frequency and risk could be achieved. The DF for the SCS design could be on the order of 1000 for fission product particulates, as compared to the DF of 10 to 100 for the suppression pool. However, because of the high cost associated with the SCS, its installation at U.S. BWRs is not expected to be cost-beneficial. Such a system is currently in use at the Barseback Nuclear Power Station in southern Sweden. A Multi-Venturi Scrubber System (MVSS) (Asea-Atom design) is being incorporated at the Oskarshamn, Forsmark, and Ringhals reactor facilities. This design uses approximately 80,000 gal of water and does not rely on any AC or DC power.<sup>38</sup> This design is expected to be less expensive than the filtra design (approximately \$5M as compared to \$30 to \$50M for the Filtra). However, because of the relatively high cost associated with both designs, external vent filters will not be quantitatively analyzed in this report.

In summary, venting has the potential to effectively mitigate the containment pressure rise during TW sequences, and delay core failure and containment failure in ATWS sequences. However, if the existing "soft" vent systems were to be used to vent containment as specified in the EPG, the soft vent systems would be likely to result in core melt (due to loss of injection) and contamination or failure of the secondary containment (direct failure of equipment or preventing equipment repair due to radiation considerations). Suppression pool bypass is likely to occur shortly after vessel failure. To overcome these problems, a filtered system capable of withstanding expected venting pressures would be required. To prevent problems with inadequate suction head to ECCS pumps, the EOPs could instruct the operator to realign the suction of ECCS pumps to another source of water, such as the CST, prior to venting. To allow operation during SBO, the vent valves would need an uninterruptible source of power. And finally, for ease of operation, interlocks could be bypassed with a keylock switch in the control room or by providing ex-panel connections for bypass jacks.

**3.3.2 Containment Sprays and Backup Water Supply.** Containment sprays could be utilized to lower containment pressure through the action of steam

a. A. Payne, Sandia National Laboratory (SNL) conference call with P.K. Niyogi, NRC, on May 1, 1989.

condensation (the use of containment sprays for debris cooling will be discussed later). Revision 4 to the Primary Containment Control portion of the EPGs directs the initiation of containment sprays when suppression chamber pressure reaches the suppression chamber spray initiation pressure, as long as suppression pool level is not too high (see EPGs for precise definition of "not too high") and drywell temperature and pressure are within the drywell spray initiation limit (also specified in the EPGs). Note that containment sprays, under the guidance given in the EPGs, would typically be initiated prior to venting, since the spray initiation pressure is less than the PCPL, at which venting is required.

The normal source of water for the containment sprays is the suppression pool, with motive force supplied by the RHR pumps. If the suppression pool flashes following venting, two problems arise. First, the suction head to the RHR pumps may be insufficient for pump operation without cavitation and damage to the pumps. Second, saturated water would not be very effective at condensing steam inside the containment. An alternate source of water, such as from the fire pumps, could be manually connected to the RHR system. Drawbacks to using the fire pumps include the manual connection that must be made to align the system, and the limited flow rates and lower discharge head that the fire pumps can produce in comparison with the RHR pumps. Note also that AC power or local manual operation would be required to operate valves, unless the valve operators are DC-powered, which typically is not the case. Another source of water could be the condensate transfer connection to the RHR system. However, the injection capacity of the condensate transfer pumps is limited by the size of the connection between the condensate transfer and RHR systems, which is typically only a few inches in diameter. Revision 4 to the EPGs does not specify either of these systems as alternative sources of water for containment spray.

The above discussion brings to light several possible improvements that could be made to enhance the availability of containment sprays for mitigating overpressurization. First of all, if the RHR pumps are capable of taking suction from a source other than the suppression pool, problems with pump cavitation could be eliminated. This would also have the benefit of providing cooler water to the sprays, thereby allowing better steam condensation in the containment. However, the more rapid depressurization associated with the cooler sprays could increase the differential pressure loading on the drywell floor beyond the ability of the vacuum breakers to relieve this differential pressure. Some

plants may already have the capability to align the RHR pumps to the CST. Others, such as Shoreham and Susquehanna, have RHR pumps that can only take suction from the suppression pool (see References 6 and 7). Using an external source of water would also add mass to the suppression pool, increasing its ability to absorb heat from the reactor. This mass addition cannot be carried out without consideration of the limits that exist on suppression pool level, and also upon drywell water level, in order to prevent structural failure of the wetwell walls or the drywell floor.

Another improvement related to the use of fire pumps for containment sprays would be a high capacity connection from the alternate water source to the RHR system. Some plants may already have such a connection; others may have only a small diameter spoolpiece or a hose connection, which would severely limit the flow rate into containment. Such an improvement could be of benefit (relative to drywell floor load considerations, see below).

If the reactor vessel has been depressurized when the backup water supply becomes available, the backup water could be directed into the reactor vessel. For accident sequences other than ATWS, the backup water supply would only have to remove the decay heat and thus could prevent core degradation or terminate core damage. For the ATWS sequence, the reactor may still be producing 25 to 30% of rated steam flow and thus, using the backup water supply would delay core damage but might not completely prevent or terminate core degradation. In both cases, injecting the water into the reactor would not prevent and might not even delay containment failure.

**3.3.3 RHR Heat Exchanger Capacity.** The rate at which heat can be removed from the suppression pool (and thus from containment) when the main condenser is not available is limited by the capacity of the RHR heat exchangers. Table 6 shows the design heat removal capacity for RHR heat exchangers at Mark II plants, both as an absolute value and as a percentage of rated thermal power (see References 12, 13, 14, 15, 16, and 17). As can be seen from this table, each of the Mark II plants has the ability to remove fission product decay energy from the containment via the suppression pool cooling mode of RHR. Bear in mind, also, that these numbers are design values; if flow and heat transfer in the RHR heat exchangers were impeded by corrosion or biofouling, the values could be significantly lower.<sup>39,40</sup> Biofouling of RHR heat exchangers could result in 100% bypass of the heat exchangers and thus, no cooling of the reactor or suppression pool water.

**Table 6.** RHR capacity as a percentage of plant thermal power rating

Plant	RHR Capacity (MBTU/h) <sup>a</sup>	Percent of Thermal Power <sup>b</sup>
Limerick	244	2.2
Susquehanna	268	2.4
La Salle	312	2.8
Nine Mile Point	190	1.7
Shoreham	178	2.1
WNP-2	244	2.2

a. Rated RHR capacity was obtained from the FSAR for DBA conditions. Typically, the pool temperature was near 212°F. At higher pool temperatures, the RHR heat exchangers would be more efficient.

b. Total RHR capacity divided by the reactor thermal power rating.

Installation of larger capacity heat exchangers is possible but not cost-effective, because of both space limitations and radiation concerns [the RHR heat exchangers are typically a "hot spot" and thus an as low as reasonably achievable (ALARA) maintenance concern]. However, to maximize the heat removal capacity of the installed heat exchangers, biofouling and corrosion need to be controlled; this requires a reliable means of controlling aquatic life, such as Asiatic clams (freshwater) and mussels (seawater), which can quickly clog the heat exchanger tube sheets. Modifications to increase the availability of the chlorination system, periodic cleaning, and heat balance (performance testing) and nondestructive examination of the heat exchangers might be required. Performance trending of vital heat exchangers can be a valuable aid in early detection of a degraded heat exchanger.

A recent review of operating experience feedback concerning service water system failures and degradations, performed by the NRC Office for the Analysis and Evaluation of Operational Data (AEOD) (see Reference 39), found that "...service water system failures and degradations have significant safety implications." The core melt frequency (for all commercial

power reactor types) was found to be in the range of  $1 \times 10^{-3}$  to  $1 \times 10^{-5}$  per reactor-year, based on the estimates derived from the review. As a result of this review, AEOD made a number of recommendations for improving service water system reliability. These recommendations did not encompass major hardware modifications; they were generally in the same vein as those discussed above. Similarly, Generic Issue 51, "Proposed Requirements for Improved Reliability of Open-Cycle Service Water Systems," made recommendations related to proper chlorination levels, operation and maintenance of the water treatment facilities, and inspection and testing of heat exchangers and piping. However, these recommendations were not found to be generically cost-effective. They might be cost-effective for some plants. The probability of non-recovery for an event (due to common mode failure from biofouling) resulting in an unmitigated severe accident has not been considered in current PRAs. This should be considered on a plant-specific basis; therefore, these recommended improvements will not be considered further in this report.

Another possibility for improving containment heat removal reliability is the installation of a dedicated heat removal system, such as the alternate residual heat removal (ARHR) system described in Reference 41. This system would utilize a high pressure injection pump, a low pressure injection pump, a separate ARHR heat exchanger sized to remove decay heat following reactor scram, a dedicated ARHR service water system, and a dedicated power supply. Most, if not all, of these components were assumed to be housed in Category I structures outside the reactor building. Because construction costs alone would be quite high (\$90 to \$500M),<sup>42</sup> addition of such a system would have to reduce risk substantially for it to be cost beneficial. It seems more likely that specific improvements on a smaller, more affordable scale could be found. Furthermore, Unresolved Safety Issue A-45, "Shutdown Decay Heat Removal Requirements," has concluded that an ARHR system would not be cost beneficial; therefore, it will not be considered any further in this report.

Another potential method of preventing containment failure from the TW sequence is to use the reactor water cleanup (RWCU) system in the blow-down mode of operation for decay heat removal. This system has proven to be capable of removing enough decay heat from the reactor to prevent overpressurization of containment in the TW sequence, thereby eliminating the need for containment venting (see References 7 and 37). This improvement is quantitatively analyzed in Section 9.

In summary, although the addition of larger RHR heat exchangers or a dedicated heat removal system does have the potential for reducing the challenge to containment from TW and some ATWS sequences, such modifications do not appear to be

cost-effective. The use of the blowdown mode of the RWCU system for decay heat removal to preserve containment integrity may be cost-effective (probably only costs related to changing procedures and operator training).

## 4. CONTAINMENT CHALLENGED AFTER CORE MELT

The sequences leading to containment challenges after core melt are discussed in this section. The primary sequences with this characteristic are transients with scram, SBO, and LOCAs. For transients, reactor scram is successful, but vessel injection is assumed to be lost. In these sequences, containment integrity is not challenged until the time of reactor vessel failure or later. Similarly, SBO sequences are a special case of transients with scram, where there is a loss of all AC power. The final sequence class is the LOCA, which was found to be a very minor contributor to core melt frequency in past PRAs (see Section 6). Containment challenges and mitigation opportunities for LOCAs are similar to transients with scram. Consequently, LOCAs will not be specifically discussed further. Note that peculiarities of design may make certain plants vulnerable to accident initiators that are not a generic concern to all Mark II BWRs. Examples of these are loss of a DC bus, loss of service water, loss of a reactor vessel level instrument reference leg, and reactor building internal flooding. Because these initiators have to be evaluated on a plant-specific basis, they also are not discussed further. The containment challenges and potential improvements are addressed in the discussion related to transients with scram.

Section 4.1 discusses the plant response during transients that lead to core damage prior to containment overpressurization. A discussion of the containment response to the challenges presented at or near the time of vessel failure is given in Section 4.2.1. Similarly, unique long-term challenges not discussed in Section 4.2.1 are presented in Section 4.2.2. A qualitative discussion of systems or actions that could potentially mitigate the consequences of these sequences is presented in Section 4.3.

### 4.1 Definition of Sequences

**4.1.1 Transients with Scram.** Transient-initiated sequences are characterized by reactor scram with a loss of coolant inventory makeup to the reactor vessel. The sequences can be divided into two groups: those where the reactor vessel remains at high pressure, and those where the vessel is depressurized enough to allow low pressure injection. The core is expected to melt rapidly in these sequences, leading to reactor vessel failure and a potential early challenge to containment integrity. The containment challenges posed by vessel failure are discussed in Section 4.2. Potential improvements to prevent core melt or delay contain-

ment failure for this class of accidents are discussed in Section 4.3.

**4.1.2 Station Blackout.** SBO sequences are a subset of the transients with scram. AC-powered vessel injection systems are presumed not to have failed but are unavailable due to a loss of power. SBO sequences are typically divided into two groups. If vessel injection is lost soon after the loss of all AC power, because of common-mode failure of the emergency batteries or mechanical failure of HPCI/HPCS and RCIC, the sequence is referred to as a short-term SBO. If injection is initially available, but is lost several hours hence because of battery depletion or by some other means, core damage is delayed and the sequence is referred to as a long-term SBO. In terms of preventing core damage, the challenge is to maintain vessel injection from DC-powered sources until AC power can be restored.

### 4.2 Definition of Containment Challenges and Failure Modes

Challenges to containment integrity that arise following melting of a significant portion of the core can be divided into two time periods: challenges at or near the time of vessel failure (early challenges), and challenges that occur several hours after vessel failure, generally after the commencement of core-concrete interactions (late challenges). Because of phenomenological uncertainties, challenges to the containment after core melt are more difficult to analyze than early overpressure challenges occurring before core melt. However, some general remarks can be made, and areas of uncertainty can be identified.

**4.2.1 Challenges At or Near the Time of Vessel Failure.** These challenges can conveniently be divided into two categories: pressure loadings in excess of the containment ultimate pressure capacity, and rapid ex-vessel steam pressurizations (including energetic fuel-coolant interactions, such as steam explosions). Overpressure challenges could result from a number of sources, including hydrogen burns (when the containment is de-inerted), direct containment heating, and failure of the containment vapor suppression function. Ex-vessel steam explosions could be the result of energetic molten fuel-coolant interactions (FCIs) in either the drywell or the wetwell. Each of these categories of containment challenge is discussed in more detail below.



**4.2.1.1 Overpressure Challenges.** In general, the containment pressure loading (not including that from steam explosions) at the time of vessel failure is likely to be lower than in a Mark I containment due to the larger size of the Mark II design. A review of past PRA calculations<sup>4,6,18,26,31,43,44,45,46</sup> shows that this type of loading has not been found to be a dominant contributor to Mark II containment failure. This is due to several factors. First, as past NUREG-1150 studies for Mark I plants have shown,<sup>8,47</sup> the melt progression in a BWR is more likely to be a flow-type melt than the slump-type predicted by the MARCH code (see Appendix A). Second, these same studies found that a high ADS reliability resulted in a corresponding high likelihood that the vessel will have been depressurized by the time of failure. Both of these factors contribute to making the likelihood of direct containment heating (DCH) low. Third, because the Mark II containment is inerted with nitrogen, there is only a small probability of hydrogen deflagration or detonation at or near the time of vessel failure. (This probability is nonzero but small, since Technical Specifications do allow operation for limited periods of time with the containment deinerted.) Finally, the high reliability of the vapor suppression function in the Mark II containment makes the probability of vapor suppression failure very small.

**4.2.1.2 Rapid Steam Pressurizations.** Fuel-coolant contact after vessel failure results in two containment challenges: steam explosions and rapid steam pressurizations. Steam explosions, as the name implies, result from a rapid transfer of energy from the melt to the coolant (time scale on the order of microseconds). Containment failure from a steam explosion would be a result of the dynamic pressure loading or impact of a missile generated by the explosion. Conversely, rapid steam pressurizations occur on a longer time scale (on the order of seconds). Here, the containment challenge is from quasistatic overpressurization. In-vessel steam explosions are believed to be far less likely than originally predicted in WASH-1400, especially for BWRs.<sup>5,48</sup> However, ex-vessel explosions and steam pressurizations due to ex-vessel FCI remain a concern for the Mark II containment. Considerable uncertainty, as well as some controversy, surrounds this issue, particularly in regard to plant-specific Mark II designs that might increase the vulnerability to this challenge. The discussion below presents both sides of this controversy for each of the U.S. Mark II design variations.

An ex-vessel steam explosion at low pressure is postulated to consist of four phases.<sup>49</sup> First, there is coarse mixing of the molten fuel and coolant, with heat

transfer at the fuel-coolant interface via film boiling. Next, a trigger (pressure pulse) is required to bring the fuel and coolant into liquid-liquid contact, resulting in a rapid increase in the rate of heat transfer from the fuel to the coolant. The third phase of the process is explosion propagation, where the heat transfer rate increases still further as the fuel fragments and steam is generated at high pressure. The final phase is expansion of the high pressure steam against its surroundings, converting thermal energy into mechanical energy. The theoretical maximum conversion ratio is approximately 30%. Note that without a sufficient triggering mechanism, the process cannot proceed beyond coarse fuel-coolant mixing. What constitutes a sufficient trigger is one of the major uncertainties surrounding the issue, and this uncertainty is compounded by a lack of applicable experimental data.

As discussed in Section 2, the Mark II design is not identical for all plants. In particular, the design of the area underneath the vessel (referred to as the in-pedestal region) differs among the Mark II plants. For the purposes of this report, the design of the in-pedestal region has been used to segregate the Mark II plants into three classes. First, there are those plants, represented by Limerick and Susquehanna, that have a level concrete floor underneath the vessel with no downcomers connecting the in-pedestal region to the suppression pool. The next group, represented by La Salle and WNP-2, has a rather large dry cavity underneath the vessel. The third group, represented by Shoreham and NMP-2, has downcomers connecting the area underneath the vessel to the suppression pool, along with some means of directing the molten corium into these downcomers. All plants, except Susquehanna, have two or four drain lines leading from the in-pedestal floor to the wetwell. The failure of these drains has been estimated to occur within 20 min after the time of vessel failure for La Salle and within approximately 6 min for Limerick (see Reference 36).<sup>a</sup> These three classes are discussed below.

(1) Flat Floor Cavity with No In-Pedestal Downcomers (Limerick and Susquehanna)

For the first group, calculations performed by the Containment Loads Working Group<sup>50</sup> indicate that a wetwell ex-vessel steam explosion, if one occurred, would not threaten the integrity of the vessel pedestal or the outer containment wall. This is because the rate processes associated with debris-spreading and heat transfer between the debris and the concrete, along with the limited flow area of the ex-pedestal

a. A. A. Payne (SNL) conference call with P. K. Niyogi (NRC) on May 1, 1989

downcomers, limit the amount of debris available to participate in a vigorous fuel-coolant interaction. Rapid quenching of the debris in the drywell cavity is not expected to fail the containment, since the resulting steam could be condensed in the suppression pool. The amount of water available to participate in the drywell cavity steam spike is determined by the accident sequence, that is, by LOCA or operation of containment sprays, operation of the sumps and drains, and the height of the downcomers above the drywell floor (18 in. at both Limerick and Susquehanna). Because LOCAs are expected to occur with low frequency (see Section 6) and spray operation during core damage is unlikely (see Section 4.3.3), and because the cavity floor is at the same level as the ex-pedestal drywell floor, significant quantities of water are not expected to be available for ex-vessel steam explosions in the drywell. The presence of drains in the in-pedestal region contributes to this low likelihood at Limerick.

Ex-vessel steam spikes in the wetwell of sufficient magnitude to fail containment are also not expected. In Brookhaven National Laboratory's review of the Limerick PRA (see Reference 4), quenching of large quantities of corium in the ex-pedestal wetwell region was not found to result in containment failure. Furthermore, time-dependent corium pour rates consistent with a flow-type melt (such as those calculated by Oak Ridge National Laboratory (ORNL) with BWRLTAS/BWRSAR/MELCOR) (see Appendix A) are expected to further reduce the likelihood that large quantities of corium would participate in ex-vessel FCIs.

## (2) Deep Cavity Below the Drywell Floor (WNP-2 and La Salle)

For the second group of plants, which have a large, dry cavity underneath the vessel, steam explosions could be a concern if a significant amount of water were to be present in the cavity at the time of vessel failure. As in the previous discussion, the amount of water participating in the drywell cavity steam spike is determined by the accident sequence, that is, by LOCA or operation of containment sprays, operation of the sumps and drains, and the volume of the cavity (e.g., ~3072 ft<sup>3</sup> below the level of the ex-pedestal drywell floor at La Salle). As above, since LOCAs are expected to occur with low frequency (see Section 6) and since spray operation during core damage is unlikely (see Section 4.3.3), significant quantities of water are not expected to be available for ex-vessel steam explosions in the drywell. At La Salle, two 4-in. lines drain the in-pedestal cavity. These two lines pass through the suppression pool air space and have been assumed for most sequences to fail within 20 min after reactor

vessel breach by the expert panel associated with the NUREG-1150 effort.<sup>a</sup> If the in-pedestal drain lines became plugged and the cavity were flooded, steam explosions could be a concern. The coolant from the ex-pedestal drywell floor communicates with the in-pedestal cavity via 8-in. lines, which extend 12 in. above the drywell floor. If the ex-pedestal drain lines became plugged, essentially no containment spray water would reach the corium and the probability of cooling the corium would be very low, that is, the CCI would continue unabated until the in-pedestal floor (or walls) failed. Structural failure of the pedestal walls and gross vessel movement capable of shearing containment penetrations are two possible failure modes. On the other hand, there is a possibility that any of the molten fuel that fell into the water-filled cavity would be quenched, without significant FCI. This is an area of uncertainty, where experimental data are needed before conclusions can be drawn.

As in the previous cavity design, the pressurization due to an in-pedestal drywell steam spike could be absorbed by the suppression pool. Steam explosions and/or steam spikes in the suppression pool at or near the time of vessel failure are considered to be unlikely for this cavity design.

## (3) Cavities With In-Pedestal Downcomers (Shoreham and NMP-2)

For the two Mark II plants with in-pedestal downcomers, there is considerable uncertainty surrounding the outcome of fuel-coolant interactions. Shoreham has installed a concrete "corium ring" to direct corium into the suppression pool via the four in-pedestal downcomers. The Shoreham PRA indicated that 33 to 47% of the corium would enter the downcomers without the corium ring, and up to 90% with the corium ring (see Reference 5). Although NMP-2 does not have a corium ring, its recessed cavity and eight in-pedestal downcomers should also direct most of the corium to the suppression pool. FCIs were considered in both the in-pedestal drywell cavity and the suppression pool at Shoreham. To eliminate concerns about in-pedestal drywell steam explosions, the amount of water that could accumulate in the in-pedestal region was reduced by lowering the height of the four in-pedestal downcomers to 1/2 in. above the drywell floor. Consequently, a maximum of 600 lbm of water at a 1/2 in. depth could participate in a steam explosion. The in-pedestal downcomer height at NMP-2 is not known. The FSAR for NMP-2 states that all

a. A. A. Payne (SNL) conference call with P. K. Niyogi (NRC) on May 1, 1989

downcomers range in height from 3 to 6 in. above the drywell floor.

Because there are no known analytical tools that can accurately predict steam explosions, there is a possibility that the Shoreham analysis could be nonconservative. Wetwell steam explosions and rapid pressurizations leading to containment failure were assessed in the Shoreham PRA to have a conditional probability of  $4.8 \times 10^{-4}$  to  $3.5 \times 10^{-4}$ , depending upon the sequence (see Reference 5). (For comparison, the Limerick PRA and the Reactor Safety Study used values ranging from  $1 \times 10^{-2}$  to  $1 \times 10^{-3}$ . These probabilities are conditional upon the occurrence of a severe accident accompanied by flow of corium into the suppression pool. Thus, the differences in the probabilities are not considered to be significant, given the total uncertainty in predicting steam explosions.) Four containment failure modes were identified in the Shoreham PRA: (a) gross movement of the vessel due to a drywell cavity steam explosion, (b) direct containment failure due to generation of a small missile, (c) failure of the outer wetwell wall during a steam explosion in the suppression pool, and (d) failure of the containment by quasistatic overpressurization. The original Shoreham PRA containment response calculations were performed with the MARCH code and incoherent flow-type pour boundary conditions (not characteristic of MARCH but thought to be likely for BWRs) were assumed to occur with a probability of 0.5. Failure of the containment was assessed to be most likely due to quasistatic overpressurization. The qualitative reasons for this conclusion are summarized below:

- There is insufficient fuel-coolant premixing.
- There is an insufficient trigger for initiating an explosion.
- There is no strong coupling mechanism, such as slug impact, that could transfer enough kinetic energy to generate a missile capable of penetrating the containment wall.

The thermal-to-mechanical energy conversion efficiency for the steam explosion calculations was taken to be 1% based on experimental data.<sup>5</sup> This value is low relative to the maximum theoretical conversion efficiency (30%) (see Reference 49). However, more research (analyses or experimental data) is necessary to make a definitive conclusion.

Although the steam explosion analyses performed for the Containment Loads Working Group were based

on the Limerick plant and had many uncertainties, the authors point out that a steam explosion in an in-pedestal downcomer (which Limerick does not have) has a much higher likelihood of failing the pedestal than does an ex-pedestal explosion (see Reference 50). This is because an in-pedestal explosion would stress the pedestal ring in tension versus a compressive stress during an ex-pedestal explosion. The authors also cautioned about the conservative and preliminary nature of the calculations.

Other calculations for Limerick show that the resulting containment pressurization rate due to rapid debris-quenching is dependent upon the amount of pool water participating in the quench (see Reference 4). Containment failure could result from a steam spike with large quantities of debris and poor circulation between the in-pedestal and ex-pedestal regions of the suppression pool. Although the calculations are bounding in nature (large corium flow rates), they do point out the potential for a steam spike challenge for sites with in-pedestal downcomers. The Shoreham PRA analyses considered the entire pool as participating in the quench (see Reference 5).

There is a possibility that wetwell steam explosions could fail one or more of the in-pedestal downcomers. Because openings exist between the in-pedestal and ex-pedestal regions of the wetwell airspace, downcomer failure would create a flow path from the drywell directly to the wetwell airspace, bypassing the water in the suppression pool. Therefore, any subsequent releases, including those resulting from wetwell venting, would be at least partially unmitigated by water scrubbing in the pool. On the other hand, if a significant portion of the debris were successfully quenched, the accident might be terminated successfully, thereby greatly reducing this effect of suppression pool bypass.

**4.2.2 Challenges after Vessel Failure (Late Challenges).** Should the containment survive these early challenges to its integrity, mitigation of challenges from CCI and high internal temperature might be necessary. Although the Mark II containment is considerably larger than the older Mark I design, late overpressure or thermal failure could still occur within a few hours to many hours after vessel failure.

**4.2.2.1 Late Overpressure Failure.** Numerous studies of Mark I and Mark II containments (see References 8, 29, 31, 43, 45, 47, 50 and Appendix A) have indicated that the generation of noncondensable gases from the interaction of molten core debris with concrete could cause the internal containment pressure to exceed the ultimate containment pressure capacity.

The likelihood of CCI cannot be predicted on a generic basis, just as in the case of ex-vessel steam explosions, because of the design variations of the in-pedestal region. However, analyses and experiments have shown that the rate of the CCI and the gas species produced do depend upon the chemical makeup of the concrete. Analysis performed by ORNL for a short-term SBO indicates that, in the absence of FCI, the concrete floor would be eaten through by CCI before the containment would be challenged by overpressurization 15 h into the sequence.

#### (1) Cavities With In-Pedestal Downcomers (Shoreham and NMP-2)

The two plants with in-pedestal downcomers would appear to be least vulnerable to CCI, because most of the core debris would be directed into the suppression pool. This direction of the corium into the suppression pool is by means of the in-pedestal floor being sloped toward the center and at a slightly lower elevation than the ex-pedestal floor (NMP-2), or by means of a curb to retain the corium until it flows down the in-pedestal downcomers (Shoreham).

A high pressure failure of the reactor vessel could result in a more severe early containment challenge. However, because the debris would be widely dispersed during a high pressure melt ejection, there would be a greater likelihood that the debris could be cooled. The Shoreham PRA only considered sustained CCIs to be a threat for the case of high pressure vessel failure (see Reference 6). Recovery of containment sprays prior to the occurrence of either containment failure or gross leakage was assumed to quench the debris. Failure of the in-pedestal downcomers due to contact with debris (or failure of the Shoreham drywell floor seal) would bypass the suppression pool and could increase the vulnerability of the containment to overpressurization (loss of suppression pool heat sink only for the high pressure vessel failure sequence). Unmitigated accidents were calculated by Lilco to lead to overtemperature or overpressure failure prior to complete erosion of the concrete.

Because low pressure vessel failures were assessed to be more likely than high pressure failures (see Section 6) in the Shoreham PRA, the most common end states involved early quenching of the core debris in the suppression pool. Late venting or recovery of injection to cool ex-vessel debris was effective in mitigating overpressure challenges following a high pressure vessel failure (see Reference 6). Thus, sustained CCI leading to containment failure was not

likely. From this perspective, the in-pedestal downcomers are a desirable feature.

#### (2) Deep Cavity Below Drywell Floor (WNP-2 and La Salle)

On the other end of the spectrum, the pedestal design with a large, dry cavity underneath the vessel would appear to be the most vulnerable to CCI. For example, the La Salle cavity is large enough to hold approximately two entire core volumes below the drywell floor grade and effectively out of reach of containment sprays. The 8-in. drain lines provide a path for spray water to flow from the ex-pedestal drywell floor to the in-pedestal cavity. The confined in-pedestal geometry would decrease the likelihood of successfully cooling the debris. Sustained in-pedestal CCI would lead to pressure loading from noncondensable gas generation and erosion of the cavity floor. At La Salle, failure of the drywell floor (3.75 ft thick) by erosion would lead to relocation of debris to a dry in-pedestal chamber in the wetwell. A large reinforced concrete plug located beneath the cavity would significantly delay challenges to the containment basemat. However, CCI could continue unabated in this region for an extended period of time. Conversely, at WNP-2, a pool of water lies below the drywell cavity. Consequently, failure of the drywell floor at WNP-2 could lead to successful quenching of the debris, but with the potential for energetic fuel-coolant interactions. An alternative drywell floor failure mode might involve the opening of a large hole in the cavity floor by molten debris flowing through the cavity floor drain lines and ablating the surrounding concrete (see Reference 31). These drain lines at La Salle were estimated by the expert elicitation panel for draft NUREG-1150 to fail shortly after vessel breach in most sequences.<sup>a</sup> It is reasonable to expect that as long as the corium is fluid, it will tend to drain through the failed drain lines and leave only a small quantity on the cavity floor. This small quantity may be insufficient to sustain the CCI in the WNP-2 design.

Wetwell venting to prevent containment overpressurization after suppression pool bypass might actually increase the offsite consequences (an earlier unscrubbed release). Sustained CCI at La Salle could lead to containment overpressure failure (see Reference 31). At WNP-2, the magnitude and rate of the FCI would determine the challenge to the containment. Based on observations by the Containment Loads Working Group (see Reference 50), factors affecting CCI include:

a. A. Payne (SNL) conference call with P. K. Niyogi (NRC) on May 1, 1989.

- Type of concrete—Higher drywell temperatures and pressures are encountered with limestone concrete, while the deepest vertical penetration occurs with basaltic concrete. The concrete composition affects the ablation temperature and the physics during CCI. Because CCI is an endothermic process, a lower ablation temperature (typical of basaltic concrete) “absorbs” more energy from the melt, but leads to higher erosion rates and greater dilution of the corium. Conversely, less energy absorbed by the concrete leads to higher radiative and convective heat transfer rates from the debris surface to the atmosphere.
- Water in the concrete—A higher percentage of water in the concrete leads to higher drywell temperatures and pressures, and greater vertical penetration. Water released during CCI promotes oxidation of metals in the melt (an exothermic reaction).
- Corium temperature—Higher initial corium temperature increases both the containment temperature and the pressure loading, as well as the concrete erosion rate.
- Steel in corium—Reducing the steel content of the corium reduces the pressure and temperature loading on the containment, but increases the concrete penetration rate, thereby decreasing the time to structural failure of the drywell floor.

In recent MARCH calculations performed for La Salle, drywell floor failure is assumed to occur when the ablation zone has progressed 1 ft into the concrete floor, that is, prior to complete erosion of the concrete floor (see Reference 31). This corresponds to a vertical distance equal to one-third of the floor's thickness. Floor failure and containment overpressurization during a high pressure short-term station blackout (TBUX) were calculated to occur at 80 and 420 min after vessel failure, respectively. As stated previously, these slump-type MARCH core melt boundary conditions may have limitations associated with melt composition and pour rates. Furthermore, failure of the 4-in. cavity drain lines was not considered in the analysis.

In summary, sustained CCI is most likely for the deep cavity design. The confined geometry of this cavity affects the coolability by limiting the heat transfer surface area. Sustained CCI could lead to drywell

floor failure and eventual containment failure. The presence of a pool beneath the WNP-2 cavity versus no pool beneath the La Salle cavity affects the challenges following drywell floor failure. Uncertainties affecting the overpressurization calculation include (a) phenomenological uncertainties related to the melt boundary conditions (flow-type versus slump-type), (b) structural integrity of the drywell floor during CCI, (c) FCI after drywell floor failure (WNP-2), and (d) debris coolability in the cavity given the late recovery of drywell sprays. Failure of the cavity drain lines is expected to result in early suppression pool bypass for both plants, although there is no analysis to support or refute this conclusion. At La Salle, the CCI could continue unabated on the dry concrete plug below the in-pedestal cavity, while the corium would be cooled by the pool below the cavity at WNP-2.

### (3) Flat Floor Cavity With No In-Pedestal Downcomers (Limerick and Susquehanna)

The plants with a level in-pedestal floor at the same elevation as the ex-pedestal drywell floor appear to lie somewhere between the other two designs as far as vulnerability to core-concrete interactions is concerned. More of the corium would be expected to spread into the ex-pedestal region of the drywell, with less of the corium quenched in the suppression pool than in the design utilizing in-pedestal downcomers. In addition to the factors affecting sustained core-concrete interactions presented in the deep cavity discussion, the following observations pertain specifically to the flat floor cavity design (see Reference 50):

- Corium temperature and spread—A higher corium temperature, which causes the corium to spread further, leads to higher drywell temperatures and pressures but less concrete penetration.
- Failure of downcomers—Failure of the downcomers, with the failure located in the wetwell airspace, would lead to suppression pool bypass and earlier failure of the containment (loss of suppression pool heat sink). Downcomer failure was not discussed in Reference 50. However, further analysis or experiments appear to be warranted to reduce the uncertainty associated with downcomer integrity. The integrity of the downcomers would have an impact on containment pressurization and on the effectiveness of any venting mitigation strategy.

- Corium drained into the suppression pool—A higher percentage of corium falling into the suppression pool via the ex-pedestal downcomers during the melt relocation reduces the amount of melt available for CCI.

**4.2.2.2 Late Thermal Failure.** If molten corium is present in the drywell, heat transfer to the drywell atmosphere and internal surfaces could cause drywell temperature to increase beyond the containment design temperature. The Containment Performance Working Group examined both thermal and pressure loadings on containments during severe accidents. Estimated leakage due to pressure loads is presented in Table 5. However, leakage due to drywell head seal degradation was not considered for the Mark II plant (Limerick) (see Reference 28). In the Mark I evaluation, leakage through the containment purge and vent valves was determined to be significant. However, for Limerick, the Containment Loads Working Group accepted the manufacturer's evaluation of these valves. All the isolation valves in Limerick had metal-to-metal contact and had been used successfully in conditions ranging from temperatures in the cryogenic range up to 900°F. Conversely, four 18-in. butterfly purge valves in the Mark I reference plant did not have a metal-to-metal seal. Based upon seal life curves, a temperature-dependent leakage model was developed. Temperature-induced leakage (of ethylene propylene seals) amounted to a 14-in.<sup>2</sup> equivalent area at temperatures above 500°F.

More recent testing performed by the NRC has examined seal behavior under a variety of conditions.<sup>52</sup> General conclusions from the study were:

1. The thermal (300°F) and radiation aging (200 Mrad at 1 Mrad/h) specified in these tests had a negligible effect on the temperature at which leakage began.
2. Metal-to-metal contact at the sealing surfaces virtually prevented the occurrence of significant leakage.
3. The temperature at which leakage began did not appear to be affected significantly by increasing the seal compression from 9 to 17%.
4. Leakage onset temperatures ranged from 626 to 669°F for the five tests of ethylene propylene rubber O-rings with a gap between the surfaces.
5. Leakage onset temperatures ranged from 486 to 592°F for the five tests of silicon rubber O-rings with a gap between the surfaces.
6. Posttest visual inspection indicated that all gaskets experienced severe degradation, including those that were tested without a gap between the sealing surfaces.

Reference 28 indicates that the Limerick drywell head originally was designed with a double tongue-and-groove seal. However, there were problems with the groove orientation and the design was changed to double gundrop with silicon rubber seals. Reference 52 only tested silicon rubber seals in a double O-ring configuration. More recent tests included silicon rubber seals with double tongue-and-groove geometry.<sup>53</sup> Six tests were conducted with gaps of 0.01 in. or with metal-to-metal contact. No leakage was observed in these tests for temperatures up to 700°F. The applicability of the results from the tongue-and-groove test with silicon rubber to the double gundrop drywell head seal design at Limerick is not known.

For the Shoreham PRA, a temperature-dependent leakage model was used (see Table 7).<sup>5,54</sup> The drywell head is sealed by a double O-ring. At temperatures between 500 and 800°F, radial shear at the drywell head anchorage caused slippage but no loss of structural integrity or increase in leakage. Seal degradation began at temperatures above 500°F; however, metal-to-metal contact between the drywell head and the flange was maintained. Above 800°F, increased slippage would lead to leakage. An upper bound analysis of the drywell head concluded that a tension failure of the drywell head would occur at approximately 1200°F, at an internal pressure of 60 psig. Temperature-dependent leakage from other isolation valves was not considered in the Shoreham PRA.

Thermal leakage can be an important challenge to the integrity of Mark II containments. Several observations can be made from existing research. First, seals with metal-to-metal contact seem to be less susceptible to leakage. Second, increasing the pressure loading may unseat seals and increase the likelihood of thermal degradation. Finally, seal leakage may occur at a variety of locations, such as at the purge and vent line penetrations and the drywell head. However, drywell head seal leakage (without water above the drywell head) would occur directly to the refueling floor and has the potential to increase the severity of offsite consequences. With the area above the drywell head flooded, the release would be scrubbed. The effect would be similar to that obtained by having the release

**Table 7.** Temperature-dependent leakage estimates for Shoreham<sup>a</sup>

Drywell Temperature (°F)	Drywell Leakage Area (in <sup>2</sup> ) <sup>b</sup>
< 500	0.002
> 500	0.025
> 600	0.050
> 700	0.075
> 800	7.2
> 1100 <sup>c</sup>	144

a. References:

1. *MAAP Analysis to Support the Shoreham 100% Power PRA*, FAI 87-80, Vol. 1, 1987.
2. *Study of the Structural Integrity of the Shoreham Primary Containment Under Accident Conditions*, 25746-1520145-B4, Stone & Webster Engineering Corporation, 1988.

b. All leakage is to the reactor building refueling floor level.

c. The drywell head would fail under tension at an internal pressure of 60 psig.

pass through the suppression pool. The elevated temperatures might also revaporize volatile fission products that have plated out on surfaces inside the containment.

**4.2.3 Discussion of Containment Failure Modes.** Containment failures resulting from sequences with challenges occurring after core melt can be the result of damage caused by pressure loads, shock waves, missile impact, or thermal loads. As discussed in Sections 4.2.1 and 4.2.2, the likelihood and magnitude of the containment challenges affect both the size and location of the failure. Each of the postulated containment failure modes is discussed below and is related to plant-specific effects when applicable.

Failures due to pressure loads fall into two classes: rapid pressurization because of steam spikes or a rapid pressure loading at vessel failure, and slow pressurization due to sustained CCI. As discussed in Section 4.2.1, the pressure loads at the time of vessel failure are not likely to cause gross containment failure, although a rapid steam spike might increase containment leakage area. As discussed in Section 4.2.1.2, plants with in-pedestal downcomers are the most susceptible to rapid steam spikes after vessel failure. In other plant designs, rapid steam spikes might occur following drywell floor failure. Depending on the magnitude of the pressure rise, steam spikes could lead to either increased leakage or containment failure. Based on the discussion in Section 3.2, increased leakage could occur through the drywell head seal and the wetwell personnel hatch, while a gross failure most likely would occur in the wetwell airspace or at the wetwell wall-to-basemat juncture.

Very rapid steam spikes or steam explosions could fail the containment by a variety of means including dynamic failure of the wetwell or pedestal walls due to shock wave impact, creation of a "missile" that penetrates the containment wall, and rapid pressurization of the in-pedestal cavity that causes gross movement of the vessel, severing lines penetrating the containment boundary (see References 5 and 50). In Reference 5, failures as a result of missile generation or gross vessel movement were assessed as unlikely. Similarly, the Containment Loads Working Group concluded that the dynamic loading from an ex-pedestal steam explosion at Limerick would not likely fail the wetwell wall (see Reference 50). Dynamic failure of the pedestal wall was not considered likely in Reference 5 due to the lack of a mixing trigger. However, the Containment Loads Working Group suggested that an in-pedestal steam explosion could challenge the structural integrity of the pedestal walls. Failure of the pedestal walls would not directly imply containment failure, but it could lead to gross movement of the vessel, which could sever lines penetrating the containment walls, or fail the pipe penetration seals. The failure location depends on the location of the steam explosion, whether there is gross vessel movement, and whether a small missile is created. Gross vessel movement most likely would lead to failure in the drywell. Direct failure of the containment structure by shock wave impact most likely would occur in the wetwell below the water line (suppression pool shock wave energy is more effectively transported through water than through air).

The final failure mode is due to excessive thermal loading. Section 4.2.2 provides a detailed discussion of this failure mode and the likely location of the failure. Thermal failures are only postulated to occur in

the drywell, with the primary locations being the drywell head seal and the various containment penetrations, including the containment isolation valves and electrical penetration assemblies. Thermal failures have potentially severe consequences, since the suppression pool would be bypassed and the release could be at a high elevation in the reactor building. However, there could be some fission product retention in the reactor building (see Section 4.3.6).

## 4.3 Potential Improvements

With the late challenges to Mark II containment integrity identified, a discussion of several improvements that have the potential for mitigating these challenges is in order.

**4.3.1 Mitigating Transients with Scram.** Mitigation focuses primarily on termination of core degradation, preventing or delaying containment failure, and reducing the offsite consequences. The sequences can be divided into two subsets: those where the vessel remains at high pressure, and those where it is depressurized to a pressure low enough to allow injection from low pressure systems. High pressure sequences will be examined first.

With the reactor at high pressure, that is, near normal operating pressure, four systems (excluding the SLCS) are capable of developing enough discharge head to inject water into the vessel: feedwater, RCIC, HPCI/HPCS, and CRD. For plants that have only turbine-driven feed pumps, feedwater injection requires that one or more main steam isolation valves (MSIVs) be open and that the main condenser be available. For plants that have a motor-driven feed pump, feedwater would be available even with the MSIVs closed, assuming that flow was throttled to the available makeup rate to the main condenser from the CST. For some transients, feedwater would initially be available and would be the preferred source of makeup to the vessel. If the transient resulted in isolation of the vessel from the main condenser, the main steam lines could be reopened under some circumstances. Otherwise, RCIC would become the preferred makeup source. Actuation of RCIC is automatic at Level 2 (RCIC actuates slightly above Level 2 at Susquehanna), which is ~10 ft above the top of active fuel (TAF). Should RCIC be unavailable, HPCI/HPCS must be relied upon for initial high pressure makeup. The actuation of HPCI/HPCS is also automatic at Level 2. Operation of RCIC and HPCI/HPCS is dependent upon the availability of emergency 125 V DC power; HPCS (BWR/5 only) also requires AC power, either from offsite sources or from its dedicated emergency

diesel generator (EDG). Service water is also required for area cooling and cooling of the EDG that is supplying the HPCS pump. Both RCIC and HPCI/HPCS initially inject water from the CST. The suction of HPCI/HPCS, and also RCIC in some plants, automatically transfers to the suppression pool when suppression pool level increases above a set level (or CST level decreases below a set level). This suction transfer becomes a concern in the case of SBO or ATWS because the high suppression pool temperature would interfere with lube oil cooling.

Each CRD pump injects at a flow rate of 40 to 70 gpm during normal operation, taking suction from the CST. Following a scram, this flow rate increases to approximately 100 gpm. Thus, the CRD pumps are a viable source of high pressure makeup. For cases where the CRD flow rate is too low to maintain vessel level, the CRD pumps are still of benefit in delaying the onset of core degradation. Operation of the CRD pumps is dependent upon cooling from one of the component cooling water systems. At some plants, the component cooling water system may isolate non-safety-related loads, such as the CRD pumps, upon receipt of an accident signal (low vessel level or high drywell pressure). Without cooling, the CRD pumps can be expected to fail within approximately 1 h (see Reference 33). The interlock that isolates component cooling water can be bypassed with electrical jumpers; however, guidance for doing so is not typically found in the current EOPs. For plants like La Salle, where the reactor building component cooling water (RBCCW) system is not designed as an Engineered Safety Feature (ESF), this is not a problem, since RBCCW should be available to cool the CRD pumps whenever the CRD pumps are available.

If no high pressure injection is available for coolant makeup, the vessel must be depressurized to allow injection from low pressure systems. Doing this is the province of the ADS, with manual depressurization by the operator as a backup should the ADS fail. Since the issuance of the TMI Action Plan in NUREG-0737,<sup>55</sup> the initiation logic for the ADS has been modified at some plants to increase the likelihood that the reactor will be depressurized when depressurization is needed. Essentially, this modification involved either the removal of the coincident high drywell pressure signal from the ADS initiation logic, or the addition of a time-delayed bypass of the high drywell pressure signal if the low vessel level signals are present. Under this revised ADS logic scheme, the reactor should automatically be depressurized upon receipt of a signal indicating that the reactor water level has fallen to Level 1 (~2 to 3 ft above the TAF), along with a confirmatory low level signal set at Level 3 (~14 ft above the



TAF), a signal that low pressure ECCS pumps are running, and time-out of the ADS timer relay (typically set at 105 seconds). (The normal operating water level is ~16 ft above the TAF.) The operator can inhibit the ADS (e.g., during an ATWS event), through the use of an inhibit switch that was also added to the system in response to NUREG-0737 (see Reference 55). The addition of these modifications is expected to significantly lower the ADS failure probability. This would, in turn, decrease the contribution to core melt frequency of the TQUX sequences, where core cooling is lost because of failure to depressurize the reactor.

Other enhancements to increase the operability of the SRVs during severe accidents have also been proposed. These include a dedicated source of DC power to the SRV solenoids, assurance that the SRVs would be capable of being opened by the operator under environmental conditions associated with severe accidents, and improved operator training and EOPs. Because of the possibility of concurrent failure of both the AC and DC power systems and the limited life of the batteries during SBO, the addition of a dedicated DC power supply for the SRV solenoids could have some potential for reducing core damage frequency. For those plants that have incorporated Revision 4 of the EPGs, the containment vent pressure is set at the primary containment pressure limit defined in the EPGs (see Reference 19). This does not approach the containment pressure at which the SRVs might be prevented from opening by a low differential pressure between the containment and the instrument air (nitrogen) used to open the valves. Therefore, this venting set point should not be a concern for the plants that have been evaluated. However, it could become a concern for plants with a higher venting set point, that is, a higher PCPL.

Revision 4 to the EPGs discusses various alternative means of depressurizing the vessel (see Reference 19). For example, interlocks could be bypassed to allow the MSIVs to be opened. This would allow use of the turbine bypass valves to reject steam to the main condenser, assuming that the main condenser was available. The use of these alternative methods is indicated if less than the minimum number of SRVs required for emergency depressurization is open, and the differential pressure between the vessel and the suppression chamber is above the minimum pressure required to open an SRV (50 psig is a typical value).

Once the vessel has been depressurized, a number of other sources can be used for low pressure makeup. These are: condensate pumps, RHR pumps in the LPCI mode, LPCS, condensate transfer pumps, fire pumps,

and service water pumps. Each of these sources is discussed below, along with possible difficulties that might have to be overcome before the source could be utilized.

1. *Condensate pumps:* Use of the condensate pumps may be limited by two basic interrelated considerations. First, condenser vacuum is required if makeup to the condenser is via a "vacuum drag" line from the CST. The available flow rate from the condensate pumps then is limited to this makeup rate because the condenser hotwell inventory is only sufficient for a few minutes of operation at full flow. Maintaining condenser vacuum could be difficult if auxiliary steam were not available as a motive force for the steam jet air ejectors. Steam from the auxiliary boiler could be used, but this would of course be dependent upon the availability of the auxiliary boiler. The mechanical air removal pumps could also be used, but these pumps discharge directly to the turbine building exhaust plenum, bypassing the offgas treatment system. Plant-specific design differences in the balance-of-plant may affect the condensate pump availability. For example, La Salle and NMP-2 utilize pumped makeup to the hotwell under normal operating conditions. La Salle also has emergency makeup pumps, while the emergency makeup at NMP-2 is via "vacuum drag" from the CST (see References 13 and 14).
2. *RHR pumps in LPCI mode:* The RHR pumps get a signal to start upon receipt of either a low vessel level signal (Level 1) or a high drywell pressure signal (approximately 2 psig). These signals also cause the RHR system to realign to the LPCI mode; the LPCI injection valves do not open, however, until vessel pressure decreases below a set value. At Susquehanna, failure of this valve interlock was found to be the dominant contributor to failure of low pressure ECCS systems (see Reference 7). Typical LPCI flow rates are on the order of 10,000 gpm per loop. The operator cannot throttle the LPCI injection flow or realign the RHR system to any other operating mode during the first few minutes of LPCI operation. However, LPCI flow can be terminated by stopping the RHR pumps. This might be an action taken during an ATWS to prevent injection of large amounts of cold water into a critical reactor.
3. *Low pressure core spray pumps:* The LPCS pumps generally receive a signal to start at approximately the same time as the RHR pumps. Either LPCS or LPCI is capable of independently coping with a design basis LOCA. The LPCS pumps are capable

of taking suction from the CST at some plants (see Reference 16); however, this is not true for all Mark II plants. This possibility has not been given credit in PRAs that have been reviewed.

4. *Condensate transfer pumps:* The above systems constitute what might be called the “normal” means of low pressure injection. The next systems to be discussed are sometimes referred to as “alternative” means of injection. The first of these is the condensate transfer pumps. The interconnection between the condensate transfer system and the RHR and LPCS systems could allow the condensate transfer pumps to be used to inject water into the vessel via the RHR or LPCS piping. Two restrictions apply, however. First, the connections are via manual valves in the reactor building; an operator would have to be dispatched to the reactor building to open these valves. Under some circumstances, the environment in the reactor building could prohibit doing this. Second, the lines are rather small (approximately 4 in. dia), thus limiting the injection flow rate. However, this is a source that should be considered when evaluating the overall failure probability of low pressure injection.
5. *Fire pumps:* Plants typically have both motor-driven and diesel-driven fire pumps, which are used to supply water to the fire mains for fire protection. However, via a hose or spoolpiece connection from the fire main to the service water system, they could also be used to inject water into the reactor vessel or the containment. The above restrictions on the use of the condensate transfer pumps also apply to the fire pumps. An operator must manually connect the fire main to the service water system, and the flow rate is limited by the size of the hose or spoolpiece. Note that AC power is required, even if the diesel fire pumps are used, unless the motor-operated valves (MOVs) connecting the service water system to the RHR system can be opened manually. Manual operation of these valves would require operator entry into the reactor building.
6. *Service water:* As a last-ditch effort, plant EOPs direct the operator to line up service water to inject into the vessel from the ultimate heat sink connection to the RHR system. These two systems are isolated from one another by two MOVs, which are operated from keylock switches in the main control room. The valves could also be opened locally, using a manual handwheel attached to the valve operator.

Typical PRAs give credit only to the first three of these systems when evaluating the availability of low pressure injection. The reason the other systems are not included is given as lack of operator familiarity with using the systems for this purpose. This is not felt to be a valid reason for excluding them from consideration, because operators receive extensive training on potential sources of water to be used in an emergency. This generally includes both classroom instruction and simulator training. The use of these systems is spelled out in Revision 4 to the EPGs, further reducing the likelihood that operators would overlook them in an emergency. Inclusion of these sources would result in a reduction in the contribution of the low-pressure sequences and TW sequences to core damage frequency.

**4.3.2 Hydrogen Control.** Because the Mark II containment is inerted under most operating conditions, hydrogen combustion is considered to be a low probability event. The only significant danger is that the containment could somehow become deinerted, for example, through venting. The plant Technical Specifications provide adequate safeguards to prevent this from happening. Therefore, no enhancements to the hydrogen control mechanisms currently in place are felt to be justified. However, hydrogen burns in the reactor building, should the primary containment fail, or in the vent path, are possible.

**4.3.3 Containment Sprays and Backup Water Supply.** There are three mitigative aspects associated with the use of containment sprays. First, by evaporative and convective cooling, sprays can reduce containment pressure. Second, they can cool debris outside the vessel, limiting CCI and drywell heatup. And third, they provide some scrubbing of aerosol fission products in the containment atmosphere, reducing the consequences of a release. The sources of water that could be used for spraying the containment have already been discussed (see Section 3.3).

There are also limitations on the use and effectiveness of containment sprays that have to be considered. First of all, since all pumps that currently can be used to spray the containment can also be used for vessel injection, there is a high probability of containment spray failure given failure of vessel injection (the presence of core debris outside the vessel implies that vessel injection has failed). Therefore, a realistic discussion of containment sprays is likely to be predicated upon the assumption that the pumps are recovered late in the sequence, or that an alternative means of spraying the containment is available, which is independent of vessel injection.

If the vessel were at high pressure without injection, there would be a possibility that containment sprays

could be available during core melt. The RHR system would require remote manual realignment from the LPCI mode to the containment spray mode. There are several implications to be considered when making this realignment. First, containment sprays might increase the likelihood of an ex-vessel steam explosion at the time of vessel failure. Conversely, because the vessel was assumed to fail at high pressure, the sprays might promote quenching of the debris during the high pressure melt ejection that accompanies this mode of vessel failure and could also reduce the fission product inventory available for release to the environment. Second, if the RHR system were still aligned in the LPCI mode at the time of vessel failure, water would be injected upon vessel depressurization and could quench debris left in the vessel and provide a source of water to the ex-vessel debris through the opening in the vessel. Steam explosions are thought to be unlikely when water is added after debris relocation. Consequently, LPCI flooding after the initial relocation of the core in-vessel could quench in-vessel debris and reduce the probability of ex-vessel steam explosions.

The EPG currently prohibits use of drywell sprays under certain combinations of drywell pressure and temperature in order to prevent containment failure or deinerting (see Reference 19). Therefore, if drywell sprays were to be used in accordance with the guidance in the EPG, they would have to be initiated relatively early in the sequence. This might be difficult if repairs had to be made to the RHR system to make the sprays available. As discussed in Section 4.3.1, other sources besides RHR can be used to spray the containment. These sources include the service water system, the fire pumps, and the condensate transfer pumps, injecting via the existing RHR piping to the containment spray headers.

To summarize, containment sprays could potentially mitigate both late overpressure and thermal failure of the containment, and could arrest or slow down corium activity and scrub fission products, thereby reducing the offsite consequences. However, some plant modifications might be needed, depending on the existing plant-specific design features and the alternative water source to be used, in order to ensure the availability of the alternative water supply. Analysis of the Mark I containment indicates that a high volume "spray" is not necessary to provide significant containment cooling and pressure reduction (see Appendix A). However, the actual benefits of anything less than a full spray pattern in the Mark II containment are uncertain. Note also that plugging of existing spray nozzles to achieve an effective spray pattern with low capacity systems was not considered viable for the Mark I plants; there-

fore, it will not be considered as an improvement for the Mark II plants.

**4.3.4 Containment Venting.** Section 3.2.1 discussed some potential benefits and downsides of venting to mitigate containment overpressurization prior to vessel failure. Containment venting might also be of limited usefulness in preventing or delaying containment challenges that occur after vessel failure. In order to keep containment pressure below the PCPL, the EPG instructs the operator to vent "...irrespective of the offsite radioactivity release" (see Reference 19). With core debris outside the vessel, following the EPG in this regard could lead to an early and possibly unscrubbed (if the suppression pool were bypassed) release of fission products from the containment. If plants have the intention of using their containment vents following vessel failure, procedures will have to be developed to supplement the guidance given in the EPG, particularly in regard to when the vents should be reclosed to limit the offsite release. A hard pipe vent system with an effluent radiation monitor interlocked to close the vent isolation valves with radiation in the vent line above a predetermined level would minimize the downsides of venting during severe accidents and any pressure relieved would reduce the peak containment pressure, potentially below the ultimate failure pressure. However, the entire vent system (actuator, seals, and control system) would have to be operable during SBO and designed and tested to ensure the availability of the sealing function under the harsh containment environment associated with a severe accident.

Venting to mitigate late thermal failure or to reduce the containment base pressure prior to an anticipated containment challenge is not addressed in the EPGs. A strategy of venting preemptively, *prior to* suppression pool bypass, could lead to a slightly higher risk because a release of noble gases could occur during the evacuation. Failure of the downcomers in the wetwell airspace would cause suppression pool bypass and loss of fission product scrubbing, and could require that the vent valves be reclosed in order to limit the offsite consequences, since wetwell venting without benefit of fission product scrubbing would increase risk. For example, a non-venting strategy (after vessel failure) with successful termination of the accident would likely result in lower consequences than a continuous venting strategy. Conversely, venting might provide some benefit in mitigating a late thermal challenge to the drywell head seal. In the worst case of downcomer failure and temperature-induced leakage from the drywell head seal, venting would reduce the driving force for leakage and release fission products (potentially at a higher rate) at a lower location in the secondary

containment. However, externally cooling the drywell head seal (discussed later in this section) appears to offer a greater benefit.

The design of the in-pedestal region also changes the effectiveness of the venting strategy. Suppression pool bypass might occur shortly after vessel failure for the cavity design with in-pedestal downcomers. In this design, most of the corium is expected to enter the suppression pool, thereby essentially eliminating CCI and providing scrubbing for most of the release. The total containment pressure is not anticipated to exceed the containment design pressure for this scenario. Suppression pool bypass in the deep cavity design would likely be delayed until core-concrete erosion failed the in-pedestal cavity (or the cavity drain lines at La Salle). The risk of suppression pool bypass for the flat pedestal design stems from a combination of the previous two challenges. Specifically, spreading of the debris could fail ex-pedestal downcomers while in-pedestal erosion might lead to floor failure. In addition, plants with in-pedestal drains into the wetwell might experience early suppression pool bypass as a result of failure of these lines.

**4.3.5 Core Debris Control.** The issue of core debris control is centered around providing a coolable debris bed following vessel failure and, at the same time, limiting the extent of CCI. As discussed earlier, individual variations in the in-pedestal design of the Mark II containments could lead to drastically different core debris end states. This section considers phenomenological uncertainties that affect the potential benefits of various modifications to enhance the control of core debris outside the reactor vessel.

**4.3.5.1 Cavities With In-Pedestal Downcomers (Shoreham and NMP-2).** The in-pedestal design at Shoreham makes use of a "corium ring" to direct the molten core debris into the suppression pool via four in-pedestal downcomers located underneath the vessel (see Figure 7). The Shoreham PRA found this configuration to be a very desirable feature, since virtually all debris was expected to be quenched in the suppression pool. As long as the vessel does not fail at high pressure, there is little concern about ex-vessel debris-cooling; it is taken care of automatically by suppression pool debris-quenching. For the same reason, CCI is not a concern. As discussed earlier, the potential that this design presents for ex-vessel steam explosions and suppression pool bypass has to be considered, since inadequate experimental and calculational data exist to exclude, with any certainty, these potential adverse effects.

A modification to seal up these in-pedestal downcomers and cover the in-pedestal floor with a layer of lead bricks has been considered. The rationale behind this suggestion is that the corium would float on top of the molten lead, since the lead would be the denser of the two materials. The molten lead would, in effect, insulate the concrete floor from attack by the corium and result in a more generic Mark II containment design. Normal refractory materials would tend to produce noncombustibles, because they cannot withstand the postulated high temperatures of the corium, and the dilution from the refractory materials is less than from using lead bricks.

The sealing of the in-pedestal downcomers could have an adverse effect on the vapor suppression capability of the containment. The design basis LOCA would have to be reanalyzed for both plants to ensure that the containment design pressure would not be exceeded. For example, at Shoreham, the maximum containment pressure during a design basis LOCA is 46 psig, already very near the containment design pressure of 48 psig. In addition, the added weight of the lead bricks could be a seismic concern. Seismic analyses would have to be redone to answer this question.

To date, no analysis has been performed quantifying the risks and benefits of the in-pedestal downcomers, and analyzing whether these downcomers really do guarantee ex-vessel debris-cooling, with negligible amounts of CCI. Furthermore, no inexpensive material has been identified that would protect the downcomers from corium attack. Therefore, this modification is not considered to be cost-effective and will not be discussed further.

**4.3.5.2 Deep Cavity Below Drywell Floor (WNP-2 and La Salle).** The deep cavity design also raises a number of concerns about the fate of the molten core debris after it leaves the vessel. The large, dry cavity underneath the pedestal presents the possibility that significant amounts of debris could become trapped, out of the reach of containment sprays (based on drawings in Reference 13, the cavity is over 9 ft deep). Should this occur, ablation of the concrete cavity floor would generate large quantities of noncondensable gases. Also, the calculated/assumed failure of the drywell floor in Reference 31 indicates that failure of the cavity floor would likely occur at about the same time that wetwell venting would take place. If this happened, the vented release would bypass the suppression pool. Another mechanism that could lead to suppression pool bypass even sooner than failure of the cavity floor is failure of the cavity floor drain lines

because of corium attack, which has been estimated to occur shortly after vessel failure for most sequences.<sup>a</sup>

If the debris attack were extensive enough to fail the cavity floor at La Salle, the corium could directly attack the large, dry concrete plug that rests on top of the containment basemat. Beyond this point, uncertainties overwhelm the ability to make realistic predictions of the outcome. The SNL analysis of the La Salle containment response to severe accidents, which is currently in progress, may help to resolve some of these issues.

**4.3.5.3 Flat Floor Cavity With No In-Pedestal Downcomers (Limerick and Susquehanna).** For the Limerick and Susquehanna designs, which have a flat floor in the in-pedestal region, the issue of core debris control is centered around preventing suppression pool bypass due to failure of the ex-pedestal downcomers or in-pedestal drain lines by debris attack. One proposed modification to enhance containment performance is to install sleeves around the most vulnerable downcomer penetrations to prevent ablation. The sleeves would have a skirt to prevent radial ablation and would be anchored to the drywell floor. However, no inexpensive materials have been identified that could withstand the high temperature attack of the corium. Therefore, this proposed modification does not appear to be cost-effective. Plugging of in-pedestal drain lines could also mitigate early suppression pool bypass.

**4.3.6 Enhanced Reactor Building Fission Product Attenuation.** As discussed in Reference 22, the secondary containment of a BWR may potentially play a significant role in mitigating severe accidents. However, because there are large differences in the design of individual secondary containments, the evaluation of the potential mitigation ability and severe accident vulnerability can only be done on a plant-specific basis. Some calculational work on the secondary containment response to primary containment failure and venting has been performed at ORNL and SNL (see References 22, 32, and 34). The following discussion is based on this work and is only applicable to the plants for which the analysis was done. Because the benefits can only be calculated on a plant-specific basis, no quantitative evaluation of these improvements is provided.

The first observation is that aerosol fission product deposition in the reactor building can be extensive as

long as reactor building integrity is maintained. The internal surfaces of the reactor building and the equipment located there provide a large heat sink and area for fission product deposition. Increased deposition is desirable because the smaller aerosol source term produces a less severe fission product release to the environment. The integrity of the secondary containment could be threatened by overpressurization as a result of a mass release rate into the secondary containment in excess of the exhaust capacity of the ventilation systems and by hydrogen burns in the reactor building.

Some reactor building design features may heighten the threat to secondary containment integrity. For example, Shoreham has an emergency reactor building ventilation system that rapidly recirculates the atmosphere in the reactor building, but filters and exhausts only a small portion of this flow to the environment. This could threaten secondary containment integrity in three ways. First, the small exhaust rate implies that the reactor building could very easily be overpressurized by containment failure or venting (recall that the vent ductwork is predicted to fail, releasing steam and noncondensable gases, including hydrogen, into the reactor building). The most likely failure location would be the refueling bay walls, which are predicted to fail at approximately 0.5 psid (Shoreham does not have blowout panels in its refueling bay) (see Reference 34). Second, given that the refueling bay walls have failed, any fission products released into the lower elevations of the reactor building by failure of the primary containment would be rapidly transported up to the refueling bay by the mixing action of the ventilation system. This would tend to lessen reactor building retention of fission products, increasing the severity of the offsite release. Finally, Reference 34 predicts that global hydrogen burns would be very likely to occur in the reactor building following primary containment failure or venting (failure or venting assumed to induce core damage). Again, this is primarily due to the mixing action of the ventilation system, which acts to limit the localized buildup of hydrogen released from the primary containment. These global hydrogen burns are predicted to result in a peak reactor building temperature of 1200°F and a peak reactor building differential pressure of 6 psi. Note that high connectivity between the different elevations of the reactor building also aids in promoting global hydrogen burns over less severe compartmentalized burns. The connectivity of the reactor building is another feature that varies widely from plant to plant.

The use of fire protection sprays to scrub fission products in the reactor building has been suggested as a possibility for some plants.<sup>22,56</sup> For example, at Browns Ferry (a Mark I plant), a large percentage of

---

a. A. Payne (SNL) conference call to P. K. Niyogi (NRC) on May 1, 1989

the reactor building receives coverage from the preaction (fusible link) fire protection sprays. At other plants, reactor building fire protection is limited to deluge sprays in areas where high concentrations of electrical cable runs are located, with only a small percentage of the reactor building protected by general area preaction sprays. In any case, unless the reactor building fire protection sprays are supplied from an independent dedicated water source, they cannot be given much credit for severe accident mitigation. This is due to the fact that any available fire protection water likely would be used for vessel injection or for spraying the primary containment. Furthermore, the fire protection system pumps are generally sized to supply water only to some small fraction of the spray nozzles, not to all of the nozzles simultaneously. Note that multiple-unit sites might be able to cross-connect their fire protection systems to overcome this limitation.

Finally, as pointed out in Reference 22, if the release from the primary containment could be directed into the lower elevations of the reactor building, the likelihood of reactor building fission product retention would be increased. In particular, those failures that result in a release directly to the refueling bay should be avoided, since they are the ones most likely to directly bypass the reactor building. From this aspect, the critical primary containment failure mode becomes high temperature deterioration of the drywell head seal.

**4.3.7 Enhanced Reactor Depressurization Capability.** Proposed enhancements to the SRVs (see Section 4.3.1) would decrease the probability of core melt at high vessel pressure and, by reducing the amount of hydrogen generated in-vessel during core damage, may reduce the probability of suppression pool bypass due to a stuck open wetwell-to-drywell vacuum breaker. Enhancing the ability to depressurize the reactor reduces the likelihood of direct containment heating, which could potentially cause rapid containment overpressurization at the time of vessel failure. It also eliminates dispersive exit of the core debris from the vessel, which could transport a large

fraction of the core to areas of the drywell located outside the pedestal region. Depressurizing also reduces the number of vacuum breaker actuations and thus the overall probability of a vacuum breaker failing open.

**4.3.8 External Cooling of the Drywell Head Seal.** A potential improvement to prevent late thermal failure of the drywell head seal is to flood the reactor cavity (the area above the drywell head and below the missile shield plugs in the refueling floor), allowing the head seal to be cooled directly. Several means for implementing this modification exist. For example, a siphon (to be installed only when needed) could be used, a hard pipe with manual isolation valves could be installed in one of the spent fuel pool-to-reactor cavity gates, or a fire hose could be employed. If cooling to the head seal were desired, an operator would be dispatched to take the appropriate action. Care would have to be used to ensure that the pool would not be drained below the minimum allowable water level needed to cool the spent fuel. Providing a remote manual capability to flood this area provides a potential method of inadvertently draining the spent fuel pool, which is not acceptable under non-severe accident conditions.

There are some potential drawbacks to this proposal. First, once the accident has progressed to the point where external cooling of the head seal is needed to prevent failure, radiation levels in the reactor building could prohibit operator entry to open the valves. Therefore, during an accident like SBO, which appears to present the greatest potential for head seal failure, the valves would have to be opened early to ensure cooling. If power is recovered prior to extensive core damage, which is very likely, the water would have to be drained and the reactor cavity decontaminated. However, the frequency of SBO is low enough that this concern is probably insignificant, particularly in light of the potential consequences should the initiating event lead to core melt and vessel failure. The quantitative benefits of flooding the drywell head will be estimated later in this report.

## 5. CONTAINMENT BYPASS

### 5.1 Definition of Challenges

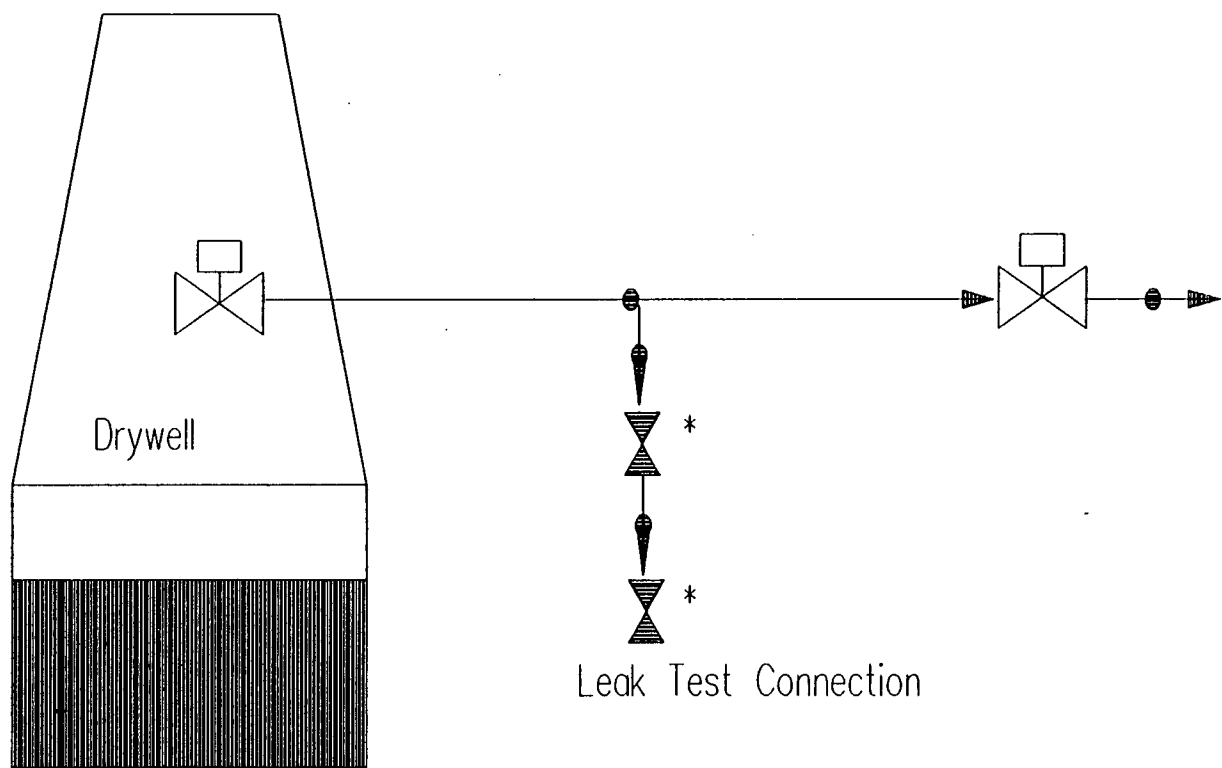
In this mode of containment failure, a release pathway is created that bypasses containment. This could happen in two general ways. First, there could be a failure to completely isolate the containment. For example, isolation valves could fail to close, manual valves could be left open following a leak rate test of a containment penetration (unlikely), or an equipment hatch could be left open (unlikely). The likelihood that a sizeable containment penetration could be left open without detection is low, since this would be indicated by excessive nitrogen makeup flow to the primary containment. However, a leak rate test connection for a primary containment isolation valve could be left open, with no indication of this condition in the control room. In an arrangement like the one shown in Figure 11, which is common to many systems with lines penetrating the primary containment, if the in-board isolation valve should fail to close during an accident, the open leak rate testing line (through the starred valves) would provide a path to bypass the containment altogether. Note that this path could be difficult or impossible to isolate following a significant release of fission products into containment, since the leak rate test valves can only be closed manually. To reduce the probability of this mode of containment bypass, the utility could require that all such valves be administratively locked closed when not in use, or the leak test piping could be capped. Note that this is a requirement of the General Design Criteria of Appendix A to 10 CFR 50; however, experience has shown that utilities may not always rigidly conform to this requirement in the case of leak testing, vent, and drain lines. With bypass through such paths

eliminated, the probability of containment bypass due to an open penetration reduces to the probability that two isolation valves in one line fail to close. This is not considered to be a significant concern.

The other way in which containment could be bypassed is by the so-called interfacing systems LOCA, also known as a V sequence in the terminology of WASH-1400.<sup>57</sup> In this sequence, there is a failure of one or more valves that form a boundary between the high pressure reactor coolant system and a low pressure system outside containment. Such sequences have been found in past PRAs to be insignificant contributors to the overall core damage frequency and risk of BWRs. However, the Office of Nuclear Reactor Regulation (NRR) has initiated an NRC review program to reevaluate the contribution of the V sequence to risk at U.S. plants. In addition, a recent report by BNL<sup>58</sup> estimated the interfacing systems LOCA core damage frequency for three U.S. BWRs. The estimate ranged from  $1.02 \times 10^{-6}$  per reactor-year for Peach Bottom to  $8.81 \times 10^{-6}$  per reactor-year at NMP-2. Therefore, depending on the outcome of the NRC review program, the improvements identified in Reference 58, and possibly others, may need to be implemented in order to lower the contribution to risk from this sequence.

### 5.2 Potential Improvements

Because these sequences have been generally found to be insignificant contributors to core damage frequency and to risk at BWRs, there is no improvement that is felt to be cost-beneficial at this time.



Mark II Containment

**Figure 11.** Typical leak test connection for containment isolation valves.



## 6. QUALITATIVE RISK ANALYSIS OF CONTAINMENT CHALLENGES AND IMPROVEMENTS

### 6.1 Core Damage Frequency

Table 8 summarizes the frequencies of the *dominant* core damage sequences from the Limerick, Susquehanna, and Shoreham risk studies. The primary challenges to core integrity come from transients, SBO, and ATWS. LOCAs are not large contributors to core damage frequency, nor are TW sequences. Note that ATWS is a fairly minor contributor for Limerick, as a result of compliance with the ATWS rule (10 CFR 50.62). For Shoreham, the contribution from SBO sequences has been drastically reduced by the addition of three additional emergency diesel generators (EDGs) (total of six) and the inclusion of a 20 MW onsite blackstart gas turbine generator in the loss of offsite power event trees. The Shoreham contribution from ATWS was reduced by the proposed installation

of the Filtra filtered containment vent system, the use of highly enriched boron in the SLCS (shutdown in 7.5 min), and the addition of an ADS inhibit switch for use during an ATWS. Note that transients are a large contributor to core damage for all of the above plants. In particular, the sequences involving a loss of feedwater with high pressure core melt (TQUX) were found to be dominant. This is in part due to the use of  $2.4 \times 10^{-3}$  as the ADS failure probability. This value was based on the ADS initiation logic in place before Reference 55 recommended logic modifications to make ADS failure less likely, such as removal of the coincident high drywell pressure signal from the set of required initiators. An updated analysis of the ADS failure probability should reduce the frequency of depressurization failure (event X), and thus reduce the contribution from the TQUX sequences.

**Table 8.** Estimated annual core damage frequencies for BWR Mark II plants (internal initiators only)

Initiator	Limerick	Shoreham	Shoreham Filtra	Susquehanna	La Salle <sup>a</sup>
Transients	5.4E-6	8.2E-6	2.1E-5	7.0E-10	$\sim 10^{-6}$
Blackout	6.7E-6	5.6E-6	4.0E-7	7.6E-8	$\sim 10^{-5}$
ATWS <sup>b</sup>	1.1E-6	1.4E-5	1.5E-6	9.3E-9	$\sim 10^{-7}$
LOCA	$\epsilon$	1.0E-6	1.5E-6	6.5E-8	$\sim 10^{-8}$
TW	5.5E-7	4.3E-6	5.9E-7	$\epsilon$	$\sim 10^{-5}$
Special <sup>c</sup>	none	6.1E-6	7.8E-6	$\epsilon$	$\epsilon$
Total	1.5E-5	4.1E-5	3.3E-5	1.5E-7	$\sim 10^{-5}$

a. Values for La Salle are preliminary estimates from June 1989.

b. Includes sequences in which core damage occurs both before and after containment failure.

c. Includes sequences initiated by loss of a DC bus, loss of service water, level instrument sensing line break, and manual shutdown due to high drywell temperature.

## 6.2 Sequence and Failure Mode Risk Significance

As a first step in *qualitatively* determining the potential impact upon risk of various containment and systems modifications, several sensitivity studies that have been performed for Susquehanna, Limerick, and Shoreham were examined.<sup>7,18,26,59</sup> These studies calculated the effects of a particular design feature, such as containment venting, or of a proposed modification, such as an enhanced SLCS, upon the frequency of each identified containment failure mode and upon risk, with risk being defined in terms of the number of expected acute and latent health effects in the surrounding population. Note: since Shoreham did not have an approved emergency plan at the time of the sensitivity study, only dose-versus-distance probabilities could be used as a measure of risk.

The first study examined was the IPE performed by Pennsylvania Power and Light (PP&L) for Susquehanna (see Reference 7). Because this was essentially a scaled-down Level 1 PRA, containment response and offsite consequences were not analyzed in detail. However, for each of the five initiator categories used in the study, PP&L proportioned the core damage frequency among four end states: core damage, core melt with vessel failure, core melt with vessel

failure and subsequent loss of containment integrity due to venting, and core melt with vessel failure and subsequent overpressure containment failure. The base case core melt frequency is  $1.5 \times 10^{-7}$  per reactor-year (refer to Table 9 for additional information).

The first sensitivity study for Susquehanna was to examine the effects of using the "traditional PRA" value of 0.1 for the probability that the operator fails to actuate the SLCS during an ATWS when SLCS actuation is required by the EOP. The base case values in Table 9 were calculated using an effective value of 0.0 for this probability, that is, the operator never fails to actuate the SLCS when it is called for in the EOP. This changes the ATWS frequency from essentially zero to  $9 \times 10^{-9}$  per reactor-year, but does not significantly affect the total core melt frequency.

In their review of the Limerick PRA, BNL calculated the effects on core damage frequency, containment failure mode frequency, and offsite consequences of not complying with the ATWS rule (see References 4 and 59). The plant modifications consisted of an ARI system and a three-pump, automatically actuated SLCS. With these changes, failure of the SLCS becomes dominated by the probability that the operator overrides the automatic SLCS actuation signal. This modification reduces core damage frequency for ATWS by an order of magnitude, but

**Table 9.** Susquehanna plant damage state estimated annual frequencies (base case values)<sup>a</sup>

Plant Damage State	Core Damage	CM With RPV Failure	CM With RPV Failure and Loss of Primary Containment Integrity	
			Wetwell Vent	Containment Failure
Transients	7.0E-10	1.9E-9	1.3E-9	1.4E-9
ATWS	9.3E-9	$\epsilon$	$\epsilon$	3.3E-11
Blackout	7.6E-8	3.9E-8	1.6E-8	1.6E-9
LOCA	5.5E-9	4.9E-10	3.0E-11	2.5E-9
LOCA/ATWS	5.9E-8	$\epsilon$	$\epsilon$	$\epsilon$
Total	1.5E-7	4.1E-8	1.7E-8	5.5E-9

a. Values taken from the 1986 Susquehanna Individual Plant Examination.

does not significantly affect the total core damage frequency from internal events.

Reference 26 analyzed the effects of venting on core damage frequency and risk at the Shoreham Nuclear Power Station. Three sensitivity cases were examined: venting via the proposed Filtra system, venting via the existing HVAC ductwork in the reactor building, and not venting. The study included a bounding analysis of the effects of venting on systems taking suction from the suppression pool, and the effects of venting on the reactor building atmosphere and on reactor building retention of fission products. The results are shown in Table 10 for the worst-case assumption that venting via existing ductwork leads to failure of equipment located in the reactor building with a release that effectively bypasses secondary containment.

As can be seen from Table 10, containment venting was found to affect only the core damage frequency of TW and ATWS sequences. Venting through Filtra was found to reduce the total core damage frequency by approximately 18%. However, with the assumption of reactor building equipment failure following venting, the use of the existing ductwork vent was found to have no benefit in reducing core damage frequency. For ATWS sequences, this was primarily due to the vent lines being too small (6 in. dia) to adequately relieve containment pressure. In the sequences involving loss of long-term containment heat removal (TW), the venting-induced equipment failures in the reactor

building were assumed to lead to loss of vessel injection and subsequent core damage.

In terms of the containment release mode, which can loosely be thought of as being equivalent to the containment failure mode used in other studies, the most favorable results are again obtained by venting through Filtra: almost 94% of all core damage sequences are recovered versus approximately 75% recovery for the existing vent and no-vent cases. In comparison with not venting, using the existing ductwork vent does reduce the probability of early overpressure containment failure (at or near the time of vessel failure), but this is offset by an increased probability of late thermal failure of the drywell head seal, and late venting with an uncontrolled release of fission products, with essentially no holdup time. Relief of containment pressure through the drywell head seal would tend to limit any potential containment pressure increase and could even reduce containment pressure.

The risk of a release at Shoreham could only be assessed in terms of the likelihood of exceeding a specified dose at a given distance from the plant. As Figures 12 and 13 show, venting through Filtra is effective in reducing risk by approximately a factor of five in comparison with both the no-vent and existing vent cases. This is due to Filtra's ability to scrub particulate fission products. On the other hand, use of the existing ductwork vent is seen, in the worst case, to actually *increase* risk in comparison with the no-vent

**Table 10.** Effects of containment venting on the estimated annual Shoreham core damage frequency

<u>Accident Class</u>	<u>Frequency With Filtra Venting</u>	<u>Frequency With Existing Vent</u>	<u>Frequency With No Venting</u>
Transients	3.0E-5	3.0E-5	3.0E-5
Blackout	4.0E-7	4.0E-7	4.0E-7
TW	1.9E-6	9.0E-6	9.0E-6
LOCA	1.3E-6	1.3E-6	1.3E-6
ATWS (CM < CF)	1.8E-8	2.5E-6	2.5E-6
ATWS (CF < CM)	3.5E-7	1.1E-6	1.1E-6
ATWS With Filtra Release	2.1E-6	0.0	0.0
Total	3.6E-5	4.4E-5	4.4E-5

## Dose Vs Distance

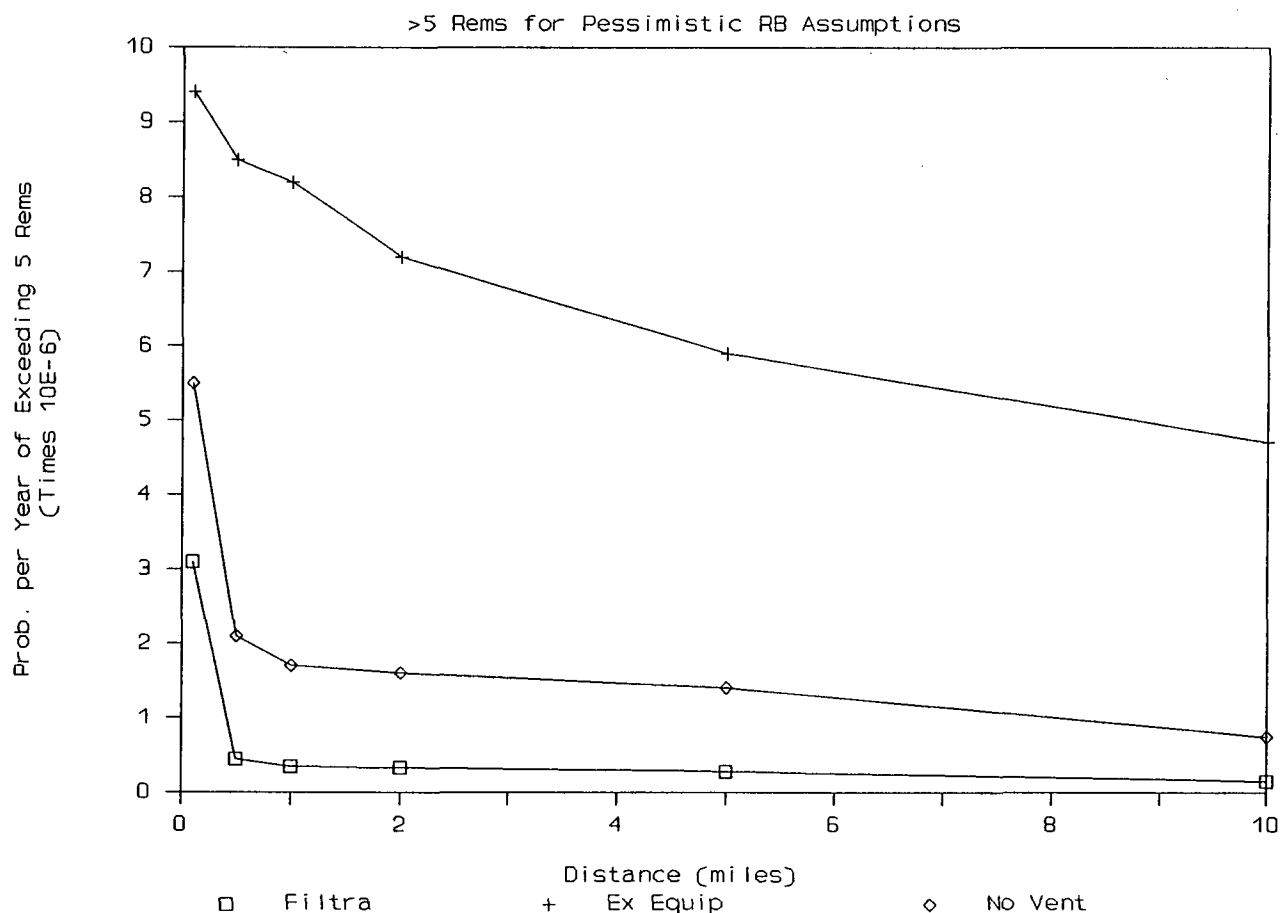


**Figure 12.** Shoreham probability of exceeding a dose of 5 rem as a function of distance.

case by a factor of approximately five. This somewhat surprising result is, as before, related to the small size of the vent lines: in order to mitigate a TW sequence, plant-specific MAAP calculations indicate that both the wetwell and drywell vent lines would have to be opened (see Reference 6). Opening the drywell line would cause fission products to bypass the suppression pool, resulting in an unscrubbed release. This is compounded by the failure of the reactor building to provide significant fission product retention, as discussed in Reference 34. This increase in risk occurs despite the reduction in the probability of early overpressure containment failure provided by venting. The reason for this is that a fraction of the early releases would be scrubbed through the suppression pool (containment failure in the wetwell airspace), reducing the severity of the release. Also, the increased probability of late thermal failure contributes to higher risk because the failure location is in the drywell head region. This produces a release to the refueling floor, directly bypassing the reactor building.

A gross estimate of the allowable costs for installing Filtra, based on the perceived reduction in risk (dose) was performed. The Shoreham base case risk was estimated at 154 man-rem per reactor-year. Using a value of five as the Filtra risk reduction factor gives a Filtra base case risk of approximately 31 man-rem per reactor-year, a net benefit of 123 man-rem per reactor-year. Therefore, the upper bound total cost benefit was estimated as

$$\begin{aligned}
 & (123 \text{ man-rem/reactor-year}) \times \\
 & (\$1000/\text{man-rem averted}) \times \\
 & (40\text{-year plant life}) = \$4.9\text{M}.
 \end{aligned}$$

The costs of actually backfitting the Filtra system to a U.S. BWR are not known. However, because of the large amount of construction required, and the need to install new lines passing through the primary containment, the allowable cost calculated above is probably

## Dose Vs. Distance

>200 Rems for Pessimistic Assumptions

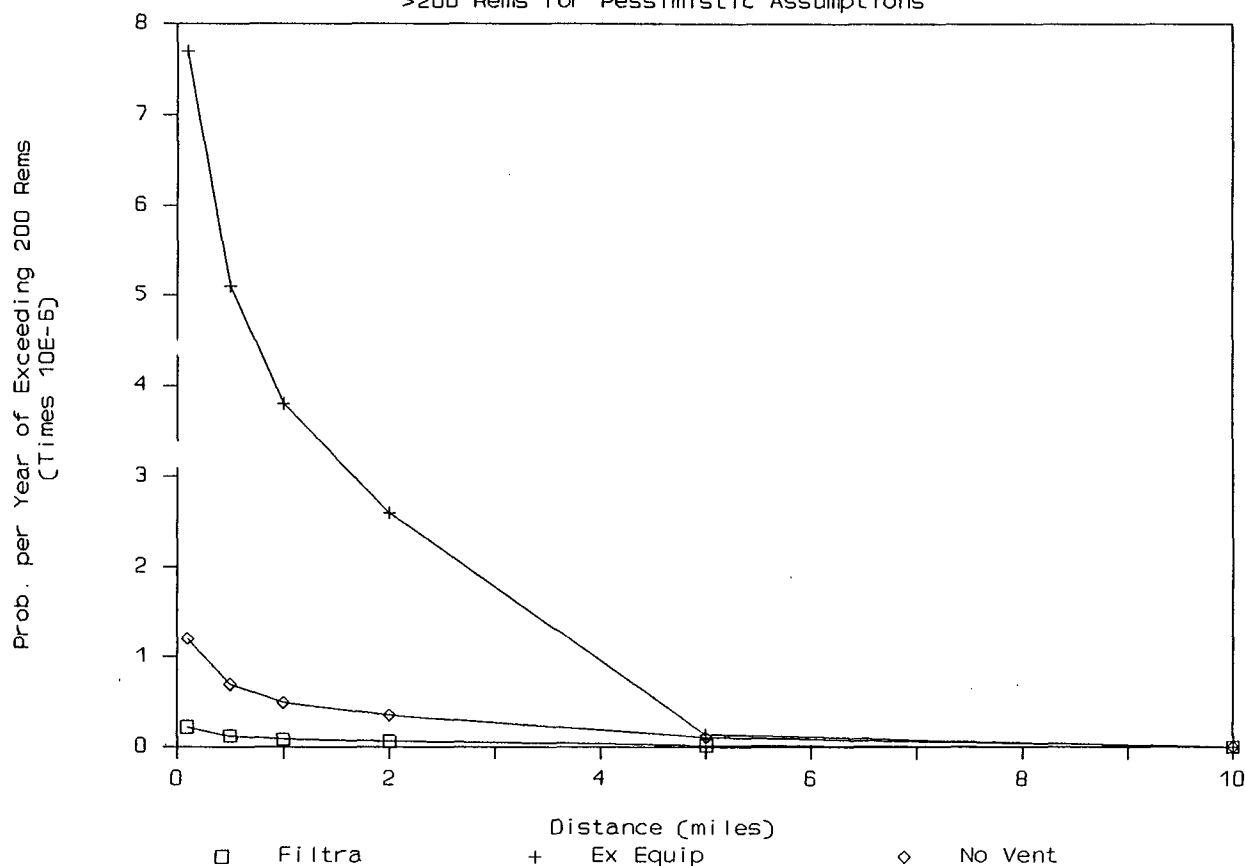


**Figure 13.** Shoreham probability of exceeding a dose of 200 rems as a function of distance.

only a small fraction of what the actual cost would be. Therefore, installation of a Filtra-type filtered containment vent system is not likely to be cost beneficial at U.S. Mark II BWRs.

### 6.3 Summary of Potential Improvements

Numerous hardware improvements and operator actions that could improve containment performance during risk-significant accidents were discussed previously in Sections 3, 4, and 5. The discussions of the potential improvements were organized by transient type, that is, containment challenged prior to vessel failure, containment challenged long after vessel failure, or containment bypass. In general, the improvements were selected to mitigate the containment challenges identified in Sections 3.2 and 4.2.

The results from the qualitative risk analyses are summarized in Table 11. Representative costs from Mark I risk reduction studies are given in Table 12. Improvement 1, a hard-pipe vent system, prevents containment failure due to overpressure failure. Containment overpressure challenges are most important in sequences where containment integrity is challenged prior to core degradation (Section 3). In particular, containment venting with continued vessel injection could prevent containment failure-induced core degradation in TW sequences and could prevent containment failure or reduce the containment pressurization rate during ATWS sequences. For sequences with core degradation prior to containment integrity challenges (Section 4), venting would at best mitigate the offsite release and, at worst, could lead to an inadvertent release or unscrubbed release. Phenomenological uncertainties related to suppression pool bypass (from downcomer or drain line failure) suggest that scrubbing of the release following vessel failure cannot be ensured (see Section 4.2 for design-specific

**Table 11.** Qualitative assessment of benefits and drawbacks of potential Mark II containment improvements

Potential Improvement	Potential Benefits	Potential Drawbacks
<b>1. Vent Systems</b>		
a. Filtered containment vent system <sup>a</sup>	<ul style="list-style-type: none"> <li>• Prevents overpressure failures for transients with scram</li> <li>• Delays overpressure failures for ATWS</li> <li>• Preemptive venting reduces base pressure before core damage</li> <li>• Mitigates hydrogen burns in secondary containment</li> <li>• Ensures scrubbing of aerosol releases</li> <li>• Unaffected by suppression pool bypass</li> </ul>	<ul style="list-style-type: none"> <li>• Filtra – very high cost (\$30–50M)</li> <li>• MVSS – high cost (~\$5M)</li> <li>• Minimal benefit if release is scrubbed by suppression pool</li> </ul>
b. Hard-pipe vent system with dedicated power source	<ul style="list-style-type: none"> <li>• Prevents overpressure failures for transients with scram</li> <li>• May delay overpressure failures for ATWS</li> <li>• Preemptive venting reduces base pressure before core damage</li> <li>• Mitigates hydrogen burns in secondary containment</li> </ul>	<ul style="list-style-type: none"> <li>• Moderately high cost (\$2.9M at Pilgrim)</li> <li>• No decontamination of release in secondary containment – increased risk if suppression pool is bypassed</li> </ul>
<b>2. Alternate containment heat removal systems<sup>a</sup></b>	<ul style="list-style-type: none"> <li>• Maintains suppression pool subcooled</li> <li>• Prevents overpressure failures for TW</li> <li>• May reduce pressurization rate for less severe ATWS</li> <li>• Low cost for use of RWCU blowdown</li> </ul>	<ul style="list-style-type: none"> <li>• Very high costs for ARHR (\$183M+) – other methods may be less expensive</li> </ul>
<b>3. Enhanced reactor depressurization capability</b>	<ul style="list-style-type: none"> <li>• Can prevent high pressure core damage and RPV failure</li> <li>• Relatively low cost (\$0.5M)</li> <li>• May reduce vacuum breaker failure</li> <li>• Can prevent core melt in long-term SBO</li> </ul>	<ul style="list-style-type: none"> <li>• None identified</li> </ul>
<b>4. Improved hydrogen control</b>	<ul style="list-style-type: none"> <li>• None for Mark II plants (inerted)</li> </ul>	<ul style="list-style-type: none"> <li>• Interferes with containment access for maintenance, testing, and leak identification</li> </ul>
<b>5. Backup water supply to RPV injection and containment sprays</b>	<ul style="list-style-type: none"> <li>• Can prevent core damage in low pressure transients with scram</li> <li>• Ex-vessel debris cooling and aerosol scrubbing</li> <li>• May mitigate thermal failure</li> <li>• Independent of RHR</li> <li>• Relatively low cost for use of fire systems</li> </ul>	<ul style="list-style-type: none"> <li>• RPV must be at low pressure for injection</li> <li>• Analysis of EPG spray initiation limit required</li> <li>• Procedures for concurrent fire if fire systems used</li> <li>• Low spray flow rate of fire systems will limit pressure reduction capability</li> <li>• Requires many operator actions and additional piping</li> </ul>

**Table 11.** (continued)

Potential Improvement	Potential Benefits	Potential Drawbacks
5. (continued))		<ul style="list-style-type: none"> <li>• May increase potential for ex-vessel steam explosions</li> </ul>
6. Core debris control		
a. Eliminating in-pedestal downcomers	<ul style="list-style-type: none"> <li>• Decreases probability of suppression pool bypass after RPV failure</li> <li>• Decreases probability of steam explosion or rapid steam spike</li> </ul>	<ul style="list-style-type: none"> <li>• Benefits uncertain due to FCI uncertainties</li> <li>• Increases probability of CCI and ex-vessel fission product release</li> <li>• Requires reanalysis of containment pressure suppression capability</li> </ul>
b. Adding in-pedestal downcomers	<ul style="list-style-type: none"> <li>• Increases probability of quenching core debris ex-vessel</li> <li>• Reduces need for containment sprays and venting</li> </ul>	<ul style="list-style-type: none"> <li>• Increases probability of steam explosion/steam spike</li> <li>• Increases probability of suppression pool bypass after RPV failure</li> <li>• May be very expensive</li> </ul>
c. Strengthening ex-pedestal downcomers <sup>a</sup>	<ul style="list-style-type: none"> <li>• Decreases probability of suppression pool bypass after RPV failure</li> </ul>	<ul style="list-style-type: none"> <li>• Few suitable materials available (high cost)</li> <li>• Increases probability of CCI</li> <li>• Does not reduce ablation of drywell floor</li> </ul>
d. Plug in-pedestal cavity penetrations	<ul style="list-style-type: none"> <li>• Decreases probability of suppression pool bypass after RPV failure</li> <li>• Decreases probability of steam explosion/steam spike</li> </ul>	<ul style="list-style-type: none"> <li>• Requires system modifications</li> <li>• May increase probability of steam explosion in deep cavity</li> <li>• Requires seismic reanalysis of primary containment</li> </ul>

**Table 11.** (continued)

Potential Improvement	Potential Benefits	Potential Drawbacks
7. External cooling of drywell head	<ul style="list-style-type: none"> <li>• Mitigates or prevents drywell head seal failure</li> <li>• Leakage scrubbed by overlying water pool</li> <li>• Low cost</li> </ul>	<ul style="list-style-type: none"> <li>• Must be manually initiated early in the accident</li> <li>• Benefits uncertain</li> <li>• Does not prevent leakage of other isolation valves or penetrations</li> </ul>
8. Use of fire protection sprays in the reactor building <sup>a</sup>	<ul style="list-style-type: none"> <li>• May scrub aerosol fission products released from primary containment</li> <li>• Hardware already in place at some plants</li> </ul>	<ul style="list-style-type: none"> <li>• Limited spray coverage</li> <li>• May provide greater benefit as alternate containment spray or RPV injection system</li> </ul>

a. These improvements are not quantitatively analyzed in this report.

**Table 12.** Summary of cost estimates from previous studies

Potential Improvement	Cost Estimate (\$)	Reference
1. Vent system		
a. Hard-pipe vent system with dedicated power source	<ul style="list-style-type: none"> <li>• 0.69M</li> <li>• 2.9M</li> <li>• 0.19M to 6.1M</li> </ul>	<ul style="list-style-type: none"> <li>• SEA Report 87-253-07-A:1</li> <li>• Estimated from Boston Edison Co. (DPU 88-28, Request No. AG 13-6) and does not include Tech. Spec. mods.</li> <li>• Draft NUREG/CR-4551, includes replacement power costs. Does not include hard pipe (only modified power supplies to vent valves).</li> </ul>
b. Filtered containment vent system (Filtru)	<ul style="list-style-type: none"> <li>• 14M-33M</li> <li>• 30M</li> </ul>	<ul style="list-style-type: none"> <li>• Draft NUREG/CR-4451, App. F, several sources</li> <li>• NUREG/CP-0095, Nov. 1988, R. O. Schlueter and R. P. Schmitz, estimate of the Swedish Filtra</li> </ul>
2. Alternate containment heat removal system	<ul style="list-style-type: none"> <li>• 61M-77M</li> <li>• 0.1M</li> </ul>	<ul style="list-style-type: none"> <li>• Draft NUREG/CR-4551, with \$845K recurring costs</li> <li>• Estimate for use of blowdown mode of RWCU</li> </ul>
3. Enhanced depressurization capability	<ul style="list-style-type: none"> <li>• 0.5M</li> <li>• 1.99M</li> <li>• 3M-14M</li> </ul>	<ul style="list-style-type: none"> <li>• SEA Report 87-253-07-A:1</li> <li>• Estimated from Boston Edison Co. (DPU 88-28, Request No. AG 13-6), does not include Tech. Spec. mods., training, etc.</li> <li>• Draft NUREG/CR-4551</li> </ul>



Table 12. (continued)

Potential Improvement	Cost Estimate (\$)	Reference
4. Enhanced containment spray system	<ul style="list-style-type: none"> <li>• 0.81M</li> <li>• 2.4M</li> </ul>	<ul style="list-style-type: none"> <li>• SEA Report 87-253-07-A:1</li> <li>• Estimated from Boston Edison Co.(DPU 88-28, Request No. AG 13-6), does not include Tech. Spec. mods., training, etc.</li> </ul>
5. Downcomers <ul style="list-style-type: none"> <li>a. Eliminating in-pedestal</li> <li>b. Adding in-pedestal</li> <li>c. Strengthening ex-pedestal</li> <li>d. Plugging in-pedestal penetrations</li> </ul>	<ul style="list-style-type: none"> <li>• Not available</li> </ul>	<ul style="list-style-type: none"> <li>• Any downcomer modification is expected to be very expensive. Improvement 5.b is expected to be the most expensive of the three options. Improvement 5.d probably has the lowest cost, but it may only be applicable to La Salle.</li> </ul>
6. External cooling to drywell head	<ul style="list-style-type: none"> <li>• Not available</li> </ul>	<ul style="list-style-type: none"> <li>• No cost estimate is available. However, the hardware costs associated with a small pump or siphon are expected to be low. Operation with the drywell head water seal, training, Tech. Specs., etc., should be considered in the system cost.</li> </ul>
7. Improved hydrogen control	<ul style="list-style-type: none"> <li>• See 1</li> </ul>	<ul style="list-style-type: none"> <li>• Primary containment is inerted. Consequently, hydrogen venting would be used to prevent burns in the secondary containment in the event of primary containment failure.</li> </ul>
8. Use of fire protection sprays in reactor building	<ul style="list-style-type: none"> <li>• Not available</li> </ul>	<ul style="list-style-type: none"> <li>• Existing fire sprays should initiate on high reactor building temperature after primary containment failure. Additional spray protection costs are not available.</li> </ul>

discussions), in contrast to the Mark I hardened vent where all releases through the vent would be scrubbed. If a reliable method of preventing suppression pool bypass were available, wetwell venting would provide a controlled release and would reduce the driving pressure for other containment failures. Although a filtered vent system would alleviate the problems associated with suppression pool bypass, the high cost of the system is expected to exceed the benefit.

Similar to containment venting, ARHR systems could prevent core degradation in TW sequences. However, the low frequency of TW sequences (see Table 8), the high system cost, and the potential for operator actions to mitigate the sequence (see Section 3.4), would likely keep this system from being cost-effective.

Enhanced reactor depressurization capability would allow reactor depressurization independently of site

DC power and would ensure operability during high temperature conditions. This capability would be particularly important during SBO sequences when DC power from the emergency station batteries would be limited or unavailable. A reliable means of depressurization would permit successful operation of safety grade or alternative low pressure injection systems. The combination of enhanced depressurization capability and the variety of low pressure injection systems would make a reduction in the core damage frequency of high pressure transients possible. No potential drawbacks were identified.

An alternative supply of water for vessel injection or containment sprays could provide both preventive and mitigative benefits. If the reactor were at low pressure, the alternative water source could be injected into the vessel to prevent or limit core damage. If the reactor vessel were failed, water injected into the vessel could

limit further core degradation and would pour out onto corium that had already exited the vessel. This could provide cooling of the ex-vessel debris and scrubbing of the non-noble gas fission products. Conversely, if the vessel were at high pressure or already failed, the water could be sprayed into the containment to mitigate (possibly prevent) the release of fission products. However, due to the low flow rate of postulated alternative pumping systems and uncertainties associated with FCI, the benefits are uncertain. In addition to cooling the debris, the containment sprays would provide some scrubbing of fission products released from the melt. Although the cost of this improvement could be low, many operator actions may be required to effectively utilize the system.

As discussed in Section 4.4.5, the potential benefits of core debris control are uncertain and plant-specific. Due to uncertainties associated with steam explosions, rapid steam spikes, and debris-spreading and coolability, the benefits of debris control improvements are unknown. In general, the costs associated with modifications to the drywell floor, downcomers, and changes in the cavity design are expected to be high. Plugging drain lines that penetrate the drywell floor may offer the greatest benefit. For example, at La Salle, drain lines in the bottom of the cavity are postulated to quickly ablate and fail in most sequences following

attack by molten corium.<sup>a</sup> In a meeting on July 27 between Philadelphia Electric Company (Limerick) and the NRC, the licensee stated that the in-pedestal drains would fail approximately 6 min after vessel failure (see Reference 36). Early failure of the in-pedestal floor drains would result in suppression pool bypass.

Flooding the drywell head has the potential for preventing or mitigating leakage through the drywell head seal. As discussed in Section 4.3, high temperature and high pressure conditions may lead to drywell head seal leakage. A pool of water above the drywell head could cool the seal and would scrub particulate fission product releases.

Hydrogen control is already provided in Mark II plants by nitrogen-inerting of the primary containment.

Past studies were identified in Section 4.4.6 that showed the potential benefits of reactor building sprays. However, use of the diesel fire pumps has been suggested as an alternate source of water for the containment sprays. It is anticipated that direct cooling of corium in the containment would provide more benefit than spraying the reactor building.

---

a. A. Payne (SNL) conference call with P. K. Niyogi (NRC) on May 1, 1989.

## 7. QUANTITATIVE RISK ANALYSIS OF ANTICIPATED TRANSIENTS WITHOUT SCRAM

ATWS sequences can be grouped into two classes, depending upon whether the containment is challenged prior to reactor vessel failure (Class IV), or upon whether core melt and vessel failure precede any challenge to containment integrity (Class IC) (see Reference 5). These accident sequence classes, which are also referred to as plant damage states, correspond to the containment vulnerable-core damage and core damage-containment vulnerable end states used in NUREG-1150. The analysis in this section was performed under the general assumption that the reactor systems are those associated with the General Electric BWR/4 product line. Detailed assumptions are described below.

### 7.1 Accident Sequence Analysis

For simplicity, the ATWS accident sequence analysis examined only a full power ATWS with isolation of the reactor from the main condenser by closure of the MSIVs. Such a sequence represents an upper bound on the severity of the BWR ATWS (see Reference 24).

The first step in the risk quantification was the construction of an event tree, which represents the sequence from the time of the initiating event until the time of either containment failure or significant core damage. Summing the end state frequencies from this event tree gives the core damage frequency for the full isolation ATWS, both for the case where loss of containment integrity precedes core damage (Class IV), and where extensive core damage occurs prior to a loss of containment integrity (Class IC).

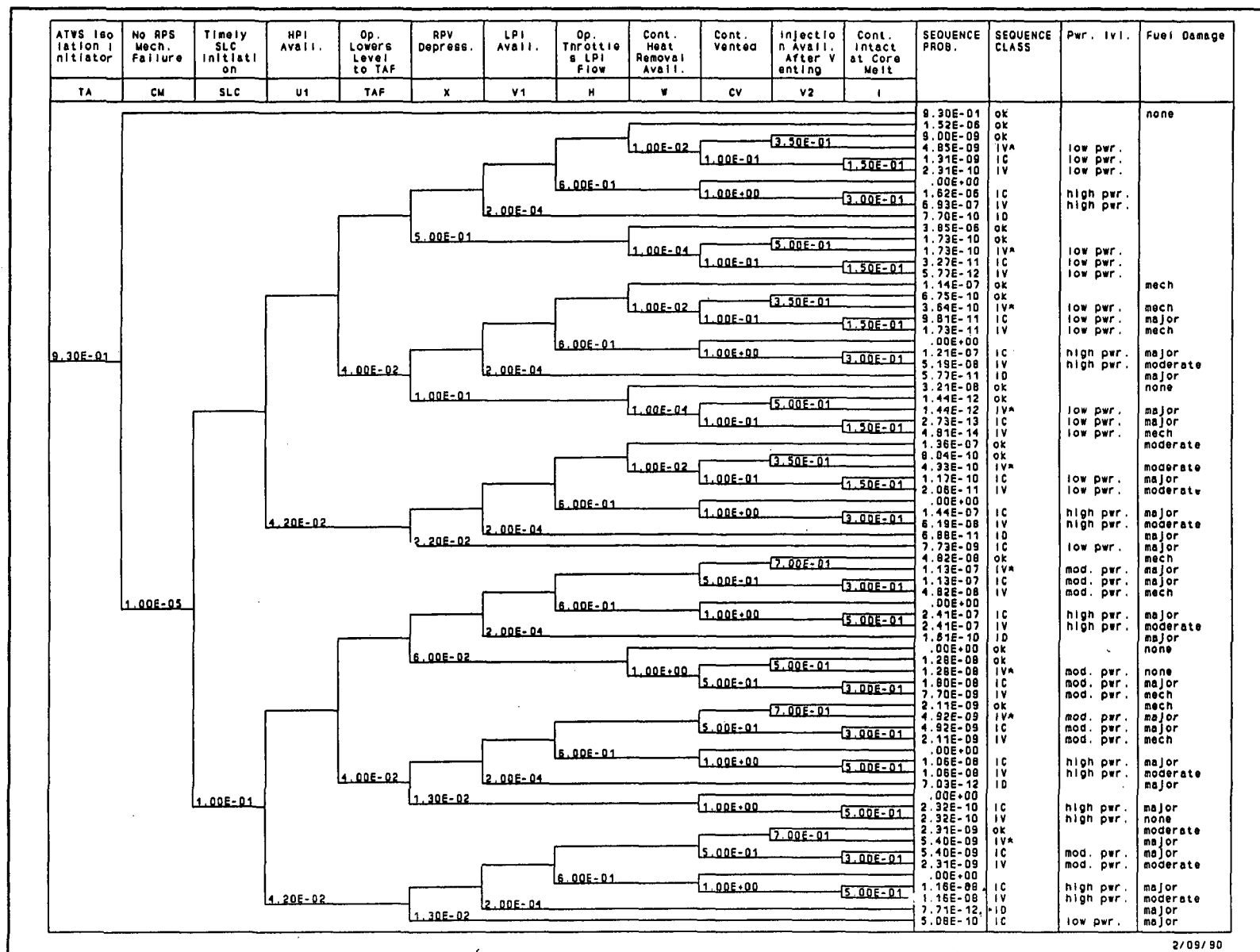
**7.1.1 Event Tree Quantification.** The following discussion gives the quantification scheme for the top events in the base case ATWS front-end event tree, which is shown in Figure 14. Changes in the quantification that were made to examine potential improvements and to assess sensitivities are discussed in Section 7.4

**Ta.** The initiating event is a transient in which the reactor is isolated from the main condenser. The frequency of 0.93 per reactor-year, taken from Table 7.9-5 in Reference 7, is a representative value. However, some variation in this value from plant to plant can be expected.

**Cm.** This is the reactor protection system (RPS) mechanical failure probability of  $1.0 \times 10^{-5}$  per demand from Reference 60. Since the values derived in Reference 60 were intended to be generic best estimates, applicable to both BWRs and PWRs, arguments presented recently by some utilities to reduce this failure probability are not felt to be sufficiently justified; based on the data currently available, the value of  $1.0 \times 10^{-5}$  per demand is most likely an upper bound on the RPS mechanical failure probability. Therefore, this value has been retained. However, as discussed in Reference 7, the installation of the ARI system does allow electrical failures of the RPS to be neglected. The reasoning for this is as follows. The failure probability of the RPS due to electrical faults was estimated by Reference 60 at  $2 \times 10^{-5}$  per demand. If ARI operates as designed, electrical failures will be recovered. Therefore, since the RPS and the ARI operate independently, the failure probability of the RPS due to electrical faults is the value of  $2.0 \times 10^{-5}$  per demand from Reference 60 multiplied by the failure probability of the ARI system, which Reference 7 estimated to be  $4.0 \times 10^{-3}$  per demand. This probability is further reduced if credit is given for operator action to vent the scram air header in accordance with the EPG. Reference 7 estimates that this action would be successful 90% of the time.

**SLC.** This is the probability that boron injection is not initiated in time to prevent the bulk suppression pool temperature from exceeding the HCTL set by the EPG (see Reference 19). For ATWS events, Reference 7 uses an elevated HCTL of 208°F, with the reactor at full operating pressure, but does not give a detailed basis to support this change. However, if such an increase in the HCTL is valid, then the allowable time for operator action to initiate boron injection is substantially increased, as indicated in Table 7.7-1 in Reference 7. Hand calculations were performed to estimate the final bulk suppression pool temperature for the case with both SLCS pumps injecting at 86 gpm and also for the case with one SLCS pump injecting at 43 gpm, with injection in both cases beginning when suppression pool temperature reaches 110°F, as per the direction given in the EPG.

For the case where both SLCS pumps inject, a final bulk suppression pool temperature of 156.4°F was calculated. This compares favorably with the value of 157.3°F calculated in Reference 7, which is well below the modified HCTL of 208°F, but is near the EPG limit of approximately 165°F. Therefore, even a small



2/09/90

Figure 14. Base case ATWS event tree.

amount of operator delay in actuating the SLCS likely would cause the EPG limit to be exceeded. For the case where only one SLCS pump injects, a final bulk temperature of 198.6°F was calculated. The value calculated by Reference 7 is 187.1°F. These values are still below the modified HCTL, but are well above the EPG limit. Therefore, for this case, if the EPG limit were followed, emergency vessel depressurization would be required during boron injection.

For the base case, the assumption is made that the EPG limit is generally valid for an ATWS sequence. The success criterion for SLCS injection is that the SLCS must be actuated in time to allow the reactor to reach a condition of hot shutdown before reaching the suppression pool HCTL (as set by the EPG). To meet this criterion, injection by both pumps is required. (The assumption is made that the generic plant has chosen to comply with the ATWS Rule<sup>61</sup> by requiring actuation of both SLCS pumps. An alternative strategy would be to increase the boron-10 isotopic enrichment so that the equivalent flow rate with one pump running would be  $\geq 86$  gpm.) Reference 7 calculates an SLCS mechanical failure probability of  $2.2 \times 10^{-2}$ , and argues that this dominates the human error probability (HEP) for failure to actuate the SLCS. If the EPG limit is followed, this is not felt to be a valid treatment, since hand calculations performed for this report and the calculations in Reference 7 show that any significant delay (more than a few minutes) in actuating the SLCS beyond the time when suppression pool temperature reaches 110°F is likely to result in suppression pool temperature exceeding the HCTL before the hot shutdown weight of boron can be injected. Therefore, the quantification of this event in some past PRAs is followed and a failure probability of 0.1 is used, based on the HEP dominating the mechanical failure probability.<sup>62</sup> This is felt to be a conservative generic approach; individual plants may be able to justify the use of a significantly lower HEP.

U1. This is the failure probability of high pressure coolant injection (HPCI), which Reference 7 calculates to be  $4.2 \times 10^{-2}$  per demand. Following the EPG would involve initial termination of all injection flow, except that provided by the CRD pumps and the SLCS, followed by restoration of flow prior to reaching Level 1, with level maintained thereafter near the TAF. The actual point at which vessel level is maintained would vary from plant to plant. Therefore, the assumption is made for the generic plant that the operators would maintain level at the bottom of the *wide range level instruments*, that is, several inches above the TAF. The validity of this assumption is borne out by experience and by discussions with licensed BWR

operator examiners. If HPCI fails, leaving RCIC and CRD as the only sources of injection, an equilibrium level is calculated, using the Chexal-Layman correlation,<sup>63</sup> which is about 6 ft below the TAF. This condition would require emergency depressurization in accordance with the EPG; therefore, the success criterion for high pressure injection is that HPCI be available. As an aside, Reference 7 calculates that HPCI should automatically actuate 95 s into the sequence, when reactor vessel downcomer water level reaches Level 2. This is approximately the time when suppression pool temperature is calculated to reach 110°F. Therefore, if the operator were to follow the EPG requirement of attempting to lower vessel level to the TAF after actuating the SLCS, the occurrence of these two events at roughly the same time would make this a very difficult action to perform successfully; the operator actions would have to be extremely well coordinated.

TAF. This is the probability that the operator does not take action to lower vessel level to the TAF in order to reduce reactor power. Because Reference 7 did not quantify this event, the failure probability of  $4.0 \times 10^{-2}$  calculated in Reference 6 is used.

X. This is the probability that the vessel is not depressurized, that is, it remains at or near normal operating pressure. The EPG instructs the operator to inhibit the ADS for an ATWS sequence, but requires emergency depressurization when level cannot be maintained above the TAF (and a source of injection is available), when level cannot be determined, or when the suppression pool HCTL is exceeded (there are other conditions requiring emergency depressurization, as well). Reference 7 strongly emphasizes that depressurization is to be avoided because of concerns about power/pressure spikes as a result of uncontrolled low pressure injection, limit cycle operation, and inadequate steam cooling of the core. With the significantly increased HCTL used in Reference 7, depressurization is not likely to be required; therefore, it is not quantified in Reference 7. However, since the base case analysis in this report is founded on the guidance given in the EPG, Event X is quantified here.

There are several paths that an isolation ATWS sequence could take, and depressurization has to be quantified separately for each of them. In the first case considered, HPCI fails, causing level to stabilize well below the TAF. In this case, the probability that the vessel is not depressurized becomes essentially the probability that the operator acts to inhibit ADS (since the ADS is quite reliable, its failure probability can be neglected for this case). Reference 6 calculated a value of  $2.2 \times 10^{-2}$  for this situation. In the second case,

SLCS injection is successful, HPCI is available, and level is controlled near the TAF. Since there is uncertainty in reactor power with vessel level maintained near the TAF (at the bottom of the wide range level instruments),<sup>64</sup> there is a corresponding uncertainty in the probability of exceeding the suppression pool HCTL prior to injecting enough boron to shut down the reactor. Therefore, the probability of depressurization was assessed to be highly uncertain. Hence, an indeterminate value of 0.5 was assigned to Event X for this case. In the third case, HPCI is running and both SLCS pumps are injecting boron into the core, with level not controlled at the TAF. Depressurization should be required only if the HCTL is exceeded. Using a limit of 165°F, hand calculations indicate that the HCTL could be exceeded before the hot shutdown weight of boron has been injected. Therefore, a probability of 0.1 is conservatively assumed for Event X (Reference 6 calculated a failure probability of 0.11). If the increased HCTL of 208°F were used, this probability would be essentially 1.0, that is, the probability of depressurization would be 0.0. The fourth case is the one where both HPCI and the SLCS fail. For this case, Reference 6 calculated a failure probability of  $1.3 \times 10^{-2}$ . The fifth case is the one where the SLCS fails but level is controlled at the TAF. For an assumed suppression pool temperature between 200 and 260°F, Reference 6 calculated a failure probability for Event X of  $6.0 \times 10^{-2}$ . With a limit of 208°F and revised procedural instructions to not depressurize with level maintained at the TAF, this probability could be significantly larger. The last case is the one where HPCI is operating, the SLCS has failed, but level is not lowered to the TAF. For this case, Reference 6 calculated a value of  $1.3 \times 10^{-2}$ .

V1. Event V1 represents the probability that low pressure injection is not available, given that the RPV has been depressurized. Because the sequence is an isolation ATWS, the conservative assumption is made that a vacuum cannot be maintained in the main condenser, resulting in insufficient makeup to the hotwell to allow use of the condensate system as a sustained source of low pressure injection. This assumption is supported by Table 7.5-3 in Reference 7, which gives a mean power conversion system (PCS) unavailability of 0.9 following an isolation ATWS. The assumption is also made that the operator will not allow LPCS to inject because of the uncertainty associated with injecting a large volume of relatively cold water directly onto a core without an adequate shutdown margin. This leaves LPCI as the only adequate source of low pressure injection. Reference 7 does not quantify LPCI unavailability for an ATWS sequence. However, a value

of  $2.0 \times 10^{-4}$  is used for other sequences. This is in line with the value of  $1.0 \times 10^{-4}$  used in Reference 6.

H. Given that LPCI is available with the vessel depressurized, the operator must take action to prevent uncontrolled injection to avoid large power/pressure spikes. Since the LPCI injection valves typically cannot be throttled during the first 5 min of LPCI operation, the operator must turn off the RHR pumps until this interlock has expired, then restart the pumps with the injection valves throttled. This action corresponds to event UH2LP in Figure H-16 in Reference 6. Case 3 (emergency depressurization) is assumed, for which Reference 6 calculated a failure probability of 0.6. The ATWS core damage frequency was found to be especially sensitive to the quantification of this event.

W. This is the probability that long-term containment heat removal is unavailable. The assumption is made that only the suppression pool cooling mode of the RHR system can be used to remove heat (containment venting is treated as a separate event), because the RHR pumps will likely be unavailable to provide containment spray if the suppression pool cooling mode of RHR is not available. Reference 7 quantifies the unavailability of the suppression pool cooling mode of RHR at  $2.0 \times 10^{-5}$  for an ATWS. Reference 6 generally used a value of  $1.0 \times 10^{-2}$ , with human error dominating the hardware unavailability of  $1.0 \times 10^{-4}$ . For cases with LPCI injecting, the HEP value of  $1.0 \times 10^{-2}$  is used in this report for the failure probability of Event W, since LPCI operation will make suppression pool cooling with RHR more difficult. For the case where the SLCS fails, but level is controlled at the TAF, a value of 1.0 is used, because the actual power level will be well above the level of decay heat, rendering RHR ineffective as a means of containment heat removal. For the case of successful SLCS injection with high pressure makeup, the equipment unavailability of  $1.0 \times 10^{-4}$  from Reference 6 is used.

CV. This is the probability that the containment is not vented or, equivalently, that the vent is too small to mitigate the pressure rise in the containment. For the base case analysis, the assumption is made that an 18-in. ductwork vent from the wetwell is available.

Venting is assumed to be initiated at the PCPL, as defined in the EPG (assumed to be ~60 psig) (see Reference 19). Critical flow calculations show that an 18-in. wetwell vent line is capable of providing adequate containment heat removal for those sequences in which reactor power is at decay heat levels. A value of 0.1 (HEP) is used for the vent unavailability in this case. If the reactor has not been shut down by injection of boron, a failure probability of

1.0 for venting is assumed (because the power level exceeds the heat removal capacity of the vent), unless level is controlled at the TAF, in which case an indeterminate value of 0.5 is used to reflect the uncertainty in reactor power with vessel level near the TAF.

V2. This is the probability that venting causes failure of injection, thus inducing core damage. Several different cases must be examined.

1. If HPCI is injecting, the suction is assumed to be from the CST, as per the guidance in the EPG (see Reference 19). Therefore, venting has no effect on NPSH. However, environmental effects (high temperature steam) in the reactor building could lead directly to loss of HPCI. Because of the uncertainty surrounding these effects, Event V2 is assigned an indeterminate failure probability of 0.5.
2. If LPCI is injecting and the reactor is subcritical because of successful boron injection, then venting would have to fail both LPCI and CRD, since the CRD pumps are capable of providing adequate flow to keep the core cooled with reactor power at decay heat levels (see Reference 23). The probability of LPCI failure has a contribution of 0.5 because of the potentially adverse reactor building environment, and 0.2 from the possible effects of venting on NPSH (see Reference 6). The CRD pumps are assumed to be located in the reactor building (not true at all plants: at Susquehanna, for example, they are in the turbine building), with suction taken from the CST. Therefore, the failure probability of Event V2 for this case is given by

$$P(V2) = (0.5 + 0.2) * (0.5) = 0.35.$$

Note: The assumption is made that the RHR and CRD pumps are sufficiently separated in the generic plant so that environmental effects are not likely to present a common mode failure mechanism. Thus, a multiplicative factor of 0.5 is used in calculating P(V2).

3. If LPCI is injecting but the reactor is not shut down, that is, boron has not been injected or LPCI has not been throttled, then the CRD pumps alone are not capable of providing adequate core cooling if LPCI is lost. Therefore, for this case, the failure probability of Event V2 is taken to be 0.7.

I. Event I probabilistically evaluates whether the containment fails prior to the onset of extensive core damage. This event was quantified in Reference 6 for the cases listed below. These values are quite uncertain and may not be applicable to all Mark II plants. Therefore, if they are to be used in a plant-specific analysis at another plant, care should be taken to ensure the applicability of the quantification methodology in Reference 6. An increase in these values will result in an increase in the Class IV ATWS frequency, whereas a decrease will result in an increase in the frequency of the Class IC ATWS sequences.

1. Boron injected, LPCI throttled, P(I) = 0.15
2. Boron injected, LPCI not throttled, P(I) = 0.3
3. Boron not injected, LPCI throttled, P(I) = 0.3
4. Boron not injected, LPCI not throttled, containment not vented, P(I) = 1.0
5. Boron not injected, level at TAF, vessel not depressurized, P(I) = 0.15
6. Boron not injected, level > TAF, LPCI throttled, P(I) = 0.3
7. Boron not injected, level > TAF, LPCI not throttled, P(I) = 0.5
8. Boron not injected, level > TAF, vessel not depressurized, P(I) = 0.5
9. Boron not injected, HPCI failed, LPCI throttled, P(I) = 0.3
10. Boron not injected, HPCI failed, LPCI not throttled, P(I) = 0.5.

The results of this analysis are the point estimate ATWS core damage frequencies shown below:

Class	Frequency (per reactor-year)
IV (CF < CM)	$1.27 \times 10^{-6}$
IC (CM < CF)	$2.30 \times 10^{-6}$

## 7.2 Containment Event Tree Analysis

Two base case SCETs were constructed to model the containment response to the challenges arising from ATWS sequences. In Class IV sequences, the

challenge to containment integrity occurs prior to core melt and vessel failure, and the predominant failure mode is quasistatic overpressurization. Conversely, in Class IC sequences, the challenge to containment integrity occurs later, generally after the time of vessel failure, with the predominant failure mode being overpressure failure in the wetwell airspace shortly after the time of vessel failure. The detailed quantification of the top events in each of these base case SCETs is given below. For a discussion of the SCET methodology, see Reference 3.

**7.2.1 Class IV SCET.** The Class IV SCET is shown in Figure 15.

**PD.** The initiating event is the Class IV plant damage state, which is defined to be an ATWS sequence that results in a challenge to containment integrity prior to extensive core damage. The conditional probability of event PD, given a Class IV end state, is 1.0.

**VE.** Event VE represents early containment venting (prior to core damage). For the base case analysis, venting is assumed to occur at the PCPL defined in the EPG (assumed to be ~60 psig) via an 18-in. wetwell vent line. Furthermore, the vent line is assumed to be connected to HVAC ductwork in the reactor building, and this ductwork is assumed to fail at the time of venting. In Class IV sequences, venting has led to a loss of injection, which results in core melt in a breached containment if the vent lines are not subsequently reclosed. However, if they are reclosed, then pressure will again build up and eventually challenge containment integrity; therefore, for the Class IV plant damage state, Event VE is assigned a conditional failure probability of 1.0.

**F1.** Event F1 models early containment failure due to overpressurization prior to the time of extensive core damage. If early venting is not successful, then early containment failure is assumed to occur; therefore,  $P(F1) = 1.0$ .

**PF.** Event PF models the energetics of the release, that is, whether there is a large driving force (such as vessel failure at high pressure), which could rapidly sweep fission products out through a breach in the containment, given that early containment failure has occurred. Because of large uncertainties in the phenomenology, event PF was assigned an indeterminate failure probability of 0.5 (see Reference 29).

**BS.** Event BS models the size of the containment break, which in turn affects the source term associated with the release. For cases of early containment failure, because of uncertainties, Event BS is assigned

an indeterminate probability of 0.5, that is, large and small breaks are considered to be equally likely (see Reference 29).

**SP.** Event SP models the effectiveness of the suppression pool in scrubbing particulate fission products from the release. Success of Event SP implies that suppression pool scrubbing is effective, while failure of SP implies that the release partially or totally bypasses the suppression pool. For this case, the resulting aerosol DF is assumed to be 1.0, that is, there is no suppression pool scrubbing. For the base case, the postulated failure of the in-pedestal drain lines shortly after vessel breach was assumed to make suppression pool bypass likely (see Reference 36).<sup>a</sup> Therefore, the conditional failure probability of Event SP was taken to be 0.9. Note that a containment failure in the drywell could also lead to pool bypass. However, failure of the in-pedestal drain lines is assumed to dominate these other modes, since vessel breach is expected to result in drain line failure and pool bypass regardless of the containment failure location. In order to constrain the size of the SCETs, no attempt was made to explicitly model the containment failure location on the event tree.

**RB.** Event RB models the effectiveness of the reactor building in retaining particulate fission products released from the primary containment. Because of the large variation in reactor building designs (see Reference 22), there is a corresponding large uncertainty in Event RB. Therefore, Event RB was assigned an indeterminate conditional failure probability of 0.5.

The conditional release probabilities are shown in Table 13 for the base case Class IV plant damage state. Refer to Appendix C for a definition of the containment release modes used in this report.

Note that all SCET end states for this ATWS plant damage state involve an early release from containment.

### 7.2.2 Class IC SCET.

The Class IC SCET is shown in Figure 16.

**PD.** The initiating event is defined to be an ATWS sequence in which core melt and vessel failure precede any challenge to containment integrity. The conditional probability of Event PD, given a Class IC end state, is 1.0.

**R1.** Event R1 represents the probability of successful in-vessel recovery. Since injection is unavailable for

---

a. A. Payne (SNL) conference call with P. K. Niyogi (NRC) on May 1, 1989.



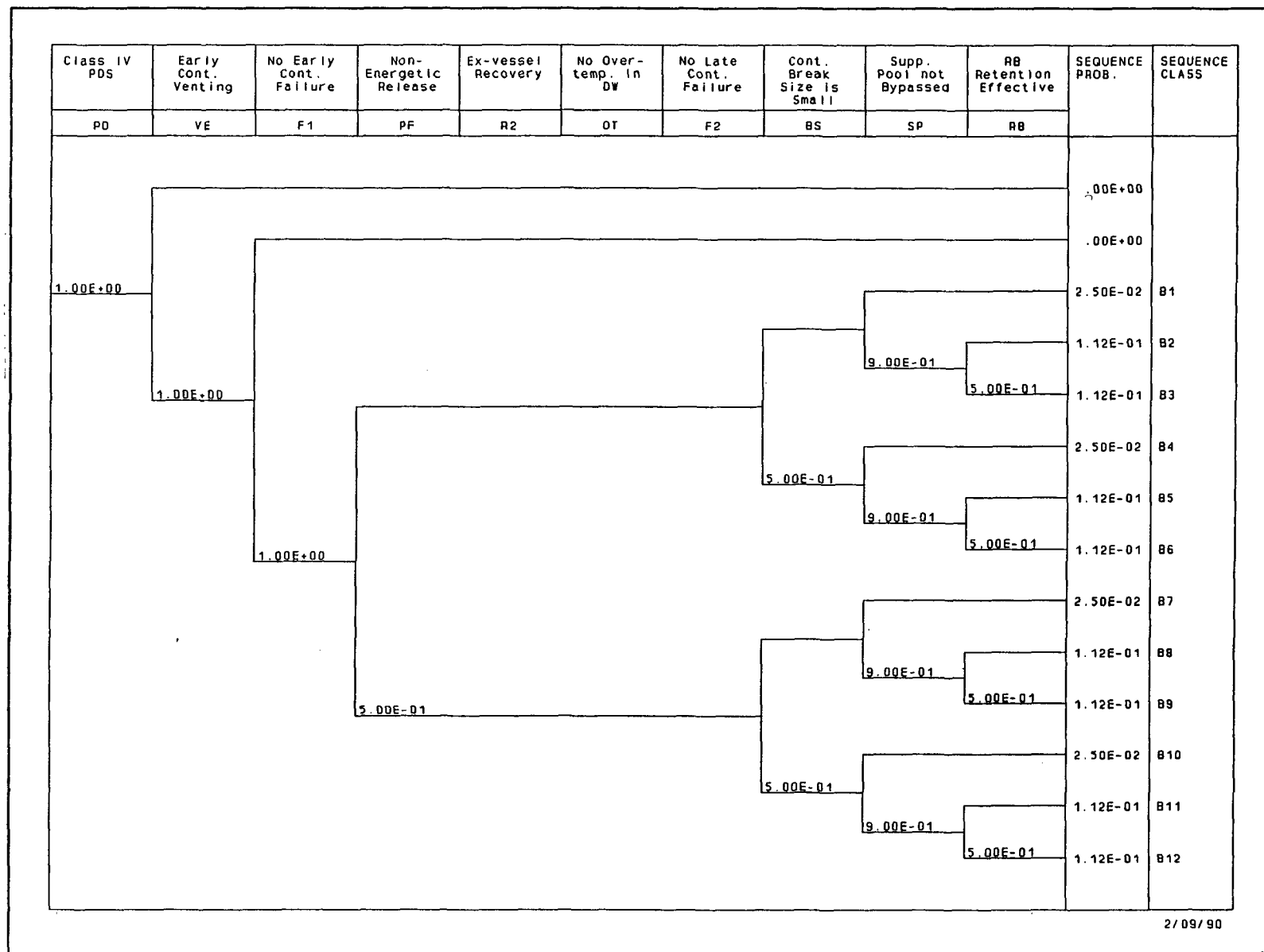
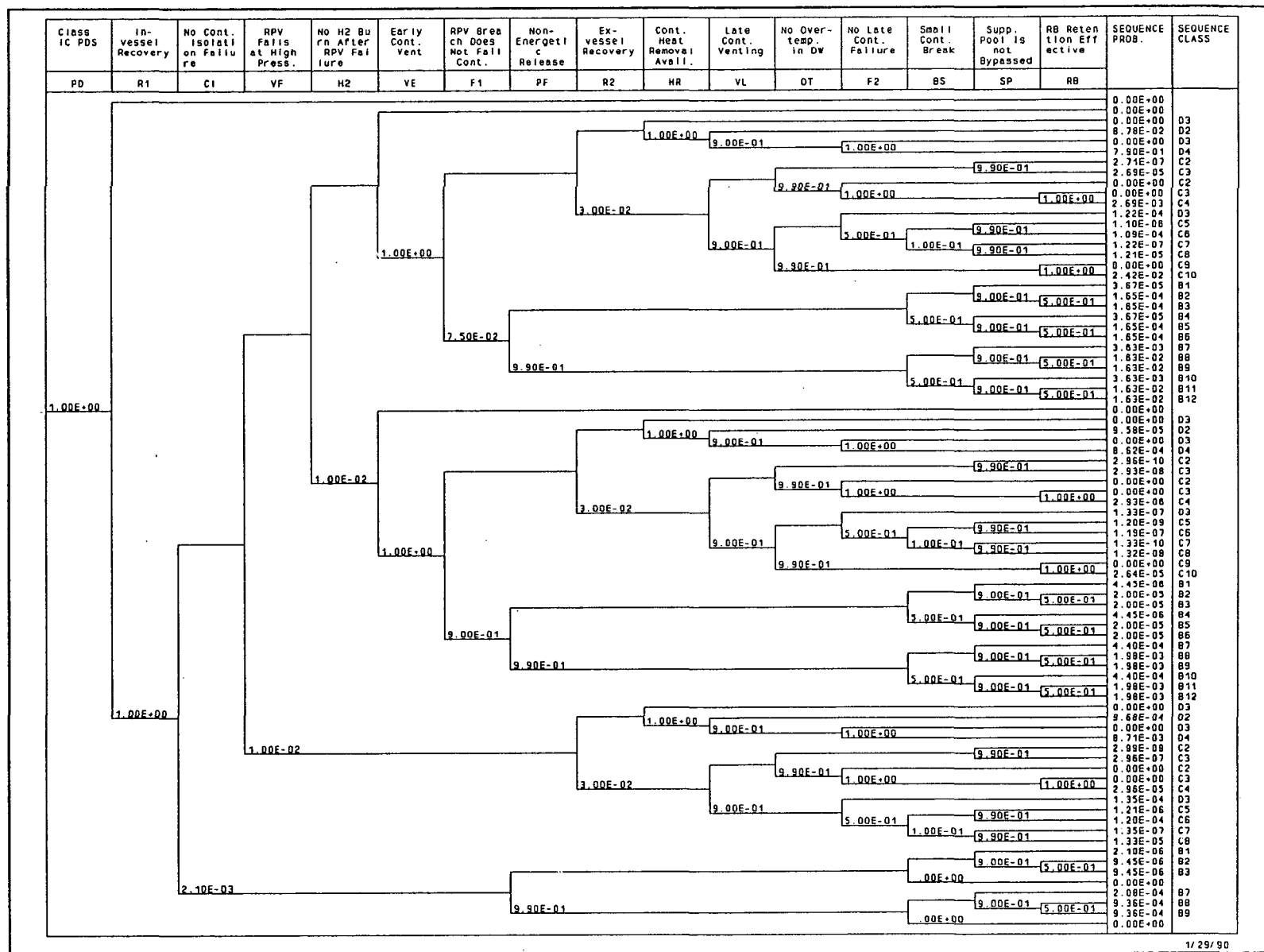


Figure 15. Class IV SCET.



1/29/90

Figure 16. Class IC SCET.

**Table 13.** Conditional containment release probabilities for the Class IV plant damage state: base case

Release Mode	Conditional Probability
B1	2.50E-02
B2	1.12E-01
B3	1.12E-01
B4	2.50E-02
B5	1.12E-01
B6	1.12E-01
B7	2.50E-02
B8	1.12E-01
B9	1.12E-01
B10	2.50E-02
B11	1.12E-01
B12	1.12E-01

the Class IC plant damage state, by definition, Event R1 is assigned a conditional failure probability of 1.0.

**CI.** Event CI models the presence of a preexisting large containment leak. Failure of Event CI is assumed to prevent further pressurization of the containment, and is modeled as a small break (large leak) for purposes of quantifying later events in the SCET and for assigning the end states of the SCET to release modes. It is analogous to the  $\delta$  containment failure mode of WASH-1400 and the Limerick PRA (see References 4 and 57). The failure probability of  $2.1 \times 10^{-3}$  used for Event CI is taken from Reference 29. This value is within the range of probabilities estimated by Reference 65 for a pre-existing large containment leak, that is, open valves.

**VF.** The upper branch of Event VF represents failure of the vessel at an elevated pressure. In the Class IC sequences, vessel failure at high pressure can result in an immediate challenge to containment integrity (see References 4 and 29), and may disperse core debris

outside the pedestal region, which can worsen the late containment challenge, especially for those plants with in-pedestal downcomers. Because the vessel is at high pressure in the Class IC plant damage state, by definition, there is assumed to be a 99% probability that the vessel will fail at high pressure. Therefore, a conditional probability of  $1.0 \times 10^{-2}$  is assigned to the lower branch of Event VF (recall that the lower branch of Event VF represents vessel failure at low pressure).

**H2.** Event H2 models a primary containment hydrogen burn at or near the time of vessel failure. A significant (but uncertain) amount of hydrogen will be present in the drywell as a result of the metal-water reaction that takes place inside the vessel during core melt. This hydrogen is transferred to the suppression pool by SRV actuation and is transported to the drywell via the wetwell-to-drywell vacuum breakers. Because the Mark II plants are allowed to operate for short periods of time with the primary containment deinerted, there is a small probability that oxygen could be present in sufficient concentrations to allow a hydrogen burn to occur at this point in the sequence. Reference 29 quantifies this possibility at  $1.0 \times 10^{-2}$ . This is also the value used in the Limerick PRA for containment *failures* induced by hydrogen burns (see Reference 4). In this report, a hydrogen burn does not necessarily result in immediate overpressure containment failure. However, this value has been retained here as the probability of occurrence of a hydrogen burn.

**VE.** Event VE models containment venting prior to or at the time of vessel breach. Because venting is failed for the Class IC plant damage state, by definition, Event VE is assigned a conditional failure probability of 1.0.

**F1.** Event F1 models overpressure failure of the containment at or near the time of vessel failure. The quantification in Reference 29 was followed, where for those sequences with vessel failure at high pressure, but with no hydrogen burn inside containment ( $\text{VF} * \text{H2}$ ), Event F1 was assigned a conditional failure probability of  $7.5 \times 10^{-2}$ . For sequences in which vessel failure at high pressure is accompanied by a hydrogen burn inside containment ( $\text{VF} * \text{H2}$ ), Reference 29 quantifies Event F1 at 0.9. If the vessel does not fail at high pressure (VF), then Event F1 is not questioned, since containment failure is judged to be extremely unlikely at this point in the sequence.

**PF.** As in the Class IV plant damage state, Event PF models the energetics of the release, given that early containment failure has occurred. In Reference 29, the major contributors to an energetic release were judged

to be prolonged suppression pool steaming and vessel failure at high pressure. Since all sequences with early containment failure (F1) involve vessel failure at high pressure, and the suppression pool can be expected to be saturated in Class IC sequences, Event PF was assigned a conditional failure probability of 0.99.

**R2.** Event R2 represents successful ex-vessel cooling of the core debris, via injection into either the failed reactor vessel or the containment spray header. The failure probability of Event R2 is based upon two factors: the likelihood that adverse suppression pool conditions (clogging of suction strainers by core debris or inadequate NPSH) will preclude operation of RHR and LPCS pumps, and the probability that operators fail to align alternate injection systems, for example, service water to the RHR ultimate heat sink connection. Since the suppression pool is likely to be saturated for these sequences (see References 4 and 9), the assumption is made that NPSH for the RHR pumps will be inadequate to prevent cavitation of the pump. Therefore, the failure probability of Event R2 reduces to the HEP for failure to align alternate injection systems. Reference 29 uses a value of  $3.0 \times 10^{-2}$  for the probability that operators fail to align alternative injection systems. The source of this value is given as the Peach Bottom Analysis done for draft NUREG-1150 (draft NUREG/CR-4550, Volume 4, October 1986). However, Reference 29 includes the diesel fire pump and the condensate system among the alternative injection sources considered available.

In the present analysis, the condensate system is assumed to be unavailable for the reasons discussed in Section 7.1 above. Additionally, the diesel or electric motor-driven fire pumps could supply water, but use of this source is not included in the base case analysis. Therefore, service water is left as the only viable means of injection should suppression pool conditions prevent the use of ECCS pumps. Note: the MAAP analysis (see Reference 9) performed for Reference 29 indicates that injection at 200 gpm into the pedestal region with the CRD pumps is sufficient for establishing a coolable debris bed. However, since Shoreham (the plant for which the analysis was done) has four in-pedestal downcomers, a large fraction of the core debris (approximately 75% in this case) is assumed to flow through these downcomers and be quenched in the suppression pool. Therefore, with only about 25% of the debris remaining in the drywell, CRD injection may be adequate. However, the generic Mark II plant is assumed not to have in-pedestal downcomers. In this case, the fraction of core debris present in the drywell is expected to be larger than 25% and CRD injection may be inadequate for establishing a coolable

debris bed. In addition, vessel failure most likely will also cause failure of the CRD injection lines, making CRD injection for debris-cooling uncertain. For these reasons, the CRD pumps were not considered in quantifying Event R2.

Alignment of service water to inject via the RHR system is assumed to require the operator to open two MOVs that are normally locked closed via a key-lock switch in the main control room. If either of these valves should fail to open upon demand, service water would be unavailable for debris-cooling. Using data from Reference 5, the probability of this happening is estimated to be  $1.5 \times 10^{-4}$  per demand. Maintenance errors could also affect ultimate heat sink availability. Maintenance unavailability is estimated (again using data from Reference 5) at  $1.4 \times 10^{-4}$ . The Reference 29 estimate of  $3.0 \times 10^{-2}$  for operator alignment error is probably conservative, since it is based on action occurring within 2 to 4 h after vessel breach (~4 to 6 h after the initiating event). As Reference 29 indicates, the minimum time window for establishing a coolable debris bed following vessel breach is more likely on the order of 10 h. However, since there is a large uncertainty associated with this human error probability, the Reference 29 value has been preserved in this report. Thus, for Class IC sequences, Event R2 is assigned a conditional failure probability of  $3.0 \times 10^{-2}$ .

**HR.** Given successful ex-vessel recovery, some means of long-term containment heat removal has to be established to prevent eventual overpressure failure (see Reference 8). Use of the RHR pumps for either suppression pool cooling or containment sprays is considered in quantifying Event HR. However, since the suppression pool is likely to be saturated for these sequences, the assumption is made that the RHR pumps will be unavailable. Therefore, Event HR is assigned a base case conditional failure probability of 1.0.

**VL.** If ex-vessel recovery fails, or if it is successful but there is a failure to establish long-term containment heat removal, then heat removal can be provided by venting the containment. Although the EPGs direct that venting take place without regard to the offsite radioactivity release (see Reference 19), the assumption is made that the extremely high radiation levels present in the containment would preclude venting 90% of the time, since the operators would probably be extremely hesitant to release a large amount of activity to the reactor building and the environment by venting. Thus, for the base case, Event VL is assigned a conditional failure probability of 0.9. Reference 8 did not consider this limitation and assigned a central estimate failure probability of  $1.0 \times 10^{-2}$  to late venting.

Another argument against using the Reference 8 value is that the probability of suppression pool bypass appears to be much higher for the Mark II containment than for the Mark I containment analyzed in Reference 8. Assuming the operators were aware of the high probability of pool bypass, they likely would be very hesitant to vent the containment, since any release would probably be unscrubbed.

**OT.** For those sequences in which ex-vessel recovery is not successful, the presence of molten core debris in the drywell can lead to very high temperatures and elevated pressures, particularly in the area of the drywell head seal (see Reference 9). Event OT evaluates the probability that temperatures  $>700^{\circ}\text{F}$  will be reached (accompanied by elevated pressures in the range of  $\sim 80$  to  $100$  psig), temperatures sufficient to cause failure of the drywell head seal or other elastomeric penetration seals. Failure of ex-vessel recovery is thought to make such high temperatures extremely likely. Therefore, for the base case,  $P(\text{OTIR2})$  is taken to be 0.99.

Note that a dichotomy exists between the industry code MAAP and the NRC-sponsored Source Term Code Package (STCP) in the calculation of late containment challenges. The MAAP code assumes more heat transfer into the containment atmosphere than into the underlying concrete, whereas the opposite is the case in STCP. Therefore, MAAP tends to predict lower noncondensable gas generation rates (from CCI) than does STCP, but with much higher containment temperatures. STCP, on the other hand, predicts higher containment pressures at an earlier time than does MAAP. The net effect is that late containment failure in the STCP analyses tends to be due to overpressurization rather than overtemperature, and occurs at an earlier time than the thermal failure predicted by MAAP.

For this report, a choice was made to incorporate the MAAP methodology. The reasons for this are as follows. First, STCP assumes that the melt ejection following vessel failure involves the entire reactor core and structural material and that it occurs instantaneously rather than in a time-dependent manner.<sup>66</sup> The majority of BWR severe accident analysts today feel that a time-dependent pour-type melt is more likely. Second, the HVAC ducting extending from just above the surface of the drywell floor to the drywell head region in the Mark II containment has not been modeled in previous STCP analyses. This ducting has the potential to allow the transport of very hot gases, which evolve from the surface of the melt as CCI progresses, to the enclosed drywell head. If this occurs,

the temperature in the vicinity of the drywell head seals could reach the experimentally observed seal failure temperature prior to a pressure rise sufficient to challenge the ultimate pressure capacity of the containment. Finally, STCP does not model the potential re-vaporization release of fission products following vessel failure (see Reference 66). This phenomenon could lead to a more severe release than that predicted by STCP.

**F2.** Event F2 probabilistically evaluates late containment failure as a result of temperature and pressure loads. For those sequences with failure of Event OT, that is, high temperatures in the vicinity of the drywell head seal, late failure of the drywell head seal is assumed to be certain. For these sequences, the conditional failure probability of Event F2 is taken to be 1.0. For sequences without excessively high drywell temperatures, the likelihood of late overpressure failure is highly uncertain. Therefore, for this case, Event F2 is assigned an indeterminate conditional failure probability of 0.5.

**BS.** Event BS models the break size, given that there has been a breach of containment. Failure of Event BS signifies a large containment break ( $>1.0$  ft<sup>2</sup>). If containment isolation has failed (CI), the failure size is assumed to be small ( $<1.0$  ft<sup>2</sup>); therefore,  $P(\text{BS}|\text{CI}) = 0.0$ . Early overpressure failure is assumed to be due to a rapid pressure rise, for which Reference 29 assigns Event BS an indeterminate conditional failure probability of 0.5 (small and large breaks equally likely). Sequences with late containment failure not caused by high drywell temperature result from a gradual pressure rise or from pressure spikes that are not sustained. For these sequences, Reference 29 assigns Event BS a probability of 0.1. For late containment failures induced by drywell temperatures in the range of  $800$  to  $1100^{\circ}\text{F}$ , containment break size was judged by Reference 29 to be uncertain and Event BS was assigned an indeterminate value of 0.5. However, since Reference 29 determines the release mode for late thermal failure, not by break size, but by whether reactor building retention of fission products is effective, Event BS was not questioned for these sequences in order to further simplify the SCET.

**SP.** Success of Event SP implies that the release passes through the water in the suppression pool where aerosol fission product scrubbing occurs. Failure implies that all or part of the release bypasses the pool. For cases with early containment failure (F1), the conditional failure probability of Event SP was taken to be 0.9, as in Class IV. For late containment challenges and late venting, this probability was increased to 0.99.

**RB.** As for the Class IV SCET discussed above, the large variation in reactor building design leads to uncertainty in the effectiveness of reactor building fission product retention. Therefore, for all sequences that do not involve late thermal failure of the drywell head seal, Event RB is assigned an indeterminate conditional failure probability of 0.5. Because failure of the drywell head seal leads to a release directly to the refueling bay, bypassing the reactor building,  $P(RB|(OT \cap F2)) = 1.0$ .

The conditional release probabilities are shown in Table 14 below for the base case Class IC plant damage state.

**Table 14.** Conditional containment release mode probabilities for Class IC plant damage state: base case

Release Mode	Conditional Probability
B1	4.33E-05
B2	1.94E-04
B3	1.94E-04
B4	4.12E-05
B5	1.85E-04
B6	1.85E-04
B7	4.28E-03
B8	1.92E-02
B9	1.92E-02
B10	4.07E-03
B11	1.83E-02
B12	1.83E-02
Early Release	8.42E-02
C2	2.74E-07
C3	2.72E-05
C4	2.72E-03
C5	2.31E-06
C6	2.29E-04
C7	2.57E-07
C8	2.54E-05
C9	0.00E+00
C10	2.42E-02
Late Release	2.72E-02
D2	8.78E-02
D3	1.09E-02
D4	7.90E-01
Ex-vessel Rec.	8.89E-01

## 7.3 Consequence Analysis

The severe accident consequence analysis was performed using a personal computer (PC) version of the MELCOR Accident Consequence Code System (MACCS) (see Reference 10). Site-specific data for the reference plant were taken from the most recent version of the draft NUREG-1150 MACCS 1.5 input deck for Peach Bottom.

Offsite release data for the reference plant are based on the results provided in Reference 67 for those cases that did not take credit for the Supplemental Containment System (SCS). The offsite release data (source terms) were generated using the MAAP program (version 3.0) (see Reference 9). Containment release modes were binned into source term release categories according to the scheme presented in Reference 29 (see Appendix C).

MACCS is composed of three modules: ATMOS, EARLY, and CHRONC, which are exercised in sequence by the code. This set of modules has been developed for the purpose of evaluating the severe accident consequences at commercial LWR power plants. MACCS 1.5 incorporates several improvements over earlier codes like CRAC2 in the treatment of variable and long-term releases, deposition modeling, dosimetry, emergency response, long-term mitigative actions, radiological health effects, and economic impacts. For a further discussion of the MACCS code, refer to Appendix D.

For this report, three risk measures were selected to be used as consequence measures: latent fatalities (cancers), population dose, and offsite costs. No early health effects are reported, since Peach Bottom is not felt to be a representative site in terms of the magnitude of the early health effects calculated by MACCS.<sup>a</sup> The dose results are based on the total whole body population dose within a 50-mi radius of the plant. The consequence results for the 10 release categories are summarized in Table 15. Note that all probabilities shown in this table are conditional upon the occurrence of a core damage sequence accompanied by a release from containment.

To obtain the risk associated with a severe accident sequence, these consequence measures are multiplied by the release probabilities and the accident sequence frequency, with a summation over the 10 release categories, as indicated by Equation 1-1. The base case results for ATWS are presented in Table 16.

a. S. A. Acharya (NRC) personal communication to R. J. Dallman (EG&G Idaho) on August 31, 1989.

**Table 15.** Conditional consequence results of the source term release categories

<u>Release Category</u>	<u>Mean Latent Fatalities</u>	<u>Mean Population Dose (man-rem)<sup>a</sup></u>	<u>Mean Offsite Costs (\$)</u>
RC1	7.23E+03	5.93E+06	4.81E+10
RC2	4.96E+03	4.26E+06	2.87E+10
RC3	7.58	1.82E+04	1.13E+06
RC4	3.03E+03	3.58E+06	5.77E+09
RC5	4.38E+03	3.94E+06	2.57E+10
RC6	2.08E+03	2.75E+06	2.99E+09
RC7	1.77E+02	3.87E+05	3.48E+07
RC8/9	3.41E+03	3.17E+06	1.22E+10
RC10	3.97	7.79E+03	1.13E+06
RC12	4.31	1.23E+04	1.52E+06

a. The population dose is that received within a 50-mi radius of the plant.

**Table 16.** Base case consequence results for ATWS sequences (per reactor-year)

<u>ATWS Class</u>	<u>Mean Latent Fatalities</u>	<u>Mean Population Dose (Man-Rem)<sup>a</sup></u>	<u>Mean Offsite Costs (\$)</u>
IC (CM < CF)	1.13E-03	1.02	6.21E+03
IV (CF < CM)	4.60E-03	4.60	1.91E+04

a. The population dose is that received within a 50-mile radius of the plant.

## 7.4 Sensitivities and Effects of Potential Improvements

A number of factors can affect the core damage frequency and thus the risk of ATWS sequences. First, a reduction in the RPS mechanical failure probability has perhaps the most direct effect, via a reduced ATWS sequence frequency, as shown in Table 17.

As can be seen from this table, lowering the RPS mechanical failure probability by one order of magnitude makes ATWS an insignificant contributor to core

damage frequency. Lowering it by two orders of magnitude, as suggested in Reference 7, makes ATWS truly inconsequential.

The next sensitivity to be evaluated is a decrease in the HEP associated with SLCS actuation. Table 18 shows the effects of a range of probabilities for Event SLC.

Note that increasing the probability of successful SLCS actuation from 0.9 to 0.99 would lower the Class IV core damage frequency by 26% and the

**Table 17.** Effect of RPS mechanical failure probability on ATWS core damage frequency

<u>P(Cm)</u>	<u>Class IV Frequency</u>	<u>Class IC Frequency</u>
1.0E-5/d (base case)	1.27E-6/y	2.30E-6/y
1.0E-6/d	1.27E-7/y	2.30E-7/y
1.0E-7/d	1.27E-8/y	2.30E-8/y

**Table 18.** Effect of SLCS failure probability on ATWS core damage frequency

<u>P(SLC)</u>	<u>Class IV Frequency</u>	<u>Class IC Frequency</u>
1.0E-1/d (base case)	1.27E-6/y	2.30E-6/y
1.0E-2/d	9.40E-7/y	2.12E-6/y
1.0E-3/d	9.07E-7/y	2.10E-6/y
0.0/d	9.03E-7/y	2.11E-6/y

Class IC frequency by 7.8%. Thus, the greater effect of more reliable SLCS injection is upon the Class IV sequences, which involve an early containment breach prior to significant core damage. Note also the somewhat surprising result that making the SLCS perfectly available actually increases the Class IC frequency slightly from the case where  $P(SLC) = 1.0 \times 10^{-3}$ . This result, which at first glance appears anomalous, was examined in some detail. The conclusion reached is that the high probability of uncontrolled low pressure injection, which would flush the boron out of the core and cause large power and pressure spikes, overrides the benefits of increased SLCS reliability in reducing the Class IC frequency. (Note that the Class IV frequency decreases monotonically as SLCS reliability increases.) As long as the probability of uncontrolled low pressure injection is greater than about 0.29, this "anomaly" is present. Thus, Event H turns out to represent a crucial point in the sequence, as discussed below.

One of the mistakes that an operator can make in responding to an ATWS is to fail to control low pressure injection following depressurization (Event H). Because depressurization for the ATWS was assessed to require emergency depressurization to <200 psig in accordance with the EPG, the conditional failure probability of Event H was calculated to be quite large, 0.6 for the base case. Because the Class IV frequency is extremely sensitive to this value, a sensitivity case was

run to examine the effects of varying the conditional failure probability of Event H. The results are shown in Table 19.

As can be seen from this table, control of low pressure injection following depressurization has a significant impact on the ATWS core damage frequency. The contribution of Event H to the ATWS core damage frequency could be decreased in one of two ways. First of all, the probability that depressurization is necessary could be lowered. This is examined further below. The second means could be to decrease the conditional failure probability of Event H through operator training on ATWS response.

One means to potentially lessen the contribution of Event H to the ATWS core damage frequency is the strategy of not following the EPG direction to lower level to the TAF, as proposed in Reference 7. This strategy has the advantage of simplicity from an operator's point of view. It also avoids the somewhat troublesome question of boron mixing efficiency in the lower plenum under low forced flow or natural circulation conditions (for those plants with a SLCS sparger located in the lower plenum, below the core plate). The potential drawback to this strategy is the decreased time available for operator action to initiate boron injection (assuming the plant conforms to the minimum requirements of Reference 61, that is, the



**Table 19.** Effect of failure to throttle low pressure injection on ATWS core damage frequency

<u>P(H)</u>	<u>Class IV Frequency</u>	<u>Class IC Frequency</u>
6.0E-1/d (base case)	1.27E-6/y	2.30E-6/y
5.0E-1/d	1.14E-6/y	1.97E-6/y
3.0E-1/d	8.74E-7/y	1.32E-6/y
1.0E-1/d	6.07E-7/y	6.63E-7/y
0.0/d	4.75E-7/y	3.37E-7/y
1.0/d	1.80E-6/y	3.60E-6/y

plant does not use very highly enriched boron, so as to achieve an equivalent SLCS flow rate in excess of 86 gpm) before reaching the suppression pool HCTL. With an 86-gpm SLCS injection rate, calculations show that even SLCS actuation at 110°F in the suppression pool might not shut down the reactor before exceeding the HCTL specified in the EPG. To avoid this problem, Reference 7 uses an elevated HCTL of 208°F for ATWS. The validity of this strategy will not be examined in detail in this report. However, some support for increasing the HCTL can be found in Reference 68.

In constructing the base case event tree for the strategy of allowing HPCI and RCIC to inject at full flow into the vessel, the EPG HCTL was used in quantifying Event X. Using the information in Reference 6, Event X was assigned a base case conditional failure probability of 0.1, that is, the reactor will be depressurized approximately 90% of the time if level is not lowered to the TAF. If the increased ATWS HCTL proposed in Reference 7 is valid, then  $P(X|TAF)$  would probably be in the range of 0.9 to 1.0. Thus, if level were lowered to the TAF in accordance with the EPG, then the conditional failure probability of Event X would also have to be in this range for the level control strategy to be effective in terms of reducing the ATWS core damage frequency. This is not felt to be likely, particularly if the EPG HCTL is also followed, because of the combined effects of suppression pool heatup and level control difficulties, that is, emergency depressurization is apt to be required. However, *if the EPG HCTL is followed* and injection is not throttled, then the probability that the reactor will have to be depressurized is high, and the strategy of lowering level to the TAF would be more effective in reducing the ATWS core damage frequency.

As discussed in Section 7.1, the current operator response to an ATWS is quite complicated because of the coincident actions that are required by the EPG, for example, the SLCS must be actuated at approximately the same time that HPCI and RCIC automatically actuate. Therefore, the probability that the operator will not be able to control level successfully in accordance with the EPG may be significantly higher than the value used in the base case analysis. This potential problem was examined in a sensitivity calculation, where the conditional failure probability of Event TAF in the base case was increased from  $4.0 \times 10^{-2}$  to 0.1. The resulting ATWS core damage frequencies were slightly higher than the base case values:

$$F_{IV} = 1.31 \times 10^{-6} \text{ per reactor-year and} \\ F_{IC} = 2.38 \times 10^{-6} \text{ per reactor-year.}$$

To compare this to the strategy of not lowering level to the TAF, the assumption was made that the elevated HCTL of 208°F is valid, accompanied by an assumed 90% probability that the reactor will not be depressurized if SLCS actuation is successful. If the SLCS fails, the probability of lowering level to the TAF to reduce power was also taken to be 0.9, that is,  $P(TAF|SLC) = 0.1$ . With these values, the ATWS core damage frequencies were calculated to be

$$F_{IV} = 6.15 \times 10^{-7} \text{ per reactor-year and} \\ F_{IC} = 8.95 \times 10^{-7} \text{ per reactor-year.}$$

Thus, the strategy of allowing HPCI and RCIC to inject at full flow during an ATWS seems to have a significant potential for reducing the ATWS core damage frequency; the new frequencies are a factor of approximately two lower than the base case. The main advantage from an operational point of view is enhanced simplicity; the current EPG guidance is complex and

operator actions have to be extremely well coordinated. However, the efficacy of not throttling the injection flow hinges on the validity of the elevated HCTL. If the HCTL cannot be increased, then allowing HPCI and RCIC to inject at full flow would essentially guarantee that emergency depressurization would be required, presenting a severe challenge to the operators. From the perspective of improved containment performance, any strategy that can reduce the ATWS core damage frequency will also reduce the challenge to containment and, therefore, can be viewed as a containment improvement; even though, in a strict sense, it may really be an accident management strategy.

The next improvement to be examined is the use of a hardened vent line leading from the wetwell airspace to an elevated release point outside the secondary containment. With a hardened vent line, the containment could be vented at an elevated pressure without releasing steam and hydrogen into the reactor building. Calculations for an 18-in. dia choke plane show that, neglecting moisture entrainment and flow resistance in the vent line, an 18-in. vent should be capable of removing approximately 10% of rated thermal power from containment (based on a rated thermal power of 3293 MW), with the containment pressure at 60 psig. Because the hardened vent is assumed to require manual actuation, the conditional failure probabilities assigned to Event CV in the base case remain unchanged, since they are dominated by failure of the operator to actuate the vent. However, the probabilities of Event V2 do change, because the effects of steam and hydrogen on equipment in the reactor building will be absent. The revised probabilities for Event V2 are listed below.

1. If HPCI is injecting, the suction is assumed to be from the CST. This is felt to be a reasonable assumption, because the latest revision to the EPG directs the operator to defeat the transfer of the HPCI suction to the suppression pool (see Reference 19). Therefore, venting has no effect on NPSH for HPCI. Because environmental effects in the reactor building are no longer a concern, Event V2 is assigned a conditional failure probability of 0.0.
2. If LPCI is injecting and the reactor is subcritical because of successful boron injection, then venting would have to fail both LPCI and CRD, because the CRD pumps are capable of providing adequate flow to keep the core cooled at this point in the sequence (see Reference 23). The probability of LPCI

failure is taken to be 0.2 due to the possible effects of venting on NPSH (see Reference 6). The CRD pumps are assumed to be unaffected by venting, because their suction is from the CST. Therefore, the failure probability of Event V2 is 0.0 as above.

3. If LPCI is injecting but the reactor is not shut down, that is, boron has not been injected or LPCI has not been throttled, then the CRD pumps alone are not capable of providing adequate core cooling. Therefore, for this case, the failure probability of Event V2 is taken to be 0.2.

With these changes, the base case ATWS core damage frequencies with hardened venting are

$$F_{IV} = 1.17 \times 10^{-6} \text{ per reactor-year and}$$

$$F_{IC} = 2.30 \times 10^{-6} \text{ per reactor-year.}$$

Note that the Class IV ATWS frequency is only slightly less than the base case frequency, and the Class IC frequency did not decrease at all. Therefore, the use of a hardened vent does not appear to be an effective strategy for ATWS mitigation. In addition, because the base case plant is assumed to have in-pedestal drain lines, which have been postulated to fail shortly after vessel breach (see Reference 36),<sup>a</sup> venting the containment could make the offsite consequences more severe if the vent valves were not closed prior to a significant release of radioactivity into the containment.

The use of containment sprays for mitigating an ATWS was not examined for the following reasons. First, if suppression pool cooling is not available, there is a high probability that the RHR system will also be unavailable for use in the containment spray mode, since failures that would disable suppression pool cooling would likely disable containment sprays, as well. Second, the diesel fire pumps, which are the other alternative spray source, are assumed to be inadequate (because of their low flow rate) for relieving the containment pressure rise expected for most ATWS sequences.

However, the diesel fire pumps may be useful for establishing a coolable debris bed in the drywell or as a means of long-term containment heat removal. To model the first possibility, the base case conditional failure probability of Event R2 in Figure 16 was reduced by a factor of 0.5. A reduction of 50% was

a. A. Payne (SNL) conference call with P. K. Niyogi (NRC) on May 1, 1989.

chosen, since the effectiveness of drywell sprays from the fire pump for cooling the core debris is highly uncertain; therefore, the failure probability of the fire system for performing this function was concluded to be indeterminate.

The conditional failure probability of Event HR is also reduced by 50% to model the potential effectiveness of containment sprays via the diesel fire pumps in removing decay heat from the containment atmosphere. Any eventual need to remove water from the suppression pool was neglected for this analysis. The effects of these changes on the offsite consequences of an ATWS sequence are shown in Table 20.

As a final sensitivity, the effect of increased HPCI system unavailability is examined. The reason for performing this sensitivity calculation is the very high

testing and maintenance unavailabilities that have recently been observed in industry.<sup>69</sup> The base case conditional failure probability of Event U1 was calculated, using data from Reference 7, with a contribution from maintenance unavailability of  $1.1 \times 10^{-2}$ . If this maintenance unavailability is increased to the value of  $5.0 \times 10^{-2}$  recommended in Reference 69, the conditional failure probability of Event U1 becomes  $8.0 \times 10^{-2}$ , which is rounded to 0.1 for the sensitivity calculation. With this higher value for Event U1, the ATWS core damage frequencies are calculated to be

$$F_{IV} = 1.31 \times 10^{-6} \text{ per reactor-year and}$$

$$F_{IC} = 2.40 \times 10^{-6} \text{ per reactor-year.}$$

Thus, the ATWS core damage frequency appears to be relatively insensitive to a significant increase in HPCI unavailability.

**Table 20.** Offsite consequences for ATWS with diesel fire pump containment sprays (per reactor-year)

ATWS Class	Mean Latent Fatalities	Mean Population Dose (Man-Rem) <sup>a</sup>	Mean Offsite Costs (\$)
IC (CM < CF)	1.00E-03	9.14E-01	5.49E+03
IV (CF < CM)	4.60E-03	4.60	1.91E+04
% decrease	2.3	1.9	2.8

a. The population dose is that received within a 50-mi radius of the plant.

## 8. QUANTITATIVE RISK ANALYSIS OF STATION BLACKOUT

SBO sequences can be grouped into two categories, based on the timing of core melt. The first, in which injection is lost soon after the loss of all AC power, is termed the short-term SBO, because core melt occurs very soon after the loss of all AC power. The other, in which injection is available for several hours and is then lost, is termed the long-term SBO, because core melt is delayed for several hours. The reference plant is assumed to be a BWR/4 with two emergency AC and two emergency DC power divisions. The primary source for unavailability data was the SBO analysis performed by SNL as part of NRC Task Action Plan A-44 (see Reference 70).

### 8.1 Accident Sequence Analysis

The accident sequence analysis for SBO was performed in a manner analogous to that of the ATWS sequences in Section 7. The base case front-end event tree is shown in Figure 17.

**8.1.1 Event Tree Quantification.** The following discussion gives the quantification scheme for the top events in the base case SBO event tree. Changes in the quantification that were made to examine potential improvements or to assess sensitivities are discussed in Section 8.4

**Te.** The initiating event is a loss of offsite power. The frequency of 0.12 per reactor-year was taken from Reference 70. Some variation in this value from plant to plant can be expected.

**DC.** This event represents a common-mode failure of the emergency station batteries, which supply power to HPCI, RCIC, and the SRV solenoids. Loss of DC power results in an immediate loss of all injection capability and the ability to depressurize the reactor. This leads to rapid core uncover and core melt with the reactor at high pressure, a short-term SBO. The failure probability of  $1.0 \times 10^{-5}$  used was taken from Reference 70.

**DG.** Event DG models the initial availability of the onsite emergency diesel generators (EDGs). The failure probability of  $1.7 \times 10^{-3}$  used was taken from Reference 70.

**B-.** Event B- represents the probability that AC power is not recovered within 30 min after the initiating event. The value of 30 min was chosen because it

represents the earliest possible time at which offsite power recovery is likely ( $>0.5$ ). The probability was calculated by modeling the time to recover offsite power as a random variable, which can be characterized by a two-parameter Weibull distribution.<sup>71</sup> Using the maximum likelihood estimates of the Weibull parameters computed in Reference 71, the probability of not recovering offsite power within 30 min is calculated to be 0.49. No credit is given for recovery of the onsite emergency diesel generators during the first 30 min.

**U1.** Event U1 represents the probability that neither HPCI nor RCIC is initially available. Using values from Reference 70, this probability is calculated to be  $2.3 \times 10^{-3}$ .

**B2.** Event B2 represents the conditional probability that AC power is not recovered within 2 h, given that it was not recovered within 30 min. Two hours represents the end of the early time phase of the accident, when core damage can be avoided by recovery of AC power (see Reference 70). The conditional probability of not recovering offsite power was calculated as for Event B- above:

$$P(\text{nOSP @ } 2 \text{ h} | \text{nOSP @ } 0.5 \text{ h}) = (0.1807)/(0.4942) = 0.366.$$

Some credit is also given for recovering the onsite emergency diesel generators during the first 2 h. Table E.4-1 in Reference 6 gives a conditional failure-to-repair probability of 0.75. Thus, the conditional probability of not recovering AC power within the first 2 h becomes

$$P(B2) = (0.366) * (0.75) = 0.27.$$

**U2.** Event U2 represents the conditional probability that neither HPCI nor RCIC continues to operate beyond the first 2 h, given that HPCI or RCIC was initially available. Each of the following three possibilities must be considered in calculating the failure probability of Event U2.

1. HPCI and RCIC are both available initially; failure of Event U2 requires failure of both HPCI and RCIC.
2. HPCI available, RCIC failed initially; failure of Event U2 requires failure of HPCI.

**Figure 17.** Base case loss of offsite power event tree.

3. RCIC available, HPCI failed initially; failure of Event U2 requires failure of RCIC.

With these three possibilities, the expression for  $P(U2)$  becomes

$$P(U2) = P[(HPCI_2 \cap RCIC_2) / (HPCI_0 \cup RCIC_0)]$$

where

$HPCI_2$  represents HPCI failure after 2 h because of conditions resulting from the prolonged loss of AC power

$RCIC_2$  represents RCIC failure after 2 h because of conditions resulting from the prolonged loss of AC power

$/HPCI_0$  represents initial availability of HPCI

$/RCIC_0$  represents initial availability of RCIC.

Using data from Reference 6 for  $HPCI_2$  and  $RCIC_2$ , and data from Reference 70 for  $/HPCI_0$  and  $/RCIC_0$ , the conditional failure probability of Event U2 is calculated to be  $5.3 \times 10^{-3}$ .

**B6.** Event B6 represents the conditional probability that AC power is not recovered within 6 h after the initiating event, given that it was not recovered within 2 h. Six hours was chosen because it represents the point at which battery depletion is assumed to become a significant concern. It is also the point at which continued HPCI operation is threatened by reactor depressurization. The conditional failure probability is calculated analogously to that of Event B2 above, using a diesel nonrecovery probability of 0.81 from Table E.4-1 in Reference 6. The resulting value is 0.14.

**X.** Event X represents the probability that the reactor is not depressurized at the time that high pressure injection is lost, or that reclosure of the SRVs causes the reactor to repressurize following the loss of high pressure injection. The failure probability is conditional upon the path taken through the event tree. Since ADS will not function during SBO (a discharge pressure signal from the low pressure ECCS pumps is needed), only manual depressurization is considered. For sequences where high pressure injection is lost in less than 6 h, the value of  $2.4 \times 10^{-3}$  from Reference 6 is

used. Reference 70 uses a value of  $5.0 \times 10^{-3}$  for operator failure to depressurize the reactor, but it is felt this is too conservative. For sequences where high pressure injection continues through the 6-h point, the continued operation of these turbine-driven injection systems is assumed to initially depressurize the reactor. However, battery depletion as a result of extended HPCI/RCIC operation is assumed to result in SRV reclosure and subsequent repressurization; therefore, the conditional failure probability of Event X is taken to be 1.0 for this case. Reference 8 uses a central estimate value of 0.99 for this event.

**V1.** Event V1 represents the use of low pressure systems to inject coolant into the reactor vessel. Using the diesel fire pumps as a source of injection is not considered, since injection would have to be aligned within approximately the first 2 h. Because all other currently available means of low pressure injection require AC power, the base case conditional failure probability of Event V1 is taken to be 1.0 for sequences where AC power has not been recovered.

**W.** Event W models long-term containment heat removal. For sequences in which AC power is recovered, Event W is quantified as follows. First of all, the assumption is made that equipment unavailability dominates the HEP for the suppression pool cooling mode of RHR. The RHR equipment unavailability is taken to be  $1.0 \times 10^{-4}$  (see Reference 6). Secondly, the probability of not recovering the PCS is taken to be

$$P(PCS) = P(\text{MSIV not open in 15 h}) + P(\text{PCS not operable}) \text{ (see Reference 6).}$$

Using data from Reference 5,

$$P(PCS) = 1.0 \times 10^{-3} + 5.0 \times 10^{-3} = 6.0 \times 10^{-3}.$$

Finally, credit is given for using the reactor water cleanup (RWCU) system in the blowdown mode of operation as a viable means of heat removal. This is based on three supporting references, which indicate that using the system for this purpose is feasible, even though past PRAs generally have not taken credit for this means of heat removal. First, calculations in Reference 7 show that using the RWCU system in the blowdown mode can be an effective means of removing decay heat from the reactor vessel and thus from the containment. Second, a hand calculation was done, based on temperature and flow data in Reference 15, which confirms the results in Reference 7. Finally,

operational experience confirms the adequacy of the RWCU system to remove decay heat from the reactor.<sup>a</sup>

Because alignment of the RWCU system to remove decay heat from the reactor would require fairly complex operator actions, the HEP is assumed to dominate the equipment unavailability. Since this would be an uncommon evolution, which would have to be performed under fairly high stress, the HEP is taken to be 0.9.

Combining these failure probabilities gives the overall failure probability for Event W for sequences where AC power is available:

$$P(W) = (1.0 \times 10^{-4}) * (6.0 \times 10^{-3}) * (0.9) \\ = 5.4 \times 10^{-7}.$$

For sequences where AC power is not available, the conditional failure probability is assumed to be 1.0, since all current means of containment heat removal are dependent upon the availability of AC power.

CV. This is the probability that the containment is not vented. For the base case analysis, the assumption is made that an 18-in. ductwork vent from the wetwell is available. A value of 0.1 is used for the vent unavailability in this case for those sequences where AC power is available. If AC power is not available, the base case conditional failure probability for containment venting is taken to be 1.0.

V2. Event V2 models the continued availability of injection in those sequences where containment venting has occurred. The value of 0.35 was derived as for the ATWS sequence in Section 7.1.

The resulting base case SBO core damage frequencies are:

- ST-SBO  $1.57 \times 10^{-6}$  per reactor-year
- LT-SBO  $3.75 \times 10^{-6}$  per reactor-year.

## 8.2 Containment Event Tree Analysis

Two base case SCETs were constructed to model the containment response to the challenges arising from

---

a. NRC Event No. 15451. April 26, 1989, event at Grand Gulf Unit One in which the RWCU system was proved to remove decay heat from the reactor vessel and was then considered as an alternate method of shutdown decay heat removal.

short-term and long-term SBO sequences. The detailed quantification of the top events in each of these base case SCETs is given below. For a more detailed discussion of the SCET methodology, see Reference 3.

### 8.2.1 Short-term SBO (Class IB1)

The base case short-term SBO SCET is shown in Figure 18.

PD. The initiating event is the short-term SBO plant damage state, which results in early loss of injection and extensive core damage within a few hours after the loss of all AC power. The conditional probability of Event PD is 1.0.

R1. Event R1 models recovery of the sequence prior to vessel failure through recovery of vessel injection. Because the dominant mode of failure for vessel injection is assumed to be the loss of AC power, Event R1 is quantified by calculating the conditional nonrecovery probability of AC power at 3 h, where 3 h is the estimated time of core plate failure (with the initiating event at time 0) calculated by ORNL using BWRLTAS/BWRSAR/MELCOR.<sup>b</sup> There is significant uncertainty as to the latest point in the sequence at which recovery of injection could successfully terminate core damage and prevent vessel failure. During discussions with analysts from ORNL, a consensus was reached that using the time of core plate failure as a surrogate for this point in the sequence is a conservative but reasonable approach. If injection were recovered prior to core plate failure, recovery would be almost certain. If injection were recovered after core plate failure, recovery might still be possible, but there is uncertainty as to what the recovery probability would be, with the uncertainty increasing with the time after core plate failure.

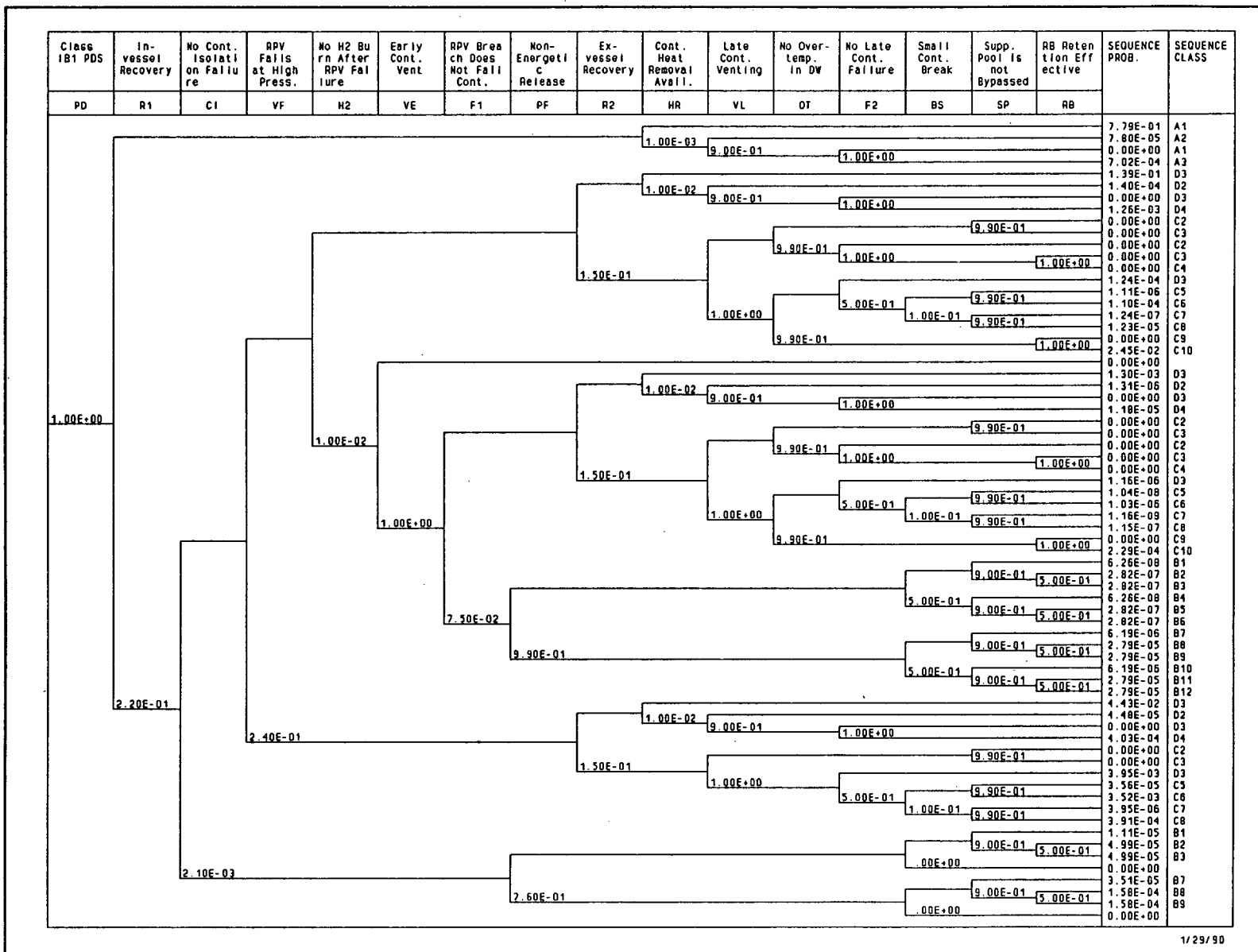
Some of the short-term SBO sequences have injection initially available, with injection being lost after 2 h. The fraction of such sequences is

$$(1.42 \times 10^{-7}) / (1.57 \times 10^{-6}) * 100\% = 9.0\%.$$

Thus, 91% of the short-term SBO sequences involve an immediate loss of injection. In quantifying Event R1, the simplifying assumption was made that all short-term SBO sequences involve an immediate loss of injection. The conditional failure probability of

---

b. ORNL analysis performed for Mark II CPI Program, as documented in ORNL Monthly Reports.



1/29/90

Figure 18. Base case short-term station blackout SCET.



Event R1 then is calculated using the two-parameter Weibull distribution of Reference 71 for the nonrecovery probability of offsite power, along with the assumption that the onsite EDGs are not recoverable during the time period spanned by the calculation. The result is

$$P(R1) = P(nOSP@3h|nOSP@0.5 h) = (0.1089)/(0.4942) = 0.22.$$

**CI.** Event CI models the presence of a preexisting large leak in containment. As in the Class IC ATWS, failure of Event CI is assumed to prevent further pressurization of the containment, and is modeled as a small break (large leak) for purposes of quantifying later events in the SCET. The failure probability of  $2.1 \times 10^{-3}$  used for Event CI is taken from Reference 29 and is in line with the estimate given in Reference 65.

**VF.** The probability that the reactor vessel fails at high pressure is calculated by determining the fraction of short-term SBO sequences where depressurization has not occurred. The probability of taking the lower branch of Event VF is then just the fraction of short-term SBO sequences where the vessel has been depressurized. From Figure 17, this fraction is

$$P(VF) = (3.71 \times 10^{-7})/(1.57 \times 10^{-6}) = 0.24.$$

**H2.** Event H2 is quantified at  $1.0 \times 10^{-2}$  as for the Class IC ATWS.

**VE.** Event VE questions whether the containment is vented prior to or at the time of vessel failure. Given that early recovery of vessel injection has failed (failure of Event R1), the assumption is made that AC power is not available. Therefore, for the base case, the conditional failure probability of Event VE is taken to be 1.0, since existing vent systems require AC control power. Preemptive venting will be considered in Section 8.4

**F1.** Event F1 models overpressure failure of the containment at or shortly after the time of vessel failure. The Reference 29 quantification was followed for this event. Since failure of the vessel at high pressure, per se, is not likely to cause containment pressure to approach the calculated ultimate pressure capacity (see Reference 29),<sup>a</sup> high pressure vessel failure alone is assumed to be incapable of causing early overpressure failure for short-term SBO sequences. If the vessel

fails at high pressure, and a hydrogen burn occurs either during or after core melt, the Reference 29 failure probability of  $7.5 \times 10^{-2}$  is used.

**PF.** A driving force for an energetic release (also known as a puff release) exists for sequences involving failure (the lower branch) of Event PF. Because a puff release is of concern only in cases of early containment failure, Event PF is questioned only for sequences with an accompanying failure of Event F1. For short-term SBO, the dominant contributor to the puff release driving force is assumed to be failure of the vessel at high pressure. Hydrogen burns are not considered, since they do not provide a sustained driving force; the pressure spike following a hydrogen burn is of too short a duration to provide a sustained energetic release. If the vessel fails at high pressure, the early release is expected to most likely be energetic. Therefore, for short-term SBO, the probability of a puff release is estimated to be 0.99 for sequences where the vessel fails at high pressure. For sequences involving failure of containment isolation (Event CI), the probability of a puff release is estimated from the likelihood of high pressure vessel failure as

$$P(PF|CI) = P(VF) = 1 - 0.24 = 0.76.$$

**R2.** As in Class IC, Event R2 models the establishment of a coolable debris bed following failure of the reactor vessel and release of core debris to the containment. However, unlike Class IC, the suppression pool is not expected to be saturated at this point in the sequence (see References 4,9,29). Therefore, the quantification of Event R1 above is followed. Thus, the failure probability of Event R2 is taken to be the conditional probability of not recovering offsite power by 4.5 h (see Reference 8), given that in-vessel recovery (Event R1) has failed. This gives

$$P(R2|R1) = P(nOSP@4.5 h)/P(R1) = (5.65 \times 10^{-2})/(0.37) = 0.15.$$

Note that there is some simplification involved in this calculation, since not all short-term SBO sequences have DC power available. Since DC control power is needed for circuit breaker control, the restoration of offsite power will be more difficult if DC power is not available. However, this added complication has been neglected. In addition, there is the assumption that covering the core debris with water will ensure coolability.

**HR.** As in the Class IC ATWS, Event HR models the availability of long-term containment heat removal, via either RHR suppression pool cooling or containment sprays, given that an ex-vessel coolable debris

a. ORNL analysis performed for Mark II CPI Program, as documented in ORNL Monthly reports.

bed has been established (success of Event R2). Reference 8 uses a central estimate failure probability of  $1.0 \times 10^{-2}$  for this sequence, assuming that the suppression pool is subcooled. If in-vessel recovery was successful (R1), this value has been further reduced by a factor of 10 to  $1.0 \times 10^{-3}$ , to reflect the additional time available for operator action.

**VL.** Event VL models containment venting after the time of reactor vessel failure. If ex-vessel recovery fails, or if it is successful but there is a failure to establish long-term containment heat removal, then heat removal can still be provided by venting the containment. The quantification of this event given for the Class IC ATWS above is followed here for those cases where AC power is available (indicated by success of Event R1 or R2). If AC power is not available (failure of Event R2), then venting is assumed to not be possible; therefore,  $P(VL|R2) = 1.0$ .

**OT.** As in the Class IC ATWS, failure of ex-vessel recovery is felt to make high temperatures in the vicinity of the drywell head seal extremely likely. Therefore, for the base case,  $P(OT|R2)$  is taken to be 0.99.

**F2.** As in the Class IC ATWS, Event F2 models late containment failure as a result of temperature and pressure loads. For those sequences with failure of Event OT, that is, high temperatures in the vicinity of the drywell head seal, accompanied by elevated pressure, late failure due to degradation of the drywell head seal is considered certain. Therefore,  $P(F2|OT)$  is taken to be 1.0. For sequences without high drywell temperatures ( $\neg OT$ ), the likelihood of late overpressure failure is highly uncertain. Therefore, for this case, Event F2 is assigned an indeterminate conditional failure probability of 0.5.

The remaining events in the SCET were quantified exactly as for the Class IC ATWS.

**8.2.2 Long-term SBO (Class IB2).** The long-term SBO SCET is shown in Figure 19.

**PD.** The initiating event is the long-term SBO plant damage state, in which core melt is delayed for several hours by the operation of HPCI or RCIC. The conditional probability of Event PD is 1.0.

**R1.** Event R1 models recovery of the sequence prior to vessel failure via recovery of vessel injection. Because the dominant mode of failure for vessel injection is again assumed to be the loss of AC power, Event R1 is quantified by calculating the conditional AC nonrecovery probability at 11.6 h, where 11.6 h is

the time by which Reference 8 calculates that injection must be restored if the sequence is to be recovered in-vessel. Therefore, the conditional failure probability of Event R1 becomes the probability of not recovering AC power by 11.6 h, given that it has not been recovered during the first 6 h. In contrast with short-term SBO, complications that battery depletion would present for the recovery of AC power cannot be neglected. For example, the assumption is made that battery depletion will prevent recovery of the onsite EDGs, since power from the site emergency batteries typically is required to flash the generator field. In addition, all large circuit breakers ( $\geq 4$  kV) will have to be operated locally, since DC control power is typically required for remote operation. To account for this, the nominal failure probability of Event R1 has been increased by an arbitrary factor of 50%. The nominal  $P(R1)$  is given by

$$P(R1) = P(\text{nOSP}@11.6 \text{ h} | \text{nOSP}@6 \text{ h}) \\ = (5.16 \times 10^{-3}) / (3.16 \times 10^{-2}) = 0.16.$$

Accounting for the lack of DC power gives

$$P(R1) = 0.16 * 1.5 = 0.24.$$

The probabilities of not recovering offsite power were calculated, as for short-term SBO, by assuming a two-parameter Weibull distribution in accordance with Reference 71.

**CI.** As for short-term SBO, the probability of a preexisting large containment leak is taken to be  $2.1 \times 10^{-3}$ , the value used in Reference 29.

**VF.** The probability that the reactor vessel fails at high pressure is calculated by determining the fraction of long-term SBO sequences where depressurization has not occurred. The failure probability of Event VF then is just the fraction of long-term SBO sequences where the vessel has been depressurized. As Figure 17 shows, there is only one sequence resulting in a long-term SBO plant damage state. For this sequence, battery depletion is assumed to result in closure of the SRVs and repressurization of the reactor vessel. Therefore, vessel failure at high pressure is extremely likely. Accordingly, the conditional probability for the lower branch of Event VF is taken to be  $1.0 \times 10^{-2}$ .

**H2.** Event H2 is quantified as before at  $1.0 \times 10^{-2}$ .

**VE.** Event VE questions whether the containment is vented prior to or at the time of vessel failure. Given that early recovery of vessel injection has failed (R1)

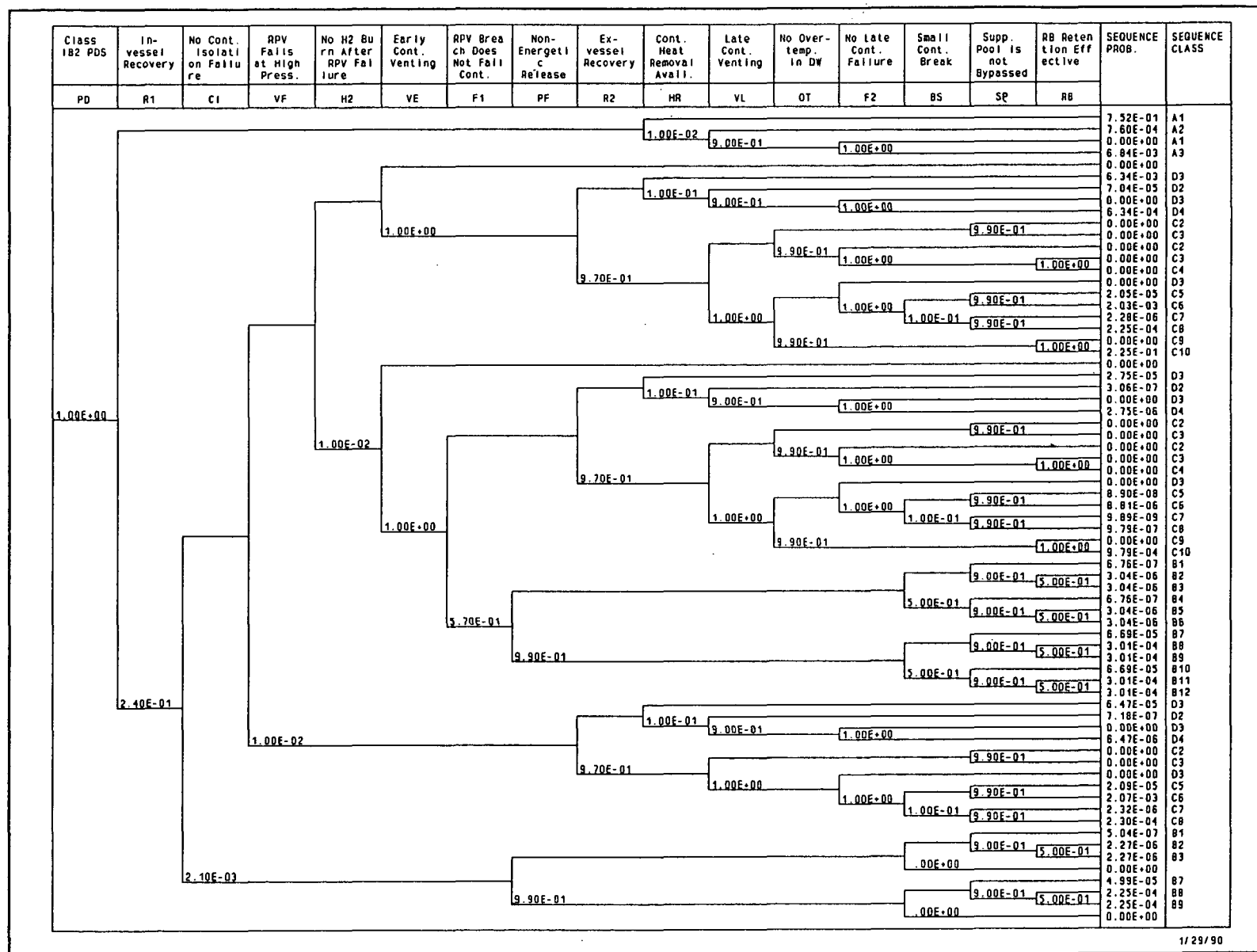


Figure 19. Base case long-term station blackout SCET.

the assumption is made that AC power is not available. Therefore, for the base case, the conditional failure probability of Event VE is taken to be 1.0, since existing vent systems require AC control power.

**F1.** As before, Event F1 models overpressure failure of the containment at or near the time of vessel failure. The Reference 29 quantification was followed for this event. Because failure of the vessel at high pressure, per se, is not likely to cause containment pressure to exceed the PCPL (see Reference 29), high pressure vessel failure alone is assumed to be incapable of causing early overpressure failure. If the vessel fails at high pressure, and a hydrogen burn occurs either during or after core melt, the Reference 29 failure probability of 0.57 is used.

**PF.** The determination of the probability of an energetic release for long-term SBO is similar to that for short-term SBO. Because the probability of high pressure vessel failure is taken to be 0.99 for long-term SBO, this becomes the failure probability of Event PF for all long-term SBO sequences involving early containment failure (CI or F1).

**R2.** As in the previous plant damage states, Event R2 models the establishment of a coolable debris bed following vessel failure. As in short-term SBO, the dominant failure mode for coolant injection is assumed to be the loss of AC power. Therefore, the failure probability of Event R2 is taken to be the conditional probability of not recovering offsite power in time to prevent significant CCI, given that offsite power was not recovered in time to prevent vessel failure. Because the batteries are depleted in the dominant long-term SBO sequence, recovery of the onsite EDGs is not considered. In addition, the lack of DC circuit breaker control power will complicate the recovery of offsite power. Therefore, as for Event R1, the nominal failure probability of Event R2 is arbitrarily increased by 50% to account for this. Thus, the conditional failure probability of Event R2 is given by

$$P(R2) = [P(nOSP @ 12.5 h) / P(nOSP @ 11 h)] * 1.5 = 0.97.$$

The times used in the calculation of P(R2) are those used by Reference 8.

**HR.** The availability of long-term containment heat removal following vessel failure is quantified as for short-term SBO, using the value from Reference 8. However, the values used for short-term SBO have been increased by a factor of 10 to account for the increased likelihood that suppression pool saturation

will cause the RHR pumps to fail as a result of inadequate NPSH.

**VL.** The quantification of late containment venting used for the previous plant damage states is followed for long-term SBO, as well.

The remaining events in the long-term SBO SCET were quantified as for short-term SBO.

Tables 21 and 22 show the conditional containment release mode probabilities for short and long-term SBO, respectively.

As these tables show, both short- and long-term SBO are most likely to result in an end state where the reactor vessel remains intact. However, there is a significant probability that long-term SBO will result in a late unscrubbed release because of failure of the dry-well head seal.

### 8.3 Consequence Analysis

The base case consequence results are presented in Table 23.

These consequences were obtained by multiplying the conditional consequences in Table 15 by the release probabilities and accident sequence frequency, then summing over the 10 release categories using Equation 1-1, as was done for ATWS sequences.

### 8.4 Sensitivities and Effects of Potential Improvements

The effects of several sensitivities and potential improvements on both core damage frequency and risk are evaluated in this section.

The first improvement to be evaluated is the addition of an onsite combustion generator, which can be started independently of both onsite and offsite power sources (the use of a small portable generator is not modeled, since such a generator would probably not be capable of providing enough power to safely shut down the plant). The assumption is made that such a generator (referred to hereafter as a blackstart gas turbine, although a diesel generator would also suffice) could be used to supply AC and DC loads needed to safely shut down the reactor, including power to the SRV solenoids that is needed for the enhanced depressurization improvement discussed in Section 6. Some plants already have such a generator. For a more detailed description of this option, as it has been implemented at one particular plant, see Reference 6. Note

**Table 21.** Conditional containment release mode probabilities for short-term SBO sequences

Release Mode	Conditional Probability
A1	7.79E-01
A2	7.80E-05
A3	7.02E-04
Recovered in-vessel	7.80E-01
B1	1.12E-05
B2	5.02E-05
B3	5.02E-05
B4	6.26E-08
B5	2.82E-07
B6	2.82E-07
B7	4.13E-05
B8	1.86E-04
B9	1.86E-04
B10	6.19E-06
B11	2.79E-05
B12	2.79E-05
Early containment failure	5.88E-04
C1	0.00
C2	0.00
C3	0.00
C4	0.00
C5	3.67E-05
C6	3.63E-03
C7	4.08E-06
C8	4.03E-04
C9	0.00
C10	2.47E-02
Late containment failure or venting	2.88E-02
D2	1.86E-04
D3	1.89E-01
D4	1.67E-03
Recovered ex-vessel	1.91E-01

**Table 22.** Conditional containment release probabilities for long-term SBO sequences

Release Mode	Conditional Probability
A1	7.52E-01
A2	7.60E-04
A3	6.84E-03
Recovered in-vessel	7.60E-01
B1	1.18E-06
B2	5.31E-06
B3	5.31E-06
B4	6.76E-07
B5	3.04E-06
B6	3.04E-06
B7	1.17E-04
B8	5.26E-04
B9	5.26E-04
B10	6.69E-05
B11	3.01E-04
B12	3.01E-04
Early containment failure	1.86E-03
C1	0.00
C2	0.00
C3	0.00
C4	0.00
C5	4.15E-05
C6	4.11E-03
C7	4.61E-06
C8	4.56E-04
C9	0.00
C10	2.26E-01
Late containment failure or venting	2.31E-01
D2	7.14E-05
D3	6.43E-03
D4	6.43E-04
Recovered ex-vessel	7.14E-03

**Table 23.** Base case consequence results for SBO sequences (per reactor-year)

	Mean Latent Fatalities	Population Dose (Rem) <sup>a</sup>	Offsite Costs (\$)
ST-SBO	2.01E-04	1.95E-01	1.09E+03
LT-SBO	2.98E-03	2.80	1.07E+04

a. The population dose is that received within a 50-mi radius of the plant.

that a dedicated safe shutdown facility, such as installed at Fermi 2, could also satisfy the needs of this improvement.

The effect of this improvement was evaluated by adding an event (GT) to the front-end SBO event tree (Figure 17) to represent the possibility of using the gas turbine to supply essential AC and DC loads. The availability of the gas turbine is questioned during the first 30 min of the sequence only; if it cannot be brought on line within the first 30 min, it is assumed to be unavailable for the remainder of the sequence. It is questioned following failure of all onsite emergency diesel generators (Event DG) and following the common-mode failure of the emergency station batteries (Event DC). Reference 61 assigns Event GT a failure probability of 0.35; this value has been retained here.

The effects of the gas turbine on the SBO core damage frequency are shown in Table 24.

**Table 24.** Effects of onsite blackstart gas turbine generator on SBO core damage frequency

Plant Damage State	Base Case Frequency	Frequency with GT
ST-SBO	1.57E-06	5.50E-07
LT-SBO	3.75E-06	1.31E-06

As this table shows, the effect of the gas turbine in reducing SBO core damage frequency is significant: the short-term and long-term SBO frequency are both reduced by approximately 65%.

The effects of the gas turbine on offsite consequences are shown in Table 25.

**Table 25.** Consequence results for SBO sequences with blackstart gas turbine (per reactor-year)

	Mean Latent Fatalities	Population Dose (Rem) <sup>a</sup>	Offsite Costs (\$)
ST-SBO	7.05E-05	6.83E-02	3.82E+02
LT-SBO	1.04E-03	9.78E-01	3.73E+03

a. The population dose is that received within a 50-mi radius of the plant.

Compared to the base case results in Table 23, the addition of the gas turbine reduces each risk measure by 65%, as expected.

The next mitigation strategy to be evaluated is preemptive venting, as has been suggested by at least one utility as a means of preventing containment failure for SBO sequences (see Reference 7). The proposed idea is to vent the containment early in the sequence before there has been a significant rise in containment pressure, which could present a personnel hazard since the vent valves would have to be opened manually under the existing vent design. Note that this differs from the venting strategy endorsed by the latest revision to the EPGs prepared by the BWR Owners' Group (see Reference 19).

For the sensitivity case, preemptive venting is included in the short-term and long-term SBO SCETs, with no provision for closing the vent valves following vessel failure. To model preemptive venting for this case, the SCETs were modified as follows. The failure probability for a preexisting large leak (Event CI) was changed to 1.0 to model the containment breach caused by opening the vent line. Because the diameter of the vent line is assumed to be 18 in., the breach caused by venting was modeled as a large break ( $>1.0$  ft<sup>2</sup>). Therefore, the conditional failure probability of Event BS was changed to 1.0. The probability of suppression pool bypass (Event SP) was assumed to be unchanged from the base case value. With the vent opened preemptively, there is assumed to be no decontamination of the release by deposition in the reactor building, since the HVAC ductwork should not be overpressurized; therefore, Event RB is assigned a conditional failure probability of 1.0.

Preemptive venting effectively changes all late releases and sequences with late (ex-vessel) recovery into early releases that occur prior to, or at the time of, vessel failure. The effect of this on the offsite consequences is shown in Table 26.

**Table 26.** Effect of preemptive venting on the consequences of SBO (per reactor-year)

	Mean Latent Fatalities	Population Dose (Rem) <sup>a</sup>	Offsite Costs (\$)
ST-SBO	1.93E-03	1.68	1.18E+04
LT-SBO	3.56E-03	3.25	2.07E+04

a. The population dose is that received within a 50-mi radius of the plant.

As this table shows, preemptive venting (with no reclosure of the vents) significantly increases the population dose, the mean number of latent fatalities, and the offsite costs associated with the release.

In order for preemptive venting to be useful, the vent valves would have to be reclosed prior to the release of a significant amount of activity to the environment. This could be done, in theory, by closing the valves when the radiation level in the vent lines exceeds a predetermined limit. This strategy presupposes the existence of independently powered radiation monitors and vent valve operators, neither of which is known to currently be in use at any Mark II plant. If the vent valves were closed prior to events that would cause a significant containment pressure rise, then preemptive venting would not lessen the challenge to the containment from overpressurization. Based on BWRLTAS/BWRSAR/MELCOR calculations performed by ORNL,<sup>a</sup> this would appear to be the case for short-term SBO, where no significant containment pressurization occurs until the time of core plate failure. If the assumption is made that the vent valves would be closed prior to core plate failure because of high vent line radiation levels resulting from core damage, then preemptive venting would not appear to be a useful strategy for mitigating short-term SBO sequences.

a. ORNL analysis performed for Mark II CPI Program, as documented in ORNL Monthly Reports.

In long-term SBO sequences, containment pressure (in the absence of venting) could be high enough at the time of core plate failure to justify preemptive venting as a means of lessening the late overpressure challenge to the containment. BWRLTAS/BWRSAR/MELCOR calculations were not available for this sequence, but the analysis in Reference 9 indicates that significant containment pressurization could occur before vessel failure (the degree of pressurization is, of course, both highly plant-specific and uncertain). However, closing the vent valves prior to vessel failure would not mitigate late thermal failure, since Reference 9 also indicates that containment temperature does not increase greatly until after vessel failure. There also is much uncertainty as to whether late containment challenges would be due to overpressure or overtemperature. On these merits, the usefulness of preemptive venting for long-term SBO is difficult to quantify.

A sensitivity case was also examined where venting is assumed to take place at the PCPL defined in Reference 19 via a hardened vent from the wetwell air-space. The vent valves are assumed to be powered from a backup source of DC power that is not affected by the availability of offsite or on-site AC power; therefore, they can be remotely operated from the control room. To model this case, the failure probability of Event VL in the short-term and long-term SBO SCETs was set to 0.1 for all branches. In addition, since the vent pipe is assumed to be able to withstand PCPL venting pressures, there should be no failure of HVAC ductwork in the reactor building. Accordingly, P(RBI/VL) was set to 1.0, that is, no reactor building decontamination of fission products occurs for the vented releases. The revised consequences are shown in Table 27.

**Table 27.** Effect of venting at the PCPL on the consequences of SBO (per reactor-year)

	Mean Latent Fatalities	Population Dose (Rem) <sup>a</sup>	Offsite Costs (\$)
ST-SBO	2.06E-04	2.09E-01	1.06E+03
LT-SBO	2.99E-03	2.81	1.07E+04

a. The population dose is that received within a 50-mi radius of the plant.

A comparison of this table with Table 23 indicates that venting at the PCPL via a hardened wetwell vent does not reduce SBO risk. In fact, risk may actually be increased somewhat, since venting takes place after reactor vessel breach, when there is a very high probability of suppression pool bypass. Also, recall that the hardened vent line bypasses the reactor building, so that there is no decontamination of the release as a result of HVAC ductwork failure.

The next improvement to be evaluated is the use of the diesel fire pump for injection into the vessel. To prevent core damage in the short-term SBO sequences, injection would have to begin within approximately 2 h. This is not likely because of the need to connect hoses via spoolpieces and manually operate large isolation valves at various locations inside the reactor building. For these reasons, the latest NUREG-1150 analysis gives no credit for using the diesel fire pumps during short-term SBO at Grand Gulf, even though substantial improvements have been made at Grand Gulf to reduce the time needed to establish injection from the firewater system.<sup>72</sup> Even if similar improvements were made at Mark II plants to allow quicker connection of the fire protection system, the high level of coordination required to successfully establish the connections and open the valves in the reactor building, under conditions of high stress, does not allow much credit to be given. Therefore, use of the diesel fire pumps for preventing core damage due to short-term SBO will not be considered further. If the diesel fire pumps were connected to the RHR system, for example, via a 6- or 8-in. pipe with double manual isolation valves, this improvement, in conjunction with enhanced depressurization capability and containment venting could reduce the SBO risk by at least an order of magnitude. This option was not quantitatively evaluated. However, the diesel fire pumps may be of use in mitigating the short-term SBO challenge to containment and the offsite release. This is discussed further below.

For long-term SBO sequences, much more time is available for operator action. Reference 72 evaluated use of the diesel fire pumps as a potential recovery action for long-term SBO sequences. There, the mean unavailability of  $3.0 \times 10^{-2}$  (at 12 h) was attributed to operator error in aligning the system. However, there is a problem with using the diesel fire pumps for long-term SBO, namely battery depletion due to continued operation of HPCI and RCIC for vessel injection during the initial portion of the sequence. Even if injection with the diesel fire pumps were successful, battery depletion would result in eventual reclosure of the SRVs and repressurization of the reactor vessel above the

shutoff head of the fire pumps. Therefore, using the diesel fire pumps would appear to be a useful strategy only in conjunction with a modification to ensure the continued availability of DC power to the SRV solenoids for the duration of the blackout.

The front-end SBO event tree (Figure 17) was modified to include credit for using the diesel fire pump for injection during long-term SBO. This was done by changing the conditional failure probability of Event V1 to 0.1: this is the HEP value of  $3.0 \times 10^{-2}$  from Reference 72, plus the probability that the diesel fire pump fails to start (the rare event approximation is used), which is estimated at  $5.0 \times 10^{-2}$ .<sup>72,73</sup> The value obtained by this method was rounded to 0.1. In addition, the failure probability of Event X for this branch was requantified at  $2.4 \times 10^{-3}$  to reflect the addition of a backup DC supply to the SRV solenoids, along with modifications to ensure SRV operability in a severe accident environment. Finally, the assumption is made that the containment vent valves have been modified to operate from DC power supplied from the new DC source. To reflect this, the conditional failure probability for containment venting was changed to 0.1. With these alterations, the core damage frequency for long-term SBO is reduced from the base case value of  $3.75 \times 10^{-6}$  per reactor-year to  $3.83 \times 10^{-7}$  per reactor-year. Note that the addition of a DC supply for the containment vent valves makes venting available for short-term SBO; however, without injection, the short-term SBO core damage frequency is unaffected.

The inclusion of these modifications also causes an apparent increase in the SBO-induced Class II (TW) core damage frequency. However, this is only an *apparent* increase, since recovery of AC power in the very long term (the dominant failure mode of containment heat removal for this sequence is loss of AC power) has not been modeled.

As mentioned earlier, the diesel fire pumps could be useful in mitigating the containment challenge and off-site release that result from a short-term SBO, since they might be useful in establishing a coolable debris bed on the drywell floor. To model this possibility, the conditional failure probability of Event R2 was reduced by a factor of 0.5. A reduction of 50% was chosen because the effectiveness of drywell sprays from the fire pump for cooling the core debris is uncertain; therefore, the failure probability of the fire system for performing this function was concluded to be indeterminate.

The conditional failure probability of Event HR is also reduced by 50% to model the potential effectiveness of containment sprays via the diesel fire pumps in



removing decay heat from the containment atmosphere. Any eventual need to remove water from the suppression pool has been neglected for this analysis. It is not thought to present a major difficulty for short-term SBO, since AC power would almost certainly be recovered before the need to remove water from the suppression pool arose.

The net reduction in offsite consequences effected by these modifications is shown in Table 28.

**Table 28.** Effects of diesel fire pump on offsite consequences of SBO (per reactor-year)<sup>a</sup>

	Mean Latent Fatalities	Population Dose (Rem) <sup>b</sup>	Offsite Costs (\$)
ST-SBO	1.06E-04	1.09E-01	5.56E+02
LT-SBO <sup>c</sup>	3.05E-04	2.86E-01	1.09E+03
Total Reduction (%)	87.1	86.8	86.0

a. This case includes backup DC power to SRV solenoids and containment vent valves, as well as modifications to ensure SRV operability in a severe accident environment.

b. The population dose is that received within a 50-mi radius of the plant.

c. The reduction in LT-SBO risk measures is due to the reduction in core damage frequency effected by using the diesel fire pumps for RPV injection.

The last sensitivity to be evaluated is the decrease in SBO risk that could be effected by deliberate flooding of the drywell head. The details of this improvement are discussed in Section 4.3.8. Essentially, a modification would be needed to allow an operator to transfer water from the spent fuel pool to the drywell head following a loss of all AC power. The potential benefits associated with drywell head flooding are twofold. First, the water may provide a large enough heat sink to prevent late thermal failure of the drywell head seal (or other elastomeric seals in the drywell head region).

Second, any release of fission products through the drywell head seal may be scrubbed to some extent by the overlying pool of water.

The assumption has been made that any cooling provided by flooding is sufficient to prevent late thermal failure of the drywell head seal 99% of the time. Thus, the conditional failure probability of Event OT in the base case SCETs for short and long-term SBO was changed to  $1.0 \times 10^{-2}$ . Furthermore, in order to model aerosol scrubbing by the overlying pool, the conditional failure probability of Event RB was changed to  $1.0 \times 10^{-2}$  for those branches involving excessively high drywell temperatures (OT). The revised offsite consequences for short and long-term SBO are shown in Table 29.

**Table 29.** Offsite consequences for SBO sequences with drywell head flooding (per reactor-year)

	Mean Latent Fatalities	Mean Population Dose (Man-Rem) <sup>a</sup>	Mean Offsite Costs (\$)
ST-SBO	9.71E-05	1.04E-01	3.27E+02
LT-SBO	2.96E-03	2.78	1.06E+04
% Total Decrease	3.9	3.7	7.3

a. The population dose is that received within a 50-mi radius of the plant.

As the table shows, drywell head flooding, if effective, has the potential to slightly reduce the offsite consequences for SBO. However, uncertainties remain as to the effectiveness of drywell head flooding for preventing thermal failure of the drywell head seal and in scrubbing the release should the head seal fail. If flooding is not as effective as assumed here, then the benefits will be correspondingly reduced.

Table 30 summarizes the effects of the various improvements and sensitivities on SBO risk that have been examined in this section.

**Table 30.** Summary of station blackout risks for the generic Mark II plant

Risk Measure (per year)	Base Case	With Blackstart Gas Turbine	With Preemptive Venting	With Venting at PCPL	With Diesel Fire Pump <sup>a</sup>	With Flooding of Drywell Head
Core Melt Freq.						
– ST–SBO	1.57E–06	5.50E–07	1.57E–06	1.57E–06	1.57E–06	1.57E–06
– LT–SBO	3.75E–06	1.31E–06	3.75E–06	3.75E–06	3.83E–07	3.75E–06
Latent Fatalities						
– ST–SBO	2.01E–04	7.05E–05	1.93E–03	2.06E–04	1.06E–04	9.71E–05
– LT–SBO	2.98E–03	1.04E–03	3.56E–03	2.99E–03	3.05E–04 <sup>b</sup>	2.96E–03
50–Mile Dose (Rem)						
– ST–SBO	1.95E–01	6.83E–02	1.68	2.09E–01	1.09E–01	1.04E–01
– LT–SBO	2.80	9.78E–01	3.25	2.81	2.86E–01 <sup>b</sup>	2.78
Offsite Costs (\$)						
– ST–SBO	1.09E+03	3.82E+02	1.18E+04	1.06E+03	5.56E+02	3.27E+02
– LT–SBO	1.07E+04	3.73E+03	2.07E+04	1.07E+04	1.09E+03 <sup>b</sup>	1.06E+04

a. Includes backup DC power to SRV solenoids and containment vent valves and modifications to ensure SRV operability in a severe accident environment.

b. Reductions in LT–SBO consequences for this case are due to a reduction in the LT–SBO core damage frequency.

## 9. QUANTITATIVE RISK ANALYSIS OF OTHER SEQUENCES (TQUX, TQUV, AND TW)

Transient-initiated sequences (T) in which feedwater (Q) and high pressure injection (U) are lost and the reactor is not depressurized (X) have been found to be dominant contributors to core damage frequency in past PRAs performed for Limerick and Shoreham (see References 4, 5, and 6). The frequency of these sequences is expected to be reduced by the modification to increase the ADS system reliability suggested by NUREG-0737 (see Reference 55 and 62). However, because these sequences have been so dominant in past studies, they are evaluated here for completeness.

### 9.1 Accident Sequence Analysis

The accident sequence analysis for the transient-initiated sequences is performed as for the previous cases of ATWS and SBO. The front-end event tree for the base case is shown in Figure 20.

#### 9.1.1 Event Tree Quantification.

**T.** The initiating event is an anticipated transient that requires the reactor to be shut down. The frequency of Event T is defined to be the sum of the following individual initiators. The frequency of these initiators will vary from plant to plant; the values used here were taken from Reference 74 and represent the frequencies expected for mature plant operation.

Initiator	Frequency (per reactor-year)
Loss of condenser vacuum	0.34
Turbine trip	5.77
MSIV closure	0.16
Loss of feedwater	0.05
Loss of offsite power	0.07
IORV	0.11
Total	6.50

**Q.** Event Q represents the probability that feedwater is available or restored following the initiating event. The assumption is made that the reference plant has

turbine-driven feedwater pumps only; therefore, at least one MSIV must be open to run the feedwater pumps. The conditional failure probability of Event Q is calculated as a weighted average of the individual conditional failure probabilities of Q for each of the initiators listed above.

Initiator	Frequency (/y)	Conditional Probability	Final Probability
Loss of vacuum	0.34	1.0	0.34
Turbine trip	5.77	0.1	0.58
MSIV closure	0.16	0.3	0.05
Loss of FW	0.05	0.14	0.01
LOSP	0.07	1.0	0.07
IORV	0.11	0.99	0.11
Total	6.50		1.16
$Q_{ave}$	$1.16/6.50 = 0.18$		

The conditional feedwater failure probability for each of the initiators was taken from Reference 6.

**U1.** Event U1 represents the failure of both HPCI and RCIC to provide injection to the vessel, given that feedwater is unavailable. Using values from Reference 70, the probability that neither HPCI nor RCIC will be available is calculated to be  $3.6 \times 10^{-3}$ .

**X.** Event X represents failure to depressurize the reactor vessel, given that feedwater, HPCI, and RCIC have all failed. The value of  $8.4 \times 10^{-4}$  is calculated under the assumption that improvements detailed in Reference 55 have been implemented at the generic plant.<sup>5,62,75</sup>

**V1.** Event V1 models the availability of low pressure injection systems following depressurization of the reactor vessel. The following systems are included in the base case quantification: LPCI, LPCS, and the condensate system. Use of the diesel fire pumps or the service water cross-tie to the RHR system is not considered for the base case analysis. The conditional failure probability of Event V1 is taken to be the product of the individual failure probabilities for each

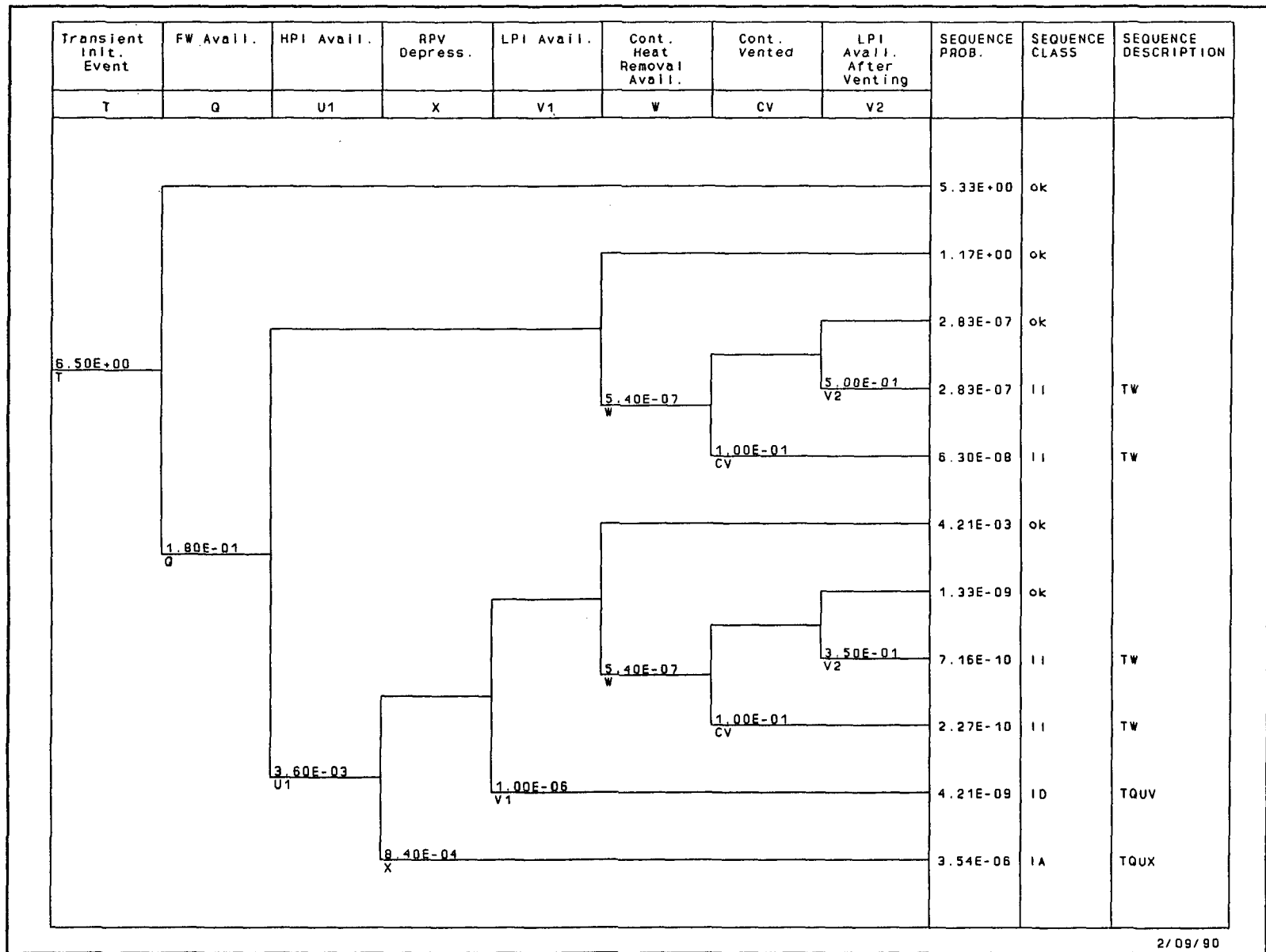


**Figure 20.** Event tree for transient-initiated sequences.

of these systems (independence is assumed for simplicity). The system unavailabilities in References 4 and 5 are comparable; however, the values in Reference 5 are somewhat easier to locate, so they are used here. The LPCI unavailability is given in Reference 5 as  $2.7 \times 10^{-3}$  and the LPCS unavailability is  $3.6 \times 10^{-3}$ . The condensate unavailability is given as 0.1 and is dominated by operator error. Multiplying these values together gives

$$P(V1) = 2.7 \times 10^{-3} * 3.6 \times 10^{-3} * 0.1 = 9.7 \times 10^{-7}$$

For this report, this value is rounded to  $1.0 \times 10^{-6}$ .

**W.** Event W, which models long-term containment heat removal, is quantified as follows. First, the assumption is made that equipment unavailability dominates the HEP for the suppression pool cooling mode of RHR. This has not always been the case in past PRAs, but is in line with more recent studies, particularly the NUREG-1150 analyses. The RHR equipment unavailability is taken to be  $1.0 \times 10^{-4}$  (see Reference 6). Second, the probability of recovering the PCS is taken to be (see Section 8)

$$P(PCS) = P(\text{MSIV not open in 15 h}) + P(\text{PCS not operable}) \text{ (see Reference 6).}$$

Using data from Reference 5,

$$P(PSC) = 1.0 \times 10^{-3} + 5.0 \times 10^{-3} = 6.0 \times 10^{-3}.$$

Finally, as discussed in Section 8, credit is given for using the RWCU system in the blowdown mode of operation as a viable means of decay heat removal. Combining these failure probabilities (again assuming independence) gives the overall failure probability of Event W:

$$P(W) = 1.0 \times 10^{-4} * 6.0 \times 10^{-3} * 0.9 = 5.4 \times 10^{-7}.$$

**CV.** This is the probability that the containment is not vented. The failure probability is taken to be 0.1, as before.

**V2.** This is the probability that venting results in the failure of injection, thus inducing core damage. Event V2 is quantified as for the Class IC ATWS in Section 7.

The results of the front-end analysis for the base case are shown in Table 31.

**Table 31.** Core damage frequency for transient initiators

Core Damage Class	Frequency (per reactor-year)
IA (TQUX)	3.54E-6
ID (TQUV)	4.21E-9
II (TW)	3.47E-7

In the above table, Class IA is made up of those sequences where core melt occurs with the reactor at high pressure (TQUX). Conversely, Class ID is made up of sequences where core melt occurs with the reactor depressurized (TQUV). Finally, the Class II sequences are those involving a loss of long-term containment heat removal (TW). As in previous Mark II PRAs, the TQUX sequences are dominant (see References 4, 5, 6, and 62).

Finally, at least one previous Mark II PRA has found that problems with reactor vessel level instrument reference legs can contribute significantly to the transient-initiated core damage frequency (see References 5, 6, and 62). In particular, loss of drywell cooling can induce flashing in the reference legs and a loss of reliable level indication. Miscalibration of the reactor level transmitters can also cause problems. Because these problems are expected to be highly plant-specific, they have not been evaluated in the present analysis. For the same reasons, other special initiators, such as loss of service water, have also been excluded.

## 9.2 Containment Event Tree Analysis

As for the preceding plant damage states, an SCET was constructed to model containment response to the Class IA (TQUX) plant damage state. The containment response to the Class ID (TQUV) and Class II (TW) plant damage states was not modeled, since the core damage frequency for each of these sequences was calculated to be significantly less than  $1 \times 10^{-6}/y$ . The quantification scheme for the top events in the SCET for the TQUX plant damage state (Figure 21) is given below.

**PD.** The initiating event is a TQUX plant damage state where all injection to the vessel has been lost and the vessel has not been depressurized. As before, the conditional probability of Event PD is 1.0.

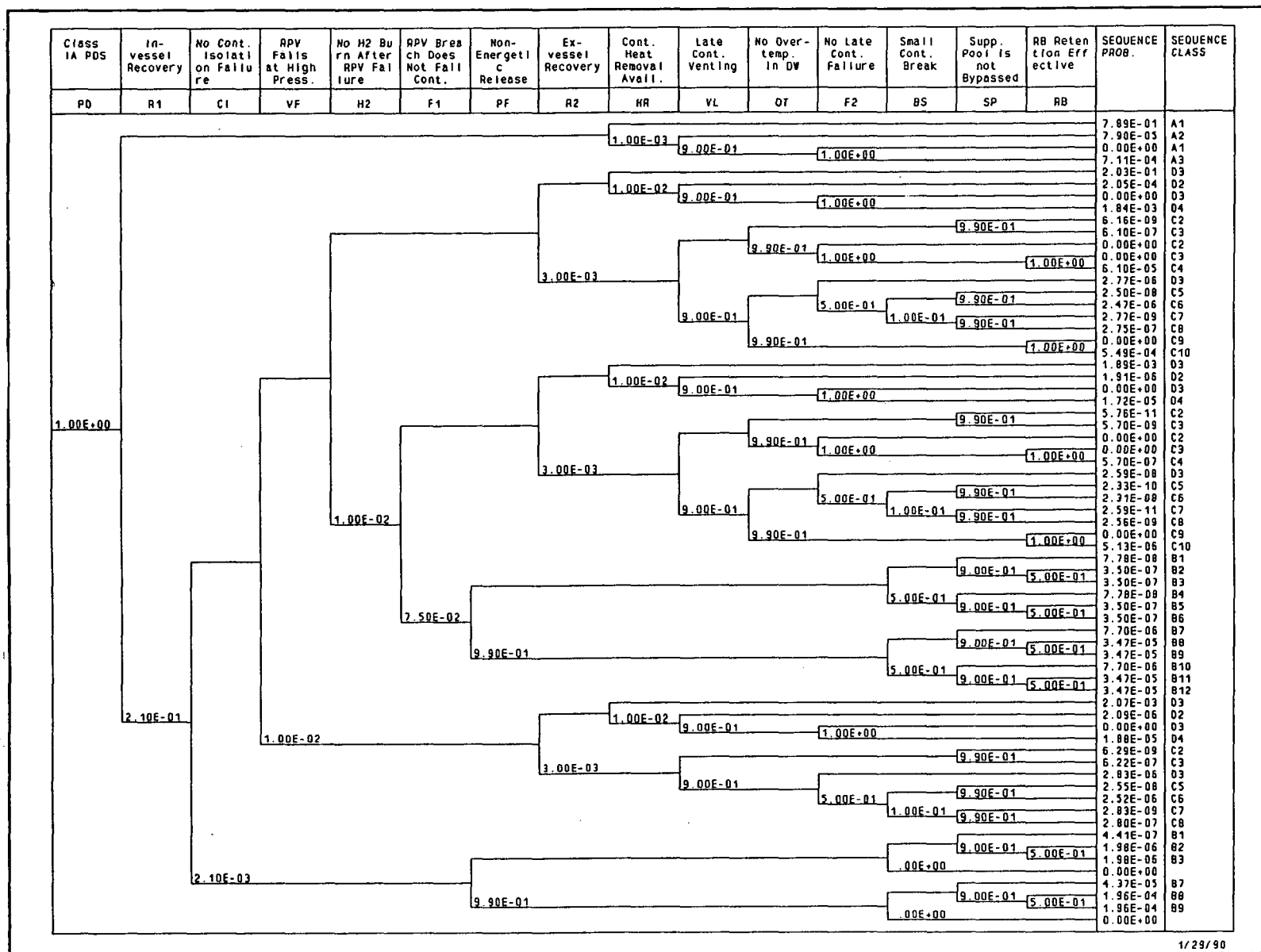


Figure 21. Base case SCET for the TQUX plant damage state.

**R1.** Event R1 evaluates the likelihood of restoring vessel injection and recovering the sequence prior to vessel failure. Because the dominant mode of loss of injection is failure to depressurize the vessel following the loss of high pressure injection, Event R1 is quantified based on the probability of depressurizing the vessel in time to prevent core melt and vessel failure, given that the vessel was not depressurized earlier. The approach taken by Reference 29 in quantifying this event was to determine the percentage of hardware failures that would disable both ADS and non-ADS SRVs. Of the ADS failure cutsets, 21% involved hardware faults that affected all SRVs. Therefore, Reference 29 assigned Event R1 a conditional failure probability of 0.21. Reference 5 used a value of 0.7, determined similarly. Since the Reference 29 quantification seemed more reasonable, the value of 0.21 was retained for Event R1.

**CI.** As for the previous plant damage states, the probability of a preexisting large containment leak (Event CI) is taken to be  $2.1 \times 10^{-3}$ , the value from Reference 29.

**VF.** Vessel failure at high pressure is extremely likely for the TQUX plant damage state. Accordingly, the conditional probability of low pressure vessel failure is taken to be  $1.0 \times 10^{-2}$ .

**H2.** Event H2 is quantified at  $1.0 \times 10^{-2}$ , as for the previous plant damage states.

**F1.** As before, Event F1 models overpressure failure of the containment at or near the time of vessel failure. The Reference 29 quantification was followed for this event. Because failure of the vessel at high pressure, per se, is not likely to cause containment pressure to exceed the PCPL (see Reference 29), high pressure vessel failure alone is assumed to be incapable of causing early overpressure containment failure. If the vessel fails at high pressure, and a hydrogen burn occurs either during or after core melt, Reference 29 calculates a failure probability of  $7.5 \times 10^{-2}$  for Event F1.

**PF.** For sequences that involve vessel failure at high pressure (/VF), the release is very likely to be energetic; therefore, for these sequences, the conditional failure probability of Event PF is taken to be 0.99. As before, Event PF is only questioned for sequences with early containment failure (F1 or CI).

**R2.** Event R2 represents successful ex-vessel cooling of the core debris, via injection into the failed reactor

vessel or into the containment spray header. The failure probability of Event R2 is based upon two factors: the likelihood that adverse suppression pool conditions (clogging of suction strainers by core debris, or inadequate NPSH) will preclude operation of RHR and LPCS pumps, and the probability that operators fail to align alternate injection systems, such as service water to the RHR ultimate heat sink connection (see Reference 29). Since the suppression pool is not likely to be saturated for these sequences (see References 4 and 9), the assumption is made that NPSH for the RHR pumps will be adequate. Therefore, the failure probability of Event R2 calculated for the Class IC ATWS is reduced by a factor of 10 to account for the ability to use the RHR pumps. Reference 29 uses a value of  $3.0 \times 10^{-2}$  for the probability that operators fail to align alternate injection systems. The source of this value is given as the Peach Bottom Analysis done for draft NUREG-1150 (1987). Applying the factor of 10 reduction to this value gives  $P(R2) = 3.0 \times 10^{-3}$ .

**HR.** As in previous plant damage states, Event HR models the availability of long-term containment heat removal, via either RHR suppression pool cooling or containment sprays, given that an ex-vessel coolable debris bed has been established (/R2) or that the sequence was recovered in-vessel (/R1). Reference 8 uses a central estimate failure probability of  $1.0 \times 10^{-2}$  for this event, assuming that the suppression pool is subcooled. If in-vessel recovery was successful (/R1), this value has been further reduced by a factor of 10 to  $1.0 \times 10^{-3}$ , to reflect the additional time available for operator action.

**VL.** Late containment venting was quantified as for the Class IC ATWS.

The remaining events in the TQUX SCET were quantified as for the preceding plant damage states.

The conditional containment release mode probabilities are shown in Table 32.

As the table shows, almost all of the end states represent successful recovery, either in the reactor vessel or on the drywell floor after the time of vessel breach.

## 9.3 Consequence Analysis

The base case consequences for Class IA (TQUX) sequences are shown in Table 33. These values were obtained analogously to those for ATWS and SBO in Sections 7 and 8, using Equation 1-1.

**Table 32.** Conditional containment release mode probabilities for TQUX sequences

Release Mode	Conditional Probability
A1	7.89E-01
A2	7.90E-05
A3	7.11E-04
Recovered in-vessel	7.90E-01
B1	5.19E-07
B2	2.33E-06
B3	2.33E-06
B4	7.78E-08
B5	3.50E-07
B6	3.50E-07
B7	5.14E-05
B8	2.31E-04
B9	2.31E-04
B10	7.70E-06
B11	3.47E-05
B12	3.47E-05
Early containment failure	5.96E-04
C1	0.00
C2	1.25E-08
C3	1.24E-06
C4	6.16E-05
C5	5.07E-08
C6	5.01E-06
C7	5.63E-09
C8	5.58E-07
C9	0.00
C10	5.54E-04
Late containment failure or venting	6.22E-04
D2	2.09E-04
D3	2.07E-01
D4	1.88E-03
Recovered ex-vessel	2.09E-01

**Table 33.** Base case consequence results for TQUX sequences (per reactor-year)

Mean Latent Fatalities	Population Dose (Rem) <sup>a</sup>	Offsite Costs (\$)
3.29E-05	5.98E-02	9.94E+01

a. The population dose is that received within a 50-mi radius of the plant.

## 9.4 Sensitivities and Effects of Potential Improvements

The effects of several sensitivities and potential improvements on both core damage frequency and risk are evaluated in this section. Only Class IA (TQUX) sequences are evaluated, since the frequency of other transient-initiated core damage sequences (TQUV and TW) is already very low ( $<1 \times 10^{-6}$  per reactor-year).

The first sensitivity case to be evaluated is the effect that in-pedestal downcomers, like those at Shoreham and Nine Mile Point 2, have on the containment release modes and offsite consequences. Sections 3.2 and 4.2 discuss the potential benefits that in-pedestal downcomers might have in mitigating CCI, as well as their potential for causing suppression pool bypass. To model the presence of these downcomers for TQUX sequences, the base case SCET (Figure 21) was modified as follows. For sequences where the reactor vessel fails at low pressure (VF), the failure probabilities of ex-vessel recovery and long-term containment heat removal (Events R2 and HR) were set to 0.0, since essentially all of the core debris is expected to flow into the suppression pool via the in-pedestal downcomers where it is assumed to be quenched by the pool water. The base case probabilities of suppression pool bypass were retained, since direct corium attack and energetic FCI are assumed to fail one or more of the in-pedestal downcomers shortly after vessel breach. The resulting containment release mode conditional probabilities are shown in Table 34.

The effects of the in-pedestal downcomers on the offsite consequences are shown in Table 35. As Table 35 shows there is essentially no difference from the base case, because the benefits of debris-quenching in the suppression pool are more than offset by the high probability of suppression pool bypass caused by the postulated failure of the in-pedestal downcomers shortly after vessel breach. If the probability of



**Table 34.** Effects of in-pedestal downcomers on the containment release mode probabilities for TQUX sequences

Release Mode	Conditional Probability	
	Base Case	Downcomers
A1	7.89E-01	7.89E-01
A2	7.90E-05	7.90E-05
A3	7.11E-04	7.11E-04
Recovered in-vessel	7.90E-01	7.90E-01
B1	5.19E-07	5.19E-07
B2	2.33E-06	2.33E-06
B3	2.33E-06	2.33E-06
B4	7.78E-08	7.78E-08
B5	3.50E-07	3.50E-07
B6	3.50E-07	3.50E-07
B7	5.14E-05	5.14E-05
B8	2.31E-04	2.31E-04
B9	2.31E-04	2.31E-04
B10	7.70E-06	7.70E-06
B11	3.47E-05	3.47E-05
B12	3.47E-05	3.47E-05
Early release	5.97E-04	5.96E-04
C1	0.0	0.0
C2	1.25E-08	6.22E-09
C3	1.24E-06	6.16E-07
C4	6.16E-05	6.16E-05
C5	5.07E-08	2.52E-08
C6	5.01E-06	2.49E-06
C7	5.63E-09	2.80E-09
C8	5.58E-07	2.78E-07
C9	0.0	0.0
C10	5.54E-04	5.54E-04
Late release	6.22E-04	6.19E-04
D1	0.0	0.0
D2	2.09E-04	2.07E-04
D3	2.07E-01	2.07E-01
D4	1.88E-03	1.86E-03
Recovered ex-vessel	2.09E-01	2.09E-01

**Table 35.** Effects of in-pedestal downcomers on the offsite consequences of TQUX sequences (per reactor-year)

	Mean Latent Fatalities	Population Dose (Rem) <sup>a</sup>	Offsite Costs (\$)
	3.29E-05	5.98E-02	9.92E+01
% Decrease	0.00	0.00	0.02

a. The population dose is that received within a 50-mi radius of the plant.

suppression pool bypass is significantly less than the assumed value of 90%, then the beneficial effects of debris-quenching will dominate and there should be a reduction in risk. This issue will be examined further in Section 10.2.

The next improvement to be examined is use of the diesel fire pumps for mitigating late containment failure. Because the TQUX sequence progresses rapidly to core damage, using the diesel fire pumps for preventing core damage is not considered (refer to the discussion in Section 8.4). However, the diesel fire pumps could be of use after vessel failure, since water from the fire protection system potentially could be used to establish a coolable debris bed and to remove heat from the containment atmosphere via the drywell sprays. This is modeled by reducing the conditional failure probabilities of Events R2 and HR in the base case SCET by 50% (see the discussion in Section 8.4 for the basis of this value). The effects of this modification on the offsite consequences are shown in Table 36.

**Table 36.** Effects of diesel fire pumps on offsite consequences of TQUX sequences (per reactor-year)

	Mean Latent Fatalities	Population Dose (Rem) <sup>a</sup>	Offsite Costs (\$)
	2.82E-05	5.56E-02	7.13E+01
% Decrease	14.3	7.02	28.3

a. The population dose is that received within a 50-mi radius of the plant.

As the table shows, the reduction in offsite consequences effected by use of the diesel fire pumps for debris-cooling and long-term containment heat removal is significant. However, there is one caveat: no consideration has been given to constraints on using drywell sprays that are currently in place in the EPGs; that is, the prohibition against using the drywell sprays at elevated temperatures and pressures inside the containment in order to prevent an excessive rate of pressure decrease that could conceivably threaten containment integrity via an excessive pressure differential (wetwell pressure > drywell pressure) (see Reference 19). Further analysis is needed to show conclusively that these constraints can be relaxed; calculations in Reference 9 indicate that initiating sprays at highly elevated containment temperatures will not result in an excessive drywell depressurization rate, but this analysis is not conclusive and is specific to one particular plant.

The next sensitivity examines the reduction in offsite consequences that would be effected if the possibility of hydrogen burns inside primary containment could be ruled out for TQUX sequences. As discussed earlier, high pressure vessel failure, per se, is not thought to present a serious challenge to the integrity of the Mark II containment. However, if the containment were not inerted with nitrogen at the time of the accident, then hydrogen burns could occur at or near the time of vessel failure, which, if accompanied by vessel failure at high pressure, could seriously challenge containment integrity relatively early in the sequence.

Technical Specifications could be revised to require Mark II plants to be inerted with nitrogen during all periods of operation. To examine the effect of

this revision on offsite consequences for a TQUX sequence, the probability of a hydrogen burn (Event H2 in the SCET) was set to 0.0. The resulting offsite consequences are shown in Table 37.

**Table 37.** Offsite consequences for TQUX sequences with no hydrogen burn (per year)

	Mean Latent Fatalities	Population Dose (Rem) <sup>a</sup>	Offsite Costs (\$)
	3.05E-05	5.76E-02	8.57E+01
% Decrease	7.3	3.7	13.8

a. The population dose is that received within a 50-mi radius of the plant.

As the table shows, setting the probability of a hydrogen burn to 0.0 does not significantly reduce the offsite consequences for the TQUX sequences. Examining the containment release mode conditional probabilities shows the reason for this. With no hydrogen burn, the conditional probability of an early release is reduced by ~26% from the base case value but the probability of a late release is unchanged. Because the late releases are sizeable contributors to the offsite consequence measures used in this report, the relatively large reduction in the early release probability yields only a small reduction in these consequences. Based on these results, the benefits to be gained by making the Technical Specification inerting requirements more stringent would probably be more than offset by increased maintenance difficulties.

## 10. TECHNICAL FINDINGS

Sections 7 to 9 of this report have presented quantitative risk results for each of the core damage sequences and corresponding plant damage states that was analyzed. In this section, these results are collocated to present a composite risk picture for the generic Mark II plant. This section closes with a discussion of what are thought to be the major limitations and uncertainties associated with the analysis performed for this report.

### 10.1 Core Damage Frequency Results

Table 38 shows the base case core damage frequencies arranged according to sequence type. These frequencies are *point estimates* derived from the accident sequence event trees discussed previously, and some uncertainty (both stochastic and due to lack of knowledge) is necessarily involved in the estimate; however, no attempt was made to quantify this uncertainty.

**Table 38.** Base case core damage frequencies for the generic Mark II plant

Sequence Accident	Frequency (per reactor-year)
Long-term SBO	3.75E-06
TQUX	3.54E-06
Short-term SBO	1.57E-06
ATWS (CM < CF)	2.30E-06
ATWS (CF < CM)	1.27E-06
TW	3.47E-07
Total	1.28E-05

Figure 22 presents this information in graphical format. In terms of core damage frequency, the dominant sequences are long-term SBO and TQUX, with significant contributions from ATWS and short-term SBO. Loss of long-term containment heat removal (TW) is not a dominant sequence, as its frequency is  $<1 \times 10^{-6}$  per reactor-year and it contributes only ~3% of the total.

These values are within the frequency ranges calculated in previous PRAs for BWR Mark II plants (see References 4, 5, 6, 36, 62); however, individual plants can be expected to have core damage frequencies that differ from the results obtained for the generic plant. In

addition, special initiators, such as loss of service water and reactor building internal flooding, and external events, such as fire and earthquake, have not been considered, since vulnerability to these initiators is highly plant-specific.

Several improvements were evaluated that have the potential for lowering the base case core damage frequency and thus providing an indirect improvement in containment performance by reducing the frequency of severe accident challenges. The results of these evaluations are summarized below.

**10.1.1 ATWS Level Control.** There are two facets to this proposed strategy, both involving modifications to the latest revision of the EPGs. Currently, the operator is instructed to terminate all injection except that from the SLCS and CRD during the initial stages of an ATWS. At least one utility has taken exception to this strategy, arguing that a simpler and more effective strategy would be to allow HPCI and RCIC to inject at their rated flow while the reactor is being shut down by boron injection from the SLCS (see References 7, 37).

As discussed in Section 7.4, the effectiveness of this strategy hinges upon the second facet, namely the use of an increased suppression pool temperature limit for ATWS to obviate the need for emergency depressurization while boron is being injected. If this higher limit is valid, then depressurization is less likely to be required, and the ATWS core damage frequency is significantly reduced, as shown in Table 39.

Along with the reduction in the ATWS core damage frequency, there is a gain in simplicity from the operator's point of view, since ATWS guidelines in the current EPG revision are quite complicated. However, if the increased suppression pool temperature limit cannot be shown to be valid, then there do not appear to be any advantages over the current procedure, since emergency depressurization would likely be required.

**10.1.2 Hardened Vent.** The next potential improvement is a hardened vent line leading from the wetwell airspace to an elevated release point outside the secondary containment. The vent line is assumed to be 18 in. in diameter; simple hand calculations show that such a vent should be capable of removing at most approximately 10% of the rated thermal power of a 3293 MW BWR. The main advantage of the hardened vent over the existing ductwork vent is that venting could be carried out at elevated containment pressures without releasing steam, hydrogen, and fission

# Mark II Base Case

## Core Damage Frequency

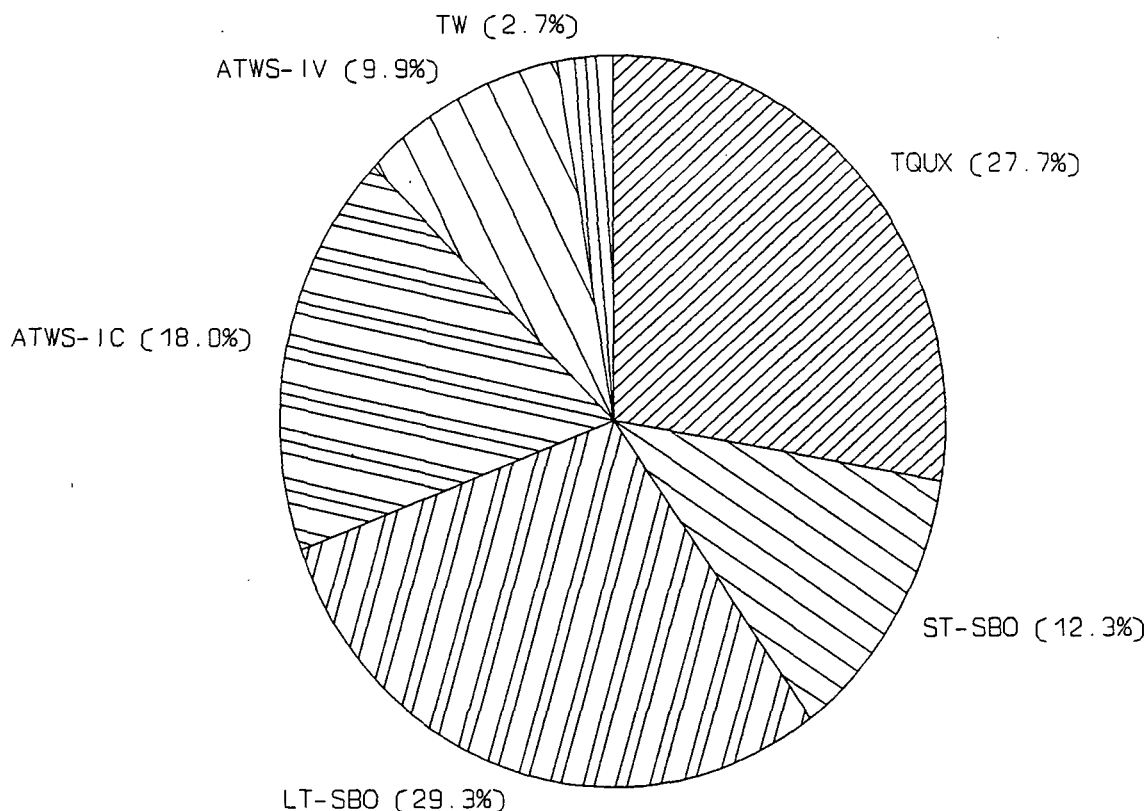


**Figure 22.** Mark II base case core damage frequency.

products into the reactor building, thus lessening the probability of equipment failure following venting. Table 40 shows the ATWS core damage frequencies with the hardened vent in place.

**Table 39.** ATWS core damage frequencies with no level control and an increased suppression pool temperature limit

Base Case Frequency (/y)	New Frequency (/y)	% Reduction
Class IV: 1.27E-06	6.11E-07	51.9
Class IC: 2.30E-06	8.94E-07	61.1

**Table 40.** ATWS core damage frequencies with hardened venting

Base Case Frequency (/y)	New Frequency (/y)	% Reduction
Class IV: 1.27E-06	1.17E-06	7.9
Class IC: 2.30E-06	2.30E-06	0.0

The hardened vent does not significantly reduce the ATWS core damage frequency. There are two reasons for this. First, venting the containment can cause a loss of adequate NPSH to low pressure ECCS pumps. Second, the 18-in. vent line cannot remove energy fast enough to prevent containment overpressurization during the more severe ATWS sequences. The hardened vent line could also be of use in mitigating

the TW sequences; however, since the TW core damage frequency already is quite low, possible further reductions effected by the use of a hardened vent were not evaluated. In addition, the in-pedestal drain lines in the reference plant are assumed to fail shortly after vessel breach, making unfiltered venting from the wetwell airspace after vessel failure unattractive, since the release through the vent line would likely be unscrubbed (see Reference 36).<sup>a</sup>

## 10.2 Containment Failure Modes

This section discusses the containment failure modes that have been identified through the use of the SCETs and gives conditional probabilities of occurrence for the base case and for the cases that examine sensitivities and potential improvements.

The end states of the SCETs were binned into containment release modes based on sequence characteristics, such as time of containment failure relative to the time of reactor vessel breach, release pathway (for example, through the suppression pool), level of decontamination provided by the reactor building, and others. The specific characteristics used to uniquely identify each release mode are listed in Appendix C. A smaller set of release mode bins was selected for presentation in this section, with the identifying characteristics given below.

Containment Failure Mode	Characteristics
REC-IV	Core melt recovered in-vessel, noble gas release or no containment failure.
REC-EV	Core melt recovered ex-vessel, noble gas release or no containment failure.
REC-TOTAL	Sum of in-vessel and ex-vessel recovery.

a. A. Payne (NSL) conference call with P. K. Niyogi (NRC) on NMay 1, 1989.

Containment Failure Mode	Characteristics
ECF-OP-SP	Early overpressure containment failure, release scrubbed through the suppression pool.
ECF-OP-nSP	Early overpressure containment failure, release bypasses the suppression pool.
LV-SP	Late vented release through the suppression pool.
LV-nSP	Late vented release bypassing the suppression pool.
LCF-OP-SP	Late overpressure containment failure, release scrubbed through the suppression pool.
LCF-OP-nSP	Late overpressure containment failure, release bypasses the suppression pool.
LCF-OT	Late overtemperature containment failure, release bypasses the suppression pool.

Some amplifying comments on these large-scale bins are in order. The suppression pool bypass in bin ECF-OP-nSP can be the result of either failure location (failure in the drywell) or failure of in-pedestal drain lines or downcomers, irrespective of the containment failure location. Because the base case plant was assumed to have in-pedestal drain lines that are postulated to fail shortly after vessel breach, this mechanism of pool bypass overshadows the containment failure location. In fact, at the level of detail provided in the SCETs, failure location is relatively unimportant for evaluating the probability of early suppression pool bypass. The same remarks also apply to cases of late overpressure containment failure.

For cases of late overtemperature failure, the failure location is assumed to be the drywell head seal. In all cases, this leads to a release that bypasses the suppression pool.

The base case conditional containment failure mode probabilities are shown in Table 41. These probabilities are a weighted average of the release probabilities for all sequences.

**Table 41.** Base case weighted-average conditional containment failure mode probabilities

Containment Failure Mode	Conditional Probability
REC-IV	5.50E-01
REC-EV	2.49E-01
REC-TOTAL	7.99E-01
ECF-OP-SP	1.18E-02
ECF-OP-nSP	1.06E-01
LV-SP	5.40E-08
LV-nSP	5.24E-04
LCF-OP-SP	1.94E-05
LCF-OP-nSP	1.93E-03
LCF-OT	7.55E-02

Table 41 shows that, given a severe core damage accident, there is a 55% chance of recovering the sequence in-vessel, with no significant release from containment. Should the sequence progress to vessel failure, there is still a 24.9% chance of establishing a coolable debris bed inside containment, again with no significant release to the environment. However, there is an 11.8% chance that a severe core damage sequence will lead to early overpressure containment failure. Of these early failures, ~90% will involve suppression pool bypass, because of either in-pedestal drain line failure or a failure location in the drywell. Should the containment survive the early challenge to its integrity, there is still a significant late challenge. By far the most significant late challenge is failure of the drywell head seal, primarily due to high temperature accompanied by elevated pressure.

Each of the suggested improvements will alter some or all of these conditional failure mode probabilities. These effects are shown in Tables 42 through 46.

**Table 42.** Effects of diesel fire pumps and enhanced depressurization capability on containment failure modes

Containment Failure Mode	Conditional Probability	
	Base Case	Revised
REC-IV	5.50E-01	4.76E-01
REC-EV	2.49E-01	3.47E-01

Containment Failure Mode	Conditional Probability	
	Base Case	Revised
REC-TOTAL	7.99E-01	8.23E-01
ECF-OP-SP	1.18E-02	1.62E-02
ECF-OP-nSP	1.06E-01	1.45E-01
LV-SP	5.40E-08	3.75E-08
LV-nSP	5.24E-04	3.60E-04
LCF-OP-SP	1.94E-05	5.82E-06
LCF-OP-nSP	1.93E-03	5.77E-04
LCF-OT	7.55E-02	1.49E-02

**Table 43.** Effects of blackstart combustion generator on containment failure modes

Containment Failure Mode	Conditional Probability	
	Base Case	Revised
REC-IV	5.50E-01	4.71E-01
REC-EV	2.49E-01	3.23E-01
REC-TOTAL	7.99E-01	7.94E-01
ECF-OP-SP	1.18E-02	1.64E-02
ECF-OP-nSP	1.06E-01	1.47E-01
LV-SP	5.40E-08	7.52E-08
LV-nSP	5.24E-04	7.30E-04
LCF-OP-SP	1.94E-05	9.92E-06
LCF-OP-nSP	1.93E-03	9.82E-04
LCF-OT	7.55E-02	4.09E-02

**Table 44.** Effects of preemptive venting (during SBO) on containment failure modes

Containment Failure Mode	Conditional Probability	
	Base Case	Revised
REC-IV	5.50E-01	5.50E-01
REC-EV	2.49E-01	2.23E-01
REC-TOTAL	7.99E-01	7.73E-01
ECF-OP-SP	1.18E-02	2.17E-02
ECF-OP-nSP	1.06E-01	1.95E-01
LV-SP	5.40E-08	5.40E-08
LV-nSP	5.24E-04	5.24E-04
LCF-OP-SP	1.94E-05	4.89E-07
LCF-OP-nSP	1.93E-03	4.83E-05
LCF-OT	7.55E-02	4.61E-03

**Table 45.** Effects of increased probability of venting at the PCPL (during SBO) on containment failure modes

Containment Failure Mode	Conditional Probability	
	Base Case	Revised
REC-IV	5.50E-01	5.50E-01
REC-EV	2.49E-01	2.50E-01
REC-TOTAL	7.99E-01	8.00E-01
ECF-OP-SP	1.18E-02	1.19E-02
ECF-OP-nSP	1.06E-01	1.06E-01
LV-SP	5.40E-08	2.18E-05
LV-nSP	5.24E-04	6.70E-02
LCF-OP-SP	1.94E-05	2.40E-06
LCF-OP-nSP	1.93E-03	2.37E-04
LCF-OT	7.55E-02	1.18E-02

**Table 46.** Effects of drywell head flooding (during SBO) on containment failure modes

Containment Failure Mode	Conditional Probability	
	Base Case	Revised
REC-IV	5.50E-01	5.50E-01
REC-EV	2.49E-01	2.50E-01
REC-TOTAL	7.99E-01	8.00E-01
ECF-OP-SP	1.18E-02	1.18E-02
ECF-OP-nSP	1.06E-01	1.06E-01
LV-SP	5.40E-08	5.40E-08
LV-nSP	5.24E-04	5.24E-04
LCF-OP-SP	1.94E-05	7.08E-04
LCF-OP-nSP	1.93E-03	7.02E-02
LCF-OT	7.55E-02	5.32E-03

The primary effect of the diesel fire pumps (with enhanced depressurization capability) is to decrease the conditional probability of late containment failure. Note that the conditional probability of recovering the sequence in-vessel decreases, with this decrease being more than offset by the increase in the conditional probability of ex-vessel recovery. This effect highlights the importance of doing a complete risk calculation. If one were to look solely at the effects of an improvement on containment failure probability, the conclusion might be reached that conditions are worse with a particular improvement than without. However, in the case of the diesel fire pumps, the reduction in long-term SBO core damage frequency (~90%), when coupled with the increase in the conditional probability

of ex-vessel recovery, affords a significant reduction in offsite consequences, as will be seen shortly.

Since the only effect of the blackstart combustion turbine is to reduce the SBO core damage frequency, a slight decrease in the late challenge to containment is seen. As in the case of the diesel fire pumps, the decrease in the conditional probability of in-vessel recovery is compensated by a reduction in SBO core damage frequency and an increase in the conditional probability of ex-vessel recovery.

Preemptive venting during SBO (with no reclosure of the vent valves) effectively changes all late releases to early releases (for SBO sequences only). Therefore, there is an increase in the overall conditional probability of an early release and a corresponding decrease in the probability of a late release.

The increased probability of venting at the PCPL (late venting) reduces the probability of late overpressure and thermal failure. This is accompanied, however, by an increased probability of a vented, unscrubbed release.

Flooding the drywell head during SBO changes all late thermal failures to late overpressure failures or to end states with ex-vessel recovery.

Because of the very preliminary nature of the evidence concerning early failure of the in-pedestal drain lines at the reference plant, a sensitivity case was run in which these drain lines were assumed not to fail shortly after vessel breach. The revised probabilities of suppression pool bypass are discussed in Section 10.3. The effects of this sensitivity on the containment failure mode conditional probabilities are shown in Table 47.

**Table 47.** Conditional containment failure mode probabilities with no early in-pedestal drain line failure

Containment Failure Mode	Conditional Probability	
	Base Case	Revised
REC-IV	5.50E-01	5.50E-01
REC-EV	2.49E-01	2.49E-01
REC-TOTAL	7.99E-01	7.99E-01
ECF-OP-SP	1.18E-02	6.51E-02
ECF-OP-nSP	1.06E-01	5.28E-02
LV-SP	5.40E-08	2.72E-06
LV-nSP	5.24E-04	5.20E-04
LCF-OP-SP	1.94E-05	9.71E-04
LCF-OP-nSP	1.93E-03	9.71E-04
LCF-OT	7.55E-02	7.55E-02

With no early failure of the in-pedestal drain lines, the probability of an early unscrubbed release decreases by approximately 50%, while the probability of a late unscrubbed release decreases by only about 1%. This very significant latter result is due to the high probability of a late unscrubbed release, given a long-term SBO plant damage state. Recall that long-term SBO is the dominant contributor to core damage frequency at the reference plant. The net result of this change is that long-term SBO replaces ATWS as the

risk-dominant sequence. This issue is examined further in Section 10.3.

## 10.3 Consequence Results

The base case consequences for the reference plant are presented in Table 48. Note that these consequences are conditional upon the occurrence of a severe core damage accident accompanied by a release from containment.

**Table 48.** Summary of results of conditional consequence analysis

Release Category	Mean Latent Fatalities	Mean Population Dose (Man-Rem) <sup>a</sup>	Mean Offsite Costs (\$)
RC1	7.23E+03	5.93E+06	4.81E+10
RC2	4.96E+03	4.26E+06	2.87E+10
RC3	7.58	1.82E+04	1.13E+06
RC4	3.03E+03	3.58E+06	5.77E+09
RC5	4.38E+03	3.94E+06	2.57E+10
RC6	2.08E+03	2.75E+06	2.99E+09
RC7	1.77E+02	3.87E+05	3.48E+07
RC8/9	3.41E+03	3.17E+06	1.22E+10
RC10	3.97	7.79E+03	1.13E+06
RC12	4.31	1.23E+04	1.52E+06

a. The population dose is that received within a 50-mi radius of the plant.

To obtain the annual frequency of these consequences (the absolute risk), the conditional probabilities above are input to Equation (1-1), along with the conditional containment release probabilities and the

accident sequence frequencies. The results are listed in Table 49 and are shown graphically in Figures 23 through 25.

**Table 49.** Base case consequence results for the generic Mark II plant (per reactor-year)

Plant Damage State	Mean Latent Fatalities	Mean Population Dose (Man-Rem) <sup>a</sup>	Mean Offsite Costs (\$)
TQUX	3.29E-05	5.98E-02	99.4
ST-SBO	2.01E-04	1.95E-01	1.09E+03
LT-SBO	2.98E-03	2.80	1.07E+04
ATWS (CM < CF)	1.13E-03	1.02	6.21E+03
ATWS (CF < CM)	4.60E-03	4.60	1.91E+04
Total	8.94E-03	8.67	3.72E+04

a. The population dose is that received within a 50-mi radius of the plant.



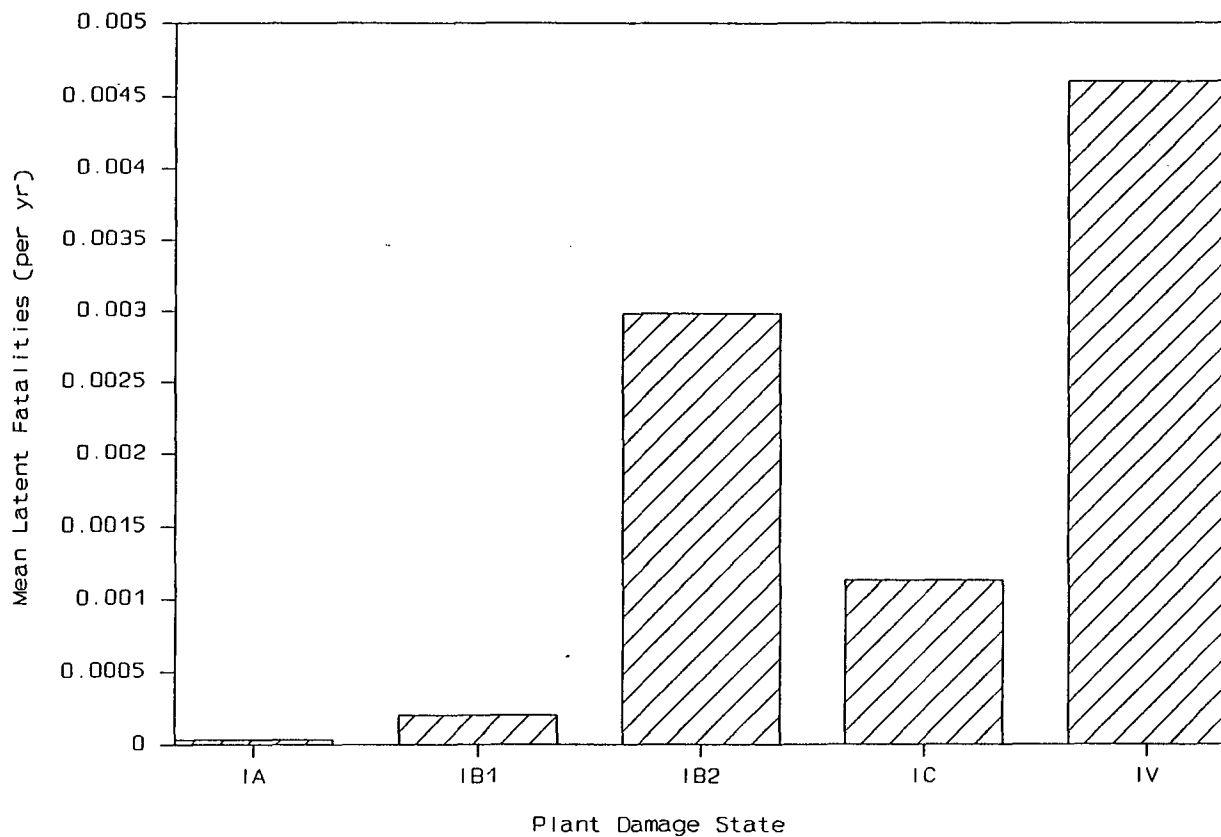


**Figure 23.** Mean latent fatalities for the reference Mark II plant.

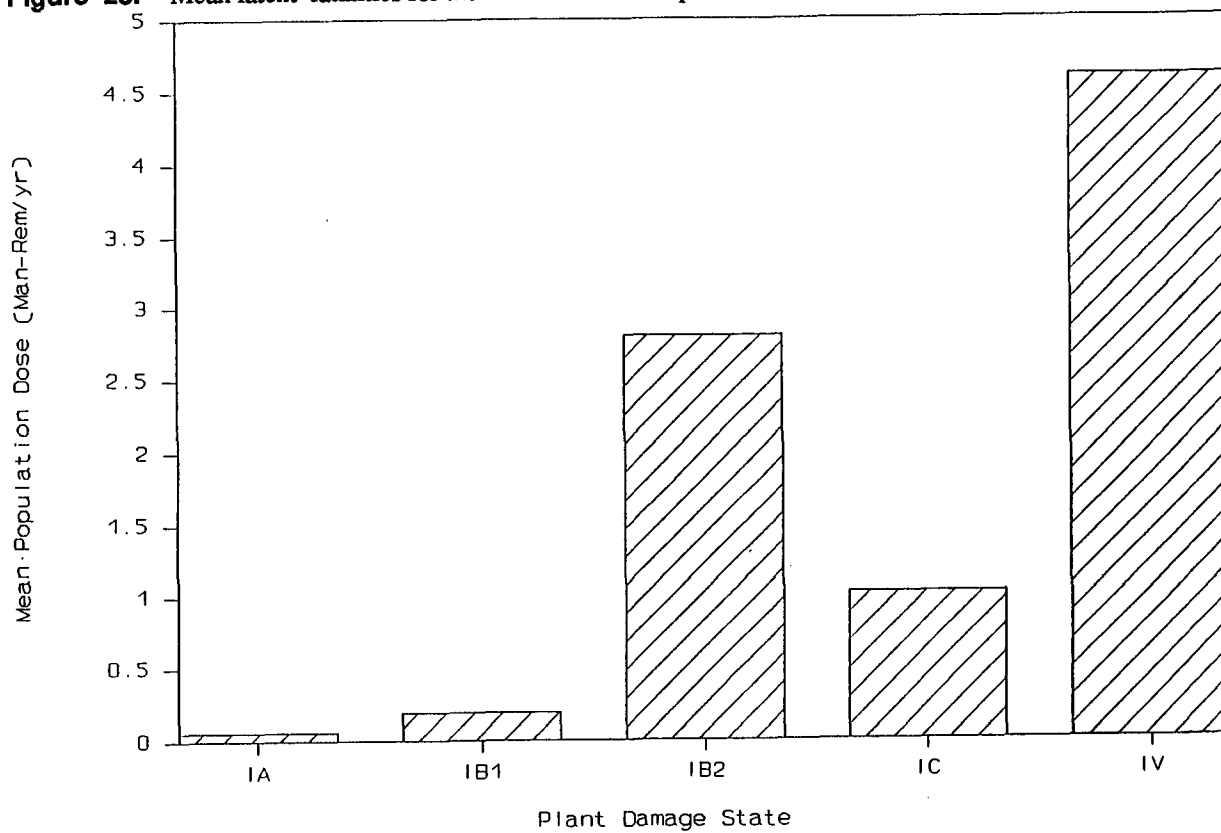


**Figure 24.** Mean population dose for the reference Mark II plant.

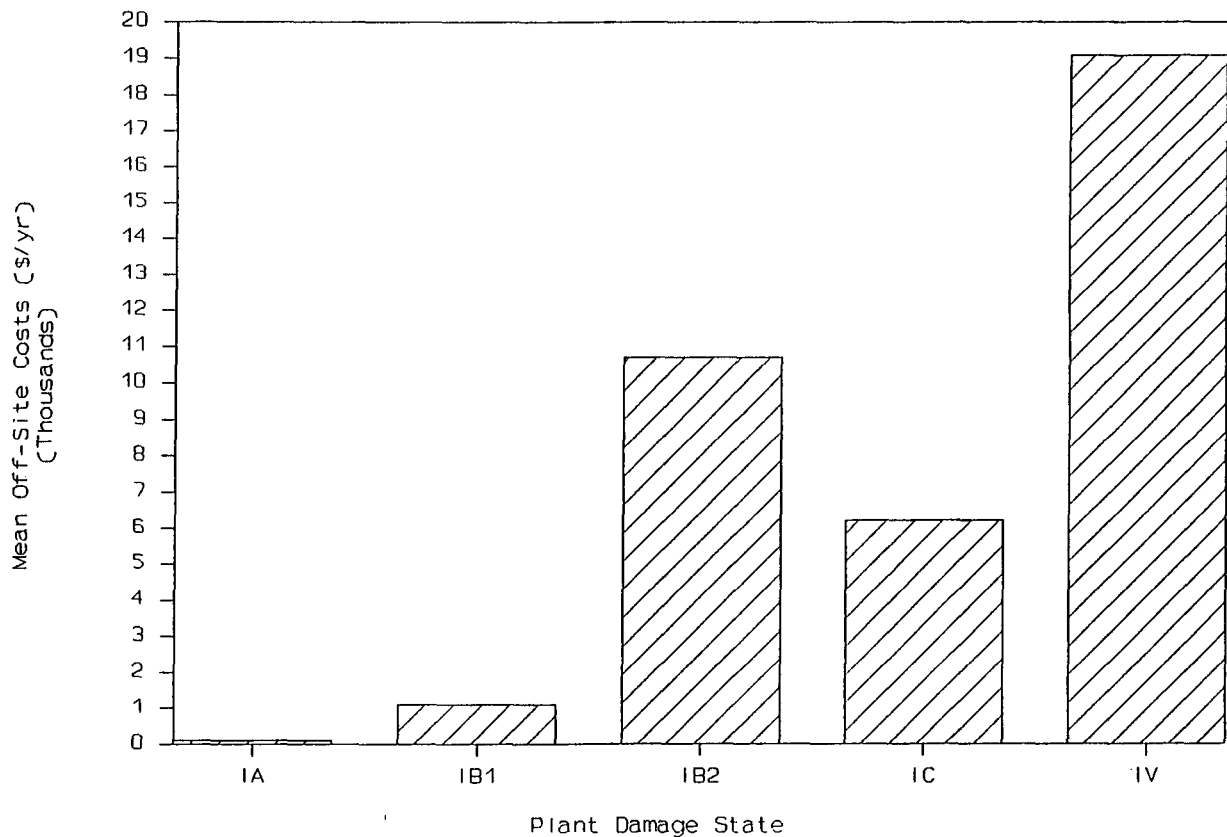


**Figure 25.** Mean offsite costs for the reference Mark II plant.

A number of potential improvements and sensitivity cases were examined that can alter the base case risk results. Each of these is discussed below.

**10.3.1 Decreased Probability of In-Pedestal Drain Line Failure.** The first sensitivity to be examined is the potential effect of a decreased probability of suppression pool bypass for a plant with no in-pedestal drain lines. For example, La Salle is reported to have two 4-in. drain lines leading from the pedestal cavity to the reactor building. These drain lines have been postulated to be likely to fail within 20 min after the time of vessel breach for most sequences.<sup>a</sup> Based on information presented to the NRC by the Philadelphia Electric Company, it appears that Limerick has drain plate covers in the in-pedestal region that could also fail shortly after vessel breach (see Reference 36). Failure of these drain lines or drain plate covers as a result of corium attack could create a path through which fission products could bypass the suppression pool. Because the reference plant was assumed to be vulnerable to early suppression pool by-

pass via this mechanism, and because there is no analytical or experimental evidence to support or refute this assumption, a sensitivity case was run in which susceptible drain lines were assumed not to be present (this is the design of Susquehanna). The probability of suppression pool bypass was recalculated using a separate containment failure mode event tree, as in Reference 29. The new values for P(SP) are listed below.

If containment isolation fails,  $P(SP) = 0.6$ .

If early overpressure failure occurs,  $P(SP) = 0.1$ .

For cases where late containment failure occurs due to combined thermal and pressure loads, Reference 29 estimates that breaks in the drywell and wetwell are equally likely. Changing the failure probability of Event DW in the early containment failure mode event tree of Reference 29 to 0.5 gives the following:

$P(SP) = 0.5$  for a small or large break.

a. A. Payne (SNL) conference call with P. K. Niyogi (NRC) on May 1, 1989.

The effects of this change on risk are shown in Table 50.

**Table 50.** Offsite consequences with no in-pedestal drain line failure at vessel breach (per reactor year)

Plant Damage State	Mean Latent Fatalities	Mean Population Dose (Man-Rem) <sup>a</sup>	Mean Offsite Costs (\$)
TQUX	2.88E-05	5.60E-02	79.1
ST-SBO	1.89E-04	1.83E-01	1.04E+03
LT-SBO	2.94E-03	2.76	1.05E+04
ATWS (CM < CF)	3.62E-04	3.38E-01	2.02E+03
ATWS (CF < CM)	2.57E-03	2.58	1.07E+04
Total	6.09E-03	5.92	2.43E+04

a. The population dose is that received within a 50-mi radius of the plant.

Comparing this table with Table 49 indicates that the effect of the postulated drain line failure on risk is quite significant. In particular, with a decreased probability of early suppression pool bypass, long-term SBO replaces ATWS as the risk-dominant sequence. Therefore, in analyzing an individual plant, the configuration of any in-pedestal drainage paths should be examined closely to determine the vulnerability of these drainage paths to corium attack and the timing of any resulting suppression pool bypass. This is especially important in evaluating proposed improvements, because plants with little or no potential for early suppression pool bypass due to drain line or in-pedestal downcomer failure may see an increased benefit for those improvements that primarily serve to mitigate late containment failure.

**10.3.2 Preemptive Venting.** As discussed in Section 8.4, at least one utility has proposed immediate opening of the containment vent lines during SBO as a strategy for mitigating containment overpressurization (see References 7, 37). The motivating concern behind this proposal is that current venting arrangements generally require AC power for remote opening of the vent valves. Since AC power is not available during SBO, operators would have to open the vent valves locally. Opening the valves locally with the containment

at high pressure could expose operators to a very hazardous environment. Therefore, to vent the containment during SBO, without exposing the operators to a hazardous environment, the suggestion has been made to open the vent valves immediately upon loss of all AC power, rather than waiting for containment pressure to rise to the PCPL.

Once the vent valves are opened, local closure of the valves after the onset of core damage may be difficult or impossible because of the potentially high radiation levels in the vent lines (due to the release of fission products through the vent line). Therefore, the open vent line was modeled as a preexisting large containment breach in the SCET. Also, the HVAC ducting will probably not be overpressurized, since the vent is opened at low containment pressure. Therefore, no credit was given for retention of fission products in the reactor building (failure probability of Event RB equals 1.0). The effect on the consequences associated with SBO is shown in Table 51.

Comparing this table with Table 49 shows that preemptive venting (with no reclosure of the vent valves) significantly increases the consequences for SBO sequences as a group. However, for the case of

**Table 51.** Effect of preemptive venting on the consequences of SBO (per reactor-year)

	Mean Latent Fatalities	Population Dose (Rem) <sup>a</sup>	Offsite Costs (\$)
ST-SBO	1.93E-03	1.68	1.18E+04
LT-SBO	3.56E-03	3.25	2.07E+04

a. The population dose is that received within a 50-mi radius of the plant.

long-term SBO with no in-pedestal drain lines, preemptive venting was found to slightly decrease the latent fatalities and population dose. This appears to be due to the absence of a late unscrubbed release (there are no late containment failures with preemptive venting); such a release would increase the fraction of particulates released from containment. This may be an artifact of the release binning scheme to some extent. At any rate, the benefit is slight and is more than offset by the increase in offsite costs associated with long-term SBO and the increase in severity associated with the short-term SBO sequences. A similar result was also seen in the Mark I Containment Performance Improvement analysis (see Reference 3).

For preemptive venting to be useful, the vent valves would have to be reclosed prior to the release of a significant amount of activity to the environment. This could be done, in theory, by closing the valves when the radiation level in the vent line exceeded a predetermined limit. This strategy presupposes the existence of independently powered radiation monitors and vent valve operators, neither of which is known to currently be in use at any U.S. Mark II plant. If the vent valves were closed prior to events that would cause a significant containment pressure rise, then preemptive venting would not lessen the challenge to containment from overpressurization. Based on BWRLTAS/BWRSAR/MELCOR calculations performed by ORNL,<sup>a</sup> this would appear to be the case for short-term SBO, where no significant containment pressurization occurs until the time of core plate failure. If the assumption is made that the vent valves would be closed prior to core plate failure because of high vent line radiation levels as a result of core damage, then preemptive venting would not appear to be a useful strategy for mitigating short-term SBO sequences.

For long-term SBO, containment pressure (in the absence of venting) could be high enough at the time of core plate failure to justify preemptive venting to lessen the late overpressure challenge to the containment. BWRLTAS/BWRSAR/MELCOR calculations were not performed for this sequence, but the analysis in Reference 9 indicates that significant containment pressurization could occur before vessel failure (the degree of pressurization is, of course, both highly plant-specific and uncertain). However, venting before vessel failure would not mitigate late thermal fail-

ure, since Reference 9 also indicates that containment temperature does not increase greatly until after vessel failure. There is also much uncertainty as to whether late containment challenges would be due to overpressure or overtemperature. On these merits, the usefulness of preemptive venting for long-term SBO is difficult to quantify.

The best argument against preemptive venting for any SBO sequence is simply that the probability of recovering AC power prior to vessel failure is very high. If AC power can be recovered, then the sequence almost certainly will be terminated with no challenge to containment. However, if the containment is preemptively vented but the sequence is terminated via the recovery of AC power prior to core damage, then any release (even a release of noble gases) will have been unnecessary. For this reason, preemptive venting during SBO does not appear to be an attractive mitigation strategy at this point.

**10.3.3 Use of Diesel Fire Pumps.** As discussed in Sections 8.4 and 9.4, the diesel fire pumps can be used to reduce the core damage frequency of long-term SBO sequences and to mitigate the challenges to containment integrity for other SBO sequences and non-blackout transient-initiated sequences where all injection is lost and the reactor is not depressurized (TQUX). Use of the diesel fire pumps for injection into the vessel during long-term SBO sequences is predicated upon the availability of a dedicated DC power supply to the SRV solenoids, since depletion of the station batteries will otherwise result in SRV closure and repressurization of the vessel above the shutoff head of the diesel fire pumps. With this modification, the long-term SBO core damage frequency is reduced from  $3.75 \times 10^{-6}$  per reactor-year to  $3.83 \times 10^{-7}$  per reactor-year. The reduction in the consequences is shown in Table 52.

As Table 52 indicates, inclusion of the diesel fire pumps and modifications to provide a dedicated source of DC power to the SRV solenoids and containment vent valves afford a significant reduction in all reported risk measures.

**10.3.4 Blackstart Combustion Generator.** Section 8.4 discussed the effects of a combustion generator with blackstart capability on the core damage frequency and consequences of SBO sequences. The effects on the SBO consequences are summarized in Table 53.

a. ORNL analysis performed for Mark II CPI Program, as documented in ORNL Monthly Reports.

**Table 52.** Offsite consequences for SBO and TQUX sequences with diesel fire pump available (per reactor-year)<sup>a</sup>

Accident Class	Mean Latent Fatalities	Population Dose (Rem) <sup>b</sup>	Offsite Costs (\$)
ST-SBO	1.06E-04	1.09E-01	5.56E+02
LT-SBO <sup>c</sup>	3.05E-04	2.86E-01	1.09E+03
TQUX	2.82E-05	5.56E-02	7.13E+01
Total	4.39E-04	4.51E-01	1.72E+03
% Reduction from Base Case	86.3	85.2	85.5

a. Includes backup DC power to SRV solenoids and containment vent valves.

b. The population dose is that received within a 50-mi radius of the plant.

c. Changes in consequences are due to the reduction in LT-SBO core damage frequency.

**Table 53.** Effects of blackstart gas turbine on consequences of SBO (per reactor-year)

	Mean Latent Fatalities	Population Dose (Rem) <sup>a</sup>	Offsite Costs (\$)
ST-SBO	7.05E-05	6.83E-02	3.82E+02
LT-SBO	1.04E-03	9.78E-01	3.73E+03

a. The population dose is that received within a 50-mi radius of the plant.

Compared to the base case results in Table 49, the addition of the gas turbine reduces all offsite consequences by approximately 65%.

**10.3.5 In-Pedestal Downcomers.** Two of the Mark II plants have downcomers located directly beneath the vessel for the purpose of directing core debris into the suppression pool should the vessel fail and release debris into containment. These downcomers were evaluated to determine if they have a significant impact on risk. As discussed in Section 9.4, the downcomers were modeled in the SCETs by setting P(R2|VF) to 0.0, that is, all debris is assumed to be quenched in the suppression pool for sequences where the vessel fails at low pressure. High pressure melt ejection is calculated to disperse approximately 25%

of the core debris to regions of the drywell outside the pedestal (see Reference 9). The calculations in Reference 9 assumed the presence of four in-pedestal downcomers, with approximately 75% of the core debris being quenched in the suppression pool. The base case failure probability of Event R2 is already quite uncertain, making any determination of the effects on P(R2) of a partial debris-quench in the suppression pool difficult. Therefore, the base case failure probability of Event R2 was retained for sequences with vessel failure at high pressure (/VF). Because direct corium attack and energetic FCIs are expected to make in-pedestal downcomer failure (and thus suppression pool bypass) very likely, the base case probabilities of suppression pool bypass were retained. Table 54 shows the consequence results with these modifications to the SCETs.

**Table 54.** Consequence results with in-pedestal downcomers and high probability of suppression pool bypass (per reactor-year)

Plant Damage State	Mean Latent Fatalities	Mean Population Dose (Man-Rem) <sup>a</sup>	Mean Offsite Costs (\$)
TQUX	3.29E-05	5.98E-02	99.2
ST-SBO	1.80E-04	1.76E-01	1.02E+03
LT-SBO	2.95E-03	2.77	1.06E+04
ATWS (CM < CF)	1.12E-03	1.02	6.20E+03
ATWS (CF < CM)	4.60E-03	4.60	1.91E+04
Total	8.88E-03	8.63	3.70E+04

a. The population dose is that received within a 50-mi radius of the plant.

Comparing this table to Table 49 indicates that the benefits of debris-quenching provided by the in-pedestal downcomers are more than offset by the high assumed probability of suppression pool bypass associated with downcomer failure. If the probability of suppression pool bypass is significantly less than the assumed value of 90%, then the beneficial effects of debris-quenching are expected to dominate and there should be a reduction in risk. Note, also, that failure of the in-pedestal downcomers would mimic failure of the in-pedestal drain lines and drain plate covers postulated in the base case, that is, failure of either drain lines or downcomers is assumed to result in early suppression pool bypass.

The overall result is that, if the presence of the in-pedestal downcomers results in a high probability of pool bypass, then the downcomers appear to be of no benefit in reducing risk. Even if the probability of pool bypass is very low, the net reduction in risk provided by these downcomers appears to be very slight. This stems directly from the fact that vessel failure at high pressure is much more likely than failure at low pressure in the dominant Mark II accident sequences. High pressure vessel failure is expected to result in a dispersive melt ejection, which is calculated to spread a significant fraction of the core debris outside the pedestal region. The debris dispersed into the exterior regions of the drywell will, if not cooled, cause heatup and pressurization of the drywell. Some of the debris trapped in the pedestal region may flow through the in-pedestal downcomers and into the suppression pool. The effect that the quenching of this debris has on the progress of the sequence is highly uncertain. However, if attack by this debris should fail one or more of the in-pedestal downcomers, then the offsite consequences of a release will increase in severity because of the loss of pool scrubbing.

**10.3.6 Drywell Head Flooding.** Drywell head flooding is a potential improvement that could prove beneficial in preventing late thermal failure of the drywell head seal during SBO, or in mitigating a release should head seal failure occur. The details of this improvement are discussed in Section 4.3.8. Essentially, a modification would be needed to allow an operator to transfer water from the spent fuel pool to the drywell head following a loss of all AC power. The potential benefits associated with drywell head flooding are twofold. First, the water may provide a large enough heat sink to prevent late thermal failure of the drywell head seal (or other elastomeric seals in the drywell head region). Second, any release of fission products through the drywell head seal may be scrubbed by the overlying pool of water.

To evaluate the effect of drywell head flooding on the offsite consequences associated with SBO, the SCETs were modified, as described in Section 8.4, to reflect both a decreased likelihood of head seal failure and the potential benefits of scrubbing through the overlying water pool. The revised offsite consequences are shown in Table 55.

Table 55 indicates that drywell head flooding, if effective, has the potential to slightly reduce the offsite consequences for SBO. However, as mentioned above, uncertainties remain as to the effectiveness of drywell head flooding in preventing failure of the drywell head seal and in scrubbing the release should the head seal fail. If flooding is not as effective as assumed here, then the benefits will be correspondingly reduced.

**10.3.7 Increased Probability of Early Containment Failure.** To examine the sensitivity of the risk results to the conditional probability of early containment failure, the failure probability of Event F1

**Table 55.** Offsite consequences for SBO sequences with drywell head flooding (per reactor–year)

	Mean Latent Fatalities	Mean Population Dose (Man–Rem) <sup>a</sup>	Mean Offsite Costs (\$)
ST–SBO	9.71E–05	1.04E–01	3.27E+02
LT–SBO	2.96E–03	2.78	1.06E+04
% Decrease From Base Case	3.9	3.7	7.3

a. The population dose is that received within a 50–mi radius of the plant.

was modified as follows. For the Class IC ATWS, the base case probabilities of  $7.5 \times 10^{-2}$  and 0.9 were increased to 0.5 and 0.99, respectively. For short-term SBO and TQUX, the base case probability was increased from  $7.5 \times 10^{-2}$  to an indeterminate value of 0.5. Finally, for long-term SBO, the base case failure probability of 0.57 was increased to 0.9. Table 56 shows the offsite consequences with these increased probabilities of early containment failure.

Increasing the probability of early containment failure leads to significantly higher offsite consequences. In particular, the consequences of an ATWS sequence with core melt prior to containment failure (Class IC) are especially sensitive to this probability.

The possible sensitivity of this result to the percentage of the population that is assumed to evacuate was also examined. The base case consequence results and the above sensitivity case of increased early containment failure probability were both obtained under the assumption that 100% of the population successfully

evacuates. However, if a certain percentage of the population did not evacuate, the risk results could potentially be quite different. To evaluate this issue, offsite consequences were recalculated with MACCS under the assumption that 5% of the population does not evacuate. The consequences for this case are shown in Table 57.

The risk per year for the sensitivity case of increased probability of early containment failure, again assuming 95% evacuation, is shown in Table 58.

Comparing Table 49 with Table 57 and Table 56 with Table 58 indicates that the percentage of the population that evacuates has essentially no impact on any of the reported risk measures, since these risk measures are dominated by the long-term chronic dose. The only risk measures that are expected to be significantly affected by the evacuation percentage are early health effects, such as prodromal vomiting and acute fatalities, but these measures are not being reported, for reasons mentioned earlier.

**Table 56.** Offsite consequences with increased probabilities of early containment failure (per reactor–year)

Plant Damage State	Mean Latent Fatalities	Mean Population Dose (Man–Rem) <sup>a</sup>	Mean Offsite Costs (\$)
TQUX	4.70E–05	7.24E–02	177
ST–SBO	2.06E–04	1.99E–01	1.11E+03
LT–SBO	2.98E–03	2.80	1.07E+04
ATWS (CM < CF)	5.34E–03	4.79	2.93E+04
ATWS (CF < CM)	4.60E–03	4.60	1.91E+04
Total	1.32E–02	12.50	6.04E+04
% Increase	47.7	44.2	62.4

a. The population dose is that received within a 50–mi radius of the plant.

**Table 57.** Offsite consequences with base case probability of early containment failure and 95% evacuation (per reactor-year)

Plant Damage State	Mean Latent Fatalities	Mean Population Dose (Man-Rem) <sup>a</sup>	Mean Offsite Costs (\$)
TQUX	3.30E-05	6.02E-02	99.4
ST-SBO	2.01E-04	1.95E-01	1.09E+03
LT-SBO	2.99E-03	2.81	1.07E+04
ATWS (CM < CF)	1.13E-03	1.02	6.21E+03
ATWS (CF < CM)	4.60E-03	4.61	1.91E+04
Total	8.95E-03	8.70	3.72E+04
% Increase	0.1	0.4	0.0

a. The population dose is that received within a 50-mi radius of the plant.

**Table 58.** Offsite consequences for the case of increased probability of early containment failure and 95% evacuation (per reactor-year)

Plant Damage State	Mean Latent Fatalities	Mean Population Dose (Man-Rem) <sup>a</sup>	Mean Offsite Costs (\$)
TQUX	4.70E-05	7.28E-02	177
ST-SBO	2.06E-04	1.99E-01	1.11E+03
LT-SBO	2.99E-03	2.81	1.07E+04
ATWS (CM < CF)	5.35E-03	4.80	2.93E+04
ATWS (CF < CM)	4.60E-03	4.61	1.91E+04
Total	1.32E-02	12.50	6.04E+04

a. The population dose is that received within a 50-mi radius of the plant.

We close this section by summarizing the quantitative benefits calculated for the potential Mark II improvements. This information is presented in Table 59. The results of the various sensitivity cases, such as ATWS level control, have not been included in the table. The risk measures presented in this table are the sum of the individual risk measures for each plant damage state.

## 10.4 Limitations and Uncertainties

The quantitative analysis performed for this report is limited in several important respects. First, the scope of the accident sequence analysis is narrower than would be performed in a typical Level 1 PRA. For example, there are areas where support system

interdependencies have been neglected. These interdependencies would be important in an analysis whose goal was to rigorously determine the core damage frequency for a specific plant. Here, however, the principal goal is to determine the *change* in the core damage frequency effected for the *generic* CPI plant by a change in hardware or operating procedure. In addition, a detailed data base of component failure rates, human error probabilities, and system unavailabilities was not developed. Instead, use was made of data from studies previously performed for similar plants.

The containment response analysis utilized SCETs. Each SCET has approximately 15 top events, rather than the 100 or more top events in the BWR accident progression event trees developed for NUREG-1150. The current uncertainties in many important phenomenological issues tend to offset attempts to



**Table 59.** Summary of quantitative benefits for potential Mark II improvements

	Hardened Vent	Diesel Fire Pump and Enhanced Depressurization	Blackstart Gas Turbine	Drywell Head Flooding	No Drain Line or Downcomer Failure
CM Frequency	↓	↓↓	↓↓	⇔	⇔
Latent Fatalities	↓	↓↓	↓↓	↓	↓↓
Population Dose	↑	↓↓	↓↓	↓	↓↓
Offsite Costs	↓	↓↓	↓↓	↓	↓↓

↑ = slight increase (< 5%)  
 ↓ = slight decrease (< 5%)  
 ↓↓ = large decrease (> 20%)  
 ⇔ = no change

include a great amount of detail in the containment event trees; even in the SCETs used here, the quantification of several important events remains indeterminate because of a lack of data, both calculational and experimental, and because some events can be precisely quantified only on a plant-specific basis. For more details on the SCET methodology, see Reference 3.

All values used to quantify the event trees, and, therefore, all results as well, are point estimates. In reality, there is a range of uncertainty (both stochastic and due to lack of knowledge) associated with each of these values and results, with this uncertainty typically being given in the form of a cumulative distribution function. Because no uncertainty analysis was performed, the uncertainty in the point estimates cannot be explicitly identified; however, in some cases, this uncertainty can be expected to span one or more orders of magnitude.

Because no Mark II plant was analyzed as part of the NUREG-1150 effort, and because only limited Mark II containment response calculations were performed by ORNL using BWRLTAS/BWRSAR/MELCOR, a choice had to be made as to what analyses to draw upon in quantifying the various branches on the SCETs. The decision was made to primarily utilize the MAAP analysis of Shoreham contained in Reference 29. This decision was made with knowledge of the recognized limitations of the MAAP code, and of the different modeling assumptions used in MAAP and STCP. Even in light of the limitations of MAAP, Reference 29 still provided the most thorough and well documented set of containment response calculations for a Mark II plant that was available for use in this project. Wherever possible, the MAAP results

from Reference 9 were supplemented or supplanted with results from other analyses.

One of the drawbacks to using the analyses in Reference 9 was that Shoreham's containment is not representative of the "generic" Mark II design, primarily because it has four in-pedestal downcomers located underneath the reactor vessel. The effect of these downcomers is that, for sequences in which the reactor vessel fails at low pressure, the MAAP code transports all core debris to the suppression pool, where the debris is assumed to be quenched. This limitation was overcome in the base case SCETs by questioning ex-vessel recovery (Event R2), even for those branches of the tree involving vessel failure at low pressure (VF). Another limitation of the Reference 9 MAAP analysis applies to those sequences involving vessel failure at high pressure (V/F), for which MAAP calculates entrainment of approximately 25% of the core debris to the ex-pedestal region of the drywell; the other 75% is transported to the suppression pool via the in-pedestal downcomers. This is not an accurate distribution for the "generic" Mark II plant, which is assumed to have a flat in-pedestal floor with no in-pedestal downcomers. This limitation was accounted for by increasing the probability of late containment failure for those sequences where ex-vessel recovery fails. Reference 29 quantified late containment failure for these sequences based on the probability of recovering a system capable of injecting water into the containment within the time to containment failure calculated by MAAP (the probability of injection recovery was quantified in Reference 29 assuming an exponential distribution for failure to repair, with a mean time-to-repair of 19 h). With ~100% of the core debris in the drywell, the time to containment failure may be significantly different than in the case with only 25% of the debris present on the drywell floor. The assumption that the debris that

enters the suppression pool is quenched is uncertain. The BWRLTAS/BWRSAR/MELCOR analysis indicates that steam spikes may be significant and sufficient to fail containment by overpressurization. Steam explosions cannot be modeled at this time, but may pose an additional challenge to containment integrity.

In the consequence analysis, original fission product transport calculations were not performed to determine source terms. Instead, the source terms calculated in Reference 9 were used as inputs to the MELCOR Accident Consequence Code System (MACCS), along with the NUREG-1150 deck for Peach Bottom (see Appendix D for more details). Again, because this report is concerned primarily with changes in offsite consequences effected by a proposed improvement, this methodology should be adequate. However, because of modeling differences between MAAP and STCP, the source terms used in this report may differ

from source terms used in NUREG-1150. This may affect some of the consequence results, as discussed in earlier sections of the report. Also, because the consequence calculations were performed using the Peach Bottom MACCS input deck from NUREG-1150, the consequence results are specific to the Peach Bottom site. Other sites with different population distributions, emergency response plans, etc., will have consequences that vary from those in this report. This should be taken into account in applying the results of this report to a specific plant.

Finally, the scope of this analysis was not to model all existing variations in the Mark II containment design and in the reactor systems. Instead, a generic plant design was decided upon, with the expectation that individual plants can use this analysis as a starting point for their own plant-specific investigations.

## 11. REFERENCES

1. U.S. Nuclear Regulatory Commission, "Integration Plan for Closure of Severe Accident Issues," SECY-88-147 (V. Stello to NRC Commissioners), May 25, 1988.
2. U.S. Nuclear Regulatory Commission, *Reactor Risk Reference Document*, NUREG-1150 (Draft), February 1987.
3. K. C. Wagner et al., *An Overview of BWR Mark I Containment Venting Risk Implications*, NUREG/CR-5225, November 1988, and Addendum 1, May 1989.
4. I. A. Papazoglou and R. Karol, *Review of the Limerick Generating Station Probabilistic Risk Assessment*, NUREG/CR-3028, February 1983.
5. Science Applications, Inc., "Probabilistic Risk Assessment, Shoreham Nuclear Power Station," Prepared for Long Island Lighting Company, June 24, 1983.
6. E. R. Burns et al., *Shoreham Nuclear Power Station Full Power PRA, PRA Update: Supplemental Containment System Implementation*, IT/Delian Corporation, Prepared for Long Island Lighting Company, February 1988.
7. Pennsylvania Power and Light, *Susquehanna Steam Electric Station Individual Plant Examination*, NPE-86-001, 1986.
8. C. N. Amos et al., *Containment Event Analysis for Postulated Severe Accidents: Peach Bottom Atomic Power Station, Unit 2*, NUREG/CR-4700, (Draft), Volume 3, May 1987.
9. Fauske and Associates, Inc., *MAAP Analyses To Support Shoreham 100% Power PRA*, Prepared for the Long Island Lighting Company, February 1988, Revised March 1988.
10. *MELCOR Accident Consequence Code System*, MACCS Version 1.5 User's Manual, NUREG/CR-4691, draft version last revised September 21, 1988.
11. "World List of Nuclear Power Plants," *Nuclear News*, 32, 2, February 1989.
12. Limerick Generating Station, "Final Safety Analysis Report," Philadelphia Electric Company, Rev. 58, June 1989.
13. La Salle County Station "Final Safety Analysis Report," Commonwealth Edison Rev. 63, July 25, 1983.
14. Nine Mile Point Nuclear Station, "Final Safety Analysis Report," Niagara Mohawk Rev. 27, July 1986.
15. Susquehanna Steam Electric Station, "Final Safety Analysis Report," Pennsylvania Power & Light.
16. Shoreham Nuclear Power Station, "Final Safety Analysis Report," Long Island Lighting Company, Rev. 34, November 29, 1984.
17. Washington Nuclear Power Station Unit 2, "Final Safety Analysis Report," Washington Public Power Supply System.
18. J. N. Castle et al., *Survey of Light Water Reactor Containment Systems, Dominant Failure Modes, and Mitigation Opportunities, Final Report*, NUREG/CR-4242, R&D Associates, January 1988.
19. General Electric Company, *BWR Owner's Group Emergency Procedure Guidelines*, NEDO-31331, Revision 4, March 1987.

20. Greimann, et al., *Final Report, Containment Analysis Techniques a State-of-the-Art Summary*, NUREG/CR-3653, March 1984.
21. R. M. Harrington and S. A. Hodge, "Containment Venting as a Severe Accident Mitigation Technique for BWR Plants With Mark I Containments," *Nuclear Engineering and Design* 108, 1988.
22. S. R. Greene, *The Role of BWR Secondary Containments in Severe Accident Mitigation: Issues and Insights From Recent Analyses*, NUREG/CP-0095, November 1988.
23. R. M. Harrington and L. J. Ott, *The Effect of Small Capacity, High Pressure Injection Systems on TQUV Sequences at Browns Ferry Unit One*, NUREG/CR-3179, September 1983.
24. R. M. Harrington and S. A. Hodge, *ATWS at Browns Ferry Unit 1, Accident Sequence Analysis*, NUREG/CR-3470, July 1984.
25. K. C. Wagner, *Analysis of a High Pressure ATWS With Very Low Make-up Flow*, DOE/ID-10211, October 1988.
26. D. L. Kelly and W. J. Galyean, "Analysis of Venting As a Severe Accident Mitigation Strategy for the BWR Mark II Containment," *IEEE Transactions on Nuclear Science*, April 1990.
27. Letter from D. Kelly (Idaho National Engineering Laboratory) to J. N. Ridgely (U.S. Nuclear Regulatory Commission) "Discussion of Core Melt Contribution from TW Sequences in BWRs," dated April 5, 1989 (DLK-03-89).
28. U.S. Nuclear Regulatory Commission, *Containment Performance Working Group*, NUREG-1037, May 1985.
29. Z. T. Mendoza et al., *Containment and Phenomenological Event Tree Evaluation at Full Power for the Shoreham Nuclear Power Station*, Science Applications International Corporation, Prepared for the Long Island Lighting Company, February 1988.
30. H. S. Blackman et al., *Containment Venting Analysis for the Peach Bottom Nuclear Power Plant*, NUREG/CR-4696, EGG-2464, December 1986.
31. M. T. Leonard and R. Freeman-Kelly, *A Preliminary Evaluation of Containment Venting at La Salle County Station, Unit 2*. Battelle Columbus Division, December 1987.
32. S. E. Dingman, *BWR Reactor Building Environment After Containment Failure*, SAND-88-1515C, December 1988.
33. T. A. Wheeler et al., *Analysis of Core Damage Frequency: Expert Judgment Elicitation on Internal Events Issues, Volume 2, Part 1—Expert Panel, and Part 2—Project Staff*, NUREG/CR-4550 (Draft), December 1988.
34. S. R. Greene, *An Assessment of the Shoreham Nuclear Power Station's Secondary Containment Mitigation Capability*, June 26, 1987.
35. Letter from D. Kelly, (Idaho National Engineering Laboratory) to J. N. Ridgely, (Nuclear Regulatory Commission), "Comments from Review of Mark II Reports by Brookhaven and R&D Associates," dated June 9, 1989, (DLK-06-89).
36. Letter from Philadelphia Electric Company to U.S. Nuclear Regulatory Commission, with Attachment, dated June 23, 1989, sent in response to a request for additional information regarding consideration of severe accident mitigation design alternatives.

37. Pennsylvania Power and Light Company, *The PP&L Approach to Risk Management and Risk Assessment*, Technical Report Number NPE-89-001, Revision 2, January 1989.
38. E. Soderman, "Mitigation of Severe Accidents," *Nuclear Europe*, November/December 1987, pp. 18-19.
39. U.S. Nuclear Regulatory Commission, *Operating Experience Feedback Report—Service Water System Failures and Degradations*, NUREG-1275, Volume 3, November 1988.
40. D. A. Neitzel et al., *Improving the Reliability of Open-Cycle Water Systems*, NUREG/CR-4626, Vol. 1, September 1986.
41. S. W. Hatch et al. *Shutdown Decay Heat Removal Analysis of a General Electric BWR/4 Mark I*, NUREG/CR-4767, July 1987.
42. U.S. Nuclear Regulatory Commission, *Regulatory and Backfit Analysis: Unresolved Safety Issue A-45, Shutdown Decay Heat Removal Requirements*, NUREG-1289, November 1988.
43. R. Erdmann et al., "Mitigating Severe Accident Consequences at the Shoreham BWR," *Proceeding from the International Meeting on Light Water Reactor Severe Accident Evaluation, August 28 to September 1, 1983*.
44. H. Ludewig et al., "An Assessment of Core Melt Accidents in the Limerick Facility," *Proceeding from the International Meeting on Light Water Reactor Severe Accident Evaluation, August 28 to September 1, 1983*.
45. K. R. Perkins et al., "Containment Performance for Core Melt Accidents in BWRs with Mark I and Mark II Containments," *Proceedings: International Topical Meeting on Probabilistic Safety Methods and Applications*, EPRI NP-3912-SR, Volume 2, Special Report, February 1985.
46. J. W. Yang and W. T. Pratt, "Mitigation of Internally Initiated Severe Accidents for a BWR Mark-II Power Plant," *Proceedings: International Topical Meeting on Probabilistic Safety Methods and Applications*, EPRI NP-3912-SR, Volume 2, Special Report, February 1985.
47. C. N. Amos et al., *Evaluation of Severe Accident Risks and the Potential for Risk Reduction: Peach Bottom, Unit 2*, NUREG/CR-4551 (Draft), Volume 3, May 1987.
48. U.S. Nuclear Regulatory Commission, *A Review of the Current Understanding and Potential for Containment Failure from In-Vessel Steam Explosions*, NUREG-1116, June 1986.
49. L. S. Tong, *Principles of Design Improvement for Light Water Reactors*, Hemisphere Publishing Corporation: Philadelphia, PA, 1988.
50. U.S. Nuclear Regulatory Commission, *Estimates of Containment Loads from Core Melt Accidents*, NUREG-1079, December 1985.
51. T. G. Theofanous et al., *An Assessment of Steam Explosion-Induced Containment Failure*, NUREG/CR-5030, February 1989.
52. D. A. Brinson and G. H. Graves, *Evaluation of Seals for Mechanical Penetrations of Containment Buildings*, NUREG/CR-5096, August 1988.
53. T. L. Bridges, *Containment Penetration Elastomer Seal Leak Rate Tests*, NUREG/CR-4944, July 1987.
54. Stone & Webster, *Study of the Structural Integrity of Shoreham Primary Containment Under Severe Accident Conditions*, Report prepared for Long Island Lighting Company, 1988.

55. U.S. Nuclear Regulatory Commission, *Clarification of TMI Action Plan Requirements*, NUREG-0737, November 1980.
56. S. J. Niemczyk, "Potential Effects of the Fire Protection System Sprays at Browns Ferry on Fission Product Transport," *Proceedings: International Topical Meeting on Probabilistic Safety Methods and Applications*, EPRI NP-3912-SR, Volume 2, Special Report, February 1985.
57. U.S. Nuclear Regulatory Commission, *Reactor Safety Study—An Assessment of Accident Risks in U.S. Commercial Nuclear Power Plants*, WASH-1400, (NUREG-75/014), October 1975.
58. T. L. Chu et al., *Interfacing Systems LOCA: Boiling Water Reactors*, NUREG/CR-5124, February 1989.
59. I. A. Papazoglou, "Risk Evaluation of the Alternate-3A Modification to the ATWS Prevention/Mitigation System in a BWR-4, Mark-II Power Plant," *Proceeding from the International Meeting on Light Water Reactor Severe Accident Evaluation, August 28 to September 1, 1983*.
60. U.S. Nuclear Regulatory Commission, *Anticipated Transients Without Scram for Light Water Reactors*, NUREG-0460, March 1980.
61. 54 FR 62, "Flow Control Conditions for the Standby Liquid Control Systems in Boiling Water Reactors," U.S. Nuclear Regulatory Commission, pp. 13361-13362, April 3, 1989.
62. D. Ilberg et al., *A Review of the Shoreham Nuclear Power Station Probabilistic Risk Assessment*, NUREG/CR-4050, November 1985.
63. B. Chexal and W. Layman, "A Correlation for Predicting Reactor Power During a BWR ATWS," *Transactions of the ANS 1986 Annual Meeting, Washington, D.C., 1986*.
64. R. J. Dallman et al., *Severe Accident Sequence Analysis Program—Anticipated Transient Without Scram Simulations for Browns Ferry Nuclear Plant Unit 1*, NUREG/CR-4165, EGG-2374, May 1987.
65. P. J. Pelto et al., *Reliability Analysis of Containment Isolation Systems*, NUREG/CR-4220, June 1985.
66. M. Khatib-Rahbar et al., "A Probabilistic Approach to Quantifying Uncertainties in the Progression of Severe Accidents," in *Nuclear Science and Engineering*, 102, 1989.
67. Pickard, Lowe, and Garrick, Inc., *Core Melt Accident Dose-Versus-Distance Probability Distributions, 100% Power Operations, Shoreham Nuclear Power Station*, Prepared for Long Island Lighting Company, February 1988.
68. T. M. Su, *Suppression Pool Temperature Limits for BWR Containments*, NUREG-0783, November 1981.
69. S. A. Eide, "Potential Underestimation of Test and Maintenance Unavailabilities in Probabilistic Risk Assessments," paper presented at *The 1989 Probabilistic Safety Assessment Conference in Pittsburgh, Pennsylvania, April 1989*.
70. A. M. Kolaczowski and A. C. Payne Jr., *Station Blackout Accident Analyses (Part of NRC Task Action Plan A-44)*, NUREG/CR-3226, May 1983.
71. R. L. Iman and S. C. Hora, "Bayesian Methods for Modeling Recovery Times with an Application to the Loss of Off-Site Power at Nuclear Power Plants," in *Risk Analysis*, 9, 1, 1989.
72. M. T. Drouin et al., *Analysis of Core Damage Frequency: Grand Gulf Unit 1 Internal Events*, NUREG/CR-4550, draft Revision 1, February 1989.
73. Northeast Utilities Service Company, "Millstone Unit 1 Probabilistic Safety Study," prepared by Probabilistic Risk Assessment Section/Safety Analysis Branch, July 1985.

74. U.S. Nuclear Regulatory Commission, *Development of Transient Initiating Event Frequencies for Use in Probabilistic Risk Assessments*, NUREG/CR-3862, May 1985.
75. J. R. Lehner et al., *Assessment of Severe Accident Prevention and Mitigation Features: BWR Mark II Containment Design*, NUREG/CR-4920, Vol. 2, July 1988.





# APPENDIX A

## PRIMARY CONTAINMENT RESPONSE CALCULATIONS FOR UNMITIGATED SHORT-TERM STATION BLACKOUT AT PEACH BOTTOM\*

with consideration of

- 1.) Separated metal and oxide pours
- 2.) Melting of reactor vessel bottom head
- 3.) Degassing of drywell concrete

S. A. Hodge  
C. R. Hyman  
L. J. Ott

Boiling Water Reactor Severe Accident Technology Program  
Oak Ridge National Laboratory  
Oak Ridge, Tennessee

---

\*Provided initially as letter report to Dr. T. J. Walker, Accident Evaluation Branch,  
Division of Systems Research, RES, USNRC dated November 28, 1988



PRIMARY CONTAINMENT RESPONSE CALCULATIONS  
FOR UNMITIGATED SHORT-TERM STATION BLACKOUT  
AT PEACH BOTTOM

with consideration of

- 1.) Separated metal and oxide pours
- 2.) Melting of reactor vessel bottom head
- 3.) Degassing of drywell concrete

S. A. Hodge  
C. R. Hyman  
L. J. Ott

Boiling Water Reactor Severe Accident Technology Program  
Oak Ridge National Laboratory  
Oak Ridge, Tennessee

November 28, 1988

Research sponsored by the U.S. Nuclear Regulatory Commission Office of Nuclear Regulatory Research under Inter-agency Agreement DOE 1886-8045-2B with the U.S. Department of Energy under contract DOE-AC05-84OR21400 with the Martin Marietta Energy Systems, Inc.

NOTICE

This report was prepared as an account of work sponsored by an agency of the United States Government. Neither the United States Government nor any agency thereof, or any of their employees, makes any warranty, expressed or implied, or assumes any legal liability or responsibility for any third party's use, or the results of such use, of any information, apparatus, product or process disclosed in this report, or represents that its use by such third party would not infringe privately owned rights.



## CONTENTS

	<u>Page</u>
EXECUTIVE SUMMARY .....	ES-1
1. INTRODUCTION .....	1-1
2. THE SHORT-TERM STATION BLACKOUT SEVERE ACCIDENT SEQUENCE .....	2-1
3. BWR SAR CALCULATIONS FOR SHORT-TERM STATION BLACKOUT WITH ADS ACTUATION .....	3-1
3.1 BWR SAR Program Severe Accident Models .....	3-1
3.2 Events Prior to Reactor Vessel Bottom Head Penetration Failure .....	3-1
3.3 Allocation of Debris Pour Between Inpedestal and Expedestal Regions of the Drywell Floor .....	3-3
4. CONTAIN CALCULATIONS OF THE CONTAINMENT RESPONSE AFTER REACTOR VESSEL BOTTOM HEAD PENETRATION FAILURE .....	4-1
4.1 The CONTAIN Model for the BWR Mark I Primary Containment .....	4-1
4.2 Primary Containment Response .....	4-1
5. CONTAIN CALCULATIONS FOR THE EFFECT OF DRYWELL SPRAYS .....	5-1
5.1 Modeling of Drywell Sprays .....	5-1
5.2 Primary Containment Response .....	5-2
6. SUMMARY OF RESULTS AND DISCUSSION OF CONCLUSIONS .....	6-1
7. RECOMMENDATIONS FOR FUTURE WORK .....	7-1
7.1 Necessary Modeling Improvements .....	7-1
7.2 Calculations Based Upon Best-Estimate Eutectic Pours from Reactor Vessel .....	7-7
7.3 Extension of Calculations Beyond Time of Exhaustion of Zirconium Inventory .....	7-7
7.4 Calculations to Estimate the Effects of Wetwell Venting .....	7-8
7.5 Calculations to Determine Expected Decontamination Factors for the Peach Bottom Secondary Containment .....	7-8
7.6 Calculations for Long-Term Station Blackout .....	7-9
7.7 Determination of Concrete Type .....	7-9
8. REFERENCES .....	8-1



PRIMARY CONTAINMENT RESPONSE CALCULATIONS  
FOR UNMITIGATED SHORT-TERM STATION BLACKOUT  
AT PEACH BOTTOM

with consideration of

- 1.) Separated metal and oxide pours
- 2.) Melting of reactor vessel bottom head
- 3.) Degassing of drywell concrete

S. A. Hodge      C. R. Hyman      L. J. Ott

Boiling Water Reactor Severe Accident Technology Program  
Oak Ridge National Laboratory  
Oak Ridge, Tennessee

EXECUTIVE SUMMARY

This report describes the results of analyses performed by the BWR Severe Accident Technology (BWRSAT) Program at Oak Ridge National Laboratory (ORNL) to estimate the conditions within the Peach Bottom drywell during an unmitigated short-term station blackout severe accident sequence. It is also the purpose of this report to discuss the efficiency of the CONTAIN code with respect to its application to calculate the response of the BWR MKI containment system to debris pours from the reactor vessel. This work was performed at the request of Dr. Thomas J. Walker, Leader of the Task Group on the BWR Mark I Shell Melt-Through Issue established by the Accident Evaluation Branch of the Nuclear Regulatory Commission (NRC) Office of Nuclear Regulatory Research. The Task Group was formed in support of an ongoing effort to determine the response of the drywell shell in the unlikely event that a severe accident were to proceed to the point of release of molten core debris from the reactor vessel.

The primary containment response calculations discussed in this report were performed with the Boiling Water Reactor Severe Accident Response (BWRSAR) code and, for the period after failure of the reactor vessel bottom head penetrations, with the CONTAIN code. The short-term station blackout accident sequence has been analyzed with the simulation based upon the existing plant configuration including representation of the concrete in accordance with recently acquired information that identifies it to be of the limestone common sand classification. It is assumed that the Automatic Depressurization System (ADS) is available and is actuated in accordance with the BWR Owners Group Emergency Procedure Guidelines. After the predicted failure of the reactor vessel bottom head penetrations, the gas blowdown rates and the core debris pouring rates calculated by the BWRSAR code are used to drive the CONTAIN calculations. It was assumed for these calculations that the core debris in the reactor vessel bottom head forms two separate mixtures during heatup after bottom head dryout: a single metallic eutectic with a melting temperature of 2750°F (1783 K) and a single oxidic eutectic with a melting temperature of 4350°F (2672 K).

It should be recognized that the authors of this report believe (and the results of recent experimental efforts by George Parker<sup>12</sup> at ORNL support the contention) that the initial pour of molten core debris from a BWR reactor vessel would be metals-rich and relatively low in temperature [about 2600°F (1700 K)]. However, we are unable to use BWR SAR code predictions based upon our best-estimates regarding the formation of low-melting-temperature eutectic alloys in the BWR reactor vessel bottom head to drive the current version (1.1) of CONTAIN, since the CORCON module within CONTAIN has no models to represent these alloys. It is for the reason of these CORCON module limitations that the BWR SAR calculations of the present report are based upon the unrealistic assumption that the metallic core debris in the reactor vessel bottom head forms a single eutectic mixture with a melting temperature higher than that of stainless steel.

In addition, while the spread of the initial metals-rich debris over the drywell floor would be expected to cause a large release of water vapor and carbon dioxide from the concrete by means of heating (even though the temperature might not be high enough to induce concrete ablation), the present released version (1.1) of CONTAIN permits none of the water vapor or carbon dioxide stored in the concrete to escape unless the overlying debris temperature is sufficient [ $>2246^{\circ}\text{F}$  (1503 K) for limestone common sand concrete] to cause ablation. Accordingly, a special version of CONTAIN provided by the code development staff at Sandia National Laboratories (SNL) was used to perform the present calculations. This special version of the code includes the necessary models for concrete degassing in the absence of ablation and for determination of the concomitant release of water vapor and carbon dioxide.

For Short-Term Station Blackout with the ADS system available, the reactor vessel is manually depressurized in accordance with the BWR Owners Group Emergency Procedure Guidelines at the time that water level indication is lost. The purpose of the rapid reactor vessel depressurization is to temporarily lower the core temperature by steam cooling, to thereby delay the onset of degradation of core geometry and the downward movement of molten core structural material, and to greatly reduce the magnitude of the direct vessel blowdown into the drywell and the concomitant containment pressure increase upon bottom head penetration failure.

Actuation of the ADS with the water level near the bottom of the core causes flashing of the vessel water inventory and early core plate dryout, predicted to occur at just 81 min after scram. Since the core plate is dry when debris relocation begins at time 132 min, local core plate failures (by overtemperature) are predicted to begin almost immediately thereafter.

Continued relocation of core debris within the reactor vessel results in bottom head dryout at time 255 min; the bottom head penetrations are predicted to fail immediately thereafter. The effect of this upon the drywell is relatively minor, however, since the reactor vessel and drywell pressures are nearly equal when the penetrations fail.



Also, since there is no great blowdown of steam through the bottom head debris bed, there is no sudden large production of hydrogen and release of energy within the debris bed upon bottom head penetration failure.

The event timing for this unmitigated severe accident sequence is provided in Table ES-1. Information concerning the amount of zirconium oxidation in the core region and in the reactor vessel bottom head as well as the total in-vessel hydrogen generation is also provided in this table, for a time sufficiently after bottom head penetration failure that the in-vessel metal-steam reactions are essentially complete.

It is important to recognize that were the reactor vessel pressurized at the time of bottom head penetration failure, the BWRSAR code would predict a large debris bed energy release provided by metal-steam reactions during vessel blowdown, and the initial pour of molten debris from the bottom head would be predicted to occur almost immediately after penetration failure, since the debris bed would quickly reheat to the assumed metallic debris melting temperature of 2750°F (1783 K). However, for the case considered here in which the ADS is actuated so that there is no large debris bed metal-steam reaction energy release, the BWRSAR code predicts an 8-min period between bottom head penetration failure and the initial pour of molten metals onto the drywell floor. Nevertheless, the pour includes a much greater proportion of unoxidized zirconium metal than would occur in the pressurized case.

CONTAIN code calculations of the containment response to the release of molten debris from the reactor vessel have been carried out for both a dry case and for a case with consideration of the effect of drywell sprays. In this connection, the advice and assistance of the CONTAIN code development staff at Sandia National Laboratories were invaluable to this project and the performance of these analyses. The following discussion pertains to the dry case, in which the only water on the drywell floor is the small amount initially in the drywell sumps, which is quickly boiled away upon the first emergence of debris.

With ADS actuation in accordance with the Emergency Procedures Guidelines, most of the energy release by oxidation of the metallic debris occurs not in the reactor vessel bottom head, but rather on the drywell floor, where the carbon dioxide and steam for the reaction are provided by the mechanisms of concrete degassing and ablation. Thus, after the initial pour from the reactor vessel begins at time 263 min after scram, the metal-CO<sub>2</sub> and metal-steam reactions in the inpedestal region of the drywell floor provide the energy to keep the floor debris molten and to provide conditions for spreading through the pedestal doorway into the expedestal region 112 min later, at time 375 min after scram.

It is instructive to consider the extent to which ADS actuation during the short-term station blackout accident sequence increases the amount of zirconium metal available for oxidation on the drywell floor. As indicated in Table ES-1, only 26% of all zirconium metal is oxidized in-vessel; this may be compared with more than 50% oxidized

in-vessel for cases in which the reactor vessel is not depressurized.<sup>7</sup> Examination of the early pours from the vessel for the present calculation reveals that 51,950 lbs (23,570 Kg) of zirconium metal reaches the inpedestal region during the 112-min period between the onset of vessel pour and the initial spread into the expedestal region; oxidation of this metal keeps the inpedestal debris hot.

At the time of initial contact with the shell at 375 min after scram, the debris layers at the shell interface introduced into the CORCON calculation consist of 0.49 in (1.24 cm) of oxide slurry at a temperature of 2592°F (1695 K) overlying 0.46 in (1.17 cm) of metals at a temperature of 2590°F (1694 K), somewhat below the solidus temperature of 2690°F (1750 K). Subsequently, the amount of debris in the expedestal region increases rapidly as the pour of molten debris from the reactor vessel continues. The debris temperature also increases rapidly, primarily due to the energy released by oxidation of the zirconium metal in the expedestal region.

The time-history of the conditions at the debris-shell interface as calculated by CONTAIN during the approximately one hour period after initial contact during which the calculated debris temperatures approach the melting temperature of carbon steel [2800°F (1810 K)] are provided in Table 4.6 of this report. The maximum debris temperature predicted for the expedestal region during this period from 375 to 435 min after scram is 2706°F (1759 K) for the metal layer at time 418 min; the calculated debris temperatures decrease rapidly after this peak. The CONTAIN code results provided in Table 4.6 are the information necessary for the performance of shell response calculations with codes such as HEATING-6 or TAC-2D. Although the predicted debris temperatures are clearly not high enough to cause shell melt-through, failure of the shell pressure boundary through loss of strength is possible. A detailed thermal and stress analysis should be performed for the drywell shell throughout the region of contact with the hot debris to address this issue.

The results presented in this report involve the first use of realistic metal and oxide pours in BWR severe accident analyses known to the authors. The report also provides the first known drywell response analyses based upon retention of the initial pours in the inpedestal region, then spreading of the debris emerging from the reactor pedestal doorway over the expedestal region of the drywell floor. As discussed in Chapter 4, the spreading into the expedestal region actually takes place in two stages with the first spread held within 800 ft<sup>2</sup> (74.3 m<sup>2</sup>) of the expedestal floor area and the second spread, occurring just three minutes later, expanding over the remaining 300 ft<sup>2</sup> (27.9 m<sup>2</sup>) of the expedestal region. The short duration of the first spread is due to the relatively rapid pour of debris from the reactor vessel occurring during this period.

Four major challenges to the continued integrity of the containment pressure boundary are identified for the case without drywell sprays in this report. First, the calculated temperature of the drywell shell in the vicinity of the head flange seals is sufficient to cause failure of

the seals. Predicted upper shell temperature is 730°F (661 K) at time 592 min; recent experiments at INEL<sup>6</sup> have shown similar seals to fail catastrophically at this temperature. At this time, the predicted drywell pressure is 126 psia (.869 MPa). Based upon recent drywell head flange leakage predictions,<sup>5</sup> seal failure at this pressure would open a 15.5 in.<sup>2</sup> (0.010 m<sup>2</sup>) leakage pathway from the drywell atmosphere to the refueling bay. The containment would then depressurize to a level consistent to maintain a continuous leakage through the drywell head flange; for these calculations, this is about 98 psia (0.676 MPa).

A second major challenge to drywell pressure boundary integrity is imposed by the high temperature of the core debris pressing against the shell around the circumference of the drywell at the level of the floor. Although the dry case results of the current analysis indicate that the maximum debris temperatures adjacent to the drywell shell are less than the shell melting temperature, previous calculations with other concrete types<sup>7</sup> indicate that the threat to drywell shell integrity is a function of the type of concrete used to construct the drywell floor. Predicted debris temperatures have been shown to be sufficient to clearly threaten shell melt-through for high limestone concrete [ablation temperature 2694°F (1752 K)], whereas expedestal debris temperatures are much lower for the same accident sequence for limestone common sand concrete [ablation temperature 2246°F (1503 K)] such as used at Peach Bottom. Thus, not only is the threat to the drywell shell accident sequence dependent (i.e., reflected through the timing, temperature, and composition of debris pours), but it is also plant specific through the concrete type.

The third major threat to drywell integrity is provided by ablation of the concrete pedestal that supports the reactor vessel. Calculations indicate that the amount of pedestal erosion is significantly affected by the amount of zirconium metal in the debris available for oxidation on the drywell floor, and this also is accident sequence dependent. For previous calculations assuming high limestone concrete,<sup>7</sup> 77% of the pedestal wall had eroded at the end of the calculation for the case of short-term station blackout with ADS actuation as opposed to 60% erosion for the same accident sequence without reactor vessel depressurization, in which much more of the zirconium metal is oxidized in-vessel. In the present calculation, the debris temperatures are much lower and a 30% reduction in pedestal wall thickness is predicted.

Finally, the fourth major challenge to the continued integrity of the containment pressure boundary is provided by the steadily increasing pressure that would have been predicted in these calculations had failure of the drywell head flange seals not been modelled. This containment pressure increase is a direct consequence of the continuing release of non-condensable gases from the core debris-concrete interaction. In this connection, it should be noted that the pressure differential required to lift the drywell head so that leakage after head flange seal failure can occur is plant-specific. For example, at Peach Bottom the drywell head is secured by 68 bolts whereas 208 bolts secure the drywell head at Browns Ferry.

As discussed previously, the dry case calculations of this report were terminated at time 900 minutes after scram. Approximately 98% of the reactor vessel bottom head debris has become molten and left the vessel by this time, and most of the lower portion of the bottom head wall has been subsumed into the debris on the drywell floor. In the expedestal region, the base of the metal layer has sunk 12.9 in (32.7 cm) beneath the original level of the floor. Although the metal layer is predicted to be frozen, it is still hot enough [2396°F (1586 K)] to cause continued ablation of the concrete immediately beneath it. Overlying the 9.6-in. (24.3 cm) thick metal layer is a 15.6-in. (39.6 cm) thickness of oxide slurry at a temperature of 2471°F (1628 K), extending to a height of 12.3 in. (31.1 cm) above the original level of the floor. Since the debris pour from the reactor vessel is virtually terminated at this point, it is expected that this is the maximum height that the debris would be predicted to achieve against the drywell shell. If the calculation were continued, the frozen metal slug and its overlying oxide slurry would merely be predicted to continue sinking slowly into the concrete remaining beneath the debris, slowly releasing additional gas. This completes the discussion concerning the results of the CONTAIN calculation for the case without sprays.

Reliable drywell spray systems that would flood the drywell floor before and during the egress of molten core and structural debris from the reactor vessel in the unlikely event that a Severe Accident were to progress this far have been proposed. One purpose of these systems would be to delay the spreading of debris toward the drywell shell. However, even if these sprays did not halt or significantly delay the movement of molten debris toward the shell (as suggested by the results of ongoing experiments at Brookhaven National Laboratory<sup>11</sup>), the presence of water over the core debris would certainly mitigate the transport of aerosols into the drywell atmosphere.

It should be noted that the existing spray system at Peach Bottom would probably not be available under the Short Term Station Blackout conditions assumed in this report. This is because the containment spray system is a subsystem of the Residual Heat Removal (RHR) system, which is a low pressure ECC system whose primary purpose is water injection into the reactor vessel under accident conditions. Thus, if containment sprays are available, then the RHR system is available, and the accident, by definition, would not have progressed to the point of bottom head penetration failure. Therefore, for the purpose of exploring the mitigative effect of sprays on severe accident progression, it has been assumed that a reliable drywell spray system has been installed that is independent of the current RHR system.

The sprays of the new system are assumed to have a capacity of 700 gpm (0.044 m<sup>3</sup>/s) and to have been introduced sufficiently before reactor vessel bottom head failure such that the drywell floor is flooded to the point of overflow to the pressure suppression pool at the time that the first debris emerges from the vessel. It is assumed that the existing spray headers are used and therefore spray is directed only into the lower expedestal regions of the drywell. Spray suction is

taken from the condensate storage tank [temperature = 90°F (305 K)] while the debris pour from the reactor vessel fills the inpedestal region sumps and during the initial spread into the expedestal region at 372 min. After the time of debris spreading around the entire periphery of the drywell (602 min), spray suction is shifted to the pressure suppression pool and the temperature of the injected spray droplets is that of the pool.

Calculated results for the wet case indicate much lower atmosphere temperatures as compared to the dry case. No conditions sufficiently harsh to cause drywell head seal degradation are predicted and therefore no direct leakage of gas and aerosols into the refueling bay is indicated. This feature, combined with the expected aerosol scrubbing by the sprays and by the subsequent water pools calculated to form on the drywell floor, makes it clear that the availability of drywell sprays during severe accidents is highly desirable.

The mitigative effect of sprays on debris/concrete phenomenology is also calculated to be substantial. Debris spreading completely around the drywell floor is delayed by approximately 3.7 h compared to the dry case, although initial debris contact with the drywell shell occurs at almost the same time. Maximum expedestal debris temperature is calculated to be 2583°F (1690 K) compared to 2706°F (1759 K) for the dry case, a reduction of 123 F° (68 K). Cumulative debris gas release at 750 min amounts to 689 lb-moles ( $3.13 \times 10^5$  gr-moles) vs 1419 lb-moles ( $6.44 \times 10^5$  gr-moles) for the dry case. Reactor pedestal ablation consumes only 0.25 ft (0.08 m) for the wet case vs 0.9 ft (0.27 m) for the dry case.

The current versions of CONTAIN and CORCON have greatly advanced the state of the art for BWR severe accident analysis. However, the present application described in this report does not permit definitive conclusions, particularly for the wet case, to be made concerning the interactions of debris with concrete, with the drywell shell, or with a postulated overlying water pool. This is partly due to uncertainties in the invessel analysis performed with the BWR SAR code that determined the debris pours used in this report. It is also due to the need for code improvements in CONTAIN and CORCON; this need arises primarily because of the evolving modeling requirements associated uniquely with the analysis of the response of the BWR MK I and MK II drywells to severe accidents. It is believed that improvements in CONTAIN/CORCON modeling capabilities should be developed according to the following recommendations:

1. Develop and incorporate into CONTAIN/CORCON a mechanistic debris spreading model. This model would allow for more accurate determination of the timing, rate, and extent of debris spreading on the flat drywell floor. Currently no such dynamic model exists for the calculation of debris/concrete interactions.

2. Improve the representation of debris melting so that various metallic, oxidic, and metallic/oxidic eutectic mixtures can be considered. This modification would allow "best estimate" debris pours to be used in calculating the debris/concrete interaction.
3. Develop an advanced concrete degassing model applicable to regions ahead of the ablation front during periods of unsteady concrete ablation. This model should be coupled with the recently developed concrete degassing model that is currently being applied in an advanced version of CONTAIN at ORNL. (The current model considers degassing only in the absence of ablation.)
4. The present representation of a layered debris configuration should be modified to allow for a homogeneous mixture of oxides and metals so that the sensitivity of calculated results to assumptions regarding layering can be addressed.
5. The debris layering scheme should be modified to allow for multiple layers of the same debris. This would improve the applicability of the current debris crusting model to layers that are simultaneously associated with radically different geometries. The concern for BWR applications is the simultaneous modeling of the drywell sump with the remainder of the inpedestal floor, which is flat. Correct modeling of the overall floor is important to the calculation of reactor pedestal erosion.
6. Allowance should be made for representation of the effect of  $B_4C$  in the debris. It is currently not considered.
7. The method of adding additional debris from the source table input to the debris already on the drywell floor should be modified to accommodate debris geometries having massive upper layers that are predicted to be completely frozen, as occurs in the wet case calculations of this report. The assumption of thermal equilibration of the added debris with the entire frozen mass of the upper layer should be eliminated and a new model should be developed that is physically more realistic.
8. The enhancement of film boiling heat transfer due to gas sparging from debris into an overlying water pool should be represented.
9. The code numerical stability should be improved so that wet case calculations are not terminated by code interrupts.

The calculations of this report, particularly those for the wet case, should be repeated after the above code improvements are made. Furthermore, it is recommended that the following additional areas be addressed in future work to assess the MK I containment response to debris pours from the reactor vessel:

1. A parameter study should be performed to identify the sensitivity of primary containment response to assumptions concerning the melting temperatures of debris in the bottom head and therefore the resulting debris pours as calculated by the BWRSAR code.
2. The type of concrete used in drywell floor construction at each of the 17 U.S. plants with BWR MK I containments should be ascertained. It is probable that no U.S. plants were built with high limestone concrete, but this should be confirmed.
3. The mitigating effects of wetwell venting should be investigated.
4. The containment analysis should be extended to include CONTAIN or MELCOR estimates of secondary containment performance after failure of the primary containment pressure boundary.
5. The present analyses should be extended beyond the time of exhaustion of the zirconium metal on the drywell floor to consider the effects of oxidation of chromium, iron, and nickel.
6. Severe accident response analyses should be performed for Long Term Station Blackout to determine the sensitivity of calculated results to parameters that are accident sequence dependent.

Table ES-1. Event timing for short-term station  
blackout with ADS actuation at Peach Bottom.

The bottom head debris is modeled as a  
mixture of metals melting at  
2750°F and a mixture of  
oxides melting at 4350°F

	Time of Event (min)
Swollen Level Below Top of Core	40.2
Open One SRV	77.0
ADS System Actuation	80.0
Core Plate Dryout	80.9
Debris Relocation Begins	132.4
First Local Core Plate Failure	132.7
Central Radial Columns Fall	222.8
Bottom Head Dryout	254.9
Bottom Head Penetration Fails	255.0
First Debris Leaves Vessel	263.1
First Debris Contact with Drywell Shell	375.0
<u>At Time 455 Minutes</u>	
Fraction of Zirconium Oxidized In vessel	
Core Region	0.179
Bottom Head Debris	0.081
Total	0.260
Total Hydrogen Generated In vessel, lbs	1,632
Bottom Head Debris Exited Vessel, lbs	475,246



## 1. INTRODUCTION

This report describes the results of analyses performed by the Boiling Water Reactor Severe Accident Technology (BWRSAT) Program at Oak Ridge National Laboratory (ORNL) to assess certain aspects of the latter phases of an unmitigated boiling water reactor severe accident involving the release of core debris from the reactor vessel. It is also the purpose of this report to discuss the efficiency of the CONTAIN code with respect to its application to calculate the response of the BWR MK I containment system to debris pours from the reactor vessel. This work was performed at the request of Dr. Thomas J. Walker, Leader of the Task Group on the BWR Mark I Shell Melt-Through Issue established by the Accident Evaluation Branch of the Division of Reactor Accident Analysis of the Nuclear Regulatory Commission (NRC) Office of Nuclear Regulatory Research. The Task Group was formed in support of an ongoing effort to determine the potential for failure of the drywell shell pressure boundary and the impact upon secondary containment (reactor building) integrity in the unlikely event that a severe accident were to proceed to the point that core debris came into contact with the drywell shell.

The specific calculations performed in this work are those specified by the Task Group Leader. These are based upon the short-term station blackout accident sequence at the Peach Bottom Atomic Power Station, which has been determined by the Accident Sequences Evaluation Program (ASEP) to provide about 20% of the total risk of core melt at this facility.<sup>1</sup> The specific case analyzed is based upon the existing plant configuration, where it is assumed that the Automatic Depressurization System (ADS) is actuated in accordance with the BWR Owner's Group Emergency Procedure Guidelines. Codes employed are BWRSAR<sup>2</sup> for the reactor vessel and the primary containment response during the first phase of the accident sequence, and BWRSAR and CONTAIN<sup>3</sup> for the debris pours from the reactor vessel and the primary containment response after reactor vessel bottom head penetration failure. For the purpose of testing the CONTAIN code in this application, it was assumed for these calculations that the core debris in the reactor vessel bottom head forms two separate mixtures during heatup after bottom head dryout: a single metallic eutectic with a melting temperature of 2750°F (1783 K) and a single oxidic eutectic with a melting temperature of 4350°F (2672 K). It is recognized that other mixtures and other melting temperatures should be included in the spectrum of possible pours; however, this is left to future work.

It was necessary in previous calculations to assume a very high melting temperature for the core debris in the reactor vessel bottom head because the CORCON module within the CONTAIN code had no models to represent low-melting-temperature eutectic alloys and because there was no model for degassing of the concrete on the drywell floor. Recent modifications provided by the CONTAIN development staff at Sandia National Laboratories (SNL) and made operational in the ORNL version have permitted the degassing restriction to be removed. In addition, local changes to the ORNL version provide a lower melting temperature of

4350°F (2672 K) for the  $\text{ZrO}_2\text{-UO}_2$  mixture recognized by the CORCON module. Therefore, we have been able for these calculations to consider more realistic lower-melting-temperature mixtures instead of the single mixture of oxides and metals melting at 4750°F (2894 K) that was considered in the previous study.<sup>4</sup>

Containment response has been analyzed for two cases differing with respect to assumptions regarding the availability of drywell sprays and the presence of water on the drywell floor. The first case, in which there are no drywell sprays and the only water on the drywell floor is the small amount initially in the drywell sumps, corresponds to the existing plant configuration. For the second case, it is assumed that a reliable independent spray system has been installed and that this system is actuated sufficiently before reactor vessel bottom head failure such that the drywell floor is flooded to the point of overflow when the first debris emerges from the vessel.

In general, the calculations whose results are represented in this report were carried out on a best-estimate basis. This includes the models employed for representation of the decay heat power as a function of time. Chapter 2 provides a description of the short-term station blackout accident sequence and a brief discussion of the motivation for consideration of the consequences of this event. The BWRSAR calculations employed to provide estimates of the debris pours from the reactor vessel for this accident sequence are discussed in Chapter 3 and a timing of events is established. Chapter 4 provides the results of CONTAIN calculations to estimate the response of the primary containment to the debris pours occurring after reactor vessel bottom head penetration failure for the dry case, the case without sprays. The CONTAIN calculations were repeated for the case with sprays and these wet case results are presented in Chapter 5.

The conclusions of this short-term station blackout analysis and the implications of the results are discussed in Chapter 6. Recommendations for future work are provided in Chapter 7, including specific suggestions for CONTAIN code improvements found necessary in attempting to apply the code to the flat-floor configuration of the BWR MK I drywell.

During the course of performing the calculations discussed in this report, there was significant consultation with the CONTAIN code development staff at SNL. Their advice in regard to the proper application of the code and their rapid response in providing on-the-spot code upgrades where necessary are greatly appreciated.

## 2. THE SHORT-TERM STATION BLACKOUT SEVERE ACCIDENT SEQUENCE

Much of the impetus for these new studies of Peach Bottom Station Blackout has derived from the most recent findings of the NRC-sponsored Accident Sequence Evaluation Program (ASEP) in support of the NUREG-1150 effort.<sup>1</sup> The final results of the ASEP Program provide the estimate that 60% of the overall risk of core melt for Peach Bottom can be attributed to the overall threat of Station Blackout.\* Historically, the station blackout accident has been considered to be the sequence initiated by loss of offsite power and reactor scram combined with failure of the station diesels to start and load. In this (long-term) accident sequence, water is injected into the reactor vessel by the steam turbine-driven HPCI or RCIC systems as necessary to keep the core covered for as long as DC power for turbine governor control remains available from the unit batteries, a period of about six hours. However, the definition of Station Blackout implemented by the ASEP Program has been expanded to include two cases that heretofore would have been classified as Loss of Injection, or TQUV in WASH-1400 parlance. In these short-term station blackout sequences, the capability for water injection to the reactor vessel is lost at the inception of the accident sequence. (The short-term designation derives from the fact that the core is uncovered relatively quickly in these sequences.)

The early total loss of injection hallmark of Peach Bottom Short-Term Station Blackout might be initiated in either of two ways. First, there might be independent failures of both the HPCI and RCIC systems when they are called upon to keep the core covered during the period while DC power remains available. Second, there might have been a common-mode failure of the DC battery systems that, upon loss of offsite power, had precluded starting of the diesel generators<sup>†</sup> and thereby was the cause of the Station Blackout; without DC power for valve operation and turbine governor control, the steam turbine-driven injection systems also would not be operable. The ASEP program results assign 17% of the overall core melt frequency for Peach Bottom to the case of Short-Term Station Blackout with independent failure of HPCI and RCIC and 3% of the frequency to the case initiated by common-mode failure of the station batteries.

---

\*The remaining risk is allocated as 31% for ATWS and 9% for all other possible accident sequences.

<sup>†</sup>It should be noted that this is a plant-specific consideration. At the Browns Ferry Nuclear Plant, for example, power for diesel generator starting and loading is independent of the unit batteries and not susceptible to common-mode failure.



### 3. BWRSAR CALCULATIONS FOR SHORT-TERM STATION BLACKOUT WITH ADS ACTUATION

This chapter describes the predicted response of a unit of the Peach Bottom Atomic Power Station to a postulated Short-Term Station Blackout caused by loss of offsite power compounded by common-mode failure of the station diesels and independent failure of the steam turbine-driven reactor vessel injection systems. In this accident sequence, there is no reactor vessel injection capability, but DC power available from the unit batteries permits the reactor vessel safety/relief valves to be operated remotely and the Automatic Depressurization System (ADS) to be actuated upon operator demand.

#### 3.1 BWRSAT Program Severe Accident Models

The Boiling Water Reactor Severe Accident Technology (BWRSAT) Program at Oak Ridge National Laboratory (ORNL) employs the BWR severe accident modeling strategy outlined in Table 3.1. The methodology described in this table has been developed at ORNL by L. J. Ott and has been incorporated into the Boiling Water Reactor Severe Accident Response (BWRSAR) code. It should be recognized that the ORNL methodology involves significantly longer times to reactor vessel bottom head penetration failure than previous analytical approaches because of our contention that the very large amount of water in the BWR reactor vessel bottom head must first be boiled away and that the quenched debris must then reheat to about 1900°F (1311 K) before the reactor vessel bottom head penetrations can fail. It should also be noted that, in general, very little of the debris in the bottom head is molten at the time of penetration failure and, therefore, the initial debris pour from the reactor vessel occurs sometime after penetration failure. However, if the reactor vessel is pressurized at the time of penetration failure, then the associated vessel blowdown through the bottom head debris would produce a large amount of hydrogen and associated energy release within the debris bed, and the initial debris pour would occur almost immediately after bottom head penetration failure.

#### 3.2 Events Prior to Reactor Vessel Bottom Head Penetration Failure

The sequence of events and event timing for the Peach Bottom short-term station blackout with ADS actuation accident sequence as calculated by the BWRSAR code are provided in Table 3.2. It is assumed that the reactor had been operating at 100% power at the time of scram and that no injection source is ever recovered.

Plots of key parameters representing events within the reactor vessel as predicted by the BWRSAR code are provided in Fig. 3.1. These plots represent events from time 35 minutes when the BWRSAR calculation

is initiated until time 300 minutes, which is about 45 minutes after reactor vessel bottom head penetration failure. As indicated in Fig. 3.1a, the ADS system is activated at time 80.0 min, when the reactor vessel water level is near the bottom of the core; this causes the opening of five safety/relief valves (SRVs). The open SRVs subsequently close whenever the reactor vessel falls to within 20 psi (0.138 MPa) of the drywell pressure and then reopen when the reactor vessel pressure has increased to 50 psi (0.345 MPa) above drywell pressure. The corresponding relief valve flows are shown in Fig. 3.1d.

The swollen reactor vessel water level, the calculation of which includes consideration of the effects of voids, is shown in Fig. 3.1b. The calculated water level rapidly falls below the core plate as a result of the water loss by flashing when the ADS valves are opened. Small temporary increases in level occur because of displacement of water in the bottom head when large masses of core debris are introduced after core plate failure. The decay heat associated with the fuel pellets relocated into the bottom head at time 222.8 min causes a boiloff of the remaining water in the reactor vessel; bottom head dryout occurs at time 254.9 min.

Plot 3.1c shows the extent of hydrogen generation by metal-steam reaction in the core region. Approximately 23% of the clad, 12% of the channel box walls, and 3% of the control blade stainless steel is predicted to be oxidized during the accident sequence, producing about 1137 lb (516 kg) of hydrogen in the core region within the reactor vessel.

Selected primary containment response characteristics predicted by the BWR SAR code for the period up to one-half hour after reactor vessel bottom head penetration failure are provided in the individual plots provided in Figs. 3.2 and 3.3. As indicated in Fig. 3.2a, ADS actuation causes a small pressure increase, but this pressure increase is erased as the containment heat sinks soak up energy after core plate dryout. The containment pressure increases significantly in response to debris relocation into the reactor vessel bottom head and after collapse of the central fuel pellet stacks. Bottom head penetration failure does not significantly increase the containment pressure because the reactor vessel was previously depressurized by means of the ADS actuation.

The drywell atmosphere temperature, shown in Fig. 3.2b, increases due to increased heat transfer from the reactor vessel whenever flow is initiated from the safety/relief valves (Fig. 3.1d), then decreases as the drywell heat sinks absorb the energy of the atmosphere. The effect of bottom head penetration failure is slight. At the completion of the reactor vessel blowdown, neither the drywell pressure nor the calculated drywell shell temperature (Fig. 3.2c) is of sufficient magnitude to threaten the integrity of the drywell shell pressure boundary.

The temperatures of the wetwell atmosphere and the torus shell respond to events within the reactor vessel as shown in Figs. 3.3a and 3.3b, but do not increase to threatening values. The wetwell atmosphere

temperature increases after reactor vessel bottom head penetration failure because of the hot gases entering the pressure suppression pool from the drywell via the vent lines and downcomers. (The pool remains sub-cooled, however. Its response is shown in Fig. 3.3d.)

A large amount of hydrogen has accumulated within the wetwell air-space (Fig. 3.3c) and the drywell (Fig. 3.2d) at the time of reactor vessel bottom head penetration failure. Some additional hydrogen [about 247 lb (112 Kg)] is generated by the passage of steam through the bottom head debris bed during the first 60 minutes after penetration failure. A slow rate of hydrogen generation by this mechanism continues as long as water remains in the downcomer region of the reactor vessel. This water is boiled by radiative and conductive (through the vessel wall) heat transfer from the bottom head debris; the steam passes through the debris bed on its way out of the vessel.

The characteristics of the debris pours from the reactor vessel bottom head as calculated by the BWRSAR code are shown in Fig. 3.4. Figure 3.4a indicates the rate of molten material release from the reactor vessel as a function of time. Although bottom head penetration failure occurs at 255 minutes, the initial pour does not occur until time 263 minutes because of the time interval required for the metallic debris to heat to its assumed melting temperature of 2750°F (1783 K). The mass-averaged temperature of the release is shown in Fig. 3.4b.

The integrated mass of debris released from the reactor vessel is indicated in Fig. 3.5a, where it is shown that about 875,000 lbs (397,000 Kg) has left the vessel by the end of the calculation, at time 900 min. This is equivalent to about 98% of the total mass of bottom head debris. The decay heat (proportional to the mass of UO<sub>2</sub>) included in the released debris is shown in Fig. 3.5b.

It should be noted that the BWRSAR code predicts that the portion of the reactor vessel bottom head beneath the point of attachment of the support skirt is completely melted through at time 483 minutes. There are no specific models within BWRSAR to address this phenomenon since it is believed that the 340,000 lbs (154,000 kg) of debris remaining within the vessel at this time would merely relocate downward about three feet (0.91 m) onto the control rod drive housing support structure (see Fig. 3.6). After relocation, the debris would continue to melt, with the molten portion flowing down onto the drywell floor in the same manner as if the reactor vessel had remained intact. Heat transfer from the debris to the reactor vessel by convection and conduction is discontinued at the time of debris relocation.

### 3.3 Allocation of Debris Pour Between Inpedestal and Expedestal Regions of the Drywell Floor

Because current versions of the CONTAIN code do not provide the capability for calculation of lateral spreading of debris over the

drywell floor, it is necessary for the user to provide CONTAIN code input tables that appropriately divide the debris pours from the reactor vessel into one flow into the inpedestal region and another flow onto the expedestal region floor. The disadvantages of this approach are discussed in Chapter 7, Section 7.1, Item 4.

As indicated in Table 3.2, reactor vessel bottom head penetration failure occurs at time 255 minutes and the initial pour from the reactor vessel begins at time 263 minutes for the short-term station blackout accident sequence considered here.

The calculated containment response to the release of core and reactor vessel structure debris from the reactor vessel depends heavily upon whether or not the drywell sprays are actuated. For the case without sprays discussed in Chapter 4, all of the debris pour from the reactor vessel is directed into the inpedestal region until time 375 minutes. At this point, the cumulative pour is sufficient to have filled the drywell sumps and to overflow the inpedestal floor area to the point that spreading into the expedestal region would be expected.

Using the method proposed by Kazimi<sup>8</sup> to estimate the extent of initial spreading over concrete, it was determined that the initial spread into the expedestal region should be modeled to cover 800 ft<sup>2</sup> (74.3 m<sup>2</sup>). The subsequent CONTAIN calculation shows that after three minutes, the conditions in the expedestal region are such that spreading of the debris over the remaining 300 ft<sup>2</sup> (27.9 m<sup>2</sup>) should be assumed.

During the three minutes of the initial debris spread into the expedestal region, the metals portion of the continuing pour from the reactor vessel is molten and superheated, while the oxide portion of the flow is frozen. Accordingly, it is assumed that 80% of the oxide flow is kept inpedestal while 20% is spread expedestal. For the metals, it is assumed that one percent is kept inpedestal due to adhesion upon the surfaces of the frozen oxides. An exception is made for the zirconium metal to model its mixing with the oxides; an additional 10% of the zirconium metal is kept inpedestal so that only 89% of this metal is directed into the expedestal region.

After time 378 minutes, when the debris expedestal is modeled to spread over the entire 1100 ft<sup>2</sup> (102.2 m<sup>2</sup>) of expedestal floor area, the apportionment of the debris pour between the inpedestal and expedestal areas remains the same as before; the basis is that the metals continue to be molten and superheated while the oxides are frozen.

After time 515 minutes, the oxide pour is molten as well as the metals. From this time until the end of the calculation, the apportionment of the predicted debris pour is made strictly according to the respective floor areas; thus, for both oxides and metals, 23% is kept inpedestal and 77% is introduced into the expedestal region.



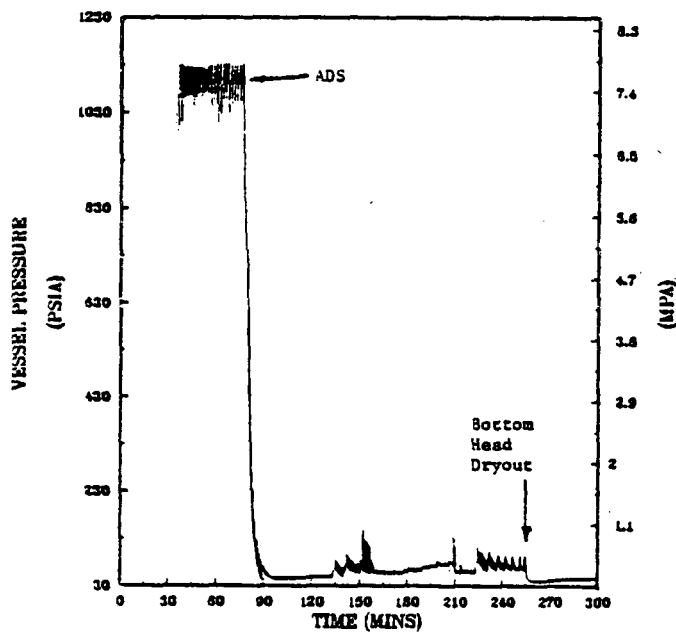
Table 3.1. BWRSAT Program Calculational Methodology Employed  
to Represent Events Between Onset of Core Degradation  
and Pour of Molten Materials from  
Reactor Vessel for BWRs

- 
1. As canister and control blade material becomes molten, it is re-located onto the core plate. This causes:
    - a. a temporarily increased steaming rate
    - b. core plate dryout and cessation of steaming
    - c. buildup of mass on the core plate and core plate heatup.
  2. Each radial region of the core plate fails due to loss of strength when its calculated temperature reaches a user-specified value. Each core plate region and its accumulated debris falls into the lower plenum, producing a burst of steam and lowering the water level there as the fallen material is quenched.
  3. Molten Zr metal flows downward over the lower core fuel rod nodes, leaving the UO<sub>2</sub> fuel pellets encased in thin ZrO<sub>2</sub> sheaths. Steam rising from the lower plenum cools the core nodes from which all unoxidized Zr has been removed. On the other hand, the rising steam causes energy release in the core peripheral nodes where Zr metal at elevated temperature still remains.
  4. The standing portions of the core fall into the lower plenum by radial column. Each core column collapses when its average clad temperature reaches a user-input value, at which time very little of the UO<sub>2</sub> mass in the region has become molten. (The actual failure mechanism is weakening, by overtemperature, of the ZrO<sub>2</sub> sheaths surrounding the UO<sub>2</sub> fuel pellets.) The falling mass is quenched by the water in the lower plenum until the time of bottom head dryout. After bottom head dryout, the debris begins to reheat.
  5. The structure of the control rod guide tubes in the lower plenum is heated by the surrounding core debris and is weakened to the point of failure when its temperature reaches a user-specified value. Failure of the control rod guide tubes causes all remaining standing portions of the core to immediately collapse. The control rod guide tube mass is added to the bottom head debris.
  6. Bottom head penetrations fail by a simulated creep-rupture mechanism as the debris mass in their vicinity reaches about 1900°F (1311 K). The reactor vessel depressurizes and equalizes with drywell pressure. When standing molten metal pools develop within debris nodes remote from the vessel wall, leakage pathways are opened through the wall via the instrument guide tubes.
  7. The individual components of the debris mass leave the vessel in the order that they reach their melting points and become liquid. Solid metallic material surrounding the lower portion of the original instrument guide tube locations is ablated into the molten material flowing from the reactor vessel via these pathways.
-

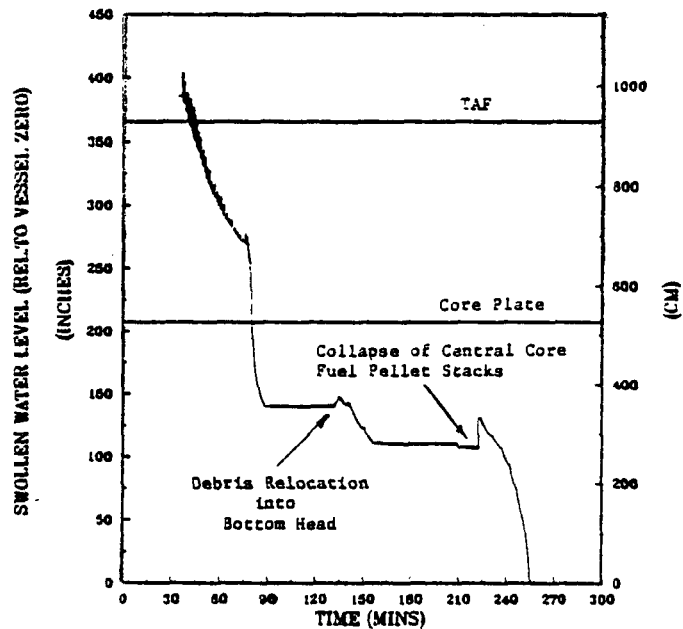
Table 3.2. Calculated sequence of events for Peach Bottom  
Short-Term Station Blackout with ADS Actuation.

The bottom head debris is modeled to separate  
into a mixture of metals melting at 2750°F  
and a mixture of oxides melting at 4350°F

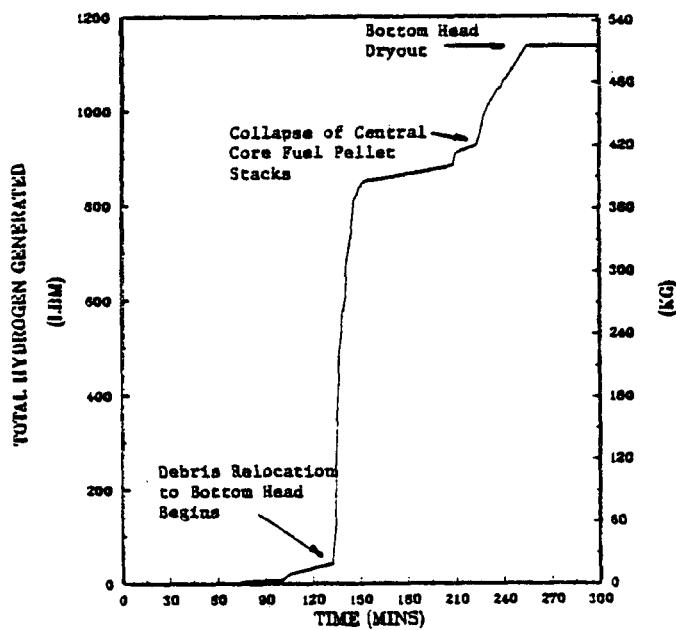
Event	Time (min)
Station blackout-initiated scram from 100% power. Independent loss of the steam turbine- driven HPCI and RCIC injection systems	0.0
Swollen water level falls below top of core	40.2
Open one SRV	77.0
ADS system actuation	80.0
Core plate dryout	80.9
Relocation of core debris begins	132.4
First local core plate failure	132.7
Collapse of fuel pellet stacks in central core	222.8
Reactor vessel bottom head dryout; structural support by control rod guide tubes fails; remainder of core falls into reactor vessel bottom head	254.9
Bottom head penetrations fail	255.0
Pour of molten debris from reactor vessel begins	263.1



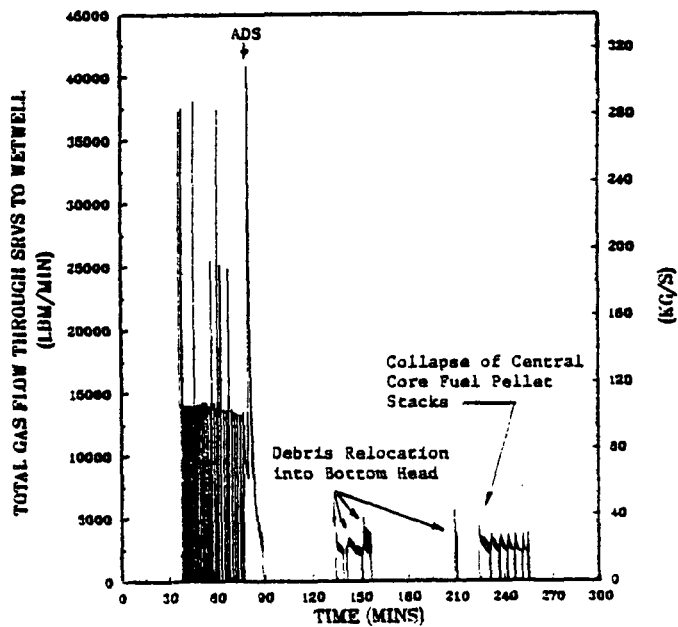
(a)



(b)

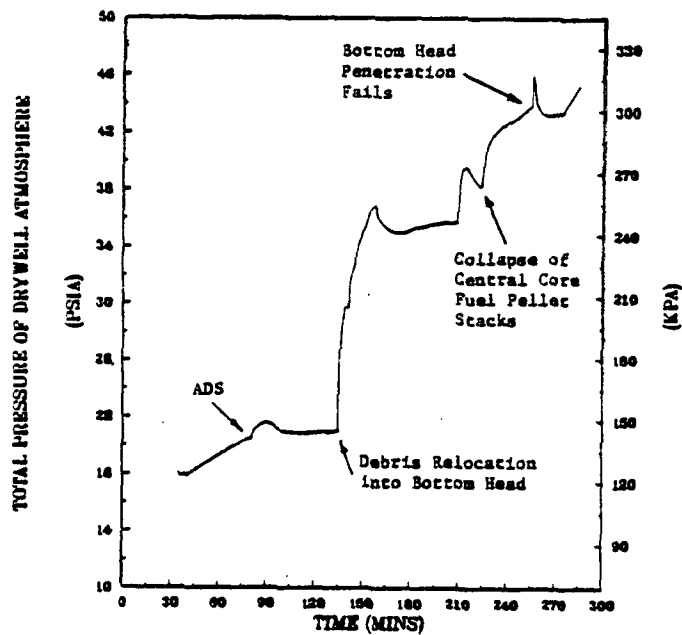


(c)

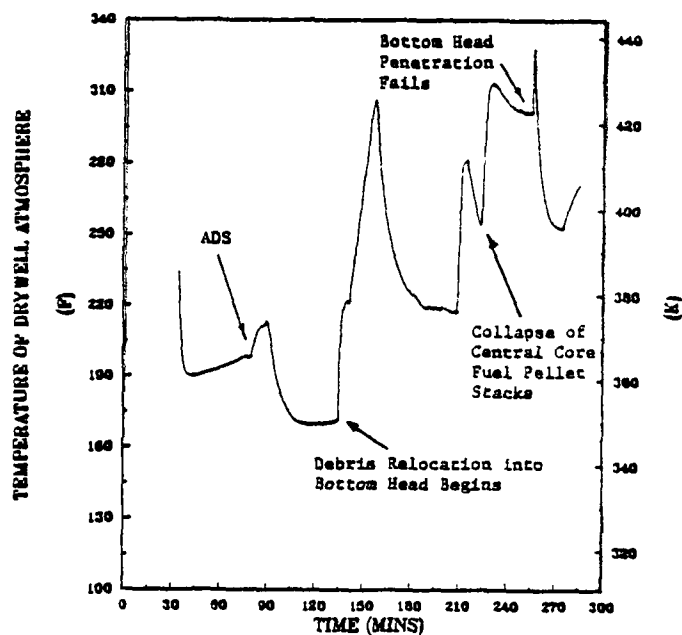


(d)

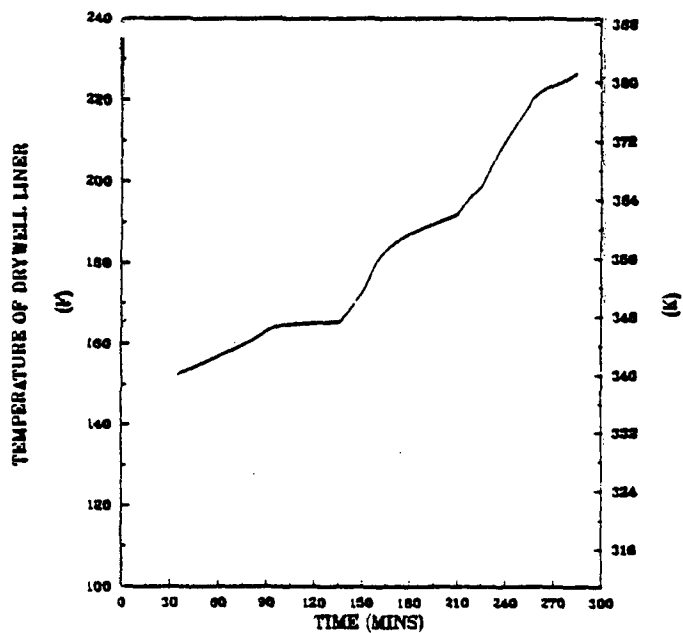
Fig. 3.1. Accident signatures for events within the reactor vessel as predicted by the BWR SAR code for the Peach Bottom short-term station blackout accident sequence with ADS.



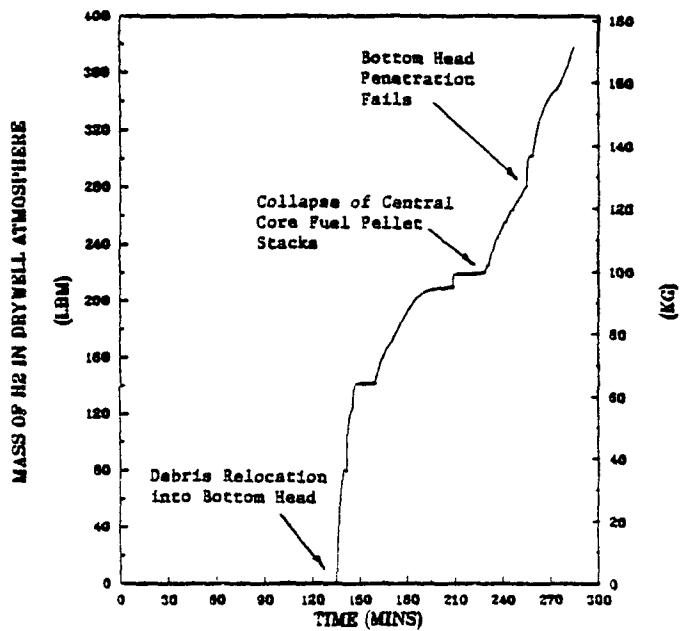
(a)



(b)



(c)



(d)

Fig. 3.2. Accident signatures for response of the drywell as predicted by the BWR SAR code for the Peach Bottom short-term station blackout accident sequence with ADS.

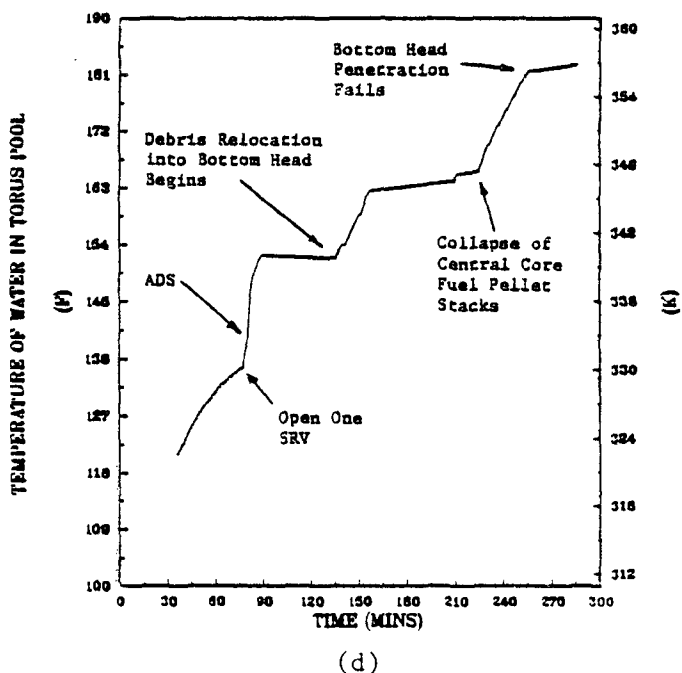
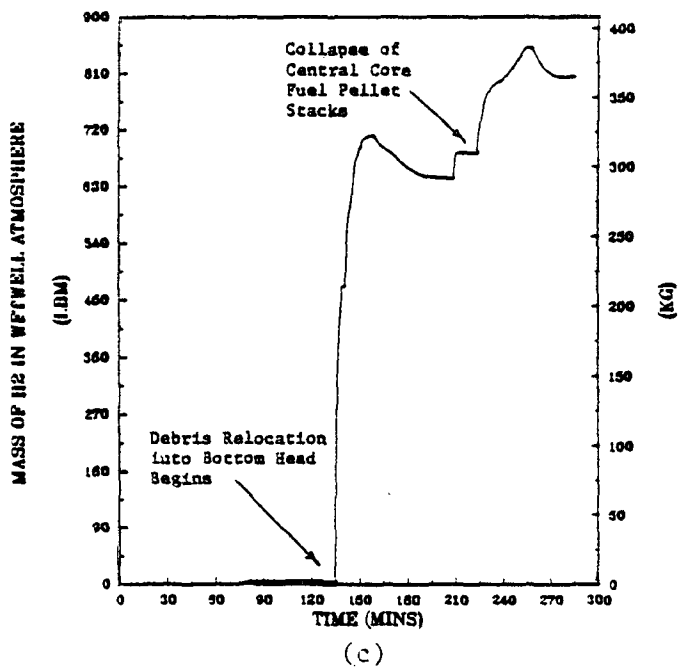
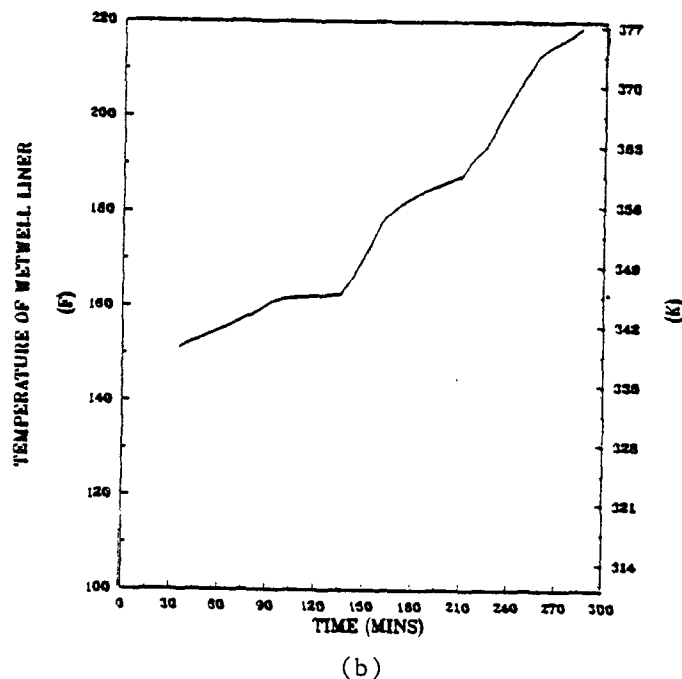
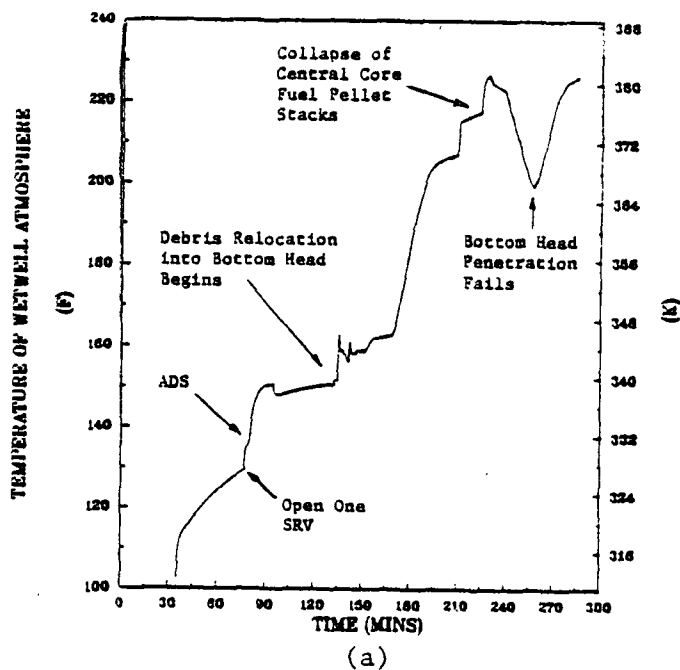


Fig. 3.3. Accident signatures for response of the wetwell as predicted by the BWR SAR code for the Peach Bottom short-term station blackout accident sequence with ADS.

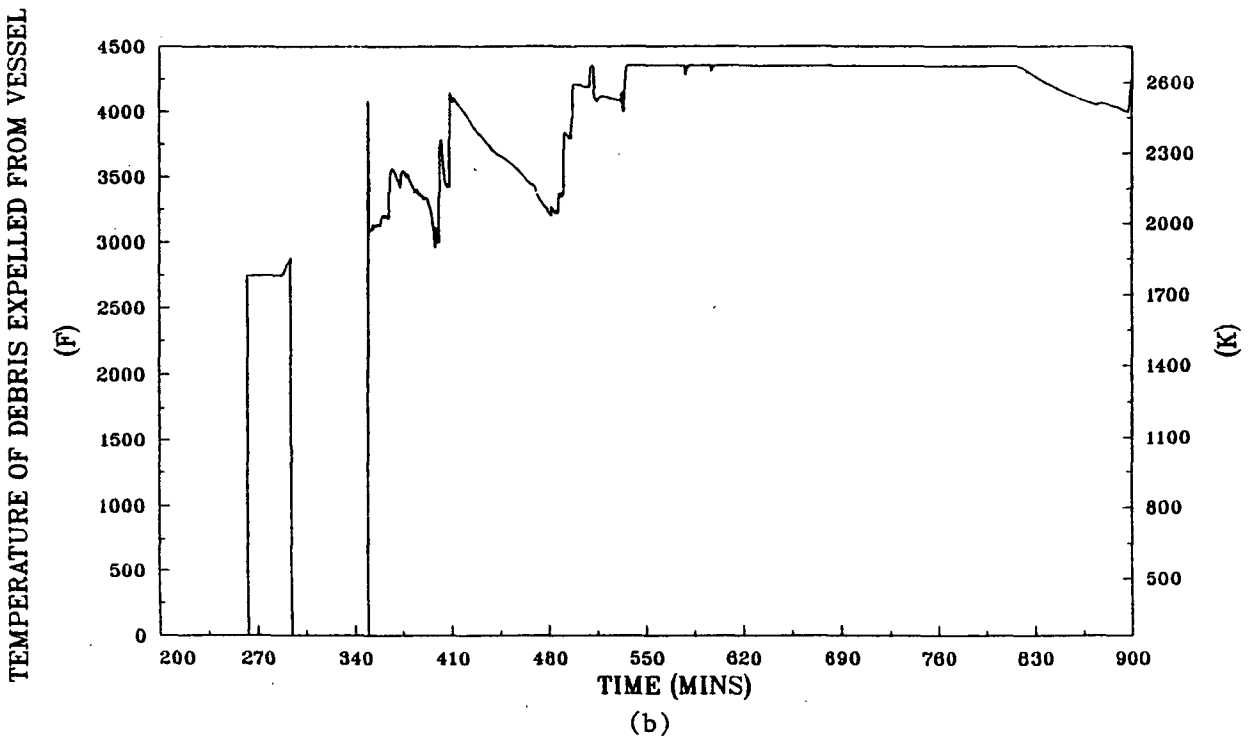
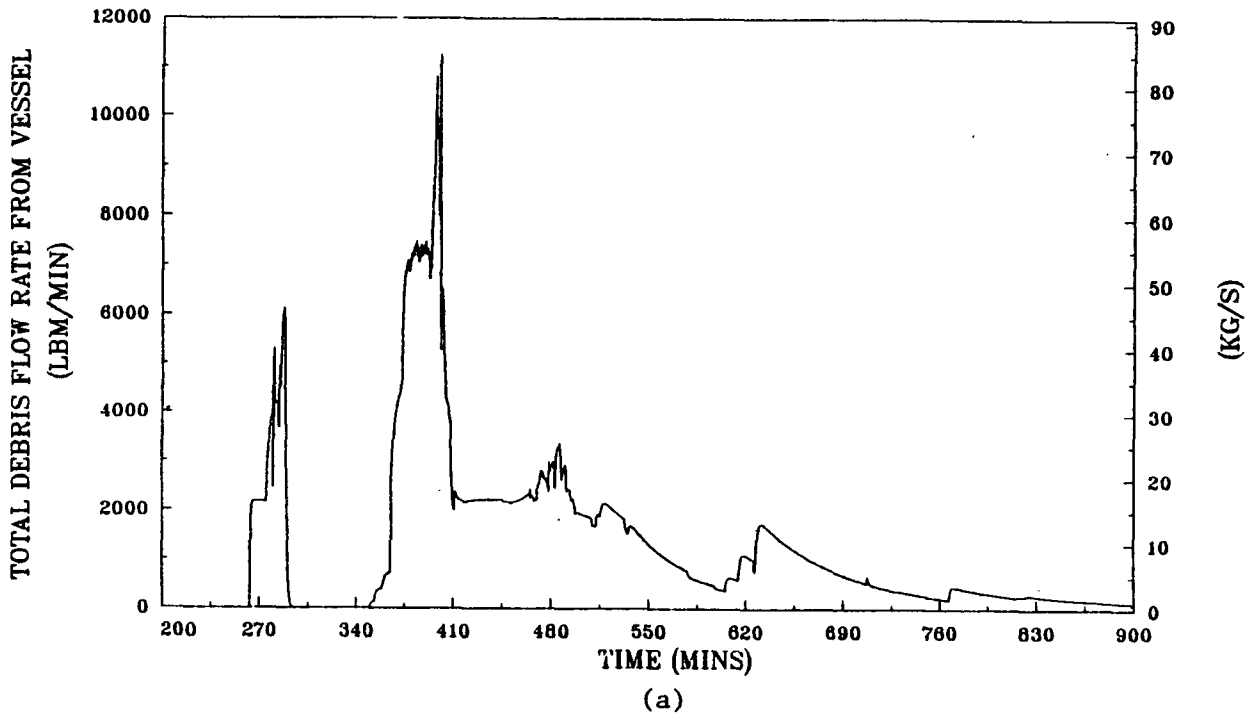
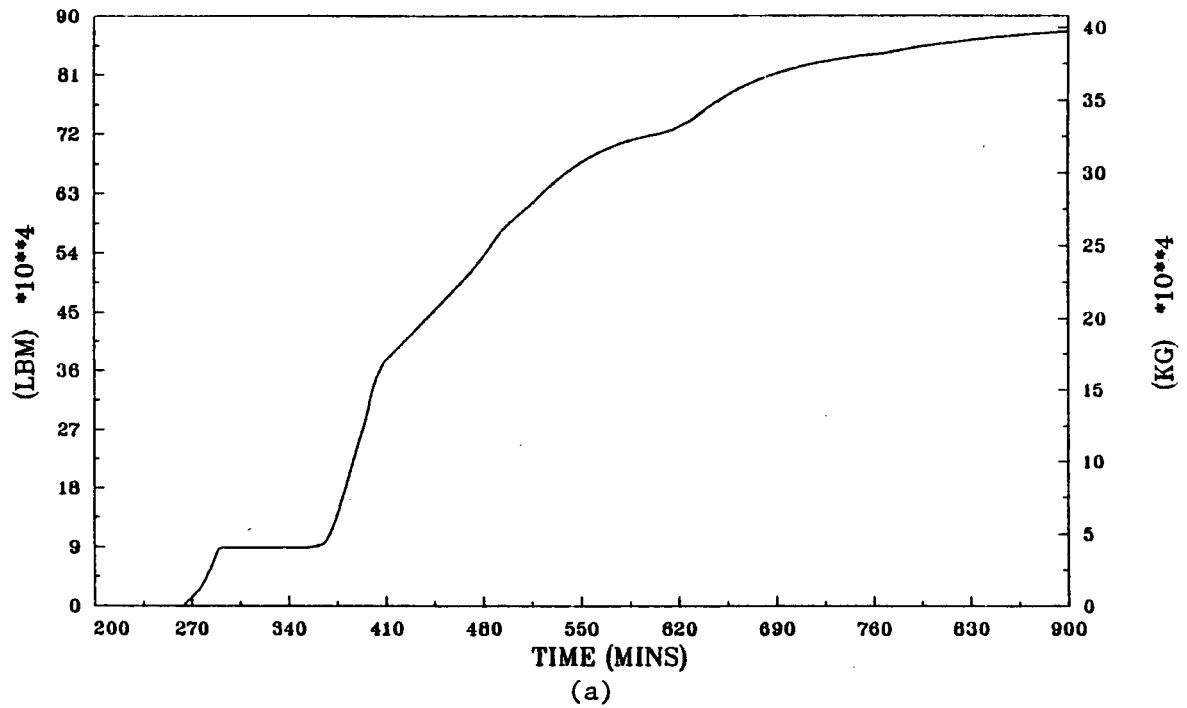


Fig. 3.4. Flow rates and temperatures of debris pours from the reactor vessel bottom head as predicted by the BWSAR code for the short-term station blackout accident sequence with ADS at a unit of the Peach Bottom Atomic Power Station.

TOTAL INTEGRATED DEBRIS MASS EXPELLED FROM VESSEL



DECAY HEAT IN EX-VESSEL DEBRIS

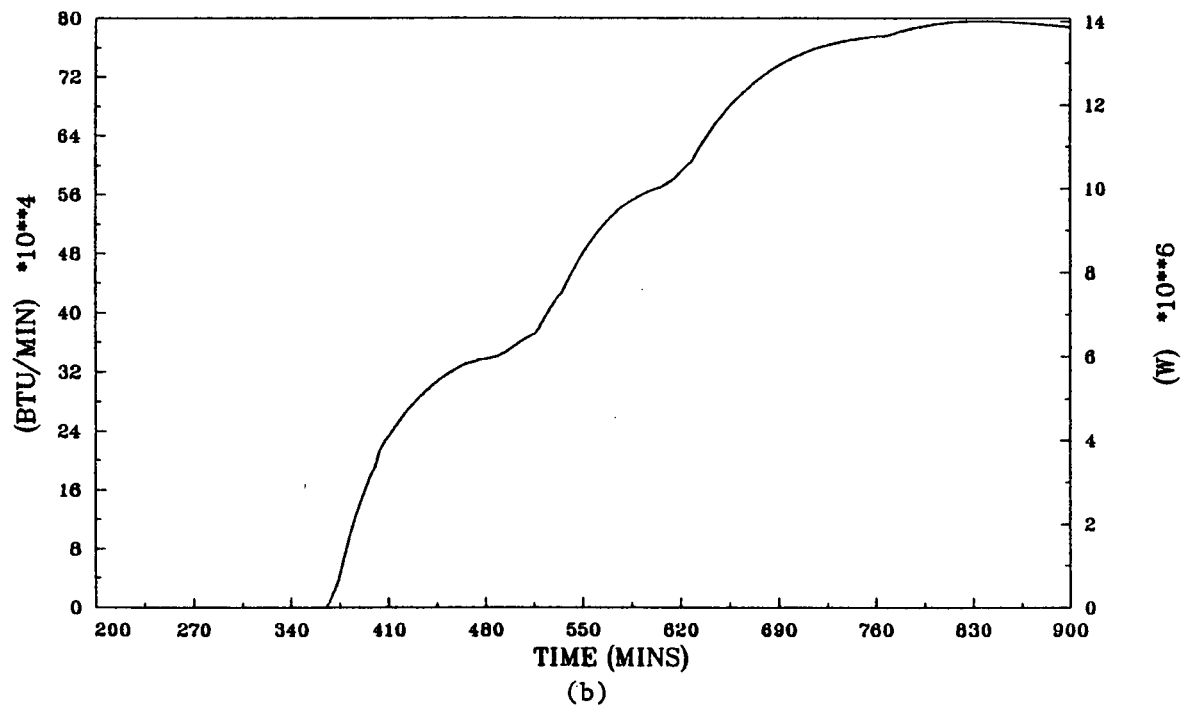


Fig. 3.5. Integrated debris mass expelled from the reactor vessel and decay heat power in the ex-vessel debris as calculated by the BWR SAR code for the short-term station blackout accident sequence with ADS at a unit of the Peach Bottom Atomic Power Station.

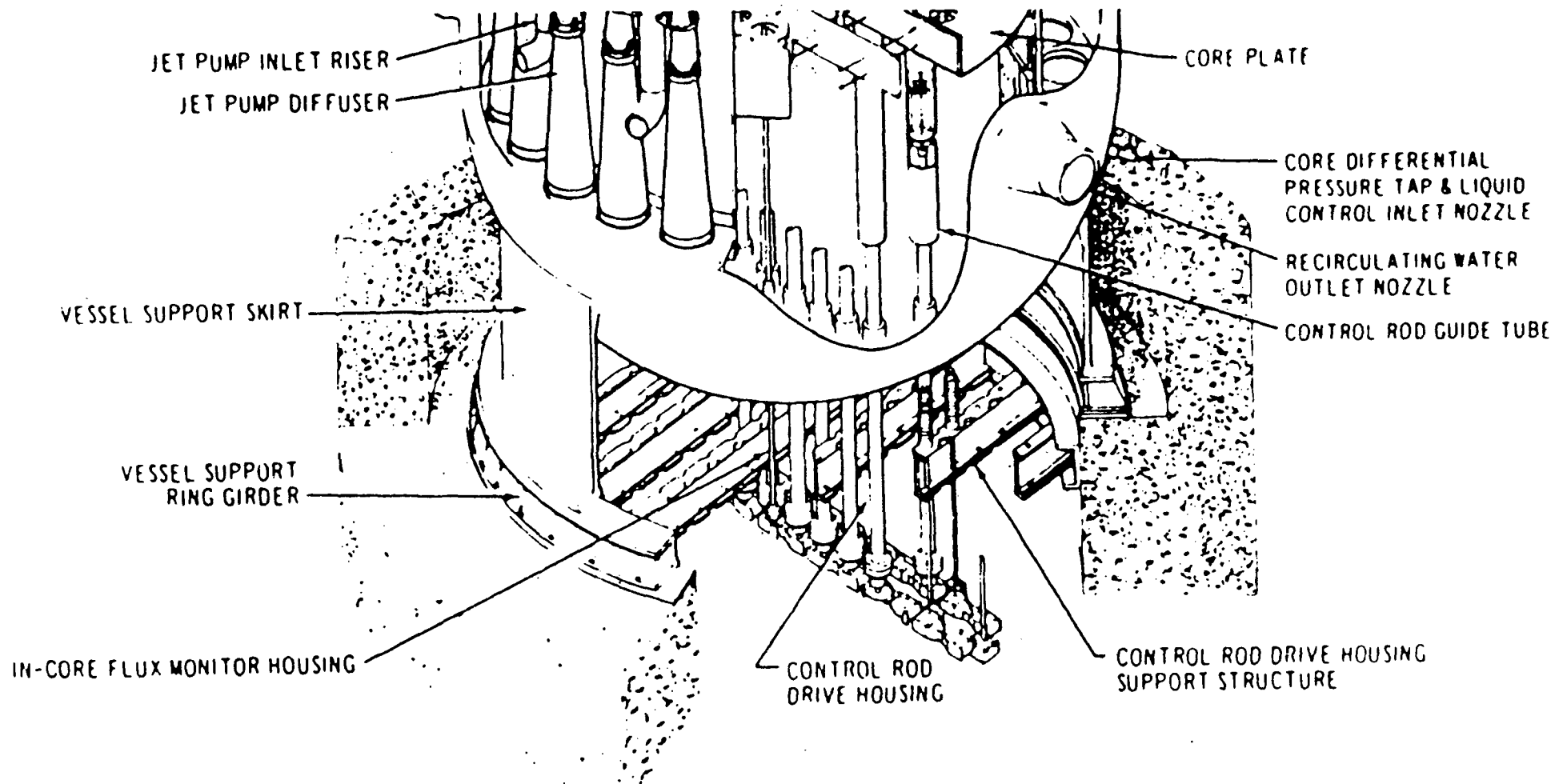


Fig. 3.6. Downward movement of separated portions of the bottom head beneath the skirt would be limited to about 34 inches by the CRD housing support structure.



## 4. CONTAIN CALCULATIONS OF THE CONTAINMENT RESPONSE AFTER REACTOR VESSEL BOTTOM HEAD PENETRATION FAILURE

### 4.1 The CONTAIN Model for the BWR Mark I Primary Containment

The BWRSAT Program at ORNL has developed a 12-cell model for use in analyses of the response of the BWR Mark I primary containment under severe accident conditions. The cell arrangement is as illustrated in Fig. 4.1. The first 9 cells are used to represent the free volume in the drywell. Core debris-concrete interactions are calculated with the CORCON module of CONTAIN for the floor of Cell 1 after the initial debris pour from the reactor vessel and also for the floor of Cell 6 when the debris has spread into the expedestal region. (The debris spreading is accomplished by stopping the initial calculation and starting a second calculation in which the debris accumulated above the inpedestal floor level during the initial calculation is now spread over both the inpedestal and expedestal floor areas.) Cell 7 represents the one-foot (0.305 m) wide annular region between the outer surface of the reactor vessel insulation and the inside surface of the concrete biological shield. Flow paths through the reactor pedestal and the biological shield are indicated by dotted lines; as shown, they connect cells 1 and 6, 2 and 5, 3 and 4, 7 and 4, and 7 and 9.

Cell 10 of the model is a large single-cell representation of the secondary containment, both reactor building and refueling bay. Its purpose is to trap leakage flows from the drywell shell either by temporary lifting of the drywell head or by burn through of the drywell shell at the level of the floor. Cell 11 represents the outside environment and collects any gases that escape from the secondary containment (cell 10) or are vented from the primary containment via the wetwell airspace, which constitutes Cell 12 of the model.

### 4.2 Primary Containment Response

In order to assess the effect of containment sprays upon calculated primary containment response, two sets of results have been calculated for the short-term station blackout with ADS accident sequence. The first set of results was calculated without consideration of containment sprays, recognizing that they would not be available with the present plant configuration under station blackout conditions; these results are described in the remainder of this chapter.

Nevertheless, future plant modifications might provide a reliable drywell spray system. To see the effect of drywell spray upon events, the short-term station blackout CONTAIN calculations for primary containment response have been repeated assuming the sprays to be available and actuated. These results are discussed in Chapter 5.

#### 4.2.1 Assumptions regarding lifting of the drywell head

The model for lifting of the drywell head used in this calculation is taken from the discussion beginning on page 58 of the recently completed Chicago Bridge and Iron Company study of Peach Bottom containment strength (Ref. 5). In recent gasket tests at Idaho National Engineering Laboratory (Ref. 6), gaskets similar to those used at Peach Bottom withstood differential pressures of 160 psi (1.103 MPa) combined with temperatures of 700°F (644 K), but then failed catastrophically as the temperature was increased to 730°F (661 K). Greg Krueger of PECO has confirmed that the drywell head gaskets at Peach Bottom are replaced each refueling. Then, with the assumption of normal (0.04 in.) gasket springback, a leakage area would not begin to open until the drywell pressure reached 175 psia (1.207 MPa).<sup>5</sup> However, recognizing that the CONTAIN results predict drywell head temperatures well in excess of 700°F (644 K), a leakage area is assumed to open for these calculations when the temperature of the drywell head reaches 730°F (661 K). As modeled, the leakage area increases linearly from zero at 97 psia (0.669 MPa) to a value of 62 in.<sup>2</sup> (0.0400 m<sup>2</sup>) as the pressure increases to 215 psia (1.482 MPa). As indicated in Figs. 4.4 and 4.6a, the predicted conditions within the drywell reach values at which leakage from the drywell head would begin at time 592 minutes.

#### 4.2.2. Calculated results

The Peach Bottom limestone common sand concrete, very similar to that used in the construction of the Browns Ferry Nuclear Plant, produces much less carbon dioxide upon attack by high-temperature core debris than would a high limestone concrete. In addition, it has an ablation temperature [2246°F (1503 K)] significantly lower than that of high limestone concrete [2694°F (1752 K)]. A comparison of the constituent weight fractions of the concretes used at Peach Bottom and Browns Ferry is provided in Table 4.1.

Diagrams indicating the directions of calculated drywell intercell gas flows and primary containment cell temperatures for Peach Bottom Short-Term Station Blackout are provided in Figs. 4.2 through 4.5. The numerical values of the intercell flows are listed in Table 4.2. The intercell flow from cell 6 to cell 10 (lower expedestal region to secondary containment by means of thermally-induced failure of the shell pressure boundary at the level of the drywell floor) by assumption remains zero throughout the calculation.

The CONTAIN calculation was initiated just before reactor vessel bottom head penetration failure with the initial drywell cell temperatures taken from BWRSAR code results. The intercell flows and cell temperatures 10 minutes after bottom head penetration failure and the beginning of gas release from the depressurized reactor vessel into the drywell are shown in Figs. 4.2a and 4.2b, respectively. The highest atmosphere temperature, as expected, is in the uppermost inpedestal cell, immediately beneath the reactor vessel.

The drywell intercell flows and the cell temperatures predicted by CONTAIN at 110 minutes after the initiation of the CORCON calculation are shown in Fig. 4.3. Up to this time, all of the debris pour has been retained within the inpedestal region. As indicated in Fig. 4.3a, two natural circulation flows are set up by the calculation: a clockwise flow between the inpedestal and the lower expedestal regions, and a counter-clockwise flow between the upper expedestal region and the annular cell 7 that represents the volume between the reactor vessel and the biological shield.

Primary containment atmosphere temperatures and flow conditions at time 593 minutes are provided in Fig. 4.4. This is about one minute after the temperature of the heat sink representing the drywell head exceeds 730°F (661 K) so that the drywell head flange seals are modeled to fail catastrophically. At the time of failure, the drywell pressure is 126 psia (0.869 MPa) and, correspondingly, the initial leakage area is 15.5 in.<sup>2</sup> (0.010 m<sup>2</sup>). It should be recognized that this leakage would directly enter the refueling bay, bypassing the reactor building.

The cell atmosphere temperatures and the intercell flows at the termination of the CONTAIN calculation at time 900 minutes are shown in Fig. 4.5. Because of the continuous concrete ablation, the associated gas release into the debris, the metal oxidation therein, and the escape into the atmosphere of gases sparged through the debris, cell temperatures are very high, particularly in the lowest cells of the inpedestal and expedestal regions (cells 1 and 6). As indicated in Fig. 4.6a, the drywell pressure in the vicinity of the drywell head flange is sufficiently high that flange separation and leakage has continued throughout the calculation.

The configurations of the debris layers on the drywell floor just before and just after initial spreading into the expedestal region are shown in Table 4.3. In particular, it can be noted that ablation of the inpedestal concrete is significant. The bottom of the debris sinks from -7.71 inches (floor of the original sump configuration) to -16.26 inches during the period 265-375 minutes.

Radial concrete ablation in the inpedestal region as calculated by CONTAIN is significant, as shown in Fig. 4.6b, which indicates the maximum radius of the lowest inpedestal cell as a function of time. The plotted curve begins when the CORCON calculation is initiated, at time 265 minutes. The initial value of 10.125 ft (3.09 m) is the radius to the inner pedestal in its original configuration. The pedestal ablation is most rapid during the early part of the calculation, when zirconium oxidation is occurring in the inpedestal region. About seven percent of the original pedestal width is predicted to be consumed during the period prior to the initial spread into the expedestal region.

Comparison of the radial concrete ablation shown in Fig. 4.6b to the axial ablation shown in Table 4.3 reveals that the radial ablation at the time (375 min.) of initial spread into the expedestal region is much less than the axial ablation (0.2 ft radial vs 0.7 ft axial).

There are two reasons for this. First, the debris consists primarily of a relatively thin layer of frozen metals so that the resistance to heat transfer by conduction in the radial direction is much larger than the resistance in the axial direction. Second, although there is no appreciable radial crust in the partially liquified layer of oxides overlying the metals, the convective heat transfer in the radial direction is limited in this layer by the stable gas film maintained at the interface between the debris and the concrete. Because the gas flow in this vertical film at the outer radius of the debris is laminar, the CORCON code assigns a Nusselt number (1.0) close to the Nusselt number (0.804) used for the horizontal gas film at the base of the frozen metallic layer. Since both of these Nusselt numbers are defined directly in terms of the gas film thickness, the thicker gas film at the vertical interface results in a convective heat transfer coefficient smaller than that for the horizontal interface, where the gas film is much thinner. Thus, the predicted downward heat transfer and ablation exceeds the radial heat transfer and ablation.

The debris temperatures for the expedestal floor area are provided in Fig. 4.6c. The debris/concrete interaction begins in the expedestal region at time 375 minutes, just after the debris inpedestal has accumulated to a sufficient depth and molten state to be modeled to flow through the pedestal doorway. Based upon a method proposed by Kazimi<sup>8</sup> for determination of debris spreading areas, the initial debris spread into the expedestal region is assigned to cover an area of 800 ft<sup>2</sup> (74.3 m<sup>2</sup>). [Total expedestal floor area is 1100 ft<sup>2</sup> (102.2 m<sup>2</sup>)].

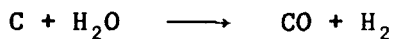
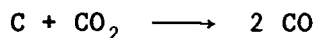
The initial spread into the expedestal region occurs during a period of rapid additional pour from the reactor vessel. (See Fig. 3.4 at time 375 min.) After just three additional minutes, the conditions in the expedestal region are such that the debris must be again modeled to spread, this time over the entire remaining 300 ft<sup>2</sup> (27.9 m<sup>2</sup>) of floor area. The debris configurations before and after this second expedestal spread are shown in Table 4.4.

As indicated in Fig. 4.6c, the debris temperatures in the expedestal region reach their maximum values during the period from 375 to 430 min. These high temperatures for the initial expedestal debris are predicted because of the calculated chemical energy release by oxidation of a large amount of zirconium metal. A comparison of powers due to chemical and decay heat sources is provided in Fig. 4.6d. Chemical power is much larger than decay power during the period before exhaustion of the zirconium metal at time 435 minutes and clearly is the reason for the calculated high debris temperatures expedestal during this period.

As indicated on Fig. 4.6d, the predicted chemical power in the expedestal region becomes a negative quantity for a very short period after exhaustion of the zirconium metal. This occurs because of an endothermic oxidation of the carbon formed by the coking reaction



during the period of zirconium oxidation. When the zirconium metal is exhausted, the CORCON module of CONTAIN models the endothermic reactions



which release large quantities of carbon monoxide and hydrogen. Subsequent to the completion of the zirconium oxidation reactions, the chemical power is primarily due to a balance between the two simultaneous endothermic carburization reactions defined above and the exothermic oxidation of chromium. The net chemical power during this time is of the order of the decay power. (The minor increase beginning at time 510 minutes and lasting until time 540 minutes is due to a late minor pour of zirconium metal occurring during this period.)

As discussed in Sect. 3.3, the debris source to the expedestal region of the drywell floor is metals-rich during the period between the initial spread into this region and the time when the temperature of the vessel pour is sufficient to maintain the oxides molten. During this 140-min period from time 375 to time 515 minutes, 89% of the zirconium and 99% of the other metals in the ongoing pour are directed into the expedestal region. For the oxides in the pour, which are frozen during this period, 80% are modeled by CONTAIN code input to flow into the inpedestal region while 20%, assumed to be carried into the expedestal region with the molten metal flow, are directed into the expedestal region.

It is obviously important to consider to what extent the calculated debris temperatures in the expedestal region are dependent upon the assumed division of metals and oxides between the inpedestal and expedestal regions of the drywell floor. To this end, the pour calculations were redone so that both metals and oxides were split between the inpedestal and expedestal regions strictly on the basis of the respective floor areas and the CONTAIN calculation of the drywell response was repeated. This exercise was performed both for the three-minute period immediately following the initial spread into the expedestal region, when the pour is divided between the 322 ft<sup>2</sup> (29.9 m<sup>2</sup>) of the inpedestal region and 800 ft<sup>2</sup> (74.3 m<sup>2</sup>) of the expedestal region, and for the final spread over the entire expedestal region.

The expedestal debris temperatures for this uniform debris composition case are shown on Fig. 4.7a and 4.7b, together with the temperatures for the best-estimate case. The overall temperature profiles for the two predictions have very similar shapes. For the metal layer (Fig. 4.7a), the peak temperature is slightly higher for the uniformly distributed case, but the period during which the temperature remains elevated is correspondingly shorter. This is consistent with the assumed partitioning of the debris pours.

From time 378 to 515 min., the best-estimate expedestal debris pour is rich in metals, incorporating 89% of the molten zirconium and 99% of the molten stainless steel leaving the reactor vessel, but only 20% of the frozen oxides. During the same period, 77% of the metals and 77% of the oxides in the ongoing pour are directed into the expedestal region for the uniform composition case. Thus, the best-estimate calculation places more zirconium metal in the expedestal region and the predicted chemical energy source and the debris temperatures remain elevated longer than in the uniform case calculation.

On the other hand, the additional oxides added to the expedestal region in the uniform composition case overlie the metals and reduce the heat loss from the metal layer to the atmosphere. This causes the peak metal layer temperature to be slightly higher for the uniform composition case and, over the long term, the predicted temperature of the metal layer for this case remains about 50 F° (30 K) higher than the metal layer temperature for the best-estimate metals-rich case.

In neither calculation do the predicted expedestal debris temperatures exceed the melting temperature of the carbon steel drywell shell [2800°F (1810 K)] and, as indicated on Figs. 4.7a and 4.7b, the calculated temperature profiles are similar. Thus, although assumptions regarding the degree of lateral separation of the molten metals from the frozen oxides have some effect upon the calculated expedestal debris temperatures, these assumptions clearly are not the dominant parameters in determining the question of shell survivability.

The question of the integrity of the reactor vessel skirt under the high-temperature conditions in the drywell is addressed in Fig. 4.8, where the temperatures of cell 3 (upper inpedestal), the skirt (which separates cells 3 and 7), and cell 7 (annular region between reactor vessel and biological shield) are plotted as functions of time. As seen, the calculated reactor vessel skirt temperature closely follows the cell 3 atmosphere temperature but does not exceed about 1700°F (1200 K). While this temperature is high enough to weaken the skirt, it should be recognized that the load supported by the skirt under these conditions is less than 10% of normal, since there is no water in the vessel and much of the core debris has escaped.

The cumulative gas release from the concrete by degassing is provided in Table 4.5 for the limestone common sand concrete considered in this report. It should be noted that most of the carbon dioxide and steam released from the concrete is consumed in metal-gas reactions within the debris; relatively little of these gases escapes from the debris surface to enter the drywell atmosphere.

A final threat to primary containment integrity is posed by the extensive predicted erosion of the reactor pedestal illustrated by Fig. 4.6b. As discussed earlier, about seven percent of the reactor pedestal is predicted to be eroded at the time of initial spreading of debris into the expedestal region. An additional 23% of the original pedestal is predicted to be eroded by the end of the calculation.

However, this predicted 30% reduction in pedestal wall thickness is probably a minimum estimate since the attack upon the pedestal wall from the other side by the expedestal debris (after time 375 minutes) is not considered in the calculation.

The pressure suppression pool is heated throughout the period of the calculation both by the decay heat energy release of the fission products trapped in the pool and by the passage of hot gases from the drywell into the pool whenever the drywell pressure rises sufficiently above the wetwell pressure to force gas flow through the downcomers. The BWRSAR calculation provides the estimate that pool fission product heating is 10.74 Mw at time 255 min, when the CONTAIN calculation is initiated; this value is used in the CONTAIN calculation until time 375 min, at which point the value is decreased to 9.83 Mw for the remainder of the calculation.

The pressure suppression pool temperature at the end of the calculation is 225°F (380 K); however, since the containment pressure at that time is 98.4 psia (0.678 MPa), which corresponds to a saturation temperature of 327°F (437 K), the pool has remained subcooled throughout the calculation.

Table 4.6 provides the time-history of the conditions at the debris-shell interface as calculated by CONTAIN for the periods during which the metal and oxide temperatures in the expedestal region are sufficiently high to challenge the integrity of the shell. As shown on Fig. 4.6c, these temperatures approach the melting temperature of carbon steel [2800°F (1810 K)] during the one hour period 375-435 minutes after scram. The maximum debris temperature predicted for the expedestal region during this period is 2706°F (1759 K) for the metal layer at time 418 minutes; the calculated debris temperatures decrease rapidly after this peak.

Conclusions regarding the effect of the debris-shell interface upon continued integrity of the drywell shell pressure boundary cannot be reached without additional calculations to determine the thermal response of the shell. Although the predicted debris temperatures are clearly not high enough to cause shell melt-through, failure of the shell pressure boundary through loss of strength is possible. A detailed thermal and stress analysis should be performed for the drywell shell throughout the region of contact with the hot debris to address this issue. It is for this purpose that the time-dependent debris conditions in the expedestal region together with the internal pressure loading of the drywell shell as calculated in this study are provided in Table 4.6. In particular, this detailed information pertaining to the calculated conditions at the interface during the period of elevated debris temperature is intended for use by interested parties who desire to perform shell response calculations with codes such as HEATING-6 or TAC-2D.

As mentioned previously, the CONTAIN calculations for this case without drywell sprays were terminated at time 900 minutes (15 hours)

after scram. Approximately 98% of the reactor vessel bottom head debris has become molten and left the vessel by this time, and most of the lower portion of the bottom head wall has been subsumed into the debris on the drywell floor. In the expedestal region, the base of the metal layer is predicted to have sunk 12.9 inches (32.7 cm) beneath the original level of the floor. All of the zirconium metal is long since oxidized, and the metal layer consists only of the frozen (but still very hot) constituents of stainless steel, whose oxidation by gases released by the continued ablation of concrete is slow. Overlying the 9.6-inch (24.3 cm) thickness of frozen metal is a 15.6-inch (39.6 cm) thickness of oxide slurry at a temperature of 2471°F (1628 K), extending to a height of 12.3 inches (31.1 cm) above the original level of the floor. Since the debris pour from the reactor vessel is for all practical purposes terminated at this point, it is reasonable to assume that this is the maximum height that the debris would reach against the drywell shell. Continuation of the CONTAIN calculation to times beyond 900 minutes would be expected only to predict that the frozen metal slug and its overlying oxide slurry would continue to slowly sink into the approximately 30 feet (9.1 M) of concrete remaining beneath the debris.



Table 4.1. Comparison of the constituent weight fractions of the limestone common sand concretes at two BWR facilities

Constituent	Peach Bottom	Browns Ferry
Al <sub>2</sub> O <sub>3</sub>	0.009	0.018
CaO	0.338	0.308
CO <sub>2</sub>	0.206	0.200
SiO <sub>2</sub>	0.358	0.388
Free H <sub>2</sub> O	0.045	0.048
Bound H <sub>2</sub> O	0.027	0.017
Other	<u>0.017</u>	<u>0.021</u>
	1.000	1.000

Table 4.2. Gas flow distribution in primary containment for Peach Bottom Station Blackout with ADS actuation for limestone common sand concrete at various times during the accident sequence

(Flows in lbm/min and time is in minutes after accident initiation)

Path <sup>a</sup>	Times			
	265.0 <sup>b</sup>	375.0 <sup>c</sup>	593.0 <sup>d</sup>	900.0 <sup>e</sup>
FLO12	213	1762	1367	953
FLO16	-213	-1756	-1352	-928
FLO23	857	2494	2474	1626
FLO25	-644	-731	-1129	-774
FLO34	857	2567	2534	1727
FLO45	859	2562	1780	1690
FLO47	-603	-2183	-2954	-1949
FLO49	610	2190	3769	1987
FLO56	221	1832	687	918
FLO610	0	0	0	0
FLO612	0	75	-701	0
FLO78	-663	-2311	-3117	-2078
FLO79	50	123	176	130
FLO89	-663	-2311	-4062	-2120
FLO810	0	0	1069	44

<sup>a</sup>Path definitions follow from the order of the indices in the path name. For path FLOIJ, the flow is from cell I to cell J if the tabulated flow is positive and from J to I if the tabulated flow is negative. See Figure 4.1 for primary containment nodalization.

<sup>b</sup>10 minutes after reactor vessel bottom head penetration failure at 255 min and immediately before inpedestal CORCON initialization.

<sup>c</sup>Immediately before 1st debris spread into expedestal area.

<sup>d</sup>0.8 min. after failure of drywell head flange seals.

<sup>e</sup>End of CONTAIN calculation.

Table 4.3. Debris configurations before and after spreading at time 375.0 min for Peach Bottom Short-Term Station Blackout with ADS actuation and limestone common sand concrete

Before Spreading			
Inpedestal only (322 ft <sup>2</sup> )			
(Inches)			
3.13	_____	Tsolidus	
		oxides	2522°F
		metals	2690°F
Floor 0.00	-----Oxides-----	Toxide	= 2654°F
		Tmetal	= 2536°F
		Mass oxides	= 73,971 lbm
		Mass metals	= 101,610 lbm
-7.01	_____		
	Metals		
-16.26	_____		
After Spreading:			
Inpedestal (322 ft <sup>2</sup> )		Expedestal (800 ft <sup>2</sup> )	
0.98	_____	_____	.94
		Oxides	
		_____	.45
Floor 0.00	-----Oxides-----	-----Metals-----	0.00 Floor
		_____	-.01
-7.98	_____		
	Metals		
-16.27	_____		
Toxide	= 2586°F	Toxide	= 2592°F
Tmetal	= 2586°F	Tmetal	= 2590°F
Mass oxides	= 65,847 lbm	Mass oxides	= 8,442 lbm
Mass metals	= 90,199 lbm	Mass metals	= 11,612 lbm

Table 4.4. Debris configurations before and after second  
expedestal region spread at time 378.0 min for  
Peach Bottom Short-Term Station Blackout

Before Second Expedestal Spread:					
Inpedestal (322 ft <sup>2</sup> )			Expedestal (800 ft <sup>2</sup> )		
	1.52	_____			
			_____	1.35	
			Oxides		
			_____	.48	
Floor	0.00	-----Oxides-----	-----Metals-----	0.00	Floor
			_____	-.32	
	-8.07	_____			
		Metals			
	-16.37	_____			
	Tsolidus oxide = 2561°F		Tsolidus oxide = 2531°F		
	Tsolidus metal = 2690°F		Tsolidus metal = 2692°F		
	Toxide = 2607°F		Toxide = 2694°F		
	Tmetal = 2591°F		Tmetal = 2695°F		
	Mass oxides = 74,275 lbm		Mass oxides = 15,065 lbm		
	Mass metals = 90,459 lbm		Mass metals = 20,309 lbm		

After Second Expedestal Spread:					
Inpedestal (322 ft <sup>2</sup> )			Expedestal (1100 ft <sup>2</sup> )		
	1.09	_____			
			_____	1.11	
			Oxides		
			_____	.40	
Floor	0.00	-----Oxides-----	-----Metals-----	0.00	Floor
			_____	-.33	
	-8.27	_____			
		Metals			
	-16.37	_____			
	Toxide = 2599°F		Toxide = 2669°F		
	Tmetal = 2598°F		Tmetal = 2669°F		
	Mass oxides = 72,423 lbm		Mass oxides = 17,275 lbm		
	Mass metals = 88,336 lbm		Mass metals = 22,639 lbm		

Table 4.5 Cumulative gas release at  
 termination of calculation for  
 Peach Bottom Station Blackout  
 with ADS actuation and lime-  
 stone common sand concrete  
 Time 900 min.

	lbs	lb-moles
<hr/>		
Gas release from concrete		
CO <sub>2</sub>	61,555	1399
H <sub>2</sub> O	<u>21,339</u>	<u>1184</u>
	82,894	2583
Gas release from debris surface		
CO <sub>2</sub>	2,180	49.5
H <sub>2</sub> O	847	47.0
CO	13,592	485.3
H <sub>2</sub>	<u>2,289</u>	<u>1135.6</u>
	18,908	1717.4
<hr/>		

Table 4.6. Expedestal debris conditions for Peach Bottom Short Term Station Blackout  
with ADS actuation and limestone common sand concrete

Time (min)	Z <sub>bot</sub> (in.)	Z <sub>MET/LOX</sub> (in.)	Z <sub>LOX/ATM</sub> (in.)	Mass metals (lbs)	T <sub>METALS</sub> (°F)	T <sub>SOLIDUS</sub> METALS (°F)	LOX-mass light oxides (lbs)	T <sub>LOX</sub> (°F)	T <sub>SOLIDUS</sub> (LOX) (°F)	Drywell Pressure (psia)
375.0	0.00	0.45	0.94	11,610	2590	2690	8,442	2592	2523	62.0
375.5	-0.04	0.46	1.00	12,860	2622	2690	9,298	2628	2526	63.7
376.0	-0.09	0.47	1.06	14,290	2654	2691	10,340	2659	2529	64.3
376.5	-0.14	0.48	1.14	15,810	2681	2691	11,430	2687	2531	64.6
377.0	-0.20	0.48	1.21	17,300	2693	2691	12,610	2692	2831	64.8
377.5	-0.26	0.48	1.28	18,810	2694	2692	13,830	2693	2531	65.0
378.0	-0.32	0.48	1.35	20,310	2695	2692	15,060	2695	2531	65.2
379.0	-0.42	0.40	1.20	25,450	2677	2692	19,610	2679	2538	65.7
380.0	-0.52	0.39	1.31	28,600	2685	2692	22,160	2685	2536	66.1
381.0	-0.63	0.39	1.42	31,890	2691	2692	24,770	2692	2534	66.5
382.0	-0.75	0.39	1.54	35,340	2693	2693	27,520	2692	2531	66.9
383.0	-0.87	0.39	1.66	38,970	2694	2693	30,310	2693	2528	67.2
384.0	-0.99	0.39	1.78	42,740	2696	2694	33,100	2695	2526	67.6
385.0	-1.11	0.38	1.90	46,460	2697	2694	35,880	2695	2523	68.0
386.0	-1.23	0.38	2.02	50,140	2697	2695	38,660	2696	2521	68.3
387.0	-1.35	0.38	2.14	54,010	2698	2695	41,440	2697	2519	68.7
388.0	-1.47	0.38	2.26	57,830	2699	2695	44,210	2697	2518	69.1
393.0	-2.07	0.40	2.89	77,700	2701	2696	58,030	2699	2510	70.5
398.0	-2.68	0.59	3.69	100,360	2701	2696	71,700	2698	2505	72.2
403.0	-3.28	0.70	4.42	127,000	2702	2696	85,720	2699	2504	74.3
408.0	-3.89	0.43	4.75	136,100	2703	2699	99,190	2700	2499	76.5
413.0	-4.50	-0.03	4.89	138,300	2704	2702	112,200	2702	2493	78.8
418.0	-5.10	-0.51	4.98	139,500	2706	2706	125,200	2695	2489	80.9
423.0	-5.54	-0.86	4.99	142,300	2680	2709	134,500	2651	2486	83.2
428.0	-5.87	-0.71	5.08	146,500	2647	2713	141,100	2609	2483	85.0
433.0	-6.16	-0.86	5.20	151,300	2630	2716	147,000	2575	2482	86.8
438.0	-6.41	-0.95	5.33	157,300	2538	2719	151,300	2545	2475	88.8
443.0	-6.59	-0.96	5.42	169,900	2472	2723	154,500	2509	2467	90.5

T<sub>SOLIDUS</sub> = Mixture temperature at which melting begins

LOX = Light oxides

HOX = Heavy oxides

Z = Elevation relative to original floor surface

MET/LOX = metal - light oxide interface

LOX/ATM = light oxide - atmosphere interface

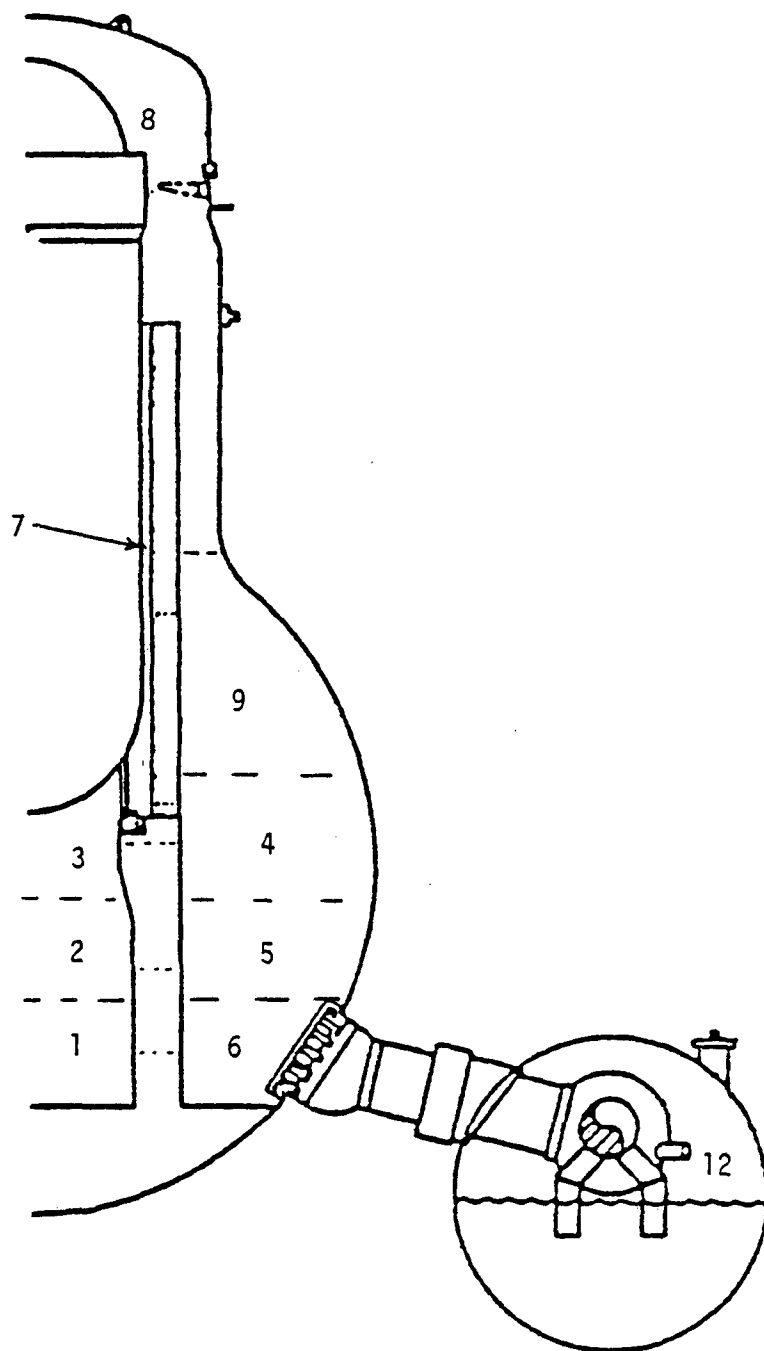


Fig. 4.1. BWRSAT Program Nodalization for the BWR Mark I Primary Containment. Not shown are cells 10 (Secondary containment) and 11 (outside environment), which make up the balance of the complete CONTAIN model used for the Peach Bottom calculations.

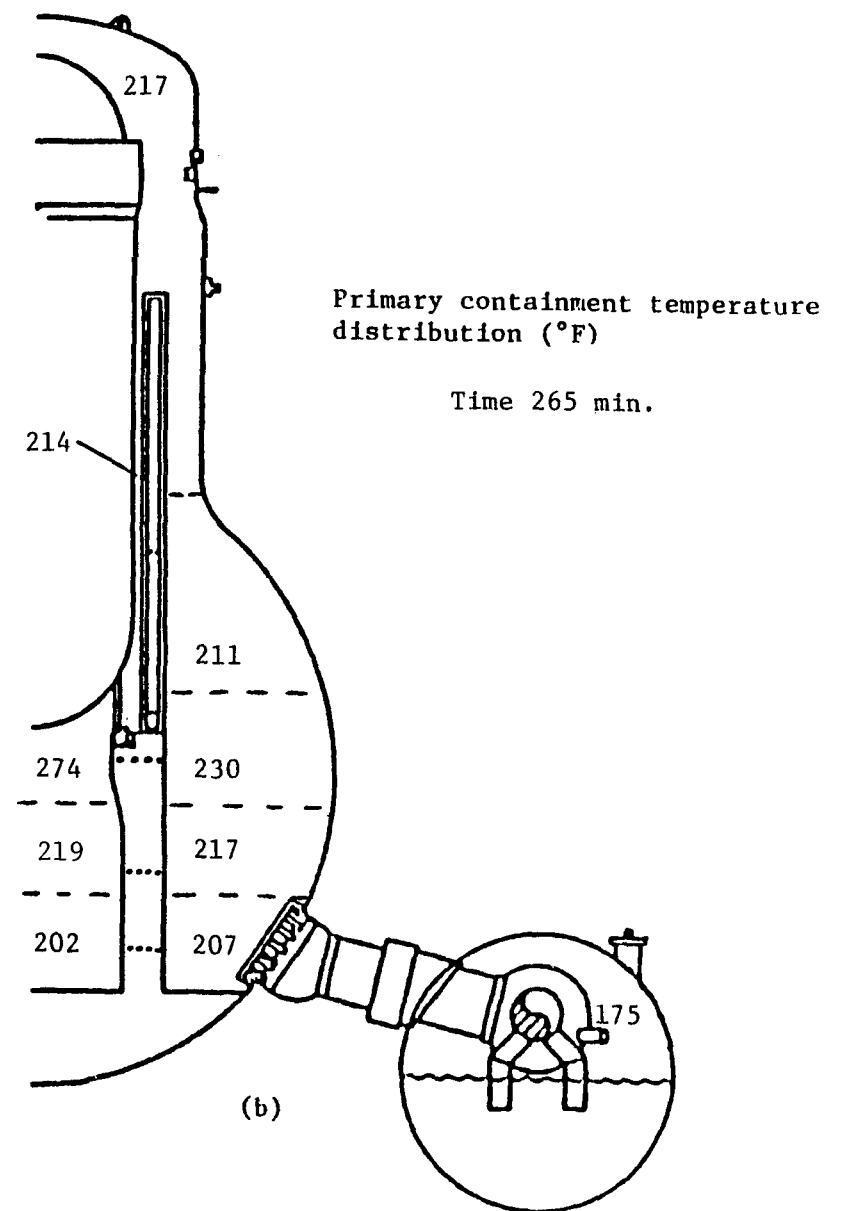
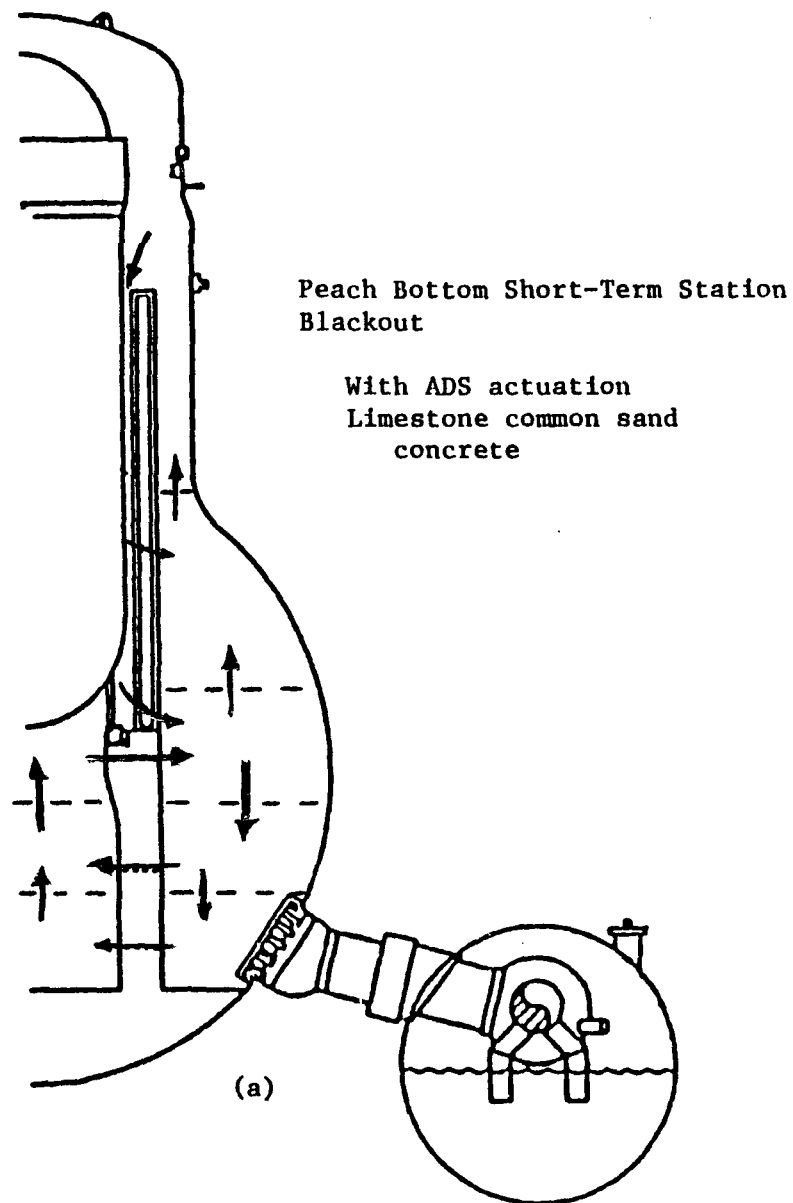


Fig. 4.2 Drywell intercell flows and cell temperatures as predicted by CONTAIN at 10 minutes after reactor vessel bottom head penetration failure and just before the inpedestal CORCON calculation is initiated.



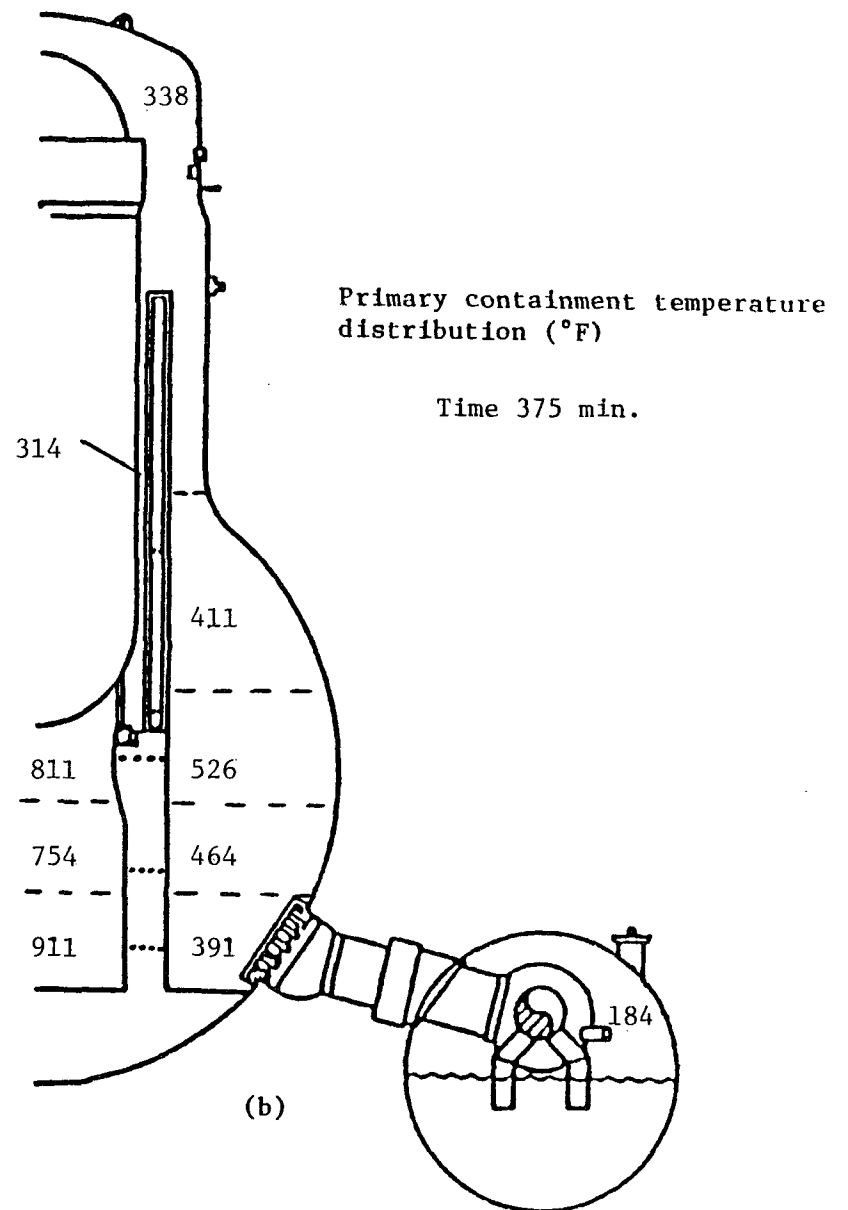
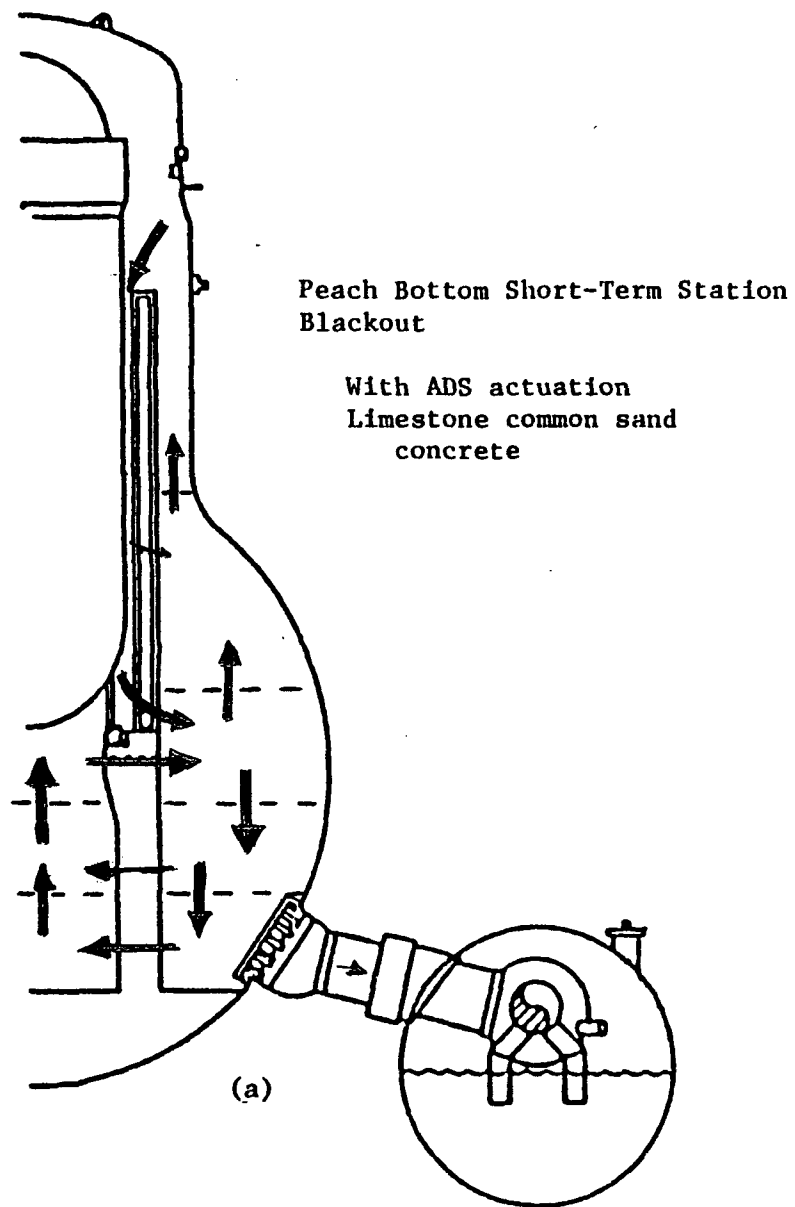


Fig. 4.3 Drywell intercell flows and cell temperatures as predicted by CONTAIN after 110 minutes of inpedestal core debris-concrete interaction calculations by CORCON. The core debris is on the verge of its initial spread into the expedestal region.

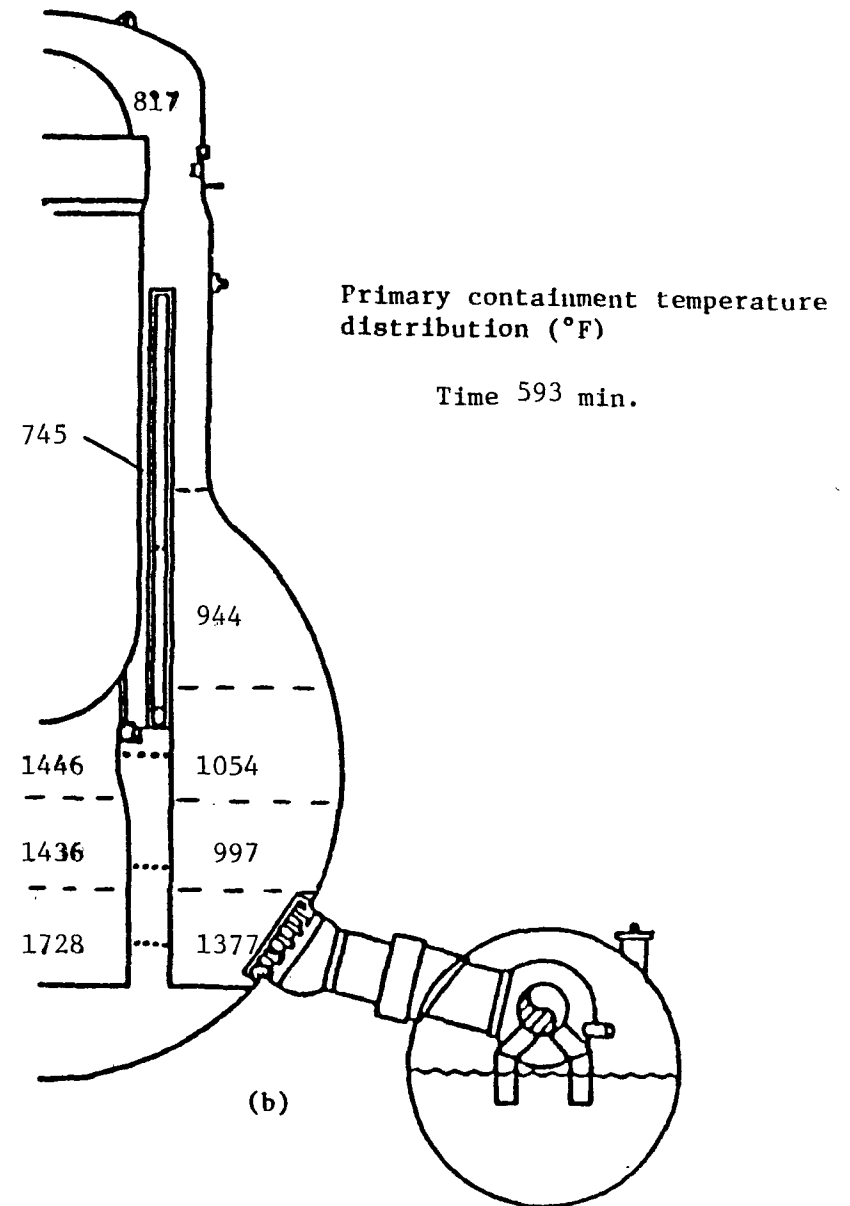
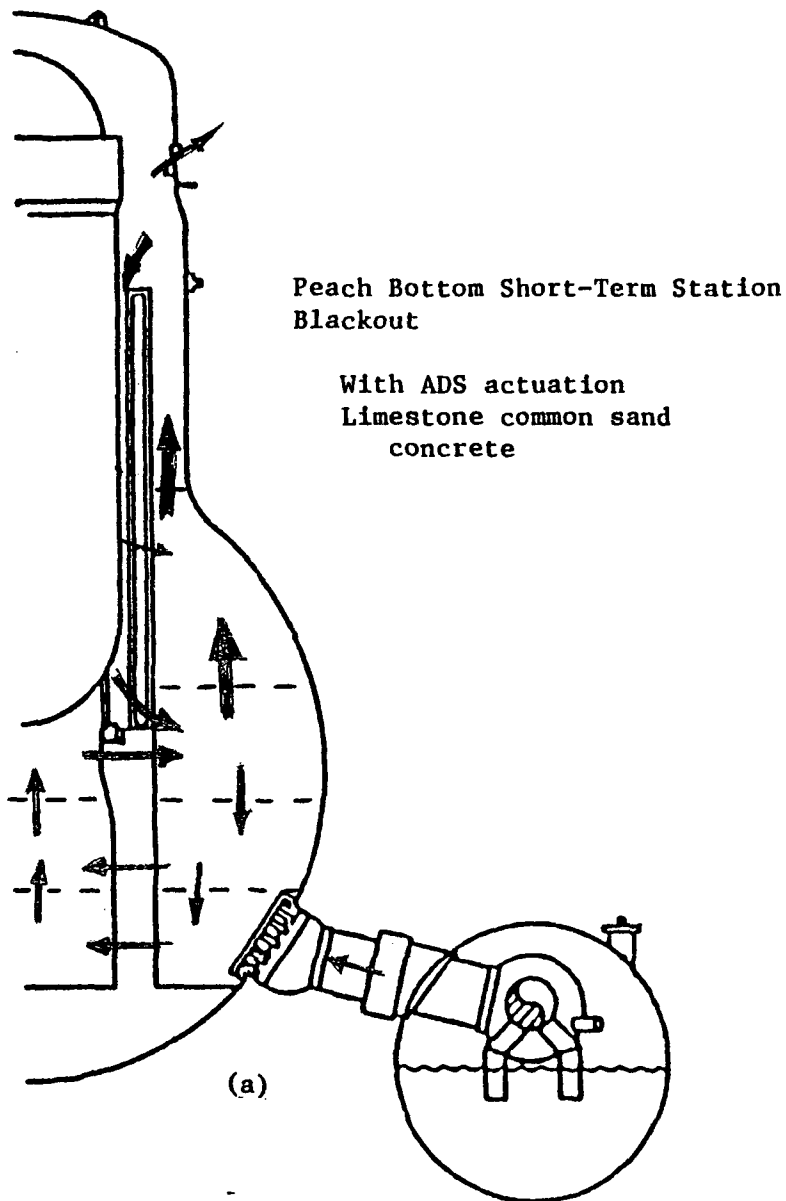


Fig. 4.4 Drywell intercell flows and cell temperatures as predicted by CONTAIN 0.8 minutes after drywell head flange leakage begins. The leakage is induced by a combination of high drywell pressure, which lifts the head and high temperature, which degrades the seals.

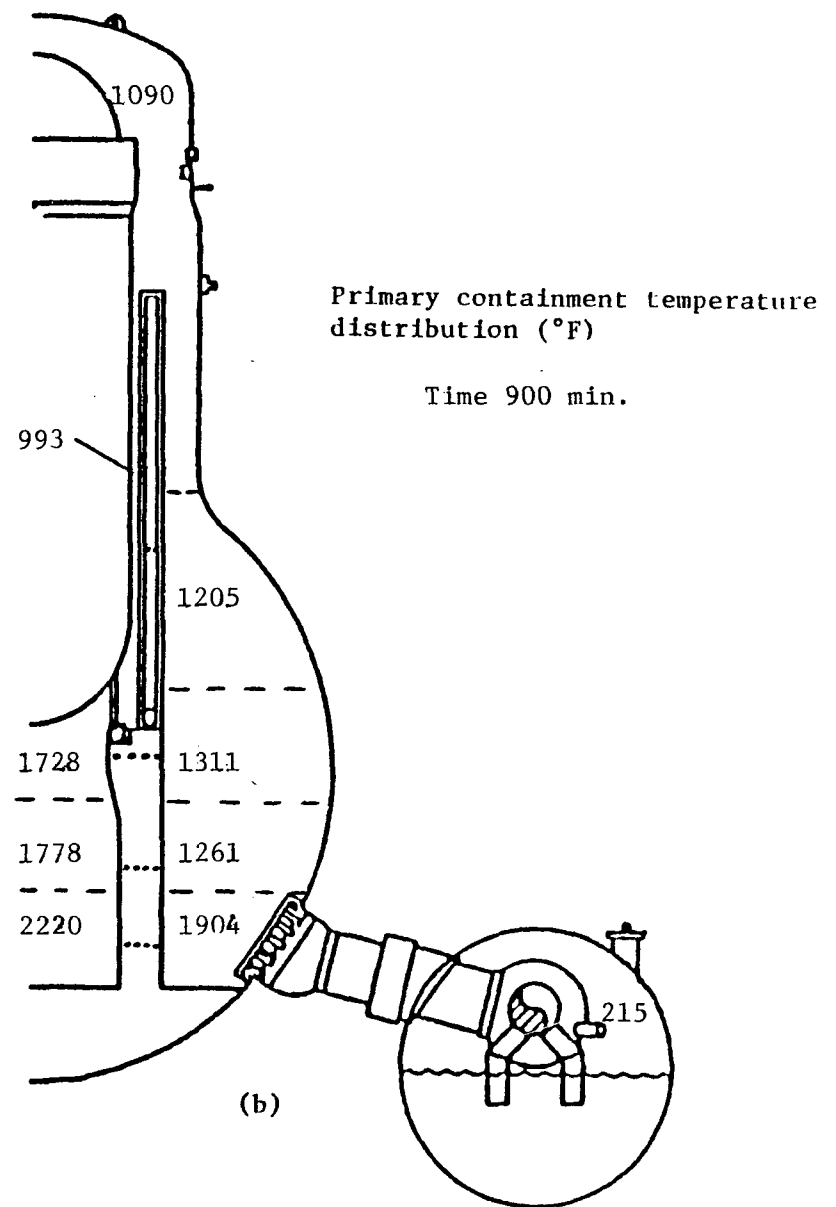
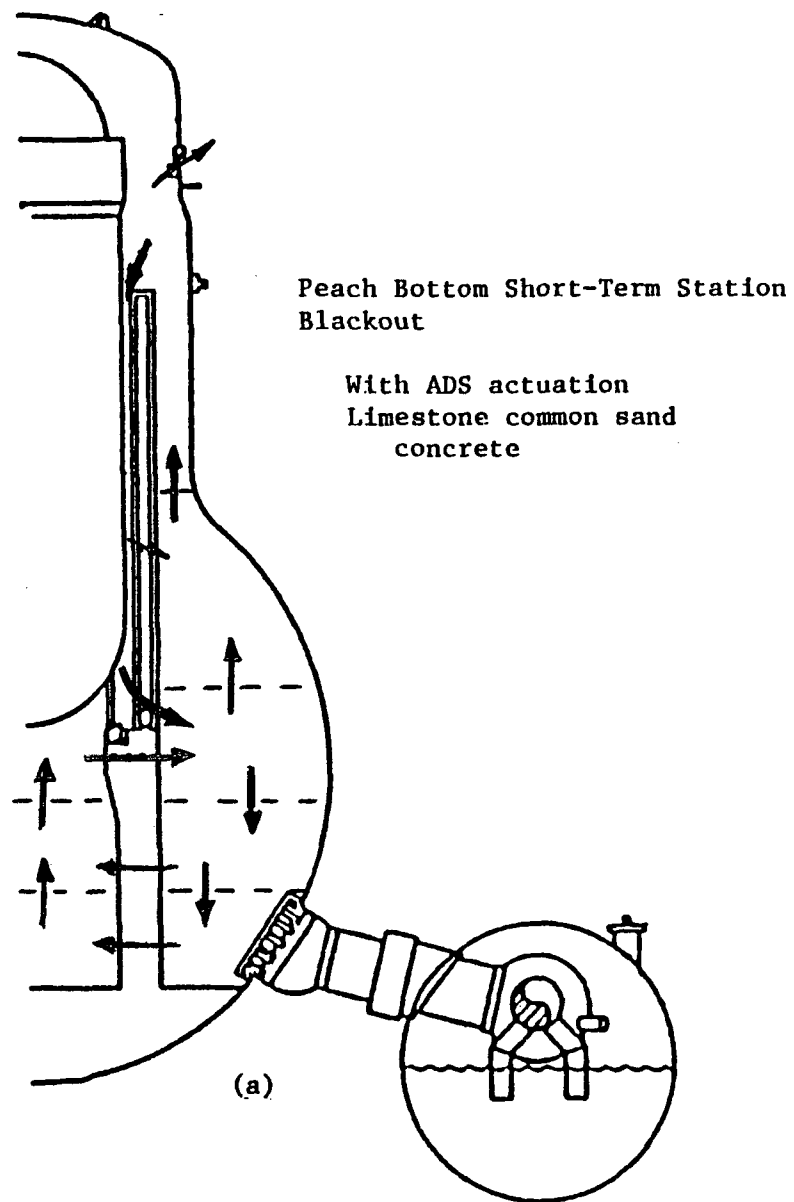


Fig. 4.5 Drywell intercell flows and cell temperatures as predicted by CONTAIN at the termination of the calculation. By assumption, there has been no failure of the drywell shell by melt-through at floor level.

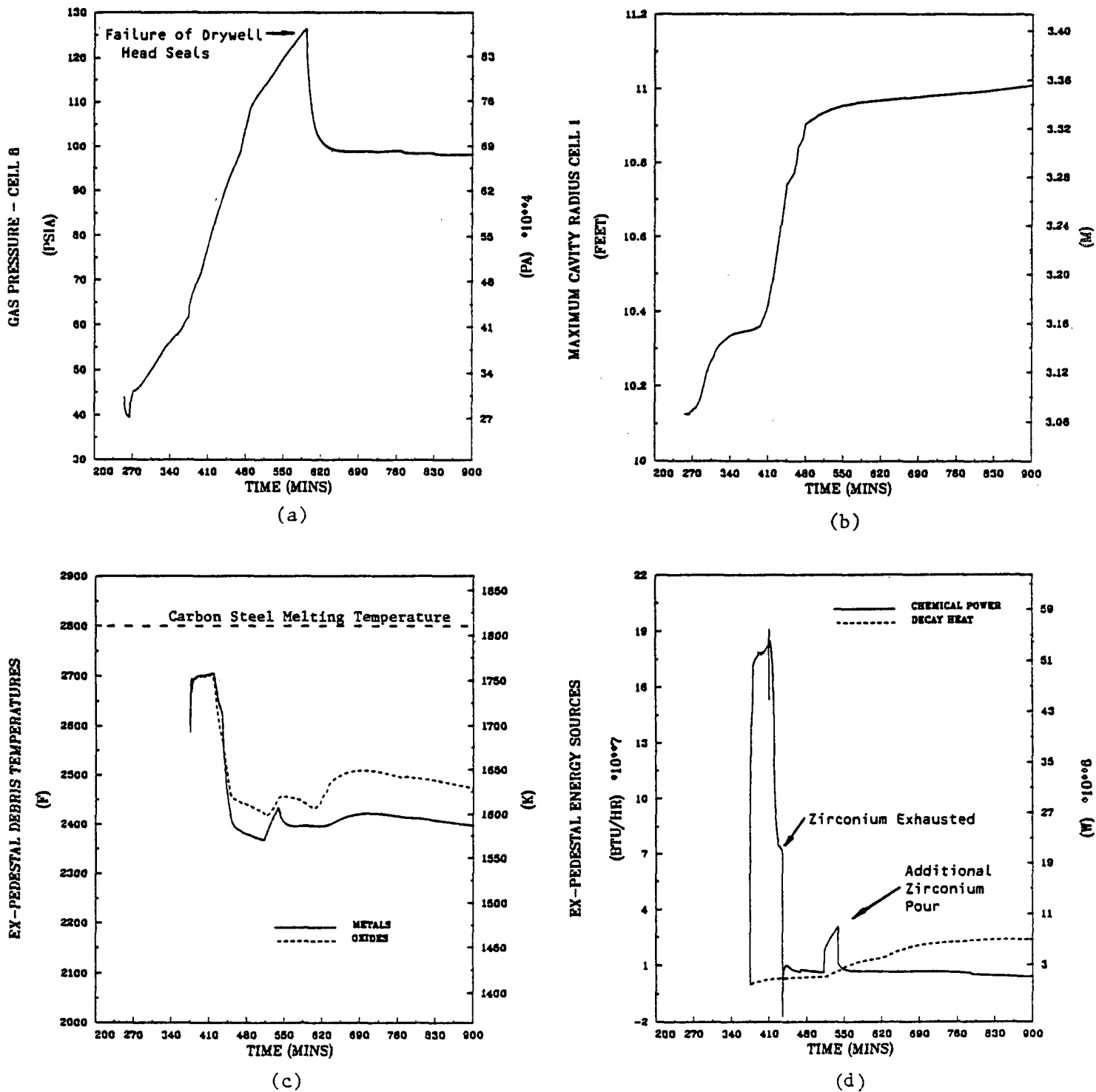


Fig. 4.6 Selected parameters relative to maintenance of drywell shell pressure boundary integrity for Peach Bottom Short-Term Station Blackout with ADS actuation. The first spread of debris into the expedestal region occurs at time 375 minutes. The floor is modeled as limestone common sand concrete without overlying water.

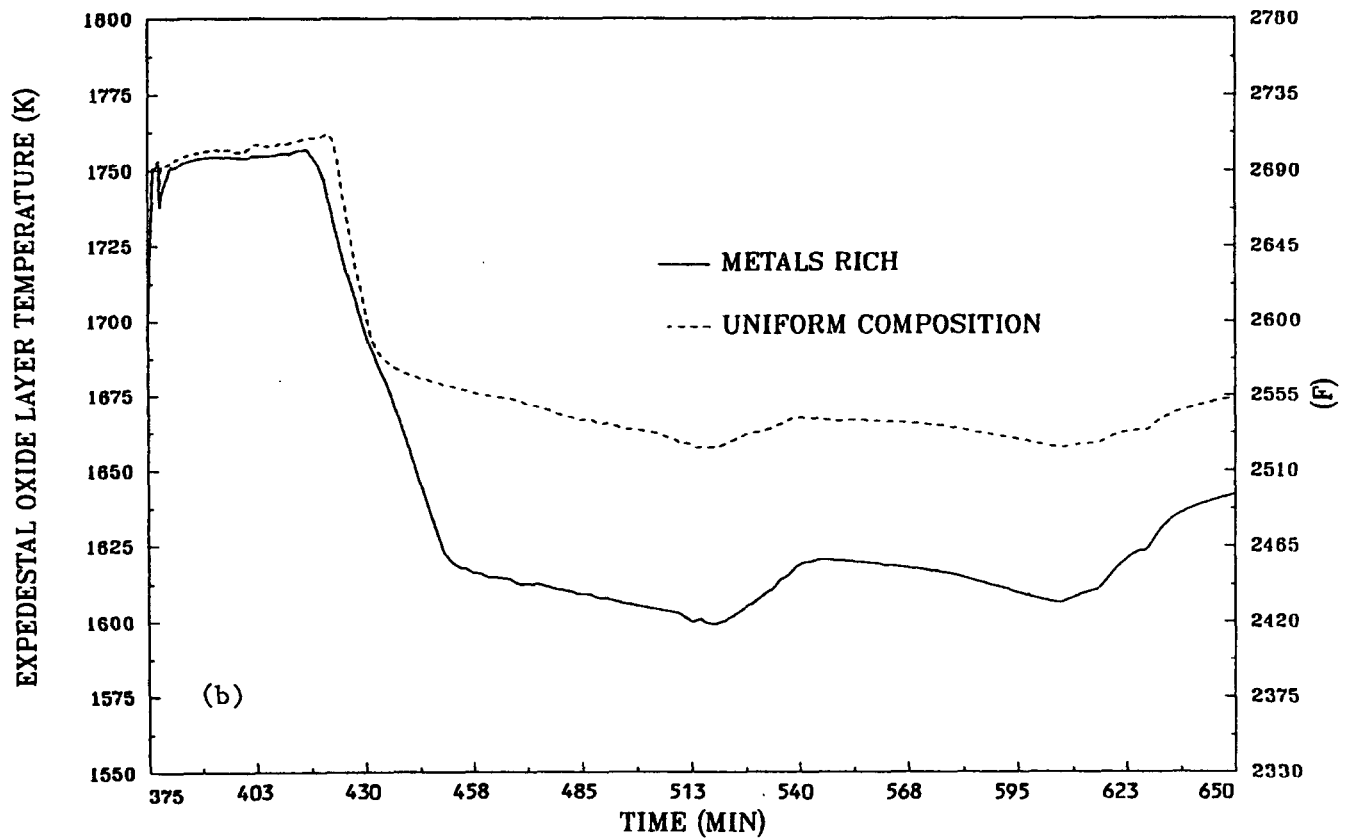
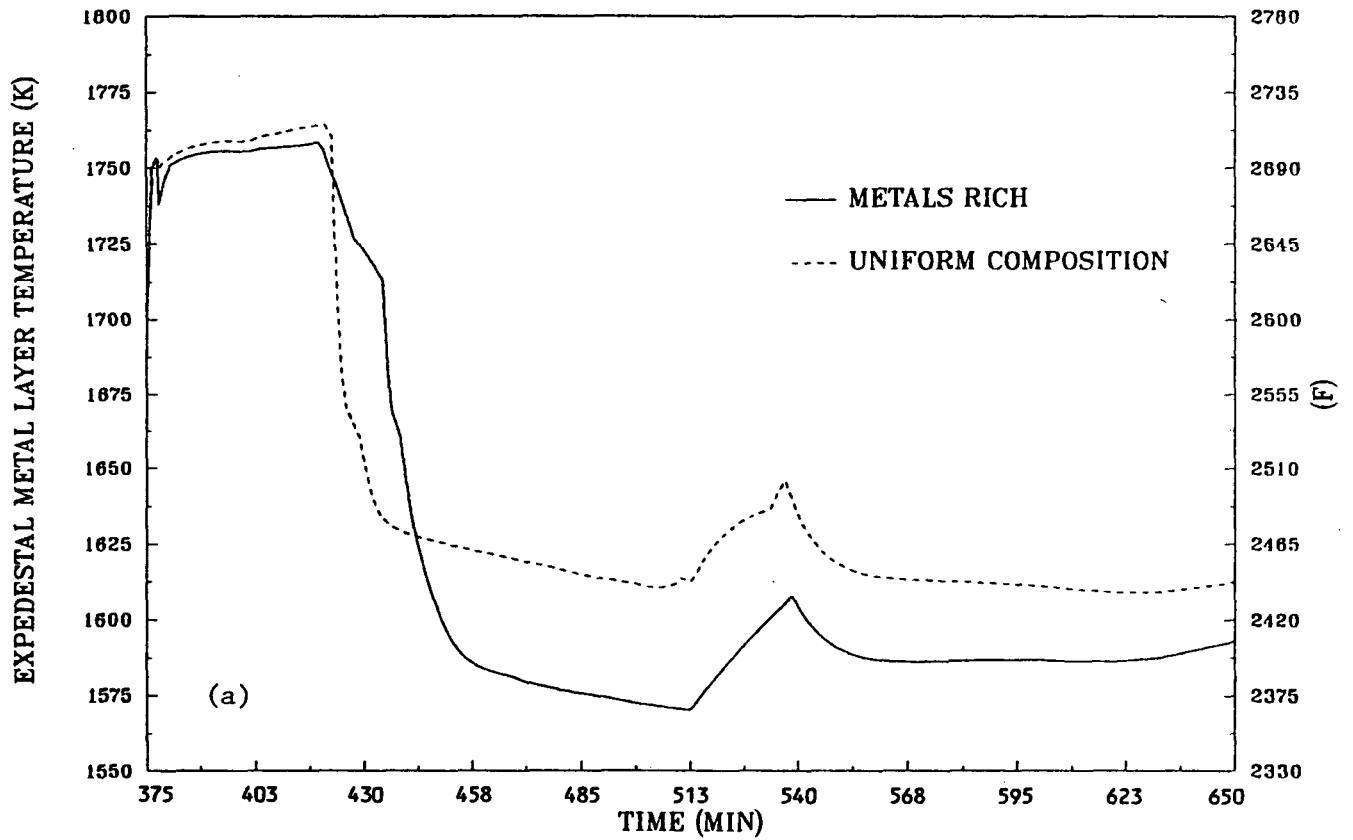


Fig. 4.7. Comparison of the debris layer temperatures in the expedestal region for the case of best-estimate (metals rich) spreading vs. the case with equal spreading of oxides and metals.

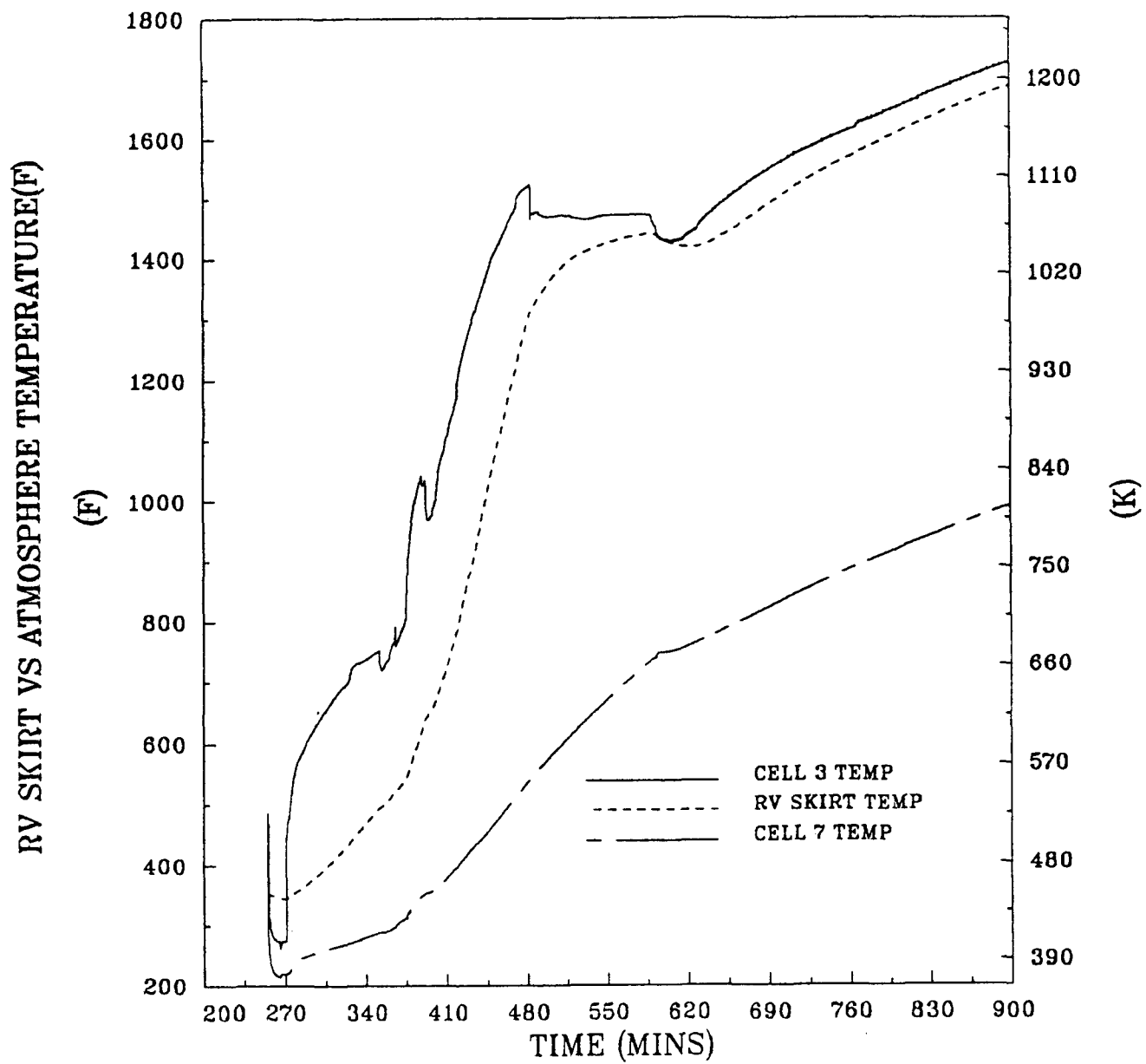


Fig. 4.8 Temperatures of the reactor vessel support skirt and the two adjoining drywell atmosphere cells.

## 5. CONTAIN CALCULATIONS FOR THE EFFECT OF DRYWELL SPRAYS

This chapter describes the predicted containment response of a Peach Bottom unit to a postulated short-term station blackout accident sequence in which the Automatic Depressurization System (ADS) is used for early depressurization of the reactor vessel in accordance with the procedures specified in the BWR Owner's Group Emergency Procedure Guidelines. The effect of the reactor vessel depressurization is to greatly reduce the magnitude of the direct vessel blowdown into the drywell and the concomitant primary containment pressure increase upon bottom head penetration failure. This is the accident sequence described in Chap. 3 for which the calculated containment response without consideration of drywell sprays is provided in Chap. 4. It is the purpose of this chapter to discuss the calculated containment response for the case with actuation of the drywell sprays.

### 5.1 Modeling of Drywell Sprays

The existing containment spray system at Peach Bottom would probably not be available under the conditions of an unmitigated severe accident that proceeded through the point of reactor vessel bottom head penetration failure and the emergence of core debris from the vessel. This is because the containment spray is a subsystem of the Residual Heat Removal (RHR) System, which is a low pressure ECCS system with primary purpose of injection into the reactor vessel under accident conditions. Thus, if containment sprays are available, then the RHR System is available, and the accident would not have progressed to the point of bottom head penetration failure. In other words, if it is hypothesized that an unmitigated severe accident has occurred at Peach Bottom, then it is reasonable to assume that the present system of containment sprays would not be operational. Nevertheless, future plant modifications might provide an independent drywell spray system. To see the effect of drywell spray upon events after bottom head penetration failure, the short-term station blackout CONTAIN calculations for primary containment response have been repeated assuming the sprays to be available and actuated.

For these calculations, a new drywell spray system is assumed that takes suction from the condensate storage tank but can be shifted to take suction from the pressure suppression pool. The spray rate is assumed to be 700 gpm (0.044 m<sup>3</sup>/s), using the existing spray headers within the drywell; these are assumed to have been fitted with nozzles that assure effective droplet formation at this reduced spray rate (existing systems have a spray rate about 5 times larger). The sprays are assumed to have been turned on sufficiently before reactor vessel bottom head penetration failure so that there is a standing pool on the drywell floor at the time of failure, with overflow through the vent pipes and downcomers to the pressure suppression pool.

As modeled, the spray initially enters cell 4 of the drywell atmosphere (see Fig. 4.1) with a droplet diameter of one millimeter. After falling through the atmosphere of cell 4, the heated flow is fed as a spray into the atmosphere of cell 5 with an increased droplet diameter of three millimeters. This increase in droplet diameter is intended to represent the effect of spray impact upon floor gratings and equipment within the drywell. The flow from cell 5 is fed as a spray (droplet diameter 3 mm) into the atmosphere of cell 6 and from there onto the pool overlying the debris on the drywell floor.

The spray is modeled to be taken from the condensate storage tank while the debris pour from the reactor vessel fills the inpedestal region and during the initial spread into the expedestal region. The temperature of the spray entering atmosphere cell 4 during this period is assumed to be 90°F (305 K). After the time that the debris spreads over the entire expedestal region (602 min), the spray is assumed to be taken from the pressure suppression pool, and its entering temperature is that of the pool.

## 5.2 Primary Containment Response

It is the purpose of this section to discuss the response of the primary containment during the portion of the short-term station blackout with ADS actuation accident sequence that occurs after failure of the reactor vessel bottom head penetrations, when there is direct blow-down of the reactor vessel to the drywell. The containment response during this period is calculated by the CONTAIN code.

Diagrams indicating the direction of calculated drywell intercell gas flows, primary containment cell temperatures and atmosphere densities for Peach Bottom Short Term Station Blackout with drywell sprays are provided in Figs. 5.1 to 5.4. The numerical values of the intercell flows are listed in Table 5.1. As in the case for the dry containment results discussed in Chap. 4, the flow from cell 6 to cell 10 (lower expedestal region to secondary containment by means of thermally-induced failure of the shell pressure boundary at the level of the drywell floor) by assumption remains zero throughout the calculation. The following discussion relies heavily upon reader familiarization with the CONTAIN nodalization diagram presented in Fig. 4.1.

The CONTAIN calculation was initiated just before reactor vessel bottom head penetration failure with the initial drywell cell temperatures taken from BWRSAR code results. The intercell flows, cell temperatures, and cell densities 10 minutes after bottom head penetration failure and the beginning of gas release from the depressurized reactor vessel into the drywell are shown in Figs. 5.1a and 5.1b, respectively. The highest atmosphere temperature, as expected, is in the uppermost inpedestal cell, immediately beneath the reactor vessel.

It should be noted that there are two clockwise natural convection flow loops indicated in Fig. 5.1a. The lower loop involves flows from



the upper inpedestal region through the pedestal wall into the expedestal region, where the action of sprays cools the atmosphere significantly. Part of this cool, more dense stream descends into the lower cells of the expedestal region, where the warmer structures heat the gas slightly. This flow returns through various pedestal openings into the inpedestal region, where the gas is heated by the reactor pedestal. It then rises to the top of the inpedestal region, where it mixes with the hot gases coming from the failed reactor vessel and begins its route once again. As seen from Table 5.1, the magnitude of this flow is on the order of 1400 lbm/min, with about 1000 lbm/min flowing from the expedestal to inpedestal regions through openings in the pedestal wall between cells 2 and 5 and with the remainder passing from cell 6 to 1 through the pedestal doorway.

The second clockwise flow path is much smaller in magnitude, 400 lbm/min, and is due to variations in gas density due to differences in gas composition and temperature. Cell 4 gas is cold and dense because of sprays; thus gas travels from cell 4 to annular cell 7 where it is heated by the relatively hot reactor vessel wall. However, because the gas is also cooled by the thick biological shield, the gas temperature in cell 7 is not as high as in the upper reaches of the drywell (cell 8) or the knuckle area of the drywell (cell 9). Because the gas is almost incompressible, flow is established from cell 7 to cell 8 with a smaller flow from cell 7 to cell 9.

It should be recognized that the above discussion depends solely on relative density differences among the cells and the relative geometrical locations of the centers of mass of each cell as located in Fig. 4.1. Nonhomogeneity in the gas density distribution is strongly affected by gas composition which, in turn, is affected by the relative rates of steam condensation on the colder structures. It is only with consideration of gas densities as well as temperatures that the relatively complicated flow patterns can be understood.

This double clockwise flow pattern is maintained at time 372 min, (the time of the initial expedestal debris spread) as indicated in Fig. 5.2. The magnitude of the flow in the upper path has decreased (Table 5.1) because of decreasing heat transfer from the structures to the gas as the gas and structure temperatures equalize. However, the magnitude of the flow in the lower cell has increased during the same period because of the release of gases from the debris/concrete interaction in the lowest inpedestal cell.

The flow pattern, atmosphere temperatures, and atmosphere densities at the time of the second expedestal spread, 602 min, are shown in Fig. 5.3. As seen from Fig. 5.3a, the flow pattern in the lower region of the drywell has become more complicated. This is because of the gas sources existing at the pool surface which consist of noncondensable gas release from the surface of the debris in cells 1 and 6, and a steam source due to boiling of the water pool in cell 1.

No steam flow source exists in cell 6 because the water pool in this cell is subcooled. The pool of cell 6 is formed directly by the coalescence of spray water in the expedestal regions of the drywell (cells 4, 5, and 6) while the water forming the pool of cell 1 is provided by the lateral runoff of water from the expedestal floor to the inpedestal floor. Thus, the water forming the pool of cell 1 has been preheated by the debris extant on the expedestal floor and thus reaches the saturation temperature [ $\sim 290^{\circ}\text{F}$  ( $417\text{ K}$ )] while the expedestal pool remains subcooled [ $276^{\circ}\text{F}$  ( $409\text{ K}$ )].

Because of the greater steam source in cell 1 compared to cell 6, the atmosphere of that cell is somewhat closer to the saturation temperature and thus is warmer than the atmosphere of cell 6, which is cooled by the sprays. Because the density of cell 1 gas is larger than the density of the gas in cell 6, gas flow is from cell 1 to cell 6 and is primarily steam. This steam is mostly condensed in cell 6, as the flow from cell 6 to cell 5 is only 5 lbm/min, while there is no flow to the pressure suppression pool.

Because there is a gas source in cell 3 from the failed reactor vessel, gas flows from cell 3 to cell 4, where it is cooled by sprays. The cold gas flows downward into cell 5 and then into cell 2 where it is mixed with the warm gas rising from cell 1. Because the gas is almost incompressible, and because cell 3 gas is less dense than cell 1 gas, the flow from cell 2 is upward into cell 3, where it is heated by the continued release from the failed reactor vessel. Thus, the gas flow pattern in the bottom region of the drywell is essentially clockwise except for the perturbation at floor level due to the strong steam source from boiling in the inpedestal region.

As seen from Fig. 5.3, the flow pattern for the upper region of the drywell has reversed its previous circulation and is now in the counter clockwise direction. The magnitude of the flow in this upper flow loop is larger than that at 372 min, and is due to the strong gas source created by boiling of the water pool of cell 1. The direction of the flow pattern is dictated by the hydraulic resistance ( $fL/D$ ), which is much smaller for the expedestal cells than for the annular cell 7. In addition, the spray by this time has reduced steam concentrations in cell 4 so that the relatively dry gas evaporates water that had previously condensed onto the cold structures during the period 372–602 min. This is the reason for the increasing flow as gas passes from cell 4 to 9 to 8 to 7 and finally back into cell 4 (Table 5.1).

The temperatures and gas flows at the end of the calculation (750 min) are shown in Fig. 5.4. This is well after the debris on the drywell floor has spread completely around the periphery of the expedestal floor (602 min). Also, the suction of the sprays has shifted from the condensate storage tank (CST) to the pressure suppression as the CST neared exhaustion at 602 min. Because of this shift, the spray water entering the drywell atmosphere is now much warmer than previously [ $214^{\circ}\text{F}$  vs  $90^{\circ}\text{F}$  ( $374\text{ K}$  vs  $306\text{ K}$ )]; thus, the water pool on the expedestal floor saturates quickly.

Because both water pools are saturated, heat transfer from the debris to the water pools results in multiple steam sources entering the drywell atmosphere — one in cell 1 and one in cell 6. These steam sources make the flow pattern in the lower regions of the drywell complicated. As seen from Fig. 5.4., there is no clear circulatory flow pattern in the lower drywell. The sprays in the steamy expedestal environment condense large amounts of steam, which reduces the pressure and allows gas to flow from the inpedestal region to the expedestal region, i.e., from cell 2 to 5 and from cell 1 to 6. Part of this outflow is compensated by the small inflow from cell 4 to cell 3, as the gas density in cell 4 is higher than in cell 3, due to the action of sprays in cell 4.

Because the spray suction has shifted to the torus pool, spray water is warmer than at earlier times, and thus is not quite as effective in condensing steam. As a result, the pressure in the drywell is high enough to cause flow to the pressure suppression pool (FLO612 in Table 5.1 at 750 min). This is also the reason for relatively high steam concentrations in the upper drywell and the resulting condensation onto cold structure surfaces. Because of the large structure surface area-to-volume ratio for the annular region composing cell 7, condensation of steam onto the cold inner surface of the biological shield results in rapid pressure reduction and permits gas flow from cell 4 to cell 7 and then from cell 7 into cell 8. Because the gas is almost incompressible, flow continues from cell 8 into cell 9 and from cell 9 back to cell 4.

The CORCON calculation was initiated for the inpedestal debris at 265 min, the same time as for the dry case reported in Chap. 4. The inpedestal calculation was continued until 372 min, when the second major debris pour was well underway. This initial spreading time is slightly earlier for the wet case than the dry case because of the reduced reactor pedestal and drywell floor erosion.

Table 5.2 reports the debris configuration both before and after the initial spreading into the expedestal region. The expedestal floor area covered by the initial spread is 800 ft<sup>2</sup> (74.3 m<sup>2</sup>). The axial erosion front is at 10.83 inches (27.51 cm) below the floor level at the time of spread. This may be compared to 16.26 in. (41.30 cm) for the dry case as indicated in Table 4.3. Pedestal erosion from 265 min to 372 min is also reduced as can be seen by comparing Fig. 5.6d to Fig. 4.6b. Because of this reduced rate of concrete ablation, the debris fills the inpedestal sump volume faster than in the dry case and is ready to spread into the expedestal floor area earlier.

As indicated in Table 5.2, the temperature of the inpedestal metal layer prior to spreading at time 372 min is only 2422°F (1601 K), well below its solidus temperature of 2687°F (1748 K), while the oxide layer temperature of 2599°F (1699 K) is only slightly below its solidus temperature. Because the metals mass is three times larger than the oxides mass, it is clear that most of the inpedestal debris is frozen at this time. However, from Fig. 3.4, it is also clear that the pour from

the reactor vessel is increasing rapidly at 372 min, and that the temperature of this pour is also increasing. Thus, even though the bulk of the inpedestal debris is frozen at 372 min, the debris pouring on top of the inpedestal debris is molten; therefore, the incoming debris was assumed to be spreadable onto the expedestal floor.

Because the bulk of the inpedestal debris is frozen at 372 min, essentially negligible amounts of debris were placed in the expedestal region initially. This is the reason for the very thin layers on the expedestal floor <.3 in. (Table 5.2) and also explains why the inpedestal debris upper surface is higher above the floor than the expedestal debris, i.e., 2.45 in. vs 0.22 in. respectively.

As discussed in Chap. 3, a method developed by Kazimi was used to determine the extent of the initial debris spread into the expedestal region for the dry case. The method predicts the amount of floor area to be covered as a function of the pour rate and the temperature of the debris emanating from the failed reactor vessel. The predicted initial spreading area for the dry case was 800 ft<sup>2</sup> (74.3 M<sup>2</sup>) expedestal. However, because the Kazimi method considers heat losses from the spreading debris to the underlying concrete to be dominant, the presence of an overlying water pool makes no difference as to the predicted extent of debris spreading. Thus, the same initial spreading area has been used for the case with drywell sprays.

As discussed in Section 3.3, the composition of the initial pour directed into the expedestal region at 372 min is 99% (by mass) of the Fe, Cr, and Ni, 89% of the Zr, and 20% of the oxides leaving the failed reactor vessel. The metals-rich composition is based upon the temperature of the debris as it leaves the failed reactor vessel. During the initial 143 minutes (372-515 min) of the first spread into the expedestal region, the metallic portion of the pour from the reactor vessel is molten [ $>2750^{\circ}\text{F}$  (1783 K), see Fig. 3.4(b)] and superheated, while the oxidic portion of the flow is frozen [ $<4350^{\circ}\text{F}$  (2672 K)]. Accordingly, it is assumed that 80% of the oxide pour is kept inpedestal while 20% is spread expedestal. For the superheated metals, it is assumed that 1% is kept inpedestal due to adhesion upon the surface of the frozen oxides. An exception is made for the zirconium metal to approximate its eutectic combination with  $\text{UO}_2$  by keeping an additional 10% of the zirconium metal inpedestal.

After time 515 min, however, the oxide pour from the vessel is molten as well as the metals. From this time until the end of the calculation at 750 min, the apportionment of the predicted vessel debris pour is made strictly according to the respective floor areas; thus, 23% of all debris pour is kept inpedestal and 77% is introduced into the expedestal region.

Table 5.3 presents the debris configurations both before and after debris spreading into the remaining expedestal floor area at 602 min. The timing of this second spread is much later than that of the dry case presented in Chap. 4 (378 min) and is due to the enhanced cooling provided by the overlying water pools created by the sprays.

As shown in Table 5.3, the average temperatures of the metal and oxide layers for both the inpedestal and expedestal debris are well below their respective solidus temperatures and one might expect that the layers are frozen. However, CORCON calculates crusting for the individual layers so that the interior temperature of the layer can be above the solidus temperature while the average temperature of the crusted regions of the layer can fall well below the solidus temperature. This is the situation shown in Table 5.3.

To further clarify this situation, the configurations of both the inpedestal debris and the expedestal debris are shown in Fig. 5.5 at three distinct times. These debris maps were constructed from the calculated results of the first expedestal debris calculation (covering 800 ft<sup>2</sup> expedestal) initialized at time 372 min. The purpose of these maps is to provide information concerning the spreadability of the debris so that an estimate of the timing of the final spread onto the remaining 300 ft<sup>2</sup> of the drywell floor can be made.

As shown at time 500 min, the inpedestal debris is calculated to have a thick metallic layer (10.2 in.) overlying a thick (14.2 in.) oxidic debris layer. Furthermore, the metallic debris is calculated to be completely frozen (shown by crosshatching) while the oxidic debris (mainly below the original floor) is calculated to have an upper crust of 1.6 in. and a lower crust of 2.0 in. The expedestal debris is calculated to have the oxides overlying the metals with a relatively thin upper oxide crust of 0.4 in. and no lower oxide crust. Again, the metal layer is completely frozen (9.8 in.). Because the inpedestal debris is completely frozen above the level of the floor, and because a substantial height (3.5 in.) of debris above the expedestal floor is also frozen (crusted), it was judged that further debris spreading would not occur at this time.

At 702 min however, (bottom of Fig. 5.5) it is seen that the inpedestal metals have become partially molten so that 5.9 in. of metals are molten with only 3.5 in. remaining frozen. This molten metal together with 5.2 in. of molten oxide results in a molten mass of debris 11.1 in. thick lying above the original level of the floor. Meanwhile, the expedestal debris consists of 13.8 in. of molten oxides above the original floor level in addition to a thick (10.2 in.) frozen metallic layer, which, by this time, has sunk below the original floor level. It is believed that debris in this configuration would readily flow over the remainder of the expedestal floor and that therefore, actual debris spreading over the remaining floor area would have occurred sometime between 500 min and 702 min.

The debris configurations at 602 min are shown in the central portion of Fig. 5.5. It is seen that considerable melting of the inpedestal metals has occurred (4.6 in.). In addition, 3.2 in. of the molten oxides extend above the floor level so that a total of 7.8 in. of molten debris exists above the floor in the inpedestal region. For the expedestal region, 9.8 in. of molten oxides overlay 10.4 in. of frozen metals. With the debris in this configuration, it was decided that the

debris would flow, and thereby the time of the final debris spread into into the remaining 300 ft<sup>2</sup> (27.9 m<sup>2</sup>) of the expedestal floor was selected to be 602 min.

Selected CONTAIN results are shown in Fig. 5.6, which is a composition of the results from three calculations. The first calculation covers the period from 255 to 372 min when the debris/concrete interaction is occurring only in the inpedestal region. The second covers the period of the initial debris spread into the expedestal area [800 ft<sup>2</sup> (74.3 m<sup>2</sup>)] from 372 to 602 min. The third CONTAIN calculation concerns the period 602 to 750 min, after the debris has spread completely around the drywell floor.

As mentioned above, the third CONTAIN calculation was terminated at 750 min. It had been intended that this calculation be extended to 900 min as in the dry case, but difficulties in code execution made this impossible. These difficulties were associated with the execution of the CORCON module for the inpedestal debris/concrete interaction and are discussed more fully in Chapter 7.

The expedestal debris temperatures are shown in Fig. 5.6a where it is seen that the initial temperatures rapidly fall so that the metals are well below their solidus temperature and are thus frozen. The oxides overlies the metals and their temperature is somewhat below the metal layer temperature.

The oxide solidus temperature is 2574°F (1685 K) and is lower than the solidus temperature of the metals [2694°F (1752 K)]. The reason for the lower oxide solidus temperature is the dilution of the oxides poured from the reactor vessel by the low melting temperature oxides arising from concrete ablation (Tablation = 1503 K). As a result, the expedestal oxides are partially molten with crusts predicted at the interface with the water (see Fig. 5.5).

Because the expedestal oxides overlies the metals, they are equilibrated directly with the incoming hot debris from the reactor vessel. Thus, the oxide layer temperature is sensitive to the rate of debris addition to the expedestal floor area. This is the reason for the drop in oxide layer temperature at 400 min when the debris pour from the failed reactor vessel sharply decreases (Fig. 3.4a).

At 550 min, the metal and oxide layer temperatures take a sharp turn downward. This corresponds to the exhaustion of the expedestal zirconium and the reduction in chemical power, which is shown in Fig. 5.6b with its magnitude contrasted with that of decay heat. It is seen that the early expedestal chemical power is from 10 to 20 times that of decay heat and is obviously the controlling factor in debris temperature.

It is also interesting to note that the zirconium inventory in the expedestal debris lasts much longer for the wet case, Fig. 5.6b, than for the dry case, Fig. 4.6d. The reason for this is the lower maximum

debris temperatures of the wet case [2583°F (1690 K)] Fig. 5.6a, compared to the dry case [2706°F (1759 K)] Fig. 4.6c, and therefore, the lower concrete ablation rate. With less ablation, there is less gas (CO<sub>2</sub> and H<sub>2</sub>O) released into the debris and less chemical power produced by Zr reaction with the gas. Therefore, the expedestal Zr inventory lasts for almost 3 h in the wet case while lasting only about 1 h for the dry case. This also explains why the debris temperature remain elevated [ $>2500^{\circ}\text{F}$  (1644 K)] for a longer period in the wet case vs the dry case.

As was the case for the dry case calculations reported in Chap. 4, no conclusion regarding the continued integrity of the drywell shell pressure boundary can be reached without additional calculations to determine the thermal response of the shell. Although the predicted debris temperatures are clearly not high enough to cause shell melt-through, failure of the shell pressure boundary through loss of strength is possible. A detailed thermal and stress analysis should be performed for the drywell shell throughout the region of contact with the hot debris to address this issue. It is for this purpose that the time-dependent debris conditions in the expedestal region together with the internal pressure loading of the drywell shell as calculated in this study are provided in Table 5.4. In particular, this detailed information pertaining to the calculated conditions at the interface during the period of elevated debris temperature is intended for use by interested parties who desire to perform shell response calculations with codes such as HEATING-6 or TAC-2D.

The calculated drywell pressure is shown in Fig. 5.6c. Although steam condensation is extensive as a result of the sprays in the lower drywell expedestal cells, there is a continuing buildup of non-condensable gases (H<sub>2</sub>, CO, and CO<sub>2</sub>) originating from the debris/concrete interaction. These gases are released throughout the calculation and would continue to be released from the debris after the calculation is terminated at 750 min. Thus, even though the assumed containment failure pressure of 175 psia (1.207 MPa)<sup>5</sup> is not reached during the course of these calculations, there is reason to believe loss of the containment pressure boundary due to overpressurization would eventually occur if not precluded by prior failure by other means.

On the other hand, it does appear that sprays would effectively preclude thermal degradation of the drywell head flange seals. As shown in Figs. 5.1 to 5.4, atmosphere temperatures remain well below the seal failure temperature of 730°F (661 K). This contrasts with the dry case, where atmosphere temperature does become high enough to fail the seals. This is important because upon seal failure, primary containment gases and aerosols have a short path to the refueling bay and the external environment. Without seal degradation, failure of the primary containment pressure boundary would occur lower in the drywell or in the wetwell airspace and would pass gases and aerosols into the secondary containment, probably into the torus room. In this way, the residence time of these gases and aerosols would increase substantially and would allow considerable aerosol deposition and retention in the secondary containment.

Cumulative gas releases from both the debris and the concrete are provided in Table 5.5 for the end of calculation at 750 min. As seen, debris cumulative gas release amounts to 689 lb-moles ( $3.13 \times 10^5$  gr-moles) and is less than one half the debris release for the dry case discussed in Chap. 4. [Dry case debris gas release at 750 min is 1419 lb moles ( $6.44 \times 10^5$  gr-moles)]. This reduction in debris gas release for the wet case is due to a reduction in calculated concrete ablation because of enhanced heat transfer to the overlying water pool. Figure 5.6d reports the reactor pedestal ablation as a function of time; only 0.25 ft of the pedestal thickness is eroded by the end of the calculation at 750 min compared to ~0.9 ft being eroded at the same time for the dry case shown in Fig. 4.6b. Thus, it appears that sprays significantly reduce calculated pedestal erosion under the conditions of this study.

The pressure suppression pool is heated throughout the period of the calculation both by the decay heat energy release of the fission products trapped in the pool and by the passage of hot gases from the drywell into the pool whenever the drywell pressure rises sufficiently above the wetwell pressure to force gas flow through the downcomers. The BWRSAR calculation provides the estimate that pool fission product heating is 10.74 Mw at time 255 min, when the CONTAIN calculation is initiated; this value is used in the CONTAIN calculation until time 372 min, at which point the value is decreased to 9.83 Mw for the remainder of the calculation.

The pressure suppression pool temperature at the end of the calculation is 235°F (386 K); however, since the wetwell pressure at that time is 83.4 psia (0.575 MPa), which corresponds to a saturation temperature of 315°F (430 K), the pool has remained subcooled throughout the calculation.



Table 5.1. Gas flow distribution in primary containment for Peach Bottom Station Blackout with ADS actuation for limestone common sand concrete and drywell sprays at various times during the accident sequence

(Flows in lbm/min and time is in minutes after accident initiation)

Path <sup>a</sup>	Times			
	265.0 <sup>b</sup>	372.0 <sup>c</sup>	602.0 <sup>d</sup>	750.0 <sup>e</sup>
FLO12	371	888	48	48
FLO16	-371	-882	277	445
FLO23	1383	1745	932	-50
FLO25	-1009	-857	-882	95
FLO34	1384	1818	974	-16
FLO45	1409	1735	876	-7
FLO47	424	80	-327	358
FLO49	-503	-77	277	-314
FLO56	413	884	-5	-359
FLO610	0	0	0	0
FLO612	0	6	0	427
FLO78	373	23	-376	335
FLO79	63	57	56	3
FLO89	405	21	-356	322
FLO810	0	0	0	0

<sup>a</sup>Path definitions follow from the order of the indices in the path name. For path FLOIJ, the flow is from cell I to cell J if the tabulated flow is positive and from J to I if the tabulated flow is negative. See Figure 4.1 for primary containment nodalization.

<sup>b</sup>10 minutes after reactor vessel bottom head penetration failure at 255 min and immediately before inpedestal CORCON initialization.

<sup>c</sup>Immediately before 1st debris spread into expedestal area.

<sup>d</sup>Immediately before 2nd debris spread into expedestal area.

<sup>e</sup>End of CONTAIN calculation.

Table 5.2 Debris configurations before and after spreading at time 372 min. for Peach Bottom Short-Term Station Blackout with ADS actuation and drywell sprays.

BEFORE SPREADING  
INPEDESTAL ONLY (322 ft<sup>2</sup>)

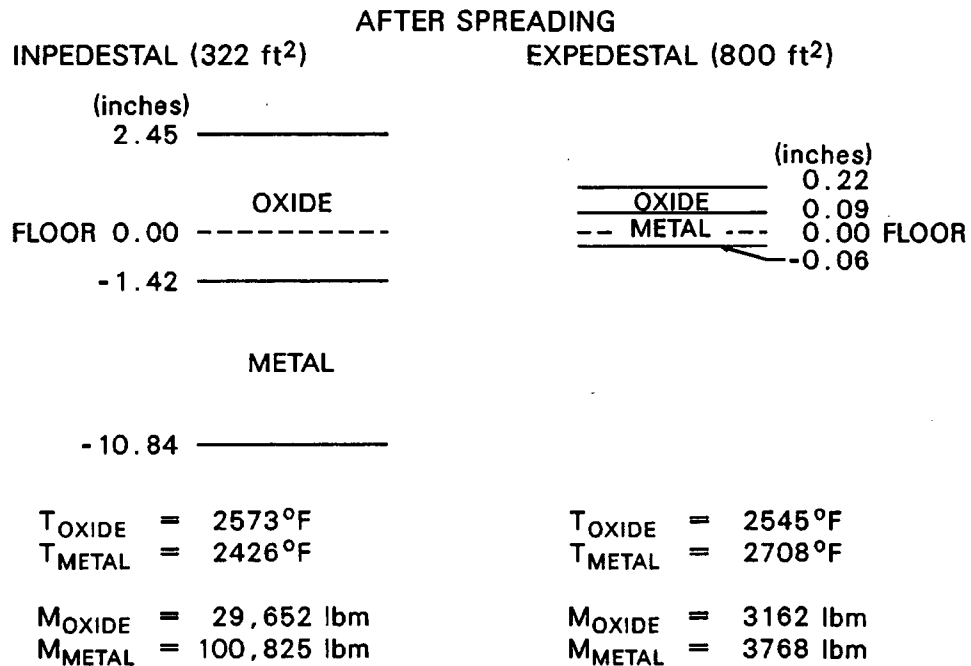


Table 5.3. Debris configurations before and after second expedestal region spread at time 602 min for Peach Bottom Short-Term Station Blackout with ADS actuation and drywell sprays.

BEFORE SECOND EXPEDESTAL SPREAD:

INPEDESTAL (322 ft <sup>2</sup> )		EXPEDESTAL (800 ft <sup>2</sup> )	
(inches)			(inches)
13.63	_____	_____	12.94
	METAL	OXIDE	
3.64	_____	=====	1.30
FLOOR 0.00	-----	METAL	0.00 FLOOR
	OXIDE	_____	-9.07
-14.63	_____		
T <sub>OXIDE</sub> = 3083°F	T <sub>SOLIDUS OXIDE</sub> = 3104°F	T <sub>OXIDE</sub> = 2432°F	T <sub>SOLIDUS OXIDE</sub> = 2562°F
T <sub>METAL</sub> = 2405°F	T <sub>SOLIDUS METAL</sub> = 2685°F	T <sub>METAL</sub> = 2451°F	T <sub>SOLIDUS METAL</sub> = 2716°F
M <sub>OXIDE</sub> = 203,206 lbm		M <sub>OXIDE</sub> = 239,067 lbm	
M <sub>METAL</sub> = 104,968 lbm		M <sub>METAL</sub> = 297,621 lbm	

AFTER SECOND EXPEDESTAL SPREAD:

INPEDESTAL (322 ft <sup>2</sup> )		EXPEDESTAL (1100 ft <sup>2</sup> )	
(inches)			(inches)
11.44	_____	_____	9.89
	METAL	OXIDE	
2.12	_____	=====	1.11
FLOOR 0.00	-----	METAL	0.00 FLOOR
	OXIDE	_____	-9.08
-14.63	_____		
T <sub>OXIDE</sub> = 2853°F		T <sub>OXIDE</sub> = 2456°F	
T <sub>METAL</sub> = 2848°F		T <sub>METAL</sub> = 2456°F	
M <sub>OXIDE</sub> = 191,553 lbm		M <sub>OXIDE</sub> = 250,817 lbm	
M <sub>METAL</sub> = 98,951 lbm		M <sub>METAL</sub> = 303,640 lbm	

Table 5.4. Expedestal debris conditions for Peach Bottom Short Term Station Blackout  
with ADS actuation, limestone common sand concrete, and drywell sprays

Time (min)	Z <sub>bot</sub> (in.)	Z <sub>MET/LOX</sub> (in.)	Z <sub>LOX/ATM</sub> (in.)	Mass metals (lb)	T <sub>METALS</sub> (°F)	T <sub>SOLIDUS METALS</sub> (°F)	LOX-mass light oxides (lb)	T <sub>LOX</sub> (°F)	T <sub>SOLIDUS (LOX)</sub> (°F)	Drywell pressure (psia)
372	-0.06	0.09	0.22	3,768	2708	2694	3,162	2545	2945	40.5
373	-0.13	0.07	0.27	4,815	2707	2695	4,322	2479	2742	40.6
374	-0.24	0.03	0.37	7,032	2643	2695	6,555	2614	2637	40.9
375	-0.34	0.04	0.49	9,644	2616	2695	8,616	2582	2612	41.1
376	-0.43	0.05	0.62	12,520	2605	2695	10,630	2580	2601	41.3
377	-0.52	0.09	0.76	15,610	2600	2694	12,610	2579	2595	41.6
387	-1.29	0.71	2.33	53,030	2589	2695	30,110	2573	2578	50.2
397	-1.93	1.79	4.17	99,590	2587	2695	44,320	2573	2574	54.7
407	-2.45	2.81	5.84	142,300	2590	2697	56,630	2545	2578	58.8
417	-2.95	2.63	6.22	151,800	2588	2704	66,670	2500	2569	60.3
427	-3.43	2.42	6.56	160,300	2582	2711	76,100	2507	2562	61.5
437	-3.89	2.30	6.95	170,900	2576	2718	84,880	2511	2556	63.0
447	-4.33	2.26	7.38	183,100	2571	2724	93,050	2510	2550	64.3
457	-4.75	2.27	7.85	196,500	2566	2729	100,600	2507	2544	65.5
467	-5.15	2.37	8.38	211,900	2562	2735	107,700	2508	2539	66.7
477	-5.53	2.62	9.03	231,300	2557	2740	114,200	2510	2534	68.0
487	-5.89	3.08	9.86	256,200	2551	2745	120,100	2515	2526	68.9
497	-6.22	3.40	10.53	275,100	2550	2746	126,100	2509	2526	69.3
507	-6.55	3.54	11.03	286,800	2552	2738	132,100	2504	2525	69.7
517	-6.88	3.57	11.44	297,400	2557	2715	139,300	2490	2525	70.0
527	-7.20	3.36	11.85	300,700	2560	2714	155,600	2486	2546	67.8
537	-7.52	3.13	12.21	302,800	2566	2714	170,600	2503	2559	66.3
547	-7.84	2.75	12.46	301,300	2574	2714	187,600	2519	2575	65.3
557	-8.16	2.39	12.66	300,200	2543	2714	201,700	2530	2577	64.6
567	-8.42	2.07	12.76	299,500	2517	2715	213,300	2520	2574	63.9

T<sub>SOLIDUS</sub> = Mixture temperature at which melting begins

LOX = Light oxides

HOX = Heavy oxides

Z = Elevation relative to original floor surface

MET/LOX = metal - light oxide interface

LOX/ATM = light oxide - atmosphere interface

Table 5.5 Cumulative gas release at  
 termination of calculation for  
 Peach Bottom Station Blackout  
 with ADS actuation and  
 drywell sprays  
 Time 750 min.

	lbs	lb-moles
<hr/>		
Gas release from concrete		
CO <sub>2</sub>	15,086	756
H <sub>2</sub> O	<u>5,228</u>	<u>640</u>
	20,314	1,396
Gas release from debris surface		
CO <sub>2</sub>	13	1
H <sub>2</sub> O	18	2
CO	626	49
H <sub>2</sub>	<u>582</u>	<u>637</u>
	1,239	689
<hr/>		

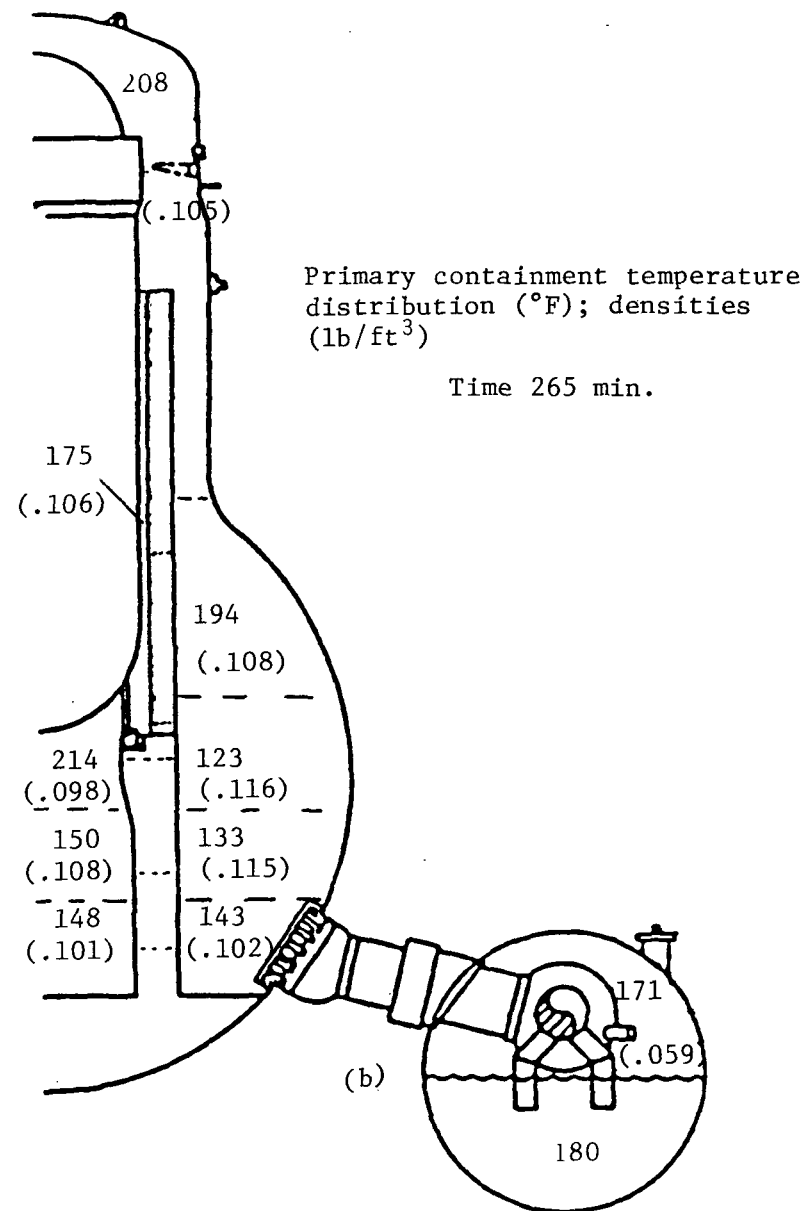
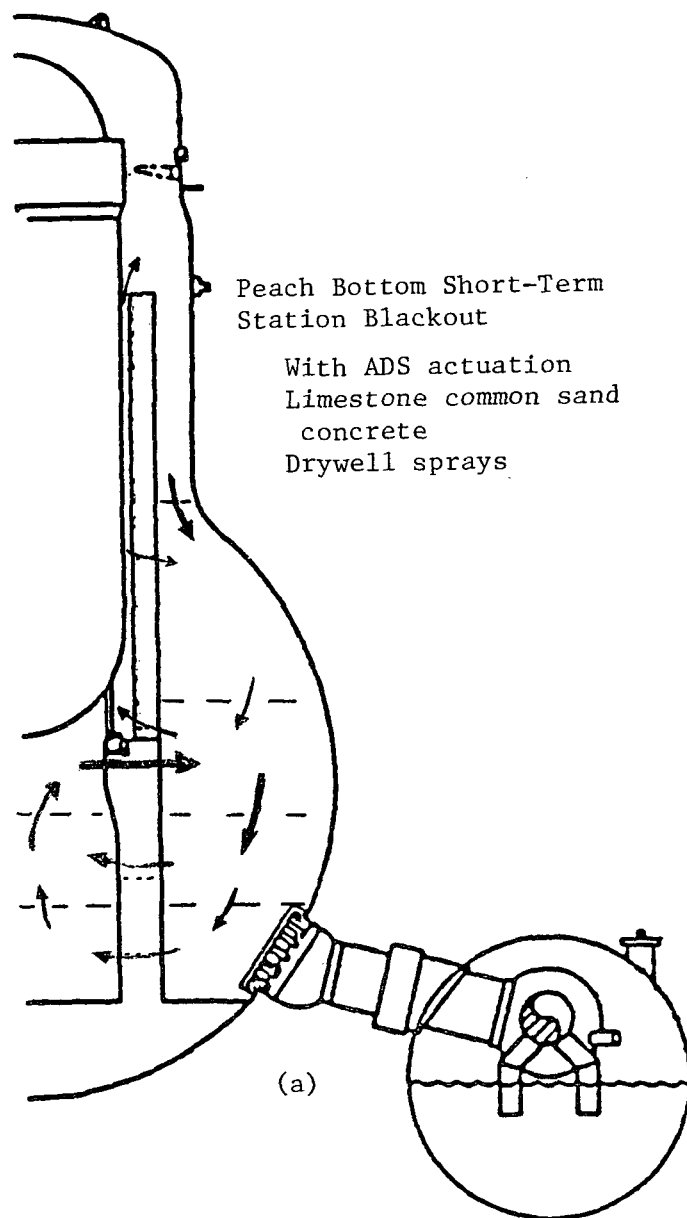


Fig. 5.1. Drywell intercell flows, cell temperatures, and densities as predicted by CONTAIN at 10 minutes after reactor vessel bottom head penetration failure and just before the inpedestal CORCON calculation is initiated.

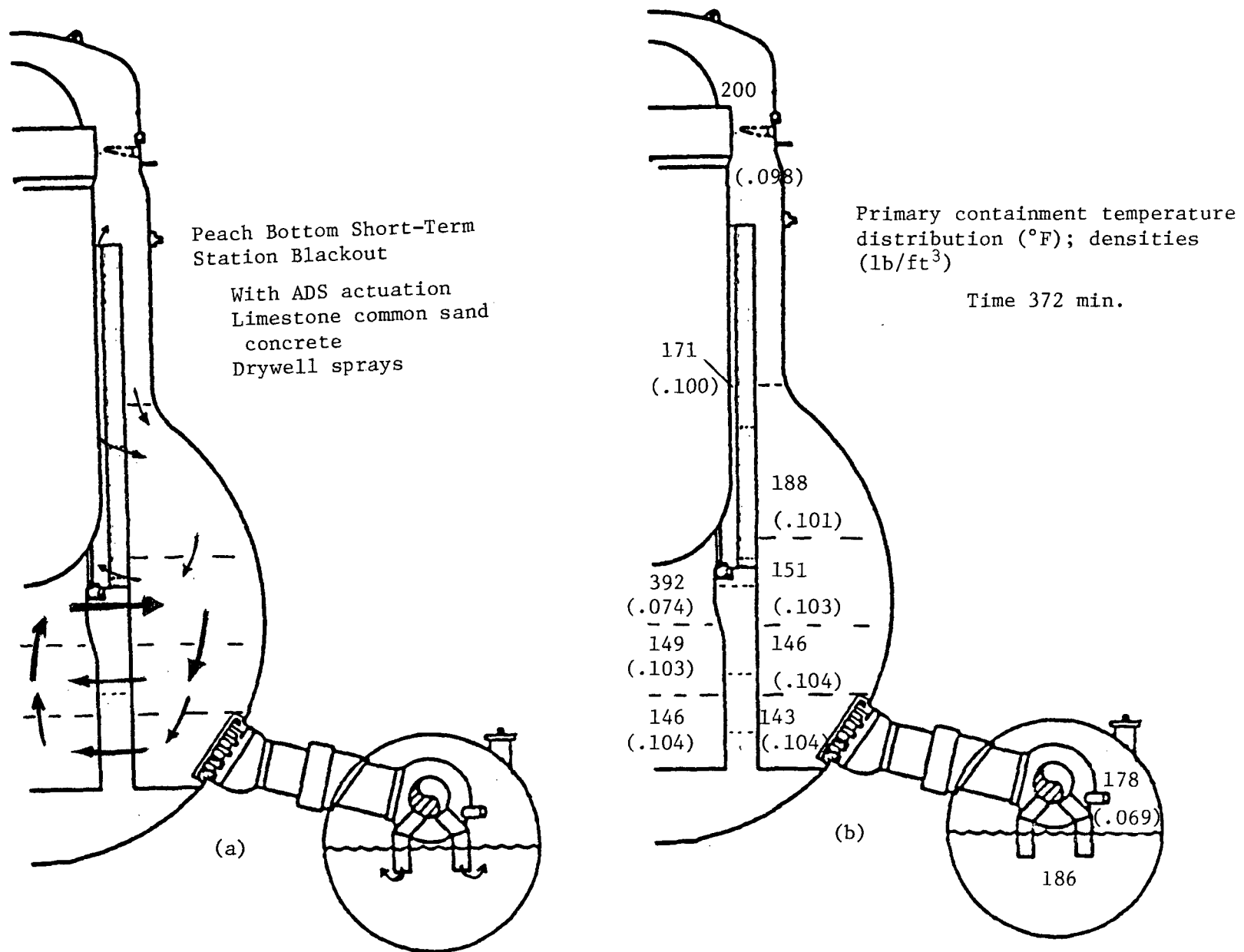


Fig. 5.2. Drywell intercell flows, cell temperatures, and densities as predicted by CONTAIN just before initial debris spread into expedestal region.

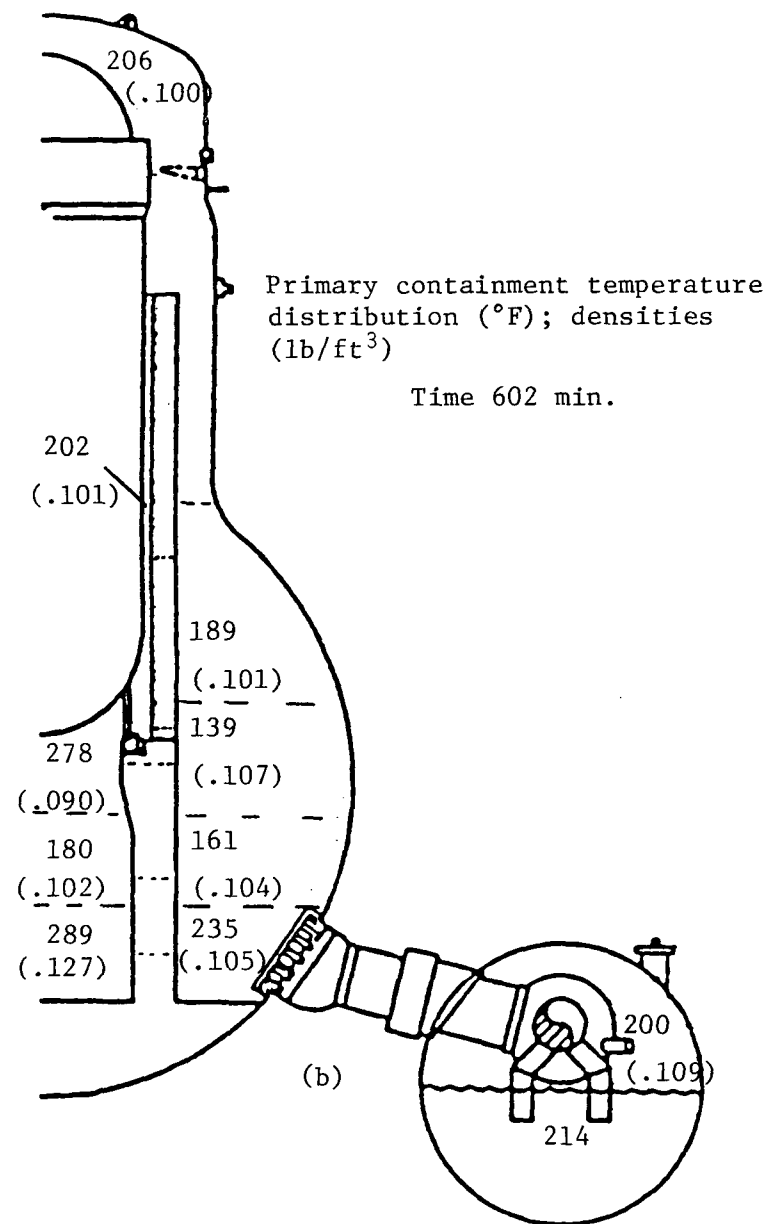
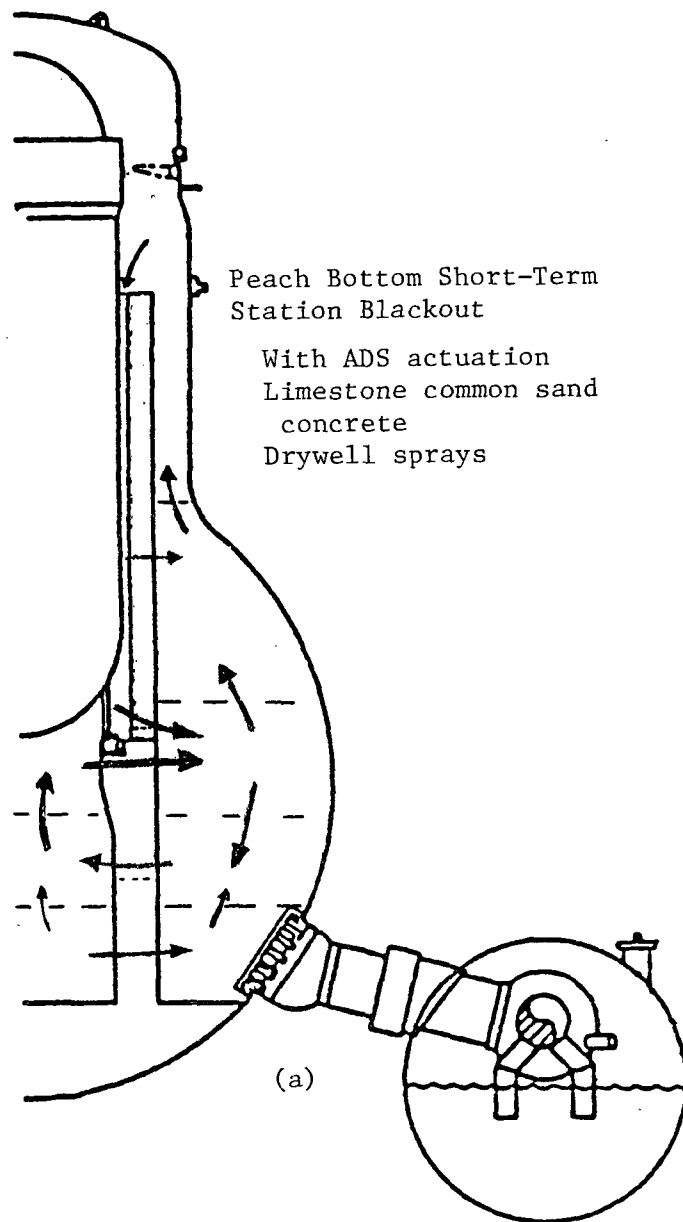


Fig. 5.3. Drywell intercell flows, cell temperatures, and densities as predicted by CONTAIN just before second debris spread into expedestal region.



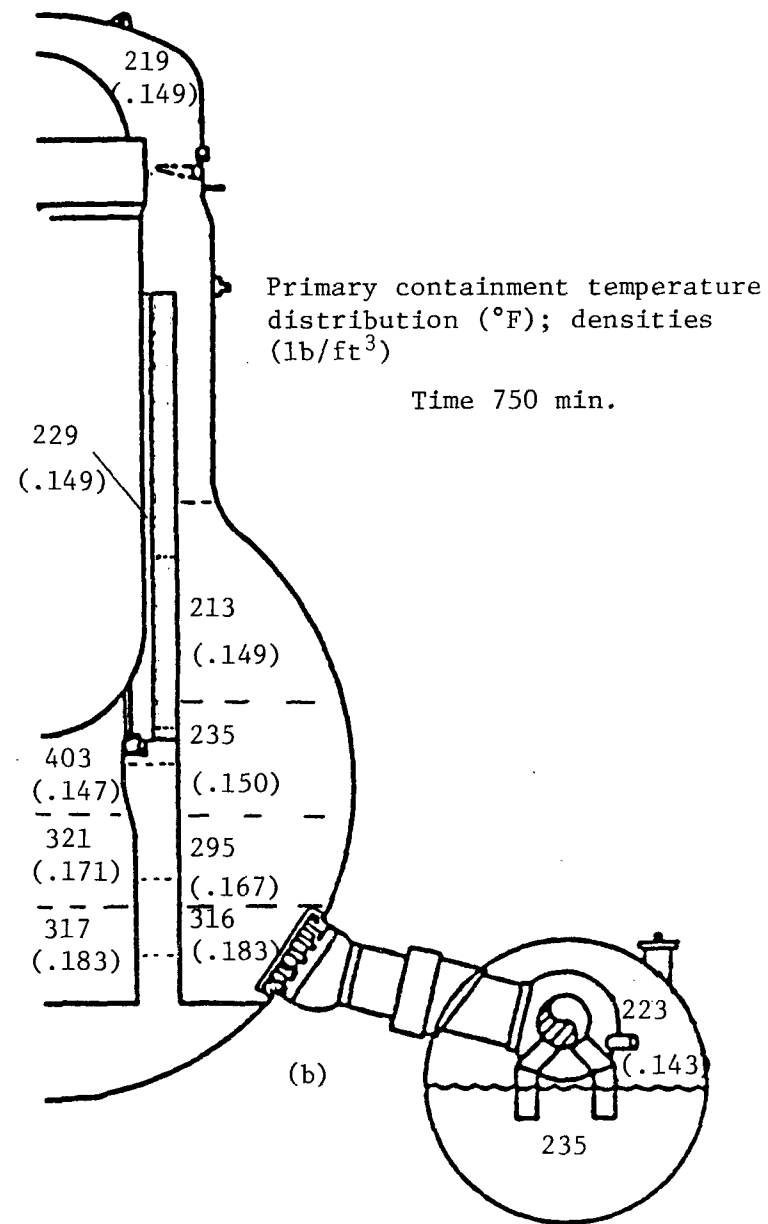
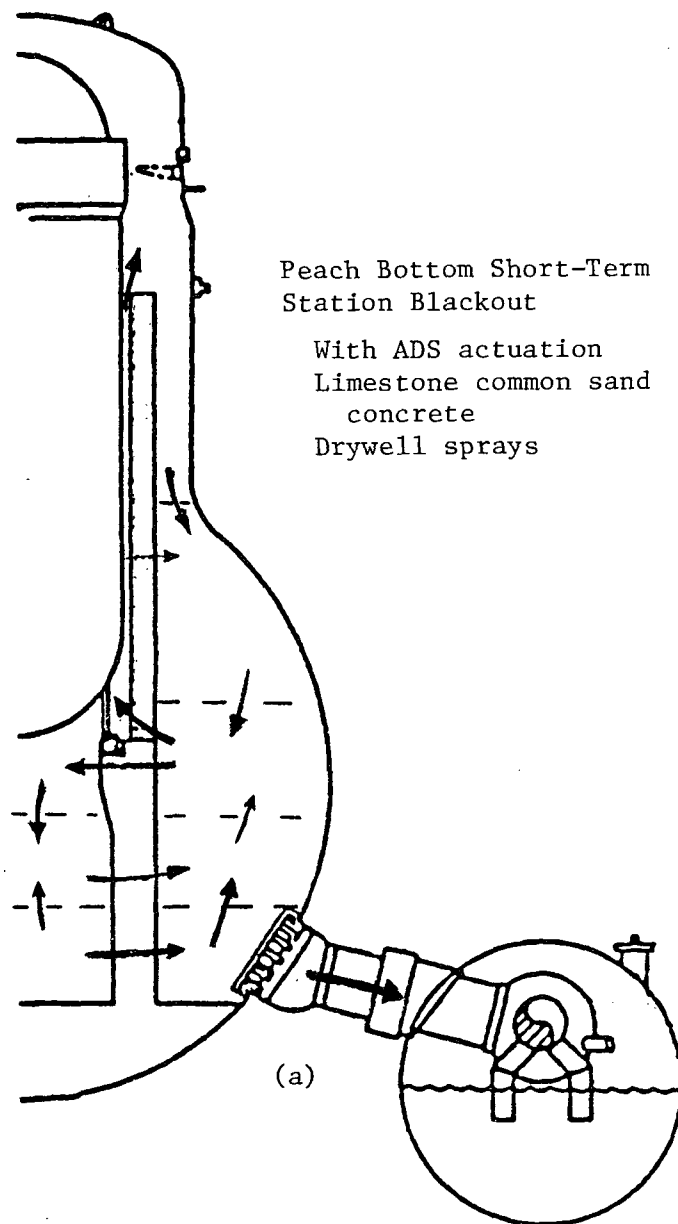


Fig. 5.4. Drywell intercell flows, cell temperatures, and densities as predicted by CONTAIN at end of calculation.

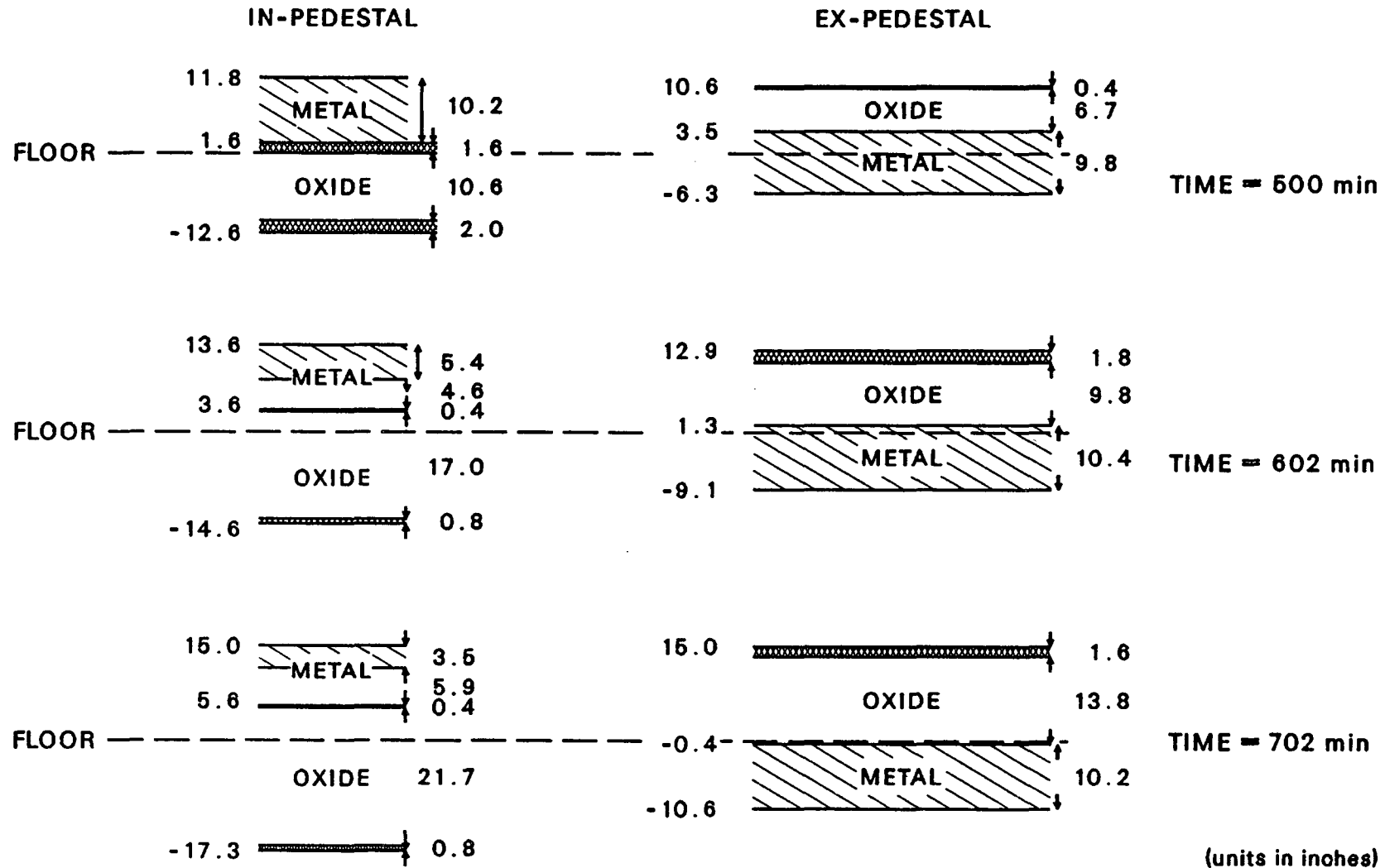
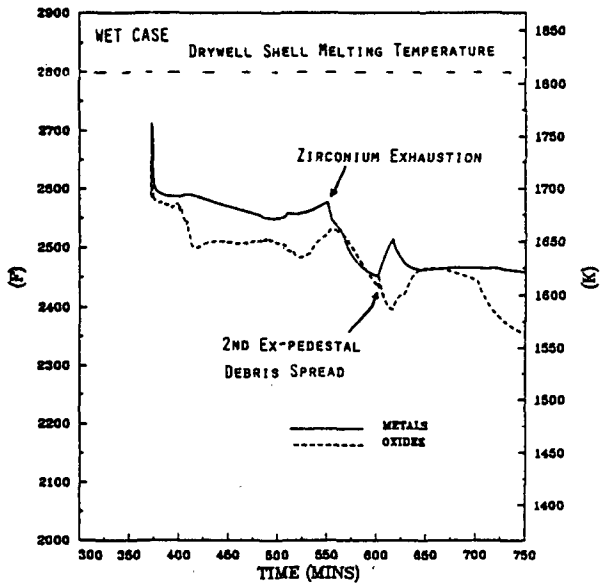


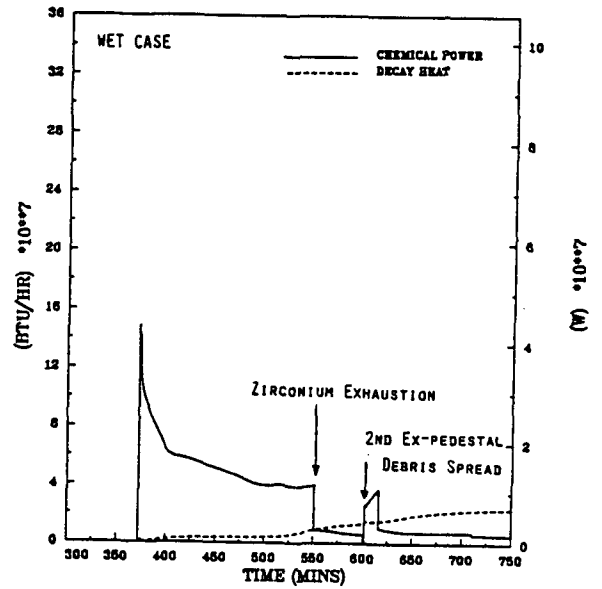
Fig. 5.5. Wet case debris configurations (inpedestal and expedestal) at three times during period of initial debris spreading onto the expedestal floor (800 ft<sup>2</sup> covered). Numbers on left of figures denote debris layer interface locations relative to original floor level, while numbers on the right denote the thicknesses of the molten and crusted portions of each layer.

EX-PEDESTAL DEBRIS TEMPERATURES



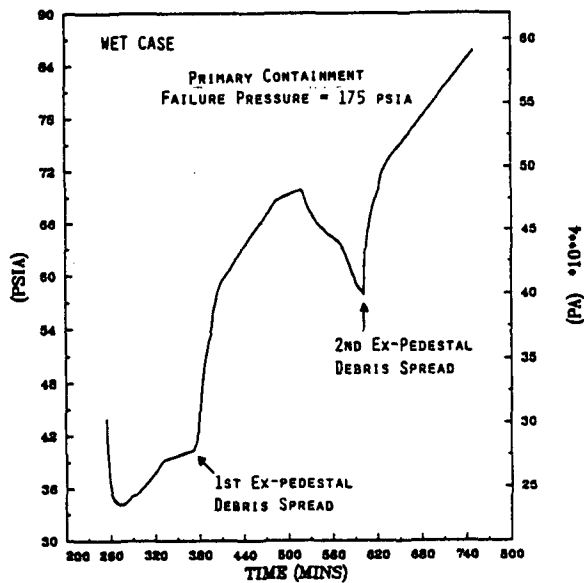
a

EXPEDISTAL ENERGY SOURCES



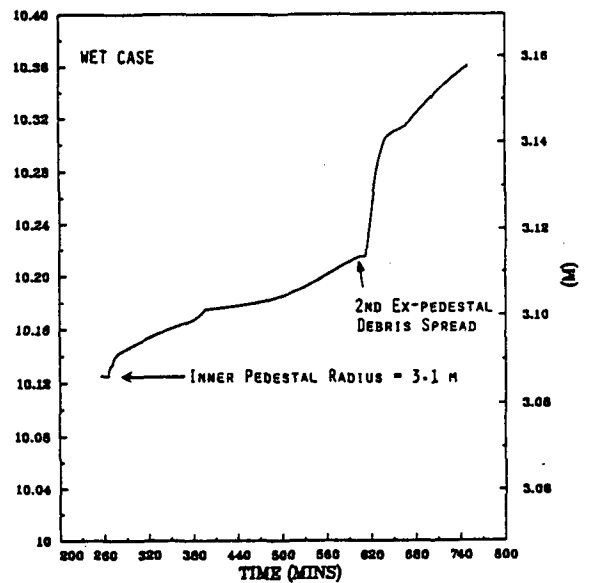
b

GAS PRESSURE - CELL 8



c

MAXIMUM CAVITY RADIUS CELL 1



d

Fig. 5.6. Selected parameters relative to maintenance of drywell shell pressure boundary integrity for Peach Bottom Short-Term Station Blackout with ADS actuation. The first spread of debris into the ex-pedestal region occurs at time 372 minutes. The floor is modeled as limestone common sand concrete with overlying water.



## 6. SUMMARY OF RESULTS AND DISCUSSION OF CONCLUSIONS

Calculations with the BWSAR and CONTAIN codes have been carried out for the Peach Bottom Short-Term Station Blackout accident sequence with ADS actuation. The reactor vessel is assumed to be depressurized when water level indication is lost, in accordance with the BWR Owners Group Emergency Procedure Guidelines.

Short-Term Station Blackout Without Depressurization and Short-Term Station Blackout with ADS Actuation differ importantly in the amount of calculated zirconium oxidation within the reactor vessel. It should be recognized that an unmitigated severe accident sequence would ultimately result in oxidation of all of the initial inventory of zirconium metal. The only question that might be resolved by these calculations is to determine how much would occur in-vessel and how much would occur on the drywell floor. The relative amounts may have important consequences. For example, if a venting strategy were employed, the early (in-vessel) hydrogen releases might be shunted around the reactor building; the associated reduction of hydrogen burns in the secondary containment structure would increase the potential of this building to mitigate fission product transport by aerosols after the onset of the core debris-concrete interaction on the drywell floor and failure of the drywell shell pressure boundary.

For the Short-Term Station Blackout accident sequence considered in this report, manual actuation of the ADS valves in accordance with the BWR Owner's Group Emergency Procedure Guidelines causes almost immediate core plate dryout, but the associated steam cooling of the upper core delays the initial melting of core structural material and the onset of core debris relocation. With the safety/relief valves opened at time 80 minutes after scram, when the reactor vessel water level is 44 inches (1.12 m) above the bottom of the core, debris relocation is predicted to begin at time 132 minutes.

Since the relocating molten debris falls upon a dry core plate, core plate heatup is rapid and initial core plate failure occurs almost immediately thereafter. The large amount of water in the reactor vessel bottom head is slowly boiled away by the structural debris that falls through the failed portions of the core plate, providing steam to the core region, where accelerated metal-water reaction occurs as a result. Bottom head dryout is hastened by the relocation of fuel, which occurs at time 223 minutes, when the  $ZrO_2$  sheath remnants of the original cladding in the central regions of the core have become too weakened by overheating to continue to support the local fuel pellet stacks. Bottom head dryout is predicted to occur at time 255 minutes, and the first penetration failure occurs immediately thereafter.

At the time of initial bottom head penetration failure, the bottom head debris is completely frozen, but the temperature is increasing under the impetus of decay heating. The assumed melting temperature of the metallic debris [2750°F (1783 K)] is reached eight minutes later so

that the initial pour from the reactor vessel begins at time 263 minutes. During the first period of debris pour, all of the pour is kept within the inpedestal region of the drywell while the sumps are being filled. Ablation of the initial floor and pedestal geometry increases the amount of pour required to raise the upper surface of the debris above the initial level of the drywell floor.

CONTAIN calculations of the primary containment response to reactor vessel bottom head penetration failure and the subsequent release of molten material from the reactor vessel have been carried out for two cases, differing with respect to assumptions made with regard to the availability of drywell sprays. For the first set of calculations, it was assumed that the containment sprays were not available. In this case, there is no water on the drywell floor at the time of bottom head penetration failure except for a small amount [3911 lbs (1775 kg)] predicted by the BWRSAR code to be present in the sump due to normal reactor vessel leakage. The CONTAIN calculation predicts this initial sump water to be quickly boiled away as the first debris enters the sump.

After about 112 minutes of debris pour for this dry case, the upper surface of the inpedestal debris is calculated to be slightly more than three inches (7.6 cm) above the initial level of the drywell floor and the temperature of the oxide layer surpasses its solidus temperature (see Table 4.3). At this point, the initial calculation is stopped and the debris is relocated as necessary to represent spreading into the expedestal area of the drywell floor. The area covered by this initial debris spread is 800 ft<sup>2</sup> (74.3 m<sup>2</sup>) and was estimated by a method proposed by Kazimi.<sup>8</sup> The length along the drywell shell contacted by this initial spread is about 100 ft (30 m) and is centered directly opposite the doorway in the reactor pedestal. After this first spread into the expedestal region at time 375 minutes, the debris height in both the inpedestal and expedestal regions is approximately one inch (2.5 cm). Subsequently, the debris levels in the inpedestal and expedestal regions increase as the additional pours from the reactor vessel are apportioned between the regions.

Metals comprise about 58% of the initial debris in the expedestal region, as indicated in Table 4.3. However, by the end of the calculation at 900 min the fraction of metals in the expedestal debris inventory is only 39%. The reason for this dilution of the metals is two-fold. First, during the period 375 to 900 min, 53% of the debris added to the drywell floor from the reactor vessel is oxidic (mainly UO<sub>2</sub> and ZrO<sub>2</sub>), and second, concrete oxides (SiO<sub>2</sub> and CaO) are added to the expedestal oxide layer as a result of concrete ablation. At the end of the calculation, there is a thick 15.6 in (0.396 m) oxide layer overlying a 9.6 in (0.243 m) thick metal layer. The height of the debris above the original floor is 12.3 in (0.312 m) while the depth of concrete ablation into the floor is 12.9 in (0.327 m).

The calculated expedestal debris temperatures for the dry case are shown in Fig. 4.6c. The maximum temperature occurs in the metal layer at 418 min and is 2706°F (1759 K). This maximum occurs during the

initial 60 min of expedestal debris/concrete interaction when debris temperatures are elevated due to the chemical energy release provided by zirconium oxidation. After zirconium exhaustion at 435 min, the expedestal debris temperatures fall rapidly.

Although dry case expedestal debris temperatures do not reach the melting temperature of the carbon steel drywell shell [2800°F (1810 K)], one cannot conclude that the drywell shell will not fail. This is because of the loss of strength of the steel shell at elevated temperatures and the simultaneously increasing drywell pressure. More detailed thermal and stress analysis should be performed for the region of debris/shell contact in order to more fully address this issue. It is for this purpose that the time-history (during the period most threatening to the shell) of the conditions at the debris shell interface as calculated by CONTAIN is provided in Table 4.6. This is the information necessary for the performance of shell response calculations with codes such as HEATING-6 or TAC-2D.

For this dry case calculation, it has been assumed that failure of the primary containment pressure boundary at the level of the drywell floor does not occur. As indicated in Fig. 4.6a, the drywell pressure is significantly reduced after failure of the drywell head flange seals caused by local high temperature at time 592 min. Subsequently, the pressure is predicted to be almost constant at 98 psia (0.676 MPa) as the drywell head lifts slightly and then reseats in response to gas releases and temperature increases within the drywell. It should be noted that gas release from the drywell by means of leakage through the drywell head flange directly enters the refueling bay and does not benefit by scrubbing processes within the reactor building. (Leakage through the drywell head flange would not be predicted, of course, if drywell pressure had previously been reduced by thermally induced failure of the shell at the floor.)

Another possible failure mechanism for the drywell shell pressure boundary involves collapse of the reactor vessel and biological shield caused by ablation of the reactor pedestal. For the calculations reported here, the thickness of the reactor pedestal is predicted to have been reduced from its original three feet (91.4 cm) to 2.13 feet (64.9 cm) at the termination of the calculation at time 900 min. However, since the weight supported by the reactor pedestal is much less than design conditions at this time, it seems reasonable to assume that collapse has not occurred.

Finally, the reactor vessel might topple within the reactor pedestal and biological shield if the vessel support skirt were weakened sufficiently by overtemperature. This possibility was examined during this study by developing a model of the skirt and calculating its temperature. As indicated in Fig. 4.8, the calculated skirt temperature at the end of the calculation is about 1700°F (1200 K), which is not sufficiently high to cause skirt collapse.

Thus, for the case without consideration of drywell sprays, the CONTAIN results indicate the following with regard to the threat posed to the integrity of the drywell shell pressure boundary:

- a) The predicted temperatures of the debris layers in the expedestal region are sufficiently high for a 60-minute period following the initial spread into the expedestal region at time 375 minutes that the shell may fail at the level of the floor due to overheating. This possibility should be examined by follow-on shell response calculations performed with HEATING-6 or TAC-2D. For this study, this failure mechanism was not modeled.
- b) If the shell pressure boundary at the floor does not fail due to direct thermal attack by debris, then the predicted containment pressure and the predicted temperature of the drywell head reach values at time 592 minutes at which, based on recent experiments at INEL, the drywell head flange seals would be expected to fail. Leakage from the drywell head flange after seal failure was modeled in these calculations.

As mentioned previously, CONTAIN calculations based upon the BWR SAR results discussed in Chap. 3. have also been performed for a case in which it is assumed that drywell sprays are available and are actuated. It is assumed that the existing spray header is used and therefore spray is directed only into cells 4, 5, and 6 (see Fig. 4.1). Spray droplet coalescence due to impact with drywell structures is accounted for by varying the input droplet size from 1 mm in cell 4 to 3 mm in cells 5 and 6. The spray flow rate is assumed to be 700 GPM (0.044 m<sup>3</sup>/s) and to have been initiated sufficiently before reactor vessel bottom head failure, such that the drywell floor is flooded to the point of overflow to the pressure suppression pool.

The source of the spray flow is assumed to be the condensate storage tank [Temp = 90°F (305 K)] while the debris pour from the reactor vessel fills the inpedestal region and during the initial spread into the expedestal regions. After the time of debris spreading around the entire periphery of drywell (602 min), the spray is assumed to be taken from the pressure suppression pool, and its injection temperature is that of the pool.

Calculated results for this wet case indicate a substantial reduction (compared to the dry case) in the atmosphere temperatures due to the sprays (Figs. 5.1 to 5.4). No drywell head flange seal degradation is predicted and no direct leakage of gas and aerosols into the refueling bay is indicated.

The pools formed by the collection of spray water on the drywell floor are calculated to have a substantial impact on the debris/concrete phenomenology. The CORCON calculation for the inpedestal area was begun at 265 min and debris was confined to this region of the drywell floor



until 372 min when, as predicted by the BWRSAR code, the second major debris pour from the reactor vessel is underway.

Table 5.2 presents the debris conditions both before and after initial debris spreading into the expedestal area of the drywell floor at 372 min. The temperatures of the inpedestal debris before spreading are such that the majority of the inpedestal debris is frozen and thus would not be able to flow into the expedestal area. However, the sumps are full and the height of the debris extends 2.8 in (7.1 cm) above the level of the drywell floor. In addition, the debris pour coming from the reactor vessel is increasing and is partially comprised of superheated liquid metals. All this information indicates probable movement of the additional debris into the expedestal area and as a result, the initial expedestal CORCON calculation was begun at this time.

The initial expedestal debris spread is slightly earlier for the wet case than the dry case (372 min vs 375 min) because of the reduced ablation of the concrete floor and reactor pedestal due to increased cooling provided by the overlying water pool. An indication of this reduced ablation can be seen by comparing Table 5.2 with Table 4.3. For the wet case at time 372 min, floor erosion results in the bottom of the debris being located at 10.8 in. (27.4 cm) below the original floor, while the dry case has floor erosion to a depth of 16.3 in. (41.4 cm) below the original floor level.

The effect of the overlying water pool is even more dramatic when considering the timing of the final debris spread around the remainder of the expedestal floor area [300 ft<sup>2</sup> (27.9 m<sup>2</sup>)]. For the dry case, this additional debris spreading is judged to occur very rapidly, i.e., at 3 min after the first debris spread at 375 min. The reason behind this is the accelerating debris pour from the reactor vessel and the continuing molten state (see Table 4.4) of the drywell floor debris.

For the wet case however, the debris remains frozen for a long period of time as shown in Fig. 5.5. Inpedestal and expedestal metal layers remain completely frozen at 500 min, a period of over 2 hours after the initial expedestal debris spread at 372 min. Gradual melting of the metal layer occurs from 500 to 602 min and combined with a thickening layer of partially molten oxides, the debris was judged to be spreadable into the remainder of the drywell floor at 602 min, a period of 3.8 hours after the initial spread into the expedestal area.

In addition to delaying the spreading of the debris completely over the drywell floor, calculated expedestal maximum temperatures for the wet case are lower than those of the dry case. The maximum temperature for the wet case is 2583°F (1690 K) compared to 2706°F (1759 K) for the dry, a reduction of 123 F° (68 K). In both cases, the maximum debris temperature is well below the carbon steel drywell shell melting temperature of 2800°F (1810 K).

Even though the maximum temperature for the wet case is less than that of the dry case, the expedestal debris temperatures remain elevated

for a longer period of time. This is because the zirconium in the expedestal region is consumed at a slower rate for the wet case compared to the dry case. This in turn is due to the slower rate of concrete ablation which follows from the lower debris temperature caused by the enhanced heat transfer to the overlying water pool. In the dry case, expedestal Zr exhaustion occurs after about an hour, whereas, wet case Zr exhaustion does not occur until almost 3 h after debris is spread into the expedestal area. Thus, expedestal wet case debris temperatures remain above 2500°F (1644 K) about 2 h longer than dry case expedestal debris temperatures.

As in the dry case, no conclusion can be reached for the wet case concerning the consequences of the threat to the drywell shell. Elevated debris temperatures persist for an extended period of time and drywell pressure continues to increase. Failure by loss of strength cannot be dismissed until detailed thermal and stress analyses are performed. For use in this endeavor, bulk debris conditions and drywell pressures for the 3 h period following initial debris/shell contact have been compiled for the wet case and are given in Table 5.4.

As further evidence of the mitigative effect of drywell sprays, cumulative gas release for the wet case amounts to 689 lb-moles vs 1419 lb-moles for the dry case at 750 min into the calculation. The reason for this is the reduced concrete ablation due to lower debris temperature which in turn is due to enhanced heat transfer to the overlying water pool. The reduction in concrete ablation can be seen by considering the calculated amounts of reactor pedestal erosion. For the dry case about 30% of the pedestal thickness is eroded, whereas, for the wet case, only about 8% of the pedestal thickness is eroded.

In conclusion, it appears that there is a high probability that primary containment integrity would be compromised for the unmitigated Peach Bottom Short-Term Station Blackout scenario occurring under the conditions assumed in this report. There are two distinct locations where the pressure boundary would be most likely to fail. First is the drywell shell at floor level for which the failure mechanism would be creep rupture induced by thermal attack by hot core debris. This failure is uncertain, however, since the results of this study indicate maximum expedestal debris temperatures less than the melting temperature of the carbon steel drywell shell. This is true both for the dry case and the wet case and is a consequence of dilution of the reactor vessel debris by concrete oxides released by ablation of the limestone common sand concrete. Detailed shell thermal response analyses are required in order to fully address this shell failure mechanism.

However, even if the drywell shell were to withstand the thermal loading imposed by the hot debris, it appears very likely that loss of pressure boundary would occur in the second failure location - the drywell head flange seals. For the dry case, calculated temperatures in the vicinity of the drywell head flange clearly exceed 730°F (661 K), the failure temperature observed in tests of seal material similar to that used for the drywell head. Because the debris/concrete interaction

continues to release gas into the primary containment, it is clear that if the shell failure does not occur at floor level, then drywell pressure will eventually increase to the point of leakage from the drywell head (leakage pressure for Peach Bottom is estimated to be 97 psia (0.669 MPa) with no seals and 175 psia (1.21 MPa) with fully intact seals). Drywell head leakage flow and subsequent gas and aerosol leakage would be into the refueling bay and therefore would have a relatively short path to the outside environment.

With consideration of the effect of addition of sprays in the wet case calculation, it appears that the threat to the drywell head flange seals can be effectively precluded. Also, the sprays and the associated water pools forming on top of the debris would scrub much of the aerosol content leaving the debris so that large reductions in aerosol emissions into the containment atmosphere would result. These two mitigative features in and of themselves make the availability of drywell sprays highly desirable.

The mitigative effect of sprays on the progression of the debris/concrete interaction is much more tenuous. Even though the current study results indicate that peak debris temperatures and concrete ablation rates are somewhat lower for the spray case than for the dry case, large uncertainties and deficiencies in the current calculational methodology make both the calculated results and comparisons of the calculated results questionable. Chapter seven identifies several current code limitations with respect to application to the BWR MK I containment response calculations discussed in this report and provides specific recommendations where it is believed that future resources toward resolution of this issue should be committed. It is clear that even though current tools such as BWRSAR, CONTAIN, and CORCON represent significant advancements in the state of the art for analysis of BWR severe accidents, much remains to be done.



## 7. RECOMMENDATIONS FOR FUTURE WORK

The purpose of this chapter is to discuss several recommendations for future work, based upon lessons learned from the current calculations and recognized limitations in the current versions of the codes from the standpoint of their application to BWR Mark I containment calculations.

### 7.1 Necessary Modeling Improvements

Although the advanced capabilities provided by CONTAIN Version 1.1 greatly improve the efficacy of the code for BWR severe accident applications, it is obvious that there are several remaining areas where the present capability must again be expanded if the code is to become adequate for BWR Mark I containment severe accident calculations in applications where core and structure debris have left the reactor vessel. Major areas include:

1. Representation of concrete degassing. Within the latest released version (1.1) of CONTAIN, none of the water vapor stored in the concrete is released unless and until the temperature of the overlying debris is sufficient to cause ablation. However, it seems reasonable to expect that the initial pours of molten core debris from a BWR reactor vessel in the unlikely event of a severe accident that progressed this far would be successive mixtures of metals at relatively low temperatures, in the range of 2100-2750°F (1420-1783 K). The spread of this initial debris over the floor of the Mark I containment drywell would be expected to cause a large release of water vapor and carbon dioxide from the concrete by means of heating, even though the temperature would not be high enough to induce concrete ablation. The degassing effect is important because the released gases pass into the core debris and cause additional energy release by means of the metal oxidation reactions.

The calculations discussed in this report were performed with an advanced version of CONTAIN provided to the BWRSAT Program at ORNL by the code development staff at SNL. This advanced version calculates the effects of concrete degassing during periods when the debris temperatures are not sufficiently high to cause concrete ablation. This can have a major impact upon the predicted containment response. The degassing models plus additional modifications made to the advanced version at ORNL permit the debris pours from the reactor vessel to be modeled much more realistically.

The debris pours predicted by BWRSAR for this study are based upon the assumption that the reactor vessel bottom head debris can be represented as a combination of a mixture of metals melting at 2750°F (1783 K) and a mixture of oxides melting at 4350°F (2672 K). With initial debris temperatures in this range, ablation

of limestone common sand concrete [ablation temperature 2246°F (1503 K)] continues throughout the dry case calculations of Chap. 4 and for most of the wet case calculations reported in Chap. 5. Therefore, for the most part, the degassing models are not exercised. This would not be true, however, for the case of high limestone concrete with its ablation temperature of 2694°F (1752 K); here concrete ablation would not be continuous and representation of the effects of degassing during periods of nonablation would be most important.

It is desirable that the CONTAIN code be further improved to provide accurate representation of the effects of concrete degassing ahead of the ablation front during periods of unsteady concrete ablation. Although the additional gas release due to accurate modeling of degassing during periods of rapidly increasing debris temperature may be only a fraction of the gas release due to ablation, there are significant periods of time during the present calculation when the metal oxidation reactions in the debris are predicted to be gas-starved. Therefore, any additional gas release from the concrete during these periods would be reflected in higher calculated metal oxidation rates and higher temperatures. It is recommended that these advanced degassing models be included in future released versions of CONTAIN.

2. Representation of debris melting. The algorithms for determination of the state of the debris components in the CORCON module of the current released version of CONTAIN are deficient for current BWR severe accident applications. Debris melting is characterized by a determination of solidus and liquidus temperatures applicable only to the vertically separated layer configuration assumed by the CORCON model. Within the metal layer, a tertiary phase diagram is used to determine the melting temperature of stainless steel according to the relative amounts of its constituent iron, nickel, and chromium. As long as stainless steel is present (there would be an enormous amount of stainless steel in BWR debris), the presence of zirconium metal is ignored and the melting temperature of the metal layer is set equal to the melting temperature of the stainless steel. In actuality, the zirconium metal would be expected to enter into the formation of a eutectic mixture with much of the stainless steel.

For the oxide layer, the  $ZrO_2$  and  $UO_2$  components are grouped as "fuel" oxides while the oxides created by concrete decomposition are treated separately. A simple phase diagram that provides a melting temperature for a  $ZrO_2$ - $UO_2$  mixture based upon the relative mole fractions is provided within the code for the fuel oxides. The composition and melting temperature of the fuel oxides is combined with that of the concrete oxides to determine the resulting solidus and liquidus temperatures of the oxide layer.

Difficulty arises with the simple CORCON phase representation for the  $ZrO_2$ - $UO_2$  mixture in that the lowest melting temperature on

the diagram is 4625°F (2825 K), which occurs at 56 mole percent  $\text{ZrO}_2$ . For example, if the BWR SAR code were to predict a pour of molten  $\text{ZrO}_2\text{-UO}_2$  eutectic at 4352°F (2673 K), the CORCON module within CONTAIN would, upon receipt of this pour, recognize it to be frozen. Thus, the latent heat of fusion for the pour would be lost from the calculation.

Therefore, in order to perform the calculations reported here, it was necessary to implement a local (ORNL) code modification to reduce the melting temperature of the  $\text{ZrO}_2\text{-UO}_2$  mixture recognized by CONTAIN/CORCON to 4350°F (2672K). With this local modification, CONTAIN/CORCON recognizes the molten oxides pouring from the reactor vessel to be molten. It is recommended that similar modifications be installed in future versions of CONTAIN/CORCON to provide a more realistic representation of the  $\text{ZrO}_2\text{-UO}_2$  phase diagram or at least, to provide the code user with the ability to set the oxide mixture melting temperatures by code input.

3. Representation of  $\text{B}_4\text{C}$  powder. Although there is a significant amount of  $\text{B}_4\text{C}$  powder within the BWR control blades [about 12 lbs (5.4 kg) per blade], the current CONTAIN/CORCON module gives no consideration to the effect of boron carbide powder upon the core debris or its interaction with the concrete floor. It is recommended that appropriate models, based upon available experimental data, be implemented.
4. Spreading of debris on the drywell floor. There are no models in the current version of CONTAIN to simulate the lateral spreading over the drywell floor of molten bottom head debris released from the reactor vessel. Such a capability should be developed and implemented into CONTAIN. The most important benefit to be gained from a mechanistic debris spreading model is the improved calculation of the oxidation of metals on the drywell floor. As discussed in Chap. 3 of this report, metal and oxide debris pours were prescribed for the various regions of the drywell floor based on the spreading analysis developed by Kazimi<sup>8</sup> and the physical state of the debris as it left the failed reactor vessel. For the metals leaving the reactor vessel, this means that independent but simultaneous metal sources appear in the separate CORCON calculations for the inpedestal and expedestal areas. This is nonrealistic because fresh metal would appear first in the inpedestal region beneath the failed reactor vessel and then flow through the pedestal doorway into and around the expedestal region, becoming progressively oxidized along the way. Thus, the chemical energy release in the expedestal region would be greater in the vicinity of the expedestal doorway and less in the more remote areas of the drywell floor. As shown in Chaps. 4 and 5, it is this chemical energy release that establishes the maximum temperature of the bulk debris adjacent to the drywell shell.

## 5. Debris Layer Modeling.

- a. The debris layer structure as currently modeled in CORCON is based upon an assumption that individual layers of oxides and metals always exist. During periods of rapid ablation, gas sparging through molten debris makes this debris layering assumption questionable. It is recommended that the CORCON module be modified so that the mixing of the metals and oxides can be calculated automatically or at least controlled by user input. It should be recognized that this in turn will lead to questions concerning the large uncertainties in the chemical and thermophysical environment existing in such a mixture of metals and oxides.
- b. A second change should be implemented in CORCON with respect to the processing of debris added via debris source tables. At present, CORCON models debris addition from source tables as initially appearing within the uppermost debris layer. The enthalphy of the debris being sourced from the tables is added to the enthalphy of the uppermost layer and a temperature corresponding to the total enthalpy is calculated. The material relocation algorithm in CORCON is then used to decide the destination layer of the newly added debris, with the equilibration process assumed to occur for each layer through which the debris travels. For massive upper layers that are calculated to be completely frozen, addition of debris sources in this manner results in temperature gradients in the upper layer crust that are of incorrect sign. This is because the CORCON model prescribes that melting of the uppermost layer be from the interior of that layer. This is inconsistent with the physical situation in which the added debris would reside on top of the upper frozen layer, and thus melting of that layer would not be from the interior but would occur from the upper surface in contact with the newly added debris.

A potential solution to this problem would be to create a new layer within the existing CORCON layering scheme. The suggested new layer would be thin and located at the top of the frozen debris. Heat and mass transfer should be across the interface of the thin molten layer with the underlying thick frozen layer.

- c. A third change in the CORCON layering scheme should be implemented to address a problem associated with modeling the BWR drywell sumps. The BWR Mark I drywell sumps are small (~6 m<sup>3</sup>) and would hold roughly 10% of the debris expected to leave a failed BWR reactor vessel. Thus, it is probable that the sumps would be completely filled with metallic debris during the initial metallic pours with sufficient metals remaining to overflow onto the rest of the inpedestal drywell floor. When this occurs with the current version of CONTAIN, there are two radically different characteristic geometries with which the



metal is simultaneously associated. The problem in the current application is the way in which the crusting model is implemented. The crusting model considers individual debris layers and represents them as cylindrical in shape, using layer thickness and layer volume to calculate an equivalent layer cross-sectional area and thus an equivalent layer radius. For the situation described above with the metals overflowing the sumps, the code simply adopts a cross-sectional area between that of the sumps and that of the inpedestal floor area. As a result of this approach, the crusting model cannot arrive at crusting estimates appropriate for either the sump or the inpedestal geometry. Since debris crusting is a dominant resistance to heat loss from the debris, a deficiency in this model is not of a minor nature. For the calculations performed for this report, the sump volume was conserved by user input, but the sump floor area was adjusted to 322 ft<sup>2</sup> (29.9 m<sup>2</sup>) – the inpedestal cross-sectional area.

A potential solution to this problem of modeling similar materials in volumes of different geometries would be to allow for multiple layers of the same debris. For metals filling the sumps and overflowing onto the drywell floor, it seems reasonable to place the metal in the sump in one layer and to place the remainder of the metal that overflows onto the floor in another layer. In this way, the crusting model as implemented in CORCON would calculate two characteristic crusts for that metal – one appropriate for the geometry of the sump and the other appropriate for the inpedestal floor area.

#### 6. Improved Debris/Water Pool Heat Transfer Modeling.

There has been recent experimental evidence<sup>9,10</sup> that indicates that heat transfer from debris to an overlying water pool is greater than that predicted within CONTAIN by the currently used flat plate film boiling correlation. The magnitude of the enhancement is the subject of present debate, and it is recommended that research should continue as necessary to resolve this issue. It is important that accurate modeling of the heat transfer phenomenon be incorporated into CONTAIN and CORCON; but until such time, modifications should be made to permit the sensitivity of calculated results to this parameter to be addressed by user input.

#### 7. Code Execution Difficulties.

Two periods of numerical instability were experienced when trying to perform the analysis of the wet case reported in Chap. 5. The instabilities concerned the convergence of the interlayer heat transfer algorithms HTRLAY and INTEMP for the inpedestal CORCON calculation.

The first instabilities occurred during the cooling period after the initial debris pour from the reactor vessel. As the metal

layer at the bottom of the debris cooled to below the ablation temperature of the concrete, 2246° F (1503 K), concrete ablation ceased and the CONTAIN degassing algorithm switched on and released gas into the metal layer. This gas reacted with unoxidized zirconium to release chemical energy; this raised the metal layer interface temperature slightly above the ablation temperature at which point the degassing algorithm turned off. Subsequently, for a few timesteps, the ablation algorithm was active and the metal layer temperature began to cool again. The temperature fell below the ablation temperature, the degassing algorithm turned on, and the cycle repeated.

During each CORCON timestep, the CORCON interlayer debris heat transfer algorithm (INTEMP) attempted to converge to a satisfactory temperature and heat flux at each layer interface within the debris and at the boundaries of the debris with its surroundings. It was at the interface at the boundary of the debris with the water pool where the initial nonconvergence occurred. A negative interface temperature was calculated and passed to the routine ATMSUR, which attempted to calculate the heat transfer into the overlying water pool. It would not converge, and the calculation was terminated.

Because the period during which the degassing algorithm was activated is very short, the wet case calculation was repeated with the degassing algorithm deactivated. The problem with the negative interface temperature did not occur although there were numerous timesteps for which subroutine INTEMP did not converge.

The second instance when convergence problems occurred was much later in the calculation (at 760 min) when CORCON was in the midst of calculating layer flip for the heavy oxide layer and the overlying metal layer. In this case, the debris/concrete interface temperature was calculated to be negative. Subroutine BUBBLE calculated a negative gas density because of the negative interface temperature. In turn, this negative gas density was passed to subroutine VSCRIT which computes the superficial gas velocity of bubbles entering the debris pool. Because the superficial velocity depends on the square root of the gas density and because the square root of a negative number is not defined, code execution terminated and no further wet case calculation could be performed.

It appears that each of the above periods of numerical convergence difficulty was not ultimately affected by CORCON timestep size. Several CORCON timesteps ranging from 0.05 s to 8 s were attempted but none resulted in a stable calculation. Although a numerically stable calculation might result from the present algorithm if the correct timestep were chosen, the analyst has only the technique of trial and error at his disposal in order to attempt to determine this correct timestep.

Because there is 26500 lb (12000 kg) of unoxidized zirconium remaining at the time of layer flip for the inpedestal CORCON calculation at termination of the calculation, it is desirable to be able

to extend the calculation until the zirconium is exhausted. As discussed in Chap. 4, reactor pedestal ablation depends directly on the temperature of the debris, which in turn is dependent on the rate of zirconium oxidation.

Therefore, it is recommended that further effort be devoted towards a better understanding of the mathematical representation of the interlayer heat transfer physics. It may be that the physics of the phenomena that are occurring at the time of the convergence difficulties are not appropriately modeled and thus the present calculational scheme cannot be expected to converge. In this case, further model development to include the new physics should be developed. On the other hand, if the modeling of the physics is adequate, then a more stable numerical algorithm should be devised.

## 7.2 Calculations Based Upon Best-Estimate Eutectic Pours from the Reactor Vessel

It is not possible to employ the BWRSAR predictions of debris pours based upon the ORNL best-estimate formation of relatively low-melting-temperature eutectic alloys in the BWR reactor vessel bottom head with the current version of CONTAIN. With the present layer configuration models and melting temperature algorithms of the CORCON module, the pour of these molten eutectic mixtures cannot be properly represented. Thus, the Peach Bottom calculations discussed in Chap. 3 of this report are based upon an assumption that the metallic core debris in the reactor vessel bottom head is in the form of a homogeneous mixture with a melting temperature of 2750°F (1783 K). With initial metallic pours at this temperature, CORCON recognizes the initial debris to be molten.

There is reason, including current results of a simple experiment by George Parker<sup>12</sup> at ORNL, to believe that the initial pour of core debris from a BWR reactor vessel would be a molten metallic eutectic mixture at relatively low temperature. Subsequent metallic pours should occur at progressively higher temperatures. The core debris-concrete interaction and spreading events on the drywell floor would be different for such pours than for the currently considered delayed pour of a single metallic mixture melting at 2750°F (1783 K). Clearly, the best-estimate eutectic pours should be considered in future calculations after the CONTAIN code has been modified to accept them.

## 7.3 Extension of Calculations Beyond Time of Exhaustion of the Zirconium Inventory

There would be a great deal of stainless steel included in the debris formed by the melting and relocation of a BWR core. In the current calculations, the stainless steel of the top guide, the control blades, the core plate, and the control rod guide tubes constitutes a total mass of approximately 275,000 lbs (125,000 kg), which is added to

the core debris. In addition, recent modifications to the BWRSAR code provide for the addition of carbon steel to the debris by means of partial melting of the bottom head. In the current calculations, about 83,000 lbs (38,000 kg) of carbon steel is so added.

With the very large amounts of chromium, iron, and nickel expected to be in BWR core debris on the drywell floor, it is important to recognize that the potential for combustible gas generation by the oxidation of these metals (4000 moles CO and 1500 moles H<sub>2</sub>) is much greater than that from the oxidation of zirconium (900 moles CO and 400 moles H<sub>2</sub>). In the current wet case calculations, the zirconium metal in the expedestal region is exhausted at time 550 minutes. However, chromium, iron, and nickel remain in this region at the end of the calculation (time 750 min). This indicates that future calculations should be carried out beyond the point of exhaustion of the inventory of zirconium to see the effect of the oxidation of the remaining metals.

#### 7.4 Calculations to Estimate the Effects of Wetwell Venting

It has been proposed that hardened vent lines be installed to permit venting of the wetwell airspace to the atmosphere outside of the secondary containment. (The presently installed primary containment venting system utilizes low-pressure ducting within the secondary containment.) The purpose of the wetwell venting would be to pass to the outside atmosphere much of the hydrogen generated within the reactor vessel or on the drywell floor before drywell shell pressure boundary failure so as to reduce the subsequent gas blowdown to the secondary containment and the combustible gas burning therein.

It is recommended that future calculations be performed to assess the potential beneficial effects of a reliable hardened system for wetwell venting to the outside atmosphere.

#### 7.5 Calculations to Determine Expected Decontamination Factors for the Peach Bottom Secondary Containment

Previous calculations (Ref. 4) demonstrate that the Peach Bottom reactor building structure would be expected to survive the deflagrations resulting from the combustible gases entering the torus room after drywell shell pressure boundary failure for cases in which the wetwell has been vented. These findings should be confirmed.

In addition, the effectiveness of the reactor building in mitigating aerosol transport should now be determined. This analysis can be performed with either the CONTAIN or MELCOR codes and will require use of the recent extension of the ORNL MELCOR model of the Peach Bottom reactor building to include the upper floors.

## 7.6 Calculations for Long-Term Station Blackout

The final results of the Accident Sequences Evaluation Program (ASEP) study of the Peach Bottom plant in support of the NUREG-1150 effort indicate that 40% of the overall risk of core melt can be attributed to Long-Term Station Blackout.<sup>1</sup> This is approximately twice the risk associated with Short-Term Station Blackout, which is the subject of the present report.

The long-term station blackout accident sequence involves several accident signatures with important differences from those of the short-term station blackout with independent loss of HPCI and RCIC accident sequence studied here. Reactor vessel bottom head penetration failure would occur much later in Long-Term Station Blackout, but the vessel would be pressurized at the time of failure and the metal-water reaction energy release caused by the steam blowdown through the debris bed would greatly accelerate the debris heatup and the rate of the initial debris pour. Thus, the initial challenge to containment would be greater for this accident sequence.

It is recommended that future calculations be performed to address the case of Long-Term Station Blackout.

## 7.7 Determination of Concrete Type

Calculations have demonstrated that the response of the BWR MK I drywell to core debris release from the reactor vessel is extremely sensitive to the type of concrete employed in the drywell construction. For high limestone concrete, there is little predicted interaction between the initial release of relatively low-temperature molten metals with the concrete and the debris tends to retain its initial temperature as it rapidly spreads over the concrete. For limestone common sand concrete with its much lower ablation temperature, the release of concrete oxides by the debris-concrete interaction rapidly dilutes the spreading debris and lowers its temperature.

The type of concrete used in drywell floor construction at each of the 17 U.S. plants with BWR MK I containments should be ascertained. (It is known that Browns Ferry and Peach Bottom employ limestone common sand concrete, leaving the status of 15 BWR sites to be resolved.) It is probable that no U.S. plants were built with high limestone concrete, but this should be confirmed.



## 8. REFERENCES

1. Personal communication with Alan Kolaczowski of the ASEP Program, July 6, 1988.
2. L. J. Ott, "Advanced Severe Accident Response Models for BWR Applications," *Proceedings of the U.S. Nuclear Regulatory Commission Fifteenth Water Reactor Safety Research Information Meeting* (to be published).
3. K. K. Murata et al., *Users' Manual for CONTAIN 1.1 - A Computer Code for Severe Nuclear Reactor Accident Containment Analysis*, SAND 87-2309 (to be published).
4. S. R. Greene et al., "Peach Bottom Containment Response Calculations for Unmitigated Short-Term Station Blackout," Letter Report to Dr. Jerry Hulman, Chief, Severe Accident Issues Branch, Division of Accident Evaluation, Office of Nuclear Regulatory Research, dated February 1, 1988.
5. CBI NA-CON, Inc., "Mark I Containment Severe Accident Analysis," for the Mark I Owners' Group (April 1987).
6. T. L. Bridges, *Containment Penetration Elastomer Seal Leak Rate Tests*, NUREG/CR-4944, July 1987.
7. S. A. Hodge et al., *Primary Containment Response Calculations for Unmitigated Short-Term Station Blackout at Peach Bottom*, Letter Report to Dr. Thomas J. Walker, BWR Mark I Shell Melt-Through Issue Task Group Leader, Office of Nuclear Regulatory Research, dated May 2, 1988.
8. M. S. Kazimi, "On the Liner Failure Potential in MARK-I BWRs," Department of Nuclear Engineering, Massachusetts Institute of Technology, April, 1988.
9. G. A. Greene, "Heat Transfer in Core-Concrete Interactions: Liquid-Liquid Film Boiling," NUREG/CR-2331, BNL-NUREG-51454, Vol. 6, No. 4, (Quarterly Progress Report October 1-December 31, 1986), April 1987.
10. R. E. Henry et al., "Experiments Relating to Drywell Shell-Core Debris Interactions," *Proceedings of the U.S. Nuclear Regulatory Commission Sixteenth Water Reactor Safety Research Information Meeting* (to be published).
11. G. A. Greene, "Experiments on Melt Spreading and Bubbling Heat Transfer," Severe Accident Research Partners Meeting, October 17-21, 1988.

12. G. Parker and S. Hodge, "Small Scale Melt Layering Experiments," *Proceedings of the U.S. Nuclear Regulatory Commission Sixteenth Water Reactor Safety Research Information Meeting* (to be published).



## **APPENDIX B**

### **ROLE OF THE BWR OWNERS GROUP EMERGENCY PROCEDURE GUIDELINES IN SEVERE ACCIDENT MANAGEMENT**

## APPENDIX B

### ROLE OF THE BWR OWNERS GROUP EMERGENCY PROCEDURE GUIDELINES IN SEVERE ACCIDENT MANAGEMENT

This appendix discusses the interface between Revision 4 to the Emergency Procedure Guidelines (EPGs) and the concept of severe accident management, that is, actions taken by the operators and plant staff to prevent or mitigate an accident that threatens the integrity of one or more barriers to the uncontrolled release of fission products to the environment. The discussion has been placed in an appendix because the information presented, while important to the overall program for responding to severe accidents in all BWR nuclear power plants, is not directly related to hardware or system aspects of improving the performance of the Mark II containment.

Revision 4 to the EPGs contains "...generic symptomatic emergency procedure guidelines"<sup>B-1</sup> to direct the operator response in the areas of reactor pressure vessel (RPV) control, primary and secondary containment control, and radioactive release control. The EPGs are written so as to be symptom-oriented rather than event-oriented. Thus, the operator is not required to diagnose the cause of an abnormal condition before taking corrective or mitigative action.

Revision 4 to the EPGs was structured to provide guidance to the operators for responding to situations that extend beyond the licensing design basis accident. However, preventive and mitigative strategies remain that Revision 4 does not address. In addition, there are questions as to whether Revision 4 provides the optimum strategy for dealing with ATWS events. These two areas of concern are the primary focus of this appendix.

#### Strategies not included in Revision 4

One strategy that is potentially useful both for preventing containment failure and for mitigating the effects of an offsite release is the use of

containment sprays. Revision 4 only addresses the use of RHR pumps, with suction from the suppression pool, as a source of containment sprays. Also, the use of containment sprays for cooling debris present on the drywell floor after reactor vessel failure is not addressed. In fact, the drywell spray initiation limit in the EPG might very well prevent the use of sprays for debris cooling. In addition, the loss of vessel level indication that would occur when the vessel failed would prompt entry into the RPV Flooding portion of the EPG, procedurally precluding the use of containment sprays for ex-vessel cooling of core debris. As discussed in Section 3.3.2, the fire pumps and the condensate transfer pumps are potential sources of containment sprays in the event that the RHR pumps are unavailable. However, with no procedural guidance on the use of these pumps for this purpose, they can be given little credit in a quantitative risk analysis (in PRAs that have been reviewed, no credit has been given to these two sources).

Another concern is the direction given to the operators for venting the primary containment. Revision 4 directs that the primary containment is to be vented to prevent exceeding the PCPL, regardless of the offsite radioactivity release. If the suppression pool were not bypassed, releases through a wetwell vent line would be scrubbed by the water in the suppression pool. However, if the suppression pool were bypassed, for example, by downcomer failure or failure of in-pedestal drain lines, the release would not be scrubbed, and the offsite consequences could be significantly more severe. This is an accident management question that the EPGs currently do not address.

#### Operator actions during an ATWS

Prevention of core damage during an ATWS focuses primarily on insertion of negative reactivity to reduce core power.<sup>B-2</sup> Failing this, actions have to be taken to prevent containment failure, since this would be likely to induce core melt. The ATWS sequence is unique in terms of operator response because it requires that actions be taken that would be inappropriate for other accidents. For example, the ADS must be initially prevented from depressurizing the reactor, since this could result in the rapid injection of

large quantities of relatively cold water into a critical core. Furthermore, vessel level might have to be lowered to the top of active fuel (TAF) in order to reduce reactor power. In addition, should depressurization become necessary after boron injection has begun, for example, to avoid exceeding the suppression pool HCTL, the operator would be faced with a severe challenge in controlling the depressurization and subsequent low pressure injection to prevent the boron that has already been injected from being flushed out of the active core region.

Entry into the ATWS portion of the EPGs is specified whenever a condition exists for which a reactor scram is required, and reactor power is above the average power range monitor low level trip setpoint (~5% of rated power is a typical value), or is undetermined. Should the entry conditions exist, the procedure then directs the operator to manually actuate ARI, if it has not already been actuated, and to trip the recirculation pumps. If ARI is successful, the ATWS will be terminated by control rod insertion. If it is not successful, tripping the recirculation pumps will cause rapid core voiding and a substantial reduction in power. Once these actions have been accomplished, the procedure then directs the performance of a number of actions concurrently, all aimed at inserting negative reactivity into the core.

The first of these actions is to inhibit the ADS and actuate the SLCS to inject boron before reaching the boron injection initiation temperature in the suppression pool (typically 110°F.). As mentioned above, a delay in operator response could make the situation worse by increasing the heat loading on the suppression pool, lessening the time until containment integrity is challenged. The procedure also outlines several alternative methods of inserting control rods into the core, including a) manual insertion of individual control rods, bypassing the rod worth minimizer and rod sequence control system as necessary to allow the insertion of high worth rods first, b) initiation of a manual scram after resetting the RPS and ARI logic to drain the scram discharge volume, and c) insertion of rods by deenergizing the scram solenoids, venting the scram air header, opening individual scram test

switches, or venting the over-piston volumes of the individual hydraulic control units.

There are a number of positive features of this procedure for ATWS mitigation. First of all, the procedure has a minimal number of entry conditions, reducing the time required for operator diagnosis of the situation. Second, should boron injection via the SLCS fail, the procedure directs the use of alternative systems (such as RCIC) for injecting boron. Third, actions that can be taken to insert control rods are detailed in the procedure. Defeat of HPCI/HPCS and RCIC suction transfer to the suppression pool is also required by the procedure. Therefore, failure of high pressure injection due to loss of lube oil cooling is not a concern if the procedure is followed.

Since the SLCS hardware is quite reliable, variations in the above value can have a profound impact upon the outcome of the analysis. At one Mark II plant, for example, the estimated frequency of overpressure containment failure due to ATWS increases from  $3.3 \times 10^{-11}$  per reactor-year to  $5.1 \times 10^{-6}$  per reactor-year when the probability of operator failure to actuate the SLCS is increased from 0.0 to 0.1.<sup>B-3</sup> With this one change, ATWS sequences become the dominant contributor to overpressure containment failure; previously, ATWS had been a negligible contributor at this plant.

Some plants have taken steps to reduce the time required for shutdown of the reactor following SLCS actuation, either by increasing the SLCS injection flow rate or, equivalently, by increasing the boron-10 isotopic concentration in the injected sodium pentaborate solution. The net effect of these changes is that the actuation of the SLCS can be delayed for a longer period of time without intolerably adverse effects. Reference B-4, for example, gives 30 minutes as an allowable delay time, based on the calculated time to shutdown of 7.5 minutes after boron injection begins.

There are also questions about how effective the guidance of the EPGs would be in terminating or mitigating an ATWS event. Concerns include 1) the efficacy of lowering the reactor vessel water level to the TAF (a RELAP5

calculation was done at INEL for a BWR/4 that predicted power in the range of 17-20% of rated thermal power with level at the TAF),<sup>B-2</sup> 2) the operator's ability to control level at the TAF due to inaccuracies in indicated level versus actual level, and 3) the potential undesirable effects associated with manual reactor pressure control. For example, reclosing SRVs following manual depressurization could generate power and pressure spikes, because the change in void fraction with respect to changes in pressure is approximately two orders of magnitude larger at 85 psig than it is at 1035 psig.

A human factors analysis of an ATWS at Browns Ferry Unit 1 found uncertainty in the timing of boron injection.<sup>B-5</sup> The uncertainty was rooted in "...the considerable difficulty operators would have in deciding to execute the task and the high level of stress accompanying the decision." A nominal human error probability of failure to initiate boron injection of  $3.69 \times 10^{-2}$  was calculated, with upper and lower uncertainty bounds of 0.259 and  $1.47 \times 10^{-2}$ , respectively. Because of the above considerations, the human factors analysis concluded that "...it may be more appropriate to take the worst case scenario and use the upper [bound] as a more conservative estimate." The estimated effect on the Susquehanna core melt frequency of increasing the probability of operator failure to actuate the SLCS from 0.0 to 0.1 is shown in Table B.1.

Table B.1 Susquehanna Plant Damage State Annual Frequencies With SLCS Failure Probability of 10%

Plant Damage State	Core Damage	CM With RPV Failure	CM With RPV Failure and Loss of Primary Containment Integrity	
			Wetwell Vent	Cont. Failure
Transients	7.0E-10	1.9E-9	1.3E-9	1.4E-9
ATWS	8.4E-9	€	€	5.1E-6
Blackout	7.6E-8	3.9E-8	1.6E-8	1.4E-9
LOCA	5.5E-9	4.9E-10	3.0E-11	2.5E-9
LOCA/ATWS	5.3E-8	€	€	5.9E-9
Total	1.4E-7	4.1E-8	1.7E-8	5.1E-6

There are also uncertainties associated with the EPG direction to control level at the top of active fuel (TAF) while boron is being injected into the core. First of all, there is uncertainty as to what reactor power would actually be with level at the TAF and pressure near normal operating pressure. As mentioned above, a RELAP5 calculation done at INEL for a BWR/4 predicted power in the range of 17-20% of rated thermal power, significantly above decay heat power.<sup>B-2</sup> However, this calculation is sensitive to the axial power profile in the core, which is in turn a function, in part, of the inlet coolant enthalpy. The inlet coolant enthalpy would depend upon the amount of feedwater heating that resulted from uncovering of the feedwater spargers as vessel level was lowered.

Another uncertainty in controlling level at TAF stems from inaccuracies in indicated level versus actual level. Since the wide range level instruments are calibrated "hot," they would give reliable indication of level during an ATWS. However, the wide range instruments do not extend to the TAF; with the wide range instruments at the bottom of their indicating range,

vessel level would still be several inches above the TAF. The post-accident flooding instrumentation does extend down below the TAF, but these instruments are calibrated "cold." Therefore, they could not generally be relied upon for accurate indication during an ATWS.

The uncertainties associated with level control could be overcome if operators were to control injection flow rate, rather than level. Since reactor power is determined by flow rate through the core during an ATWS, a flow rate could be specified that would place reactor power near the decay heat removal capabilities of the RHR system. Flow control has been shown to be an effective means of controlling the reactor power and slowing the containment heatup rate. Very low flow rates would result in very low reactor power (~4%) and would significantly slow the containment pressurization rate.<sup>B-2, B-5, B-6</sup> However, on the downside, very low flow rates may lead to partial core uncover with core cooling provided by steam flow. Core heatups might lead to significant zircaloy cladding oxidation and to increased hydrogen production.<sup>B-7</sup> Perhaps a flow rate that is as low as possible, while still maintaining adequate steam cooling, could prevent core degradation and minimize the containment heatup rate.

There could also be undesirable effects associated with operator attempts to control pressure in accordance with the EPGs during an ATWS. First of all, the operator is directed to depressurize the reactor if the suppression pool heat capacity temperature limit (HCTL) is exceeded. As noted in the EPGs, this would be a complete depressurization to below 200 psi.<sup>B-1</sup> If condensate pumps were running, this could result in injection of cold water into the vessel. There is also a concern that LPCI and LPCS could inject very large quantities of water since both are actuated automatically at Level 1. The operator is relied upon to terminate all sources of vessel injection except CRD and the SLCS. Also, if the RHR system were being used for suppression pool cooling when vessel level dropped below Level 1, it would automatically realign to the LPCI mode. Because of this interlock, continuous heat removal from the suppression pool could prove to be difficult until level is permanently restored above Level 1.



Conflicts might also arise between different sections of the EPGs when responding to the ATWS. For example, emergency depressurization would be required if suppression pool temperature could not be maintained below the HCTL. However, rapid depressurization could result in boron being flushed out of the core, along with the need to control high capacity low pressure injection from the condensate system, LPCI, and LPCS in order to avoid recriticality and power/pressure spikes. To obviate this concern, PP&L has instituted a special ATWS HCTL of 208°F to allow more time for boron to be injected before approaching conditions in the suppression pool that would require emergency depressurization. PP&L also takes exception to the EPG instruction to lower level to the TAF, because of the possibility that the ADS would depressurize the reactor; PP&L instead advocates allowing HPCI, RCIC, and CRD to inject at full flow (~5700 gpm), with level stabilizing below Level 2 but well above the TAF. Doing this would also promote efficient boron mixing in the lower plenum, avoiding the need to carefully restore level after the necessary amount of boron has been injected, thus also avoiding the potential for thermal shock to the core and reactor vessel.

An analysis is not given in Reference B-3 to justify the use of this special ATWS HCTL. However, if raising this limit could be substantiated, then the allowable operator delay in initiating boron injection could be significantly increased. This would in turn lower the probability of operator failure to initiate boron injection in a timely fashion. Consequently, there would be a greater probability of successfully terminating the ATWS with no core degradation or challenge to containment integrity.

The strategy of allowing high pressure systems to inject at rated flow during an ATWS, rather than lowering level to the TAF, is also predicated upon the use of a higher HCTL for ATWS. This is because the equilibrium reactor power with an injection flow rate of 5700 gpm is approximately 28% of rated power, resulting in a rapid heatup of the suppression pool. If injection were not throttled, the HCTL specified in the EPG would quickly be reached. Again, the use of an increased HCTL for ATWS would allow additional time for injection of boron, even for the case with unthrottled flow from the high pressure injection systems.

In summary, an ATWS sequence might be effectively terminated by taking the actions outlined in the EPGs. Calculations done by ORNL using BWR-LTAS show that either SLCS actuation or manual rod insertion (at normal speed) alone is sufficient to bring the reactor to a shutdown condition, with no challenge to containment integrity from over-pressurization.<sup>B-5</sup> However, as mentioned above, there are concerns that adherence to the EPGs might not successfully terminate or mitigate the consequences of an ATWS event. There may be alternative actions that are easier to perform than the actions specified in the EPGs. For example, if the MSIVs could be opened (by bypassing interlocks in accordance with the EPGs), then the turbine bypass valves could be used to reject heat to the main condenser. Drywell sprays could be used to condense steam in the containment, but this would be a temporary measure, unless water could be removed from the suppression pool, since high suppression pool level would eventually require that sprays be terminated.

## REFERENCES

- B-1. General Electric Company, BWR Owners Group Emergency Procedures Guidelines, NEDO-31331, Rev. 4, March 1987.
- B-2. R. J. Dallman et al., Severe Accident Sequence Analysis Program - Anticipated Transient Without Scram Simulations for Browns Ferry Nuclear Plant Unit 1, NUREG/CR-4165, EGG-2374, May 1987.
- B-3. Pennsylvania Power & Light, Susquehanna Steam Electric Station Individual Plant Examination, NPE-86-001, 1986.
- B-4. Burns, E. R., et al., Shoreham Nuclear Power Station Full Power PRA, PRA Update: Supplemental Containment System Implementation, IT/Delian Corporation, prepared for Long Island Lighting Company, February, 1988.
- B-5. M. E. Harrington and S. A. Hodge, ATWS at Browns Ferry Unit 1, Accident Sequence Analysis, NUREG/CR-3470, July 1984.
- B-6. K. C. Wagner, Analysis of a High Pressure ATWS With Very Low Make-up Flow, DOE/ID-10211, October 1988.
- B-7. R. Chambers, "Integrated SCDAP/RELAP5 Analysis of a BWR High Pressure Boiloff", Proceedings of the Fourteenth Water Reactor Safety Information Meeting, Gaithersburg, Maryland, October 27-31, 1986,

**APPENDIX C**  
**SOURCE TERM BINNING METHODOLOGY**

## APPENDIX C

### SOURCE TERM BINNING METHODOLOGY

The end states of the SCETs were assigned alphanumeric designators to indicate the containment release mode. The scheme outlined in Reference C-1 for mapping SCET end states to containment release modes was used in this report. For convenience, this scheme is reproduced below.

Release Mode	Attributes
A1	In-vessel recovery, no cont. failure
A2	In-vessel recovery, cont. vented
A3	In-vessel recovery, cont. failed
B1	Early small break, release through supp. pool
B2	Early small break bypassing the supp. pool, with reactor bldg. retention
B3	Same as B2, but with no reactor bldg. retention
B4	Early slow release through the supp. pool
B5	Early slow release bypassing the supp. pool but with reactor bldg. retention
B6	Same as B5 but with no reactor bldg. retention
B7	Early moderate release through the supp. pool
B8	Early moderate release bypassing the supp. pool but with reactor bldg. retention
B9	Same as B8 but with no reactor bldg. retention
B10	Early energetic release through the supp. pool
B11	Early energetic release bypassing the supp. pool but with reactor bldg. retention
B12	Same as B11 but with no reactor bldg. retention
C1	Late vented release with Filtra holdup maintained (not applicable)
C2	Late vented release
C3	Late vented release bypassing the supp. pool but with reactor bldg. retention
C4	Same as C3 but with no reactor bldg. retention
C5	Late overpressure cont. failure with release through the supp. pool
C6	Late overpressure cont. failure bypassing the

	supp. pool
C7	Late large overpressure cont. failure with release through the supp. pool
C8	Same as C7 but bypassing the supp. pool
C9	Late thermal failure in the drywell with reactor bldg. retention
C10	Same as C9 but with no reactor bldg. retention
D1	Ex-vessel recovery with cont. vented through Filtra (not applicable)
D2	Ex-vessel recovery with cont. vented through the supp. pool
D3	Ex-vessel recovery with no cont. failure or venting
D4	Ex-vessel recovery with late cont. failure, noble gas release mitigated by small leakage rates

To reduce the number of source term calculations, Reference C-1 further bins these containment release modes into eleven release categories. Source terms were then calculated with MAAP for each of these release categories.<sup>C-2</sup> The scheme for grouping the release modes into release categories is shown below.

<u>Release Category</u>	<u>TQUX</u>	<u>ST-SB0</u>	<u>LT-SB0</u>	<u>ATWS-IC</u>	<u>ATWS-IV</u>
RC1	B12	B12		B12	B12
RC2	B11,B9	B11,B9		B11,B9	B11,B9
RC3	B10,B7,B4,B1	B10,B7,B4,B1		B10,B7,B4,B1	B10,B7,B4,B1
RC4	B8,B6,B5,B3, B2	B8,B6,B5,B3, B2		B8,B6,B5,B3, B2	B8,B6,B5,B3, B2
RC5	C10,C4	C10,C4	B12,B11,B9	C10,C4	
RC6	C9,C3	C9,C3	B8,B6,B5,B3, B2	C9,C3	
RC7	C2	C2	B10,B7,B4,B1	C2	
RC8	C8	C8	C10,C8,C4	C8	
RC9	C6	C6	C9,C6,C3	C6	
RC10	C5,C7,D4,A3	C5,C7,D4,A3	C5,C7,C2,D4	C5,C7,D4	
RC12	D3,D2,D1,A2, A1	D3,D2,D1,A2, A1	D3,D2,D1,A1	D3,D2,D1,A1	

Reference C-3 lists the source terms calculated for each of these release categories. This information was used as input to the MACCS consequence code in calculating the risk measures for this report. For further details, refer to Appendix D.

#### REFERENCES

- C-1. Z. T. Mendoza et al., Containment and Phenomenological Event Tree Evaluation At Full Power for the Shoreham Nuclear Power Station, Science Applications International Corporation, prepared for the Long Island Lighting Company, February 1988.
- C-2. Fauske and Associates, Inc., MAAP Analyses To Support Shoreham 100% Power PRA, prepared for the Long Island Lighting Company, February 1988. Revised March 1988.
- C-3. Pickard, Lowe, and Garrick, Inc., Core Melt Accident Dose-Versus-Distance Probability Distributions. 100% Power Operations, Shoreham Nuclear Power Station, prepared for Long Island Lighting Company, February 1988.





**APPENDIX D**  
**DETAILED INPUTS TO THE MACCS CONSEQUENCE ANALYSIS**

**APPENDIX D**  
**DETAILED INPUTS TO THE MACCS CONSEQUENCE ANALYSIS**

Table of Contents

<u>Section</u>	<u>Description</u>	<u>Page</u>
1.0	Discussion . . . . .	D-3
2.0	ATMOS Input Data . . . . .	D-5
3.0	EARLY Input Data . . . . .	D-25
4.0	CHRONC Input Data . . . . .	D-43
5.0	Auxiliary Input Files . . . . .	D-62
6.0	Results . . . . .	D-63
<hr/>		
<u>Appendix</u>	<u>Description</u>	
D.1	Documentation of PC Version of MACCS 1.5.9 . . .	D-68

## 1.0 Discussion

This calculation package documents the details of the severe accident consequence analysis for the reference BWR Mark II containment utilizing a PC version of the MELCOR Accident Consequence Code System Version 1.5.9 (MACCS 1.5.9).<sup>D-1</sup> For the purpose of this analysis, site-specific data for the reference BWR Mark II are based on the most recent version of the NUREG-1150 MACCS 1.5.9 input decks for Peach Bottom. These files differ in some places from those used in the pre-decisional draft of NUREG-1150, which utilized version 1.5.5 of MACCS. These changes reflect additions to improve the code and to correct input errors.

A series of changes to MACCS are in process to update the code from the version used for this analysis (Version 1.5.9) to the release version of MACCS 1.5 (Version 1.5.11). The major change that affects this analysis is in the interdiction model. The code inadvertently ties the number of interdiction periods to the user-specified number of decontamination levels. For this analysis (as well for the NUREG-1150 analyses) the maximum interdiction period was only 5 years instead of the intended 30 years. SNL has performed comparisons of results for the two code versions, using a Surry NUREG-1150 input deck. The 0 to 50-mile population dose calculated by the new code for a medium size NUREG-1150 source term was 7% higher than the old code, with the 0 to 50-mile economic costs decreasing by 5%. These changes are principally due to a 32% decrease in the amount of property condemned due to uninhabitability in that region, as the old code was mistakenly condemning property based on a five-year maximum interdiction period, instead of the intended 30-year interdiction period. The results for a larger source term from the NUREG-1150 set showed a smaller difference in the calculated results.

Offsite release data for the reference plant are based on the results provided in PL&G report PLG-0614 for the Shoreham Nuclear Power Station, Reference D-2. Results were utilized from the PL&G report for the cases which did not take credit for the Supplemental Containment System (no-Filtra cases). The PL&G analysis utilized the MAAP program to generate offsite release data,

consisting of 10 representative accident sequences that result in unique release categories.

MACCS 1.5 is comprised of a single FORTRAN-77 program, which consists of three basic modules, ATMOS, EARLY, and CHRONC, which are exercised in sequence. MACCS has been developed for the purpose of evaluating the consequences of severe accidents at commercial LWR power plants. It incorporates several improvements over earlier modeling capabilities available in CRAC2 for the treatment of variable and/or long-term releases, deposition modeling, dosimetry, emergency response, long-term mitigative actions, radiological health effects and economic impacts.

The ATMOS module calculates the air and ground isotope concentrations, plume dispersion, and timing information for all plume segments as a function of downwind distance. Atmospheric transport is modeled in ATMOS using a straight line Gaussian plume treatment. Plume depletion occurs during transport as a result of radioactive decay and deposition of the material onto the ground. Wet and dry deposition models are treated as independent processes in ATMOS.

The types of consequences calculated by MACCS 1.5 include early health effects, chronic health effects, and economic impacts. Four exposure pathways are utilized in EARLY to model doses received in the early (typically 7-day) time period. These pathway models are cloudshine, inhalation from the plume, groundshine, and inhalation of resuspended ground contamination. CHRONC utilizes three exposure pathways to model chronic doses. These pathway models are groundshine, inhalation of resuspended ground contamination, and ingestion of contaminated food and water. The economic effects models of MACCS 1.5 are designed to estimate the direct offsite costs resulting from a severe accident. These costs include the emergency response costs associated with the early mitigative actions of evacuation and relocation, the costs of long-term mitigative actions, including extended relocation, decontamination, interdiction, condemnation, crop disposal, and control of food production.

## 2.0 ATMOS Input Data

Variable Name - **ATNAM1**

Purpose - Identifier for specific ATMOS case (Case Specific). Titles correspond to the release categories and representative sequences defined in PLG-0614, Table 3

CASE 1:

RIATNAM1001 'Shoreham PLG-0614 RC 1, Rep. Seq. IVA.1A, Peach Bottom Site'

CASE 2:

RIATNAM1001 'Shoreham PLG-0614 RC 2, Rep. Seq. IVA.1B, Peach Bottom Site'

CASE 3:

RIATNAM1001 'Shoreham PLG-0614 RC 3, Rep. Seq. IVA.1BM, Peach Bottom Site'

CASE 4:

RIATNAM1001 'Shoreham PLG-0614 RC 4, Rep. Seq. IIID.1, Peach Bottom Site'

CASE 5:

RIATNAM1001 'Shoreham PLG-0614 RC 5, Rep. Seq. SBORC5A, Peach Bottom Site'

CASE 6:

RIATNAM1001 'Shoreham PLG-0614 RC 6, Rep. Seq. TDIQRC6A, Peach Bottom Site'

CASE 7:

RIATNAM1001 'Shoreham PLG-0614 RC 7, Rep. Seq. TQUVRC7, Peach Bottom Site'

CASE 8:

RIATNAM1001 'Shoreham PLG-0614 RC 8/9, Rep. Seq. IIA.1, Peach Bottom Site'

CASE 9:

RIATNAM1001 'Shoreham PLG-0614 RC 10, Rep. Seq. IIA.1M1, Peach Bottom Site'

CASE 10:

RIATNAM1001 'Shoreham PLG-0614 RC 12, Rep. Seq. TQUXRC12, Peach Bottom Site'

Variable Name - **ENDAT1**

Purpose - Flag to indicate that this is the last program in the series to be run.

Source - NUREG-1150 MACCS 1.5.9 Peach Bottom Model.

OCENDAT1001 .FALSE. (SET THIS VALUE TO .TRUE. TO SKIP EARLY AND CHRONC)

Variable Name - **NUMRAD**

Purpose - Number of radial spatial elements defined in the model.

Source - NUREG-1150 MACCS 1.5.9 Peach Bottom Model.

GENUMRAD001 26

Variable Name - **SPAEND**

Purpose - Distance in meters to the end of the spacial intervals.

Source - NUREG-1150 MACCS 1.5.9 Peach Bottom Model.

\* PEACH BOTTOM

\*

GESPAEND001	.40	.82	1.21	1.61	2.43
GESPAEND002	3.22	4.02	4.83	5.63	8.05
GESPAEND003	11.27	16.09	20.92	25.75	32.19
GESPAEND004	40.23	48.28	64.37	80.47	112.65
GESPAEND005	160.93	241.14	321.87	563.27	804.67
GESPAEND006	1609.34				

Variable Name - **NUMISO**

Purpose - Number of nuclides defined in the model.

Source - NUREG-1150 MACCS 1.5.9 Peach Bottom Model.

ISNUMISO001 60

Variable Name - MAXGRP  
 Purpose - Number of nuclide groups defined in the model.  
 Source - NUREG-1150 MACCS 1.5.9 Peach Bottom Model.

#### ISMAXGRP001 9

Variable Name - WETDEP  
 Purpose - Logical flag for each of the nuclide groups that indicates whether they are subject to wet deposition.  
 Source - NUREG-1150 MACCS 1.5.9 Peach Bottom Model.

Variable Name - DRYDEP  
 Purpose - Logical flag for each of the nuclide groups that indicates whether they are subject to dry deposition.  
 Source - NUREG-1150 MACCS 1.5.9 Peach Bottom Model.

	WETDEP	DRYDEP
*		
*		
ISDEPFLA001	.FALSE.	.FALSE.
ISDEPFLA002	.TRUE.	.TRUE.
ISDEPFLA003	.TRUE.	.TRUE.
ISDEPFLA004	.TRUE.	.TRUE.
ISDEPFLA005	.TRUE.	.TRUE.
ISDEPFLA006	.TRUE.	.TRUE.
ISDEPFLA007	.TRUE.	.TRUE.
ISDEPFLA008	.TRUE.	.TRUE.
ISDEPFLA009	.TRUE.	.TRUE.

Variable Name - NUCNAM  
 Purpose - Identifying name associated with each of the nuclides.  
 Source - NUREG-1150 MACCS 1.5.9 Peach Bottom Model.

Variable Name - PARENT  
 Purpose - Name of parent nuclide, if any.  
 Source - NUREG-1150 MACCS 1.5.9 Peach Bottom Model.

Variable Name - **IGROUP** - Chemical group to which nuclide is assigned.  
 Purpose - Chemical group to which nuclide is assigned.  
 Source - NUREG-1150 MACCS 1.5.9 Peach Bottom Model.

Variable Name - **HAFLIF** - Half-life of the isotope in seconds.  
 Purpose - Half-life of the isotope in seconds.  
 Source - NUREG-1150 MACCS 1.5.9 Peach Bottom Model.

\* NUCLIDE GROUP DATA FOR 9 NUCLIDE GROUPS

	NUCNAM	PARENT	IGROUP	HAFLIF
ISOTPGRP001	CO-58	NONE	6	6.160E+06
ISOTPGRP002	CO-60	NONE	6	1.660E+08
ISOTPGRP003	KR-85	NONE	1	3.386E+08
ISOTPGRP004	KR-85M	NONE	1	6.13E+04
ISOTPGRP005	KR-87	NONE	1	4.560E+03
ISOTPGRP006	KR-88	NONE	1	3.008E+04
ISOTPGRP007	RB-86	NONE	3	1.611E+06
ISOTPGRP008	SR-89	NONE	5	4.493E+06
ISOTPGRP009	SR-90	NONE	5	8.865E+08
ISOTPGRP010	SR-91	NONE	5	3.413E+04
ISOTPGRP011	SR-92	NONE	5	9.756E+03
ISOTPGRP012	Y-90	SR-90	7	2.307E+05
ISOTPGRP013	Y-91	SR-91	7	5.080E+06
ISOTPGRP014	Y-92	SR-92	7	1.274E+04
ISOTPGRP015	Y-93	NONE	7	3.636E+04
ISOTPGRP016	ZR-95	NONE	7	5.659E+06
ISOTPGRP017	ZR-97	NONE	7	6.048E+04
ISOTPGRP018	NB-95	ZR-95	3	1.033E+06
ISOTPGRP019	MO-99	NONE	6	2.377E+05
ISOTPGRP020	TC-99M	MO-99	6	2.167E+04
ISOTPGRP021	RU-103	NONE	6	3.421E+06
ISOTPGRP022	RU-105	NONE	6	1.598E+04



ISOTPGRP023	RU-106	NONE	6	3.188E+07	
ISOTPGRP024	RH-105	RU-105	6	1.278E+05	
ISOTPGRP025	SB-127	NONE	4	3.283E+05	
ISOTPGRP026	SB-129	NONE	4	1.562E+04	
ISOTPGRP027	TE-127	SB-127	4	3.366E+04	
ISOTPGRP028	TE-127M	NONE	4	9.418E+06	
ISOTPGRP029	TE-129	SB-129	4	4.200E+03	
ISOTPGRP030	TE-129M	NONE	4	2.886E+06	
ISOTPGRP031	TE-131M	NONE	4	1.080E+05	
ISOTPGRP032	TE-132	NONE	4	2.808E+05	
ISOTPGRP033	I-131	TE-131M	2	6.947E+05	
ISOTPGRP034	I-132	TE-132	2	8.226E+03	
ISOTPGRP035	I-133	NONE	2	7.488E+04	
ISOTPGRP036	I-134	NONE	2	3.156E+03	
ISOTPGRP037	I-135	NONE	2	2.371E+04	
ISOTPGRP038	XE-133	I-133	1	4.571E+05	
ISOTPGRP039	XE-135	I-135	1	3.301E+04	
ISOTPGRP040	CS-134	NONE	3	6.501E+07	
ISOTPGRP041	CS-136	NONE	3	1.123E+06	
ISOTPGRP042	CS-137	NONE	3	9.495E+08	
ISOTPGRP043	BA-139	NONE	9	4.986E+03	NEW
ISOTPGRP044	BA-140	NONE	9	1.105E+06	
ISOTPGRP045	LA-140	BA-140	7	1.448E+05	
ISOTPGRP046	LA-141	NONE	7	1.418E+04	NEW
ISOTPGRP047	LA-142	NONE	7	5.724E+03	NEW
ISOTPGRP048	CE-141	LA-141	8	2.811E+06	PARENT ADDED
ISOTPGRP049	CE-143	NONE	8	1.188E+05	
ISOTPGRP050	CE-144	NONE	8	2.457E+07	
ISOTPGRP051	PR-143	CE-143	8	1.173E+06	
ISOTPGRP052	ND-147	NONE	7	9.495E+05	
ISOTPGRP053	NP-239	NONE	8	2.030E+05	
ISOTPGRP054	PU-238	CM-242	8	2.809E+09	
ISOTPGRP055	PU-239	NP-239	8	7.700E+11	
ISOTPGRP056	PU-240	CM-244	8	1.133E+11	
ISOTPGRP057	PU-241	NONE	8	4.608E+08	

ISOTPGRP058	AM-241	PU-241	7	1.366E+10
ISOTPGRP059	CM-242	NONE	7	1.408E+07
ISOTPGRP060	CM-244	NONE	7	5.712E+08

Variable Name - CWASH1  
 Purpose - Linear term of the washout factor.  
 Source - NUREG-1150 MACCS 1.5.9 Peach Bottom Model.

WDCWASH1001 9.5E-5 (HELTON AFTER JONES, 1986)

Variable Name - CWASH2  
 Purpose - The exponential term for the washout factor.  
 Source - NUREG-1150 MACCS 1.5.9 Peach Bottom Model.

WDCWASH2001 0.8 (HELTON AFTER JONES, 1986)

Variable Name - NPSGRP  
 Purpose - The number of particle size groups that is used for dry deposition.  
 Source - NUREG-1150 MACCS 1.5.9 Peach Bottom Model.

DDNPSGRP001 1

Variable Name - VDEPOS  
 Purpose - The representative dry deposition velocity associated with each of the particle size groups.  
 Source - NUREG-1150 MACCS 1.5.9 Peach Bottom Model.

DDVDEPOS001 0.01 (VALUE SELECTED BY S. ACHARYA, NRC)

Variable Name - CYSIGA  
 Purpose - The linear term in the expression for sigma-y for the six stability classes.  
 Source - NUREG-1150 MACCS 1.5.9 Peach Bottom Model.

\* STABILITY CLASS: A            B            C            D            E            F  
\*

DPCYSIGA001    0.3658    0.2751    0.2089    0.1474    0.1046    0.0722

Variable Name    - CYSIGB

Purpose            - The exponential term of the expression for sigma-y, six stability classes.

Source            - NUREG-1150 MACCS 1.5.9 Peach Bottom Model.

\* STABILITY CLASS: A            B            C            D            E            F  
\*

DPCYSIGB001    .9031    .9031    .9031    .9031    .9031    .9031

Variable Name    - CZSIGA

Purpose            - The linear term of the expression for sigma-z, six stability classes.

Source            - NUREG-1150 MACCS 1.5.9 Peach Bottom Model.

\* STABILITY CLASS: A            B            C            D            E            F  
\*

DPCZSIGA001    2.5E-4    1.9E-3    .2        .3        .4        .2

Variable Name    - CZSIGB

Purpose            - The exponential term of the expression for sigma-z, six stability classes.

Source            - NUREG-1150 MACCS 1.5.9 Peach Bottom Model.

\* STABILITY CLASS; A            B            C            D            E            F  
\*

DPCZSIGB001    2.125    1.6021    .8543    .6532    .6021    .6020

Variable Name    - YSCALE

Purpose            - The linear scaling factor for the sigma-y function.

Source            - NUREG-1150 MACCS 1.5.9 Peach Bottom Model.

DPYSCALE001 1. 3 3 3 8 A 122A10 YTL118ATZ \*

Variable Name **DPZSCALE** 1.0 3.0 3.0 3.0 3.0 3.0 1000000000  
 Purpose - The linear scaling factor for the sigma-z function.  
 Source - NUREG-1150 MACCS 1.5.9 Peach Bottom Model.

DPZSCALE001 1.27

Variable Name **TIMBAS**  
 Purpose - The time base for the expansion factor (seconds)  
 Source - NUREG-1150 MACCS 1.5.9 Peach Bottom Model.

PMTIMBAS001 600. (10 MINUTES)

Variable Name **BRKPNT**  
 Purpose - The break point in the formula used for calculating the  
 plume meander expansion factor.  
 Source - NUREG-1150 MACCS 1.5.9 Peach Bottom Model.

PMBRPNT001 3600. (1 HOUR)

Variable Name **XPFAC1**  
 Purpose - Exponential expansion factor number 1.  
 Source - NUREG-1150 MACCS 1.5.9 Peach Bottom Model.

PMXPFAC1001 0.2

Variable Name **XPFAC2**  
 Purpose - Exponential expansion factor number 2.  
 Source - NUREG-1150 MACCS 1.5.9 Peach Bottom Model.

PMXPFAC2001 0.25

Variable Name - SCLCRW

Purpose - Scaling factor for the critical wind speed for entrainment of a buoyant plume.

Source - NUREG-1150 MACCS 1.5.9 Peach Bottom Model.

PRSCLCRW001 1.

Variable Name - SCLADP

Purpose - Scaling factor for the adiabatic plume rise formula.

Source - NUREG-1150 MACCS 1.5.9 Peach Bottom Model.

PRSCCLADP001 1.

Variable Name - SCLEFP

Purpose - Scaling factor for the effective plume rise formula.

Source - NUREG-1150 MACCS 1.5.9 Peach Bottom Model.

PRSCLEFP001 1.

Variable Name - BUILDW

Purpose - Width of the reactor building in meters.

Source - NUREG-1150 MACCS 1.5.9 Peach Bottom Model.

WEBUILDW001 50. \* PEACH BOTTOM

Variable Name - BUILDH

Purpose - Height of the reactor building in meters.

Source - NUREG-1150 MACCS 1.5.9 Peach Bottom Model.

WEBUILDH001 50. \* PEACH BOTTOM

Variable Name - CORINV

Purpose - Defines the total core inventory in becquerels for each nuclide, NUCNAM.

Source - MACCS 1.5 User's Manual.

\* 3578 MWTH BWR CORE INVENTORY, 80 O/O CAPACITY, 3/3 SHUTDOWN INVENTORY  
 \* SUPPLIED BY D.E. BENNETT, 6/17/86

	NUCNAM	CORINV(BQ)
RDCORINV001	CO-58	2.024E+16
RDCORINV002	CO-60	2.423E+16
RDCORINV003	KR-85	3.317E+16
RDCORINV004	KR-85M	1.206E+18
RDCORINV005	KR-87	2.193E+18
RDCORINV006	KR-88	2.960E+18
RDCORINV007	RB-86	1.856E+15
RDCORINV008	SR-89	3.673E+18
RDCORINV009	SR-90	2.599E+17
RDCORINV010	SR-91	4.771E+18
RDCORINV011	SR-92	4.984E+18
RDCORINV012	Y-90	2.783E+17
RDCORINV013	Y-91	4.482E+18
RDCORINV014	Y-92	5.004E+18
RDCORINV015	Y-93	5.690E+18
RDCORINV016	ZR-95	5.899E+18
RDCORINV017	ZR-97	6.073E+18
RDCORINV018	NB-95	5.581E+18
RDCORINV019	MO-99	6.436E+18
RDCORINV020	TC-99M	5.554E+18
RDCORINV021	RU-103	4.877E+18
RDCORINV022	RU-105	3.254E+18
RDCORINV023	RU-106	1.327E+18
RDCORINV024	RH-105	2.429E+18
RDCORINV025	SB-127	3.077E+17
RDCORINV026	SB-129	1.068E+18
RDCORINV027	TE-127	2.979E+17
RDCORINV028	TE-127M	4.010E+16
RDCORINV029	TE-129	1.002E+18

RDCORINV030	TE-129M	2.634E+17
RDCORINV031	TE-131M	5.058E+17
RDCORINV032	TE-132	4.944E+18
RDCORINV033	I-131	3.417E+18
RDCORINV034	I-132	5.020E+18
RDCORINV035	I-133	7.172E+18
RDCORINV036	I-134	7.850E+18
RDCORINV037	I-135	6.751E+18
RDCORINV038	XE-133	7.182E+18
RDCORINV039	XE-135	1.707E+18
RDCORINV040	CS-134	5.596E+17
RDCORINV041	CS-136	1.501E+17
RDCORINV042	CS-137	3.350E+17
RDCORINV043	BA-139	6.612E+18
RDCORINV044	BA-140	6.522E+18
RDCORINV045	LA-140	6.655E+18
RDCORINV046	LA-141	6.145E+18
RDCORINV047	LA-142	5.912E+18
RDCORINV048	CE-141	5.922E+18
RDCORINV049	CE-143	5.765E+18
RDCORINV050	CE-144	3.841E+18
RDCORINV051	PR-143	5.643E+18
RDCORINV052	ND-147	2.522E+18
RDCORINV053	NP-239	7.516E+19
RDCORINV054	PU-238	5.226E+15
RDCORINV055	PU-239	1.325E+15
RDCORINV056	PU-240	1.659E+15
RDCORINV057	PU-241	2.856E+17
RDCORINV058	AM-241	2.903E+14
RDCORINV059	CM-242	7.667E+16
RDCORINV060	CM-244	4.137E+15

Variable Name - SCLCRW

Purpose - Scaling factor to adjust the core inventory.

Source - SCLCRW is the ratio of core thermal power level assumed for the analysis to the value for the reference BWR. The Peach Bottom rated core thermal power level is assumed for this analysis. SCLCR is then:

$$SCLCRW = 3293 \text{ MWth} / 3578 \text{ MWth}$$

$$SCLCRW = 0.920$$

RDCORSCA001 0.920 \* PEACH BOTTOM

Variable Name - PSDIST

Purpose - Particle size distribution for each nuclide group.

Source - NUREG-1150 MACCS 1.5.9 Peach Bottom Model.

RDPSDIST001 1.

RDPSDIST002 1.

RDPSDIST003 1.

RDPSDIST004 1.

RDPSDIST005 1.

RDPSDIST006 1.

RDPSDIST007 1.

RDPSDIST008 1.

RDPSDIST009 1.

Variable Name - IDEBUG

Purpose - Debug output flag (0 = no debug).

Source - NUREG-1150 MACCS 1.5.9 Peach Bottom Model.

OCIDEBUG001 0

Variable Name - METCOD

Purpose - Meteorological sampling option code.

metcod = 1, user specified day and hour in the year, 2, weather category bin sampling,



3, 120 hours of weather specified on the ATMOS user input file,

4, constant met, (2\N) 1000

5, stratified random samples for each day of the

year. Variable Name - M2M2M

Source - NUREG-1150 MACCS 1.5.9 Peach Bottom Model - Purpose

Source - NUREG-1150 MACCS 1.5.9 Peach Bottom Model - Purpose

M1METCOD001 2

(THIS NUMBER SHOULD BE SET TO 4 FOR RISK ASSESSMENT) 1000

Variable Name - LIMSPA

Purpose - Last Spatial Interval for Measured Weather - Variable Name

Source - NUREG-1150 MACCS 1.5.9 Peach Bottom Model - Purpose

Source - NUREG-1150 MACCS 1.5.9 Peach Bottom Model - Purpose

M2LIMSPA001 25

1000

Variable Name - BNDMXH

Purpose - Boundary weather mixing layer height - Variable Name

Source - NUREG-1150 MACCS 1.5.9 Peach Bottom Model - Purpose

Source - NUREG-1150 MACCS 1.5.9 Peach Bottom Model - Purpose

M2BNDMXH001 1000. (METERS)

1000 1000 1000 1000 1000 1000 1000 1000 1000 1000

Variable Name - IBDSTB

Purpose - Boundary weather stability class index - Variable Name

Source - NUREG-1150 MACCS 1.5.9 Peach Bottom Model - Purpose

Source - NUREG-1150 MACCS 1.5.9 Peach Bottom Model - Purpose

M2IBDSTB001 4 (D-STABILITY)

1000

Variable Name - BNDRAN

Purpose - Boundary weather rain rate. - Variable Name

Source - NUREG-1150 MACCS 1.5.9 Peach Bottom Model - Purpose

(mm/hr)

M2BNDRAN001 5. (MM/HR)

Variable Name - BNDWND

1000

Purpose - Boundary weather wind speed.

Source - NUREG-1150 MACCS 1.5.9 Peach Bottom Model.

M2BNDWNO01 4. (M/S)

Variable Name - NSMPLS

Purpose - Number of samples per bin.

Source - NUREG-1150 MACCS 1.5.9 Peach Bottom Model.

M4NSMPLS001 4 (THIS NUMBER SHOULD BE SET TO 4 FOR RISK ASSESSMENT)

Variable Name - NNRINT

Purpose - Number of rain distance intervals for binning.

Source - NUREG-1150 MACCS 1.5.9 Peach Bottom Model.

M4NNRINT001 6

Variable Name - RNDSTS

Purpose - Endpoints of the rain distance intervals (kilometers).

Source - NUREG-1150 MACCS 1.5.9 Peach Bottom Model.

M4RNDSTS001 3.22 5.63 11.27 20.92 40.23 80.47 KM

Variable Name - RNRATE

Purpose - Number of rain intensity breakpoints.

Source - NUREG-1150 MACCS 1.5.9 Peach Bottom Model.

M4NRINTN001 3

Variable Name - RNRATE

Purpose - Rain intensity breakpoints for weather binning  
(millimeters per hour).

Source - NUREG-1150 MACCS 1.5.9 Peach Bottom Model.

M4RNRATE001 2. 4. 6.

Variable Name - IRSEED  
Purpose - Initial seed for random number generator.  
Source - NUREG-1150 MACCS 1.5.9 Peach Bottom Model.

M4IRSEED001 79

Variable Name - ATNAM2  
Purpose - Descriptive text identifying the source term. This text is used to identify specific source terms in the output.  
Source - Arbitrary selection, only one source term is used for each case.

RDATNAM2001 'SOURCE TERM 1'

Variable Name - OLARM  
Purpose - Time after accident initiation when the accident reaches general emergency conditions (as defined in NUREG-0654), or when plant personnel can reliably predict that general emergency conditions will be attained.  
Source - OLARM was estimated from the sequence descriptions presented in the "MAAP Analysis to Support Shoreham 100% PRA," (reference 4).

CASE 1, OLARM = 0.5 hrs:

RDOALARM001 1800.

CASE 2, OLARM = 0.5 hrs:

RDOALARM001 1800.

CASE 3, OLARM = 0.5 hrs:

RDOALARM001 1800.

CASE 4, OLARM = 0.5 hrs:

RDOALARM001 1800.

CASE 5, OLARM = 1.0 hrs:

RDOALARM001 3600.

CASE 6, OLARM = 1.0 hrs:

RDOALARM001 3600.

CASE 7, OLARM = 0.5 hrs:

RDOALARM001 1800.

CASE 8, OLARM = 16. hrs:

RDOALARM001 57600.

CASE 9, OLARM = 16. hrs:

RDOALARM001 57600.

CASE 10, OLARM = 1.0 hrs:

RDOALARM001 3600.

Variable Name - NUMREL

Purpose - Number of plume segments that are released.

Source - PLG-0614, Table 3

RDNUMREL001 1

Variable Name - MAXRIS

Purpose - Selection of risk-dominant plume.

Source - Single plume release.

RDMAXRIS001 1

Variable Name - REFTIM

Purpose - Reference time for dispersion and radioactive decay.

Source - A value of 0.50 is assumed for this analysis. This results in the midpoint of the plume's release period being used as

the representative time point for the dispersion, dry deposition, and radioactive decay models.

RDREFTIM001	0.50		
Variable Name	- PLHEAT		
Purpose	- Heat content of plume release (W).		
Source	- PLG-0614, Table 3		
RDPLHEAT001	0.0		
Variable Name	- PLHITE		
Purpose	- Height of plume segments at release (m).		
Source	- PLG-0614, Table 3		
RDPLHITE001	10.		
Variable Name	- PLUDUR		
Purpose	- Duration of plume segments (s) (Case Dependent).		
Source	- PLG-0614, Table 3		
CASE 1:			
RDPLUDUR001	7200.		
CASE 2:			
RDPLUDUR001	7200.		
CASE 3:			
RDPLUDUR001	7200.		
CASE 4:			
RDPLUDUR001	36000.		
CASE 5:			
RDPLUDUR001	7200.		

CASE 6:  
RDPLUDUR001      28800.

CASE 7:  
RDPLUDUR001      27000.

CASE 8:  
RDPLUDUR001      7200.

CASE 9:  
RDPLUDUR001      7200.

CASE 10:  
RDPLUDUR001      72000.

Variable Name    - PDELAY  
Purpose           - Time of release for each plume segment (s) (Case Dependent).  
Source            - PLG-0614, Table 3

CASE 1:  
RDPDELAY001      7200.

CASE 2:  
RDPDELAY001      7200.

CASE 3:  
RDPDELAY001      7200.

CASE 4:  
RDPDELAY001      3600.

CASE 5:  
RDPDELAY001      57600.

CASE 6:

RDPDELAY001      50400.

CASE 7:

RDPDELAY001      32400.

CASE 8:

RDPDELAY001      140400.

CASE 9:

RDPDELAY001      140400.

CASE 10:

RDPDELAY001      90000.

Variable Name    - RELFAC

Purpose            - Release fractions for isotope groups in release (Case  
Dependent).

Sources          - Xe/Kr - PLG-0614, Table 3.  
                  I    - PLG-0614, Table 3. (Inorganic I)  
                  Cs   - PLG-0614, Table 3.  
                  Te   - PLG-0614, Table 3.  
                  Sr   - PLG-0614, Table 3.  
                  Ru   - PLG-0614, Table 3.  
                  La   - PLG-0614, Table 3. (0.0 for all cases)  
                  Ce   - assumed to be 0.0 for all cases.  
                  Ba   - assumed to be 0.0 for all cases.

Ce and Ba releases are assumed to be zero.

\* isotope groups:

*	Xe/Kr	I	Cs	Te	Sr	Ru	La	Ce	Ba
---	-------	---	----	----	----	----	----	----	----

CASE 1:

RDRELFR001	1.0E+0	4.0E-1	4.9E-1	1.0E-5	2.0E-3	6.0E-4	0.0E+0	0.0	0.0
------------	--------	--------	--------	--------	--------	--------	--------	-----	-----

CASE 2:

RDRELFRC001 1.0E+0 2.0E-1 2.3E-1 1.0E-5 1.0E-3 3.2E-4 0.0E+0 0.0 0.0

CASE 3:

RDRELFRC001 1.0E+0 1.0E-5 1.0E-5 1.0E-5 1.0E-5 1.0E-5 0.0E+0 0.0 0.0

CASE 4:

RDRELFRC001 1.0E+0 7.0E-2 7.0E-2 3.0E-5 1.8E-3 5.0E-4 0.0E+0 0.0 0.0

CASE 5:

RDRELFRC001 1.0E+0 1.0E-1 1.9E-1 1.0E-5 3.5E-4 1.0E-4 0.0E+0 0.0 0.0

CASE 6:

RDRELFRC001 7.0E-1 4.0E-2 4.0E-2 1.0E-5 8.0E-4 3.0E-5 0.0E+0 0.0 0.0

CASE 7:

RDRELFRC001 1.0E+0 2.0E-3 2.0E-3 1.0E-5 1.0E-5 2.0E-5 0.0E+0 0.0 0.0

CASE 8:

RDRELFRC001 1.0E+0 9.0E-2 9.9E-2 1.0E-5 6.0E-4 2.0E-4 0.0E+0 0.0 0.0

CASE 9:

RDRELFRC001 1.0E+0 1.0E-5 1.0E-5 1.0E-5 1.0E-5 1.0E-5 0.0E+0 0.0 0.0

CASE 10:

RDRELFRC001 1.0E-2 3.0E-5 3.9E-5 1.0E-5 1.0E-5 1.0E-5 0.0E+0 0.0 0.0



### 3.0 EARLY Input Data

Variable Name - EANAM1  
Purpose - General descriptive title describing this "EARLY" input file.

MIEANAM1001 'EARLY Input - Shoreham PLG-0614 Releases using PB Surrogate Site'

Variable Name - ENDAT2  
Purpose - Flag to indicate if this is the last program in the series to be run.  
Source - NUREG-1150 MACCS 1.5.9 Peach Bottom Model.

MIENDAT2001 .FALSE. (SET THIS VALUE TO .TRUE. TO SKIP CHRONC)

Variable Name - IPLUME  
Purpose - Defines the dispersion model option used.  
Dispersion model option code: 1 - straight line  
2 - wind-shift with rotation  
3 - wind-shift without rotation  
Source - NUREG-1150 MACCS 1.5.9 Peach Bottom Model.

MIIPLUME001 2

Variable Name - NUMFIN  
Purpose - Defines the number of fine grid subdivisions used by the model. (3, 5, or 7 allowed)  
Source - NUREG-1150 MACCS 1.5.9 Peach Bottom Model.

MINUMFIN001 7 (3, 5, OR 7 ALLOWED)

Variable Name - IPRINT  
Purpose - Level of debug output required, normal runs should specify zero

Source - NUREG-1150 MACCS 1.5.9 Peach Bottom Model.

MIIPRINT001 0

Variable Name - **OVRRID**

Purpose - Flag indicating if wind-roses from ATMOS are to be overridden.

Source - NUREG-1150 MACCS 1.5.9 Peach Bottom Model.

MIOVRRID001 .FALSE. (USE THE WIND ROSE CALCULATED FOR EACH WEATHER BIN)

Variable Name - **RISCAT**

Purpose - Logical flag signifying that the breakdowns of risk by weather category bin are to be presented to show their relative contribution to the mean.

Source - NUREG-1150 MACCS 1.5.9 Peach Bottom Model.

MIRISCAT001 .FALSE.

Variable Name - **POPFLG**

Purpose - Location of population distribution data.

Source - NUREG-1150 MACCS 1.5.9 Peach Bottom Model.

PDPOPFLG001 .FILE

Variable Name - **NUMORG**

Purpose - Number of organs defined for health effects.

Source - NUREG-1150 MACCS 1.5.9 Peach Bottom Model.

ODNUMORG001 9

Variable Name - **ORGNAM**

Purpose - Names of organs defined for health effects.

Source - NUREG-1150 MACCS 1.5.9 Peach Bottom Model.

ODORGNAM001 'SKIN', 'EDEWBODY', 'LUNGS', 'RED MARR', 'LOWER LI', 'STOMACH',  
ODORGNAM002 'THYROIDH', 'BONE SUR', 'BREAST'

Variable Name - CSFACT

Purpose - Cloud shielding factor; three values of each protection factor are supplied, one for each type of activity:  
1 - evacuees while moving  
2 - normal activity in sheltering and evacuation zone  
3 - sheltered activity

Source - NUREG-1150 MACCS 1.5.9 Peach Bottom Model.

\* evacuees normal shelter  
\*

SECSFACT001 1. 0.75 0.50 \* PEACH BOTTOM SHELTERING VALUE

Variable Name - PROTIM

Purpose - Inhalation protection factor; three values of each protection factor are supplied, one for each type of activity.

Source - NUREG-1150 MACCS 1.5.9 Peach Bottom Model.

SEPROTIM001 1. 0.41 0.33 \* VALUES FOR NORMAL ACTIVITY AND  
\* SHELTERING SELECTED BY S. ACHARYA,  
NRC

Variable Name - BRRATE

Purpose - breathing rate (cubic meters per second) ; three values are supplied, one for each type of activity.

Source - NUREG-1150 MACCS 1.5.9 Peach Bottom Model.

SEBRRATE001 2.66E-4 2.66E-4 2.66E-4

Variable Name - SKPFAC

Purpose - Skin protection factor; three values are supplied, one for each type of activity.

Source - NUREG-1150 MACCS 1.5.9 Peach Bottom Model.

SESKPFAC001 1.0 0.41 0.33 \* VALUES FOR NORMAL ACTIVITY AND  
\* SHELTERING SELECTED BY S. ACHARYA,  
NRC

Variable Name - GSHFAC

Purpose - Ground shielding factor; three values are supplied, one for each type of activity.

Source - NUREG-1150 MACCS 1.5.9 Peach Bottom Model.

SEGSHFAC001 0.5 0.33 0.1 \* VALUE FOR NORMAL ACTIVITY SELECTED BY  
\* S. ACHARYA, NRC; PEACH BOTTOM SHEL.  
VALUE

Variable Name - RESCON

Purpose - Resuspension inhalation model concentration coefficient (/meter). RESCON = 1E-4 is appropriate for mechanical resuspension by vehicles. RESAF = 2.11 days causes 1E-4 to decay in one week to 1E-5, the value of RESCON used in the first term of the long-term resuspension equation used in CHRONC.

Source - NUREG-1150 MACCS 1.5.9 Peach Bottom Model.

SERESCON001 1.E-4 (RESUSPENSION IS TURNED ON)

Variable Name - RESHAF

Purpose - Resuspension concentration coefficient half-life (sec).

Source - NUREG-1150 MACCS 1.5.9 Peach Bottom Model.

SERESHAF001 1.82E5 (2.11 DAYS)

Variable Name - EANAM2

Purpose - Specific description of the emergency response scenario being used.

Source - NUREG-1150 MACCS 1.5.9 Peach Bottom Model.

EZEANAM2001 'EVACUATION WITHIN 10 MILES, RELOCATION MODELS APPLY ELSEWHERE'

Variable Name - WTNAME

Purpose - The type of weighting to be applied to the emergency response scenarios; must supply a value of either 'TIME' or 'PEOPLE'.

Source - NUREG-1150 MACCS 1.5.9 Peach Bottom Model.

EZWTNAME001 'PEOPLE'

Variable Name - WTFRAC

Purpose - Weighting fraction applicable to this scenario.

Source - NUREG-1150 MACCS 1.5.9 Peach Bottom Model.

EZWTFRAC001 0.95

Variable Name - ESPEED

Purpose - Radial evacuation speed (M/S).

Source - NUREG-1150 MACCS 1.5.9 Peach Bottom Model.

EZESPEED001 4.8 \* PEACH BOTTOM

Variable Name - LASMOV

Purpose - The last ring in the movement zone.

Source - NUREG-1150 MACCS 1.5.9 Peach Bottom Model.

\* LAST RING IN THE MOVEMENT ZONE

\*

EZLASMOV001 15 (EVACUEES DISAPPEAR AFTER TRAVELING TO 20 MILES)

Variable Name - INIEVA

Purpose - The first spatial interval in the evacuation zone.

Source - NUREG-1150 MACCS 1.5.9 Peach Bottom Model.

EZINIEVA001        1        (NO INNER SHELTER ZONE)

Variable Name    - LASEVA

Purpose            - The outer bounds of distance intervals for the three evacuation zones.

Source           - NUREG-1150 MACCS 1.5.9 Peach Bottom Model.

EZLASEVA001       0    0    12 (SINGLE EVACUATION ZONE OUT TO 10 MILES)

Variable Name    - EDELAY

Purpose            - Evacuation delay times for the three evacuation zones (sec).

Source           - NUREG-1150 MACCS 1.5.9 Peach Bottom Model.

EZEDELAY001    0.   0.       5400.

Variable Name    - TTOSH1

Purpose            - The time to take shelter in the inner shelter zone (sec).

Source           - NUREG-1150 MACCS 1.5.9 Peach Bottom Model. (No inner shelter zone.)

SRTTOSH1001      0.       (THERE IS NO INNER SHELTER ZONE)

Variable Name    - SHELT1

Purpose            - The shelter duration in the inner shelter zone (sec).

Source           - NUREG-1150 MACCS 1.5.9 Peach Bottom Model. (No inner shelter zone.)

SRSHELT1001      0.       (THERE IS NO INNER SHELTER ZONE)

Variable Name    - LASHE2

Purpose            - The last ring of the outer shelter zone.

Source           - NUREG-1150 MACCS 1.5.9 Peach Bottom Model.

SRLASHE2001      0        (THERE IS NO OUTER SHELTER ZONE)

Variable Name - TTOSH2  
Purpose - The time to take shelter in the outer shelter zone (sec).  
Source - NUREG-1150 MACCS 1.5.9 Peach Bottom Model. (No outer shelter zone.)

SRTTOSH2001 0. (THERE IS NO OUTER SHELTER ZONE)

Variable Name - SHEL2  
Purpose - The shelter duration in the outer shelter zone (sec).  
Source - NUREG-1150 MACCS 1.5.9 Peach Bottom Model. (No outer shelter zone.)

SRSHEL2001 0. (THERE IS NO OUTER SHELTER ZONE)

Variable Name - ENDEMP  
Purpose - Duration of the emergency phase (seconds from plume arrival).  
Source - NUREG-1150 MACCS 1.5.9 Peach Bottom Model.

SRENDEMP001 604800. (ONE WEEK)

Variable Name - CRIORG  
Purpose - Critical organ for relocation decisions.  
Source - NUREG-1150 MACCS 1.5.9 Peach Bottom Model.

SRCRIORG001 'EDEWBODY'

Variable Name - TIMHOT  
Purpose - Hot spot relocation time (seconds from plume arrival).  
Source - NUREG-1150 MACCS 1.5.9 Peach Bottom Model (same as TIMHOT).

SRTIMHOT001 43200. (ONE-HALF DAY)

Variable Name - TIMNRM

Purpose - Normal relocation time (seconds from plume arrival).  
Source - NUREG-1150 MACCS 1.5.9 Peach Bottom Model (same as TIMNRM).

SRTIMNRM001 86400. (ONE DAY)

Variable Name - DOSHOT  
Purpose - Hot spot relocation dose criterion threshold (sieverts).  
Source - NUREG-1150 MACCS 1.5.9 Peach Bottom Model (same as DOSHOT).

SRDOSHOT001 0.5 (50 REM DOSE TO WHOLE BODY IN 1 WEEK TRIGGERS RELOCATION)

Variable Name - DOSNRM  
Purpose - Normal relocation dose criterion threshold (sieverts).  
Source - NUREG-1150 MACCS 1.5.9 Peach Bottom Model (same as DOSHOT).

SRDOSNRM001 0.25 (25 REM DOSE TO WHOLE BODY IN 1 WEEK TRIGGERS RELOCATION)

Variable Name - NUMEFA  
Purpose - Number of early fatality effects.  
Source - NUREG-1150 MACCS 1.5.9 Peach Bottom Model.

EFNUMEFA001 3

Variable Name - EFFACA  
Purpose - The alpha factor in the hazard function associated with the target organ.

Variable Name - EFFACB  
Purpose - The beta (exponential) factor in the hazard function associated with the target organ.  
Source - NUREG-1150 MACCS 1.5.9 Peach Bottom Model.

Variable Name - EFFTHR  
Purpose - The threshold dose associated with the target organ.  
Source - NUREG-1150 MACCS 1.5.9 Peach Bottom Model.



\*  
 \* LD50 BY T  
 \* ORGNAM EFFACA EFFACB EFFTHR 1 7 14 30 200 365  
 \*

EFATAGRP001 'RED MARR' 4. 6. 1.5 4 8 16  
 EFATAGRP002 'LUNGS' 10.0 7. 5.0 10 160 370 920  
 EFATAGRP003 'LOWER LI' 15. 10. 7.5 15 35

\*  
 \* NOTE: LUNG PARAMETERS TAKEN FROM LETTER FROM B. SCOTT TO N. WALD DATED  
 3/7/87,  
 \* SHAPE FACTOR OF 7 IS APPROPRIATE FOR EXTERNAL AND INTERNAL DOSE  
 DELIVERED  
 \* AT THE SAME TIME.

Variable Name - NUMEIN  
 Purpose - The number of early injury effects.  
 Source - NUREG-1150 MACCS 1.5.9 Peach Bottom Model.

EINUMIN001 7

Variable Name - EINAM  
 Purpose - The name of the early injury effect.

Variable Name - ORGNAM  
 Purpose - The name of the target organ for this early injury effect.

Variable Name - EISUSC  
 Purpose - The fraction of the population that is susceptible to this  
 early injury effect.

Variable Name - EITHRE  
 Purpose - The threshold dose below which the risk of the injury is  
 zero.

Variable Name - EIFACA  
 Purpose - The alpha factor in the hazard function for the injury.

Variable Name - EIFACB  
 Purpose - The beta factor in the hazard function for the injury.  
 Source - NUREG-1150 MACCS 1.5.9 Peach Bottom Model.

							D50 VS T			
*	EINAME	ORGNAM	EISUSC	EITHRE	EIFACA	EIFACB	1	7	10	21
*	EINJUGRP001	'PRODROMAL VOMIT'	'STOMACH'	1.	.5	2.	3.	2	5	
	EINJUGRP002	'DIARRHEA'	'STOMACH'	1.	1.	3.	2.5	3	6	
	EINJUGRP003	'PNEUMONITIS'	'LUNGS'	1.	5.	10.	7.	=	DEATH	
	EINJUGRP004	'SKIN ERYTHEMA'	'SKIN'	1.	3.	6.	5.	6	20	
	EINJUGRP005	'TRANSEPIDERMAL'	'SKIN'	1.	10.	20.	5.	20	80	
	EINJUGRP006	'THYROIDITIS'	'THYROIDH'	1.	40.	240.	2.			240
	EINJUGRP007	'HYPOTHYROIDISM'	'THYROIDH'	1.	2.	60.	1.3			60

\*  
 \* NOTE: THYROIDH ACUTE DOSE CONVERSION FACTORS ARE USED TO CALCULATE  
 \* THYROID INJURIES. WHEN THESE DOSE FACTORS WERE CALCULATED,  
 \* INHALATION DOSE FACTORS FOR IODINE ISOTOPES WERE REDUCED BY A  
 \* FACTOR OF FIVE TO ACCOUNT FOR THE REDUCED EFFECTIVENESS OF DOSE FROM  
 \* IODINE ISOTOPES.  $0.0048 = 0.012 \times 0.4$ ;  $0.0053 = 0.012 \times (17X7)/270$ .

Variable Name - NUMACA  
 Purpose - The number of acute exposure cancer effects.  
 Source - NUREG-1150 MACCS 1.5.9 Peach Bottom Model.

LCNUMACA001 7

Variable Name - ACTHRE  
 Purpose - The dose threshold for linear dose response (Sv).  
 Source - NUREG-1150 MACCS 1.5.9 Peach Bottom Model.

LCACTHRE001 1.5

Variable Name - ACNAME

Purpose - The name of the latent cancer effect.

Variable Name - **ORGNAM**

Purpose - The name of the target organ for this latent cancer effect.

Variable Name - **ACSUSC**

Purpose - The fraction of the population that is susceptible to this latent cancer effect.

Variable Name - **DOSEFA**

Purpose - The alpha factor of dose dependence in the cancer risk model.

Variable Name - **DOSEFB**

Purpose - The beta factor of dose dependence in the cancer risk model.

Variable Name - **CFRISK**

Purpose - The lifetime risk factor for cancer death.

Variable Name - **CIRISK**

Purpose - The lifetime risk factor for cancer injury.

Source - NUREG-1150 MACCS 1.5.9 Peach Bottom Model.

*	ACNAME	ORGNAM	ACSUSC	DOSEFA	DOSEFB	CFRISK	CIRISK
*							
LCANCERS001	'LEUKEMIA'	'RED MARR'	1.	.39	.61	3.7E-3	3.7E-3
LCANCERS002	'BONE'	'BONE SUR'	1.	.39	.61	1.5E-4	1.5E-4
LCANCERS003	'BREAST'	'BREAST'	1.	1.	0.	6.0E-3	1.7E-2
LCANCERS004	'LUNG'	'LUNGS'	1.	.39	.61	5.1E-3	5.7E-3

LCANCERS005	'THYROID'	'THYROIDH'	1.	1.	0.	7.2E-4
7.2E-3						
LCANCERS006	'GI'	'LOWER LI'	1.	.39	.61	1.5E-2
2.5E-2						
LCANCERS007	'OTHER'	'LOWER LI'	1.	.39	.61	7.5E-3
1.3E-2						

\*

\* NOTE: THYROIDH LIFETIME DOSE CONVERSION FACTORS ARE USED TO CALCULATE  
 \* THYROID CANCERS. WHEN THESE DOSE FACTORS WERE CALCULATED, INHALATION  
 \* AND INGESTION DOSE FACTORS FOR IODINE ISOTOPES WERE REDUCED BY A  
 \* FACTOR OF THREE TO ACCOUNT FOR THE REDUCED EFFECTIVENESS OF DOSE FROM  
 \* IODINE ISOTOPES.  $0.74 = (17 + 9)/(17 + 9 + 9)$  AND  $0.26 = 1.0 - 0.74$ .

Results Name - TYPE1OUT

Purpose - Total number of a given effect (latent cancer, early death,  
 early injury)

\* NUMBER OF DESIRED RESULTS OF THIS TYPE

\*

TYPE1NUMBER 35

\*

TYPE1OUT001	'ERL FAT/TOTAL'	1	26	CCDF (0 TO 1000 MILES)
TYPE1OUT002	'ERL INJ/PRODROMAL VOMIT'	1	26	CCDF
TYPE1OUT003	'ERL INJ/DIARRHEA'	1	26	
TYPE1OUT004	'ERL INJ/PNEUMONITIS'	1	26	
TYPE1OUT005	'ERL INJ/THYROIDITIS'	1	26	
TYPE1OUT006	'ERL INJ/HYPOTHYROIDISM'	1	26	
TYPE1OUT007	'ERL INJ/SKIN ERYTHEMA'	1	26	
TYPE1OUT008	'ERL INJ/TRANSEPIDERMAL'	1	26	
TYPE1OUT009	'CAN FAT/TOTAL'	1	26	CCDF
TYPE1OUT010	'CAN FAT/LUNG'	1	26	
TYPE1OUT011	'CAN FAT/THYROID'	1	26	
TYPE1OUT012	'CAN FAT/BREAST'	1	26	
TYPE1OUT013	'CAN FAT/GI'	1	26	
TYPE1OUT014	'CAN FAT/LEUKEMIA'	1	26	

TYPE1OUT015	'CAN FAT/BONE'	1	26	
TYPE1OUT016	'CAN FAT/OTHER'	1	26	
TYPE1OUT017	'CAN INJ/TOTAL'	1	26	
TYPE1OUT018	'ERL FAT/TOTAL'	1	19	(0 TO 50 MILES)
TYPE1OUT019	'ERL INJ/PRODRIMAL VOMIT'	1	19	
TYPE1OUT020	'ERL INJ/DIARRHEA'	1	19	
TYPE1OUT021	'ERL INJ/PNEUMONITIS'	1	19	
TYPE1OUT022	'ERL INJ/THYROIDITIS'	1	19	
TYPE1OUT023	'ERL INJ/HYPOTHYROIDISM'	1	19	
TYPE1OUT024	'ERL INJ/SKIN ERYTHEMA'	1	19	
TYPE1OUT025	'ERL INJ/TRANSEPIDERMAL'	1	19	
TYPE1OUT026	'CAN FAT/TOTAL'	1	19	
TYPE1OUT027	'ERL FAT/TOTAL'	1	12	(0 TO 10 MILES)
TYPE1OUT028	'ERL INJ/PRODRIMAL VOMIT'	1	12	
TYPE1OUT029	'ERL INJ/DIARRHEA'	1	12	
TYPE1OUT030	'ERL INJ/PNEUMONITIS'	1	12	
TYPE1OUT031	'ERL INJ/THYROIDITIS'	1	12	
TYPE1OUT032	'ERL INJ/HYPOTHYROIDISM'	1	12	
TYPE1OUT033	'ERL INJ/SKIN ERYTHEMA'	1	12	
TYPE1OUT034	'ERL INJ/TRANSEPIDERMAL'	1	12	
TYPE1OUT035	'CAN FAT/TOTAL'	1	12	

Results Name - TYPE2OUT

Purpose - The furthest distance at which a given risk of early death is exceeded.

\* NUMBER OF DESIRED RESULTS OF THIS TYPE

\*

TYPE2NUMBER 1

\*

\* FATALITY RISK THRESHOLD

\*

TYPE2OUT001 0.

Results Name - TYPE3OUT

Purpose - The number of people whose acute dose to a given organ exceeds a given threshold.

\* NUMBER OF DESIRED RESULTS OF THIS TYPE

\*

TYPE3NUMBER 3

\*

	ORGAN NAME	DOSE THRESHOLD (SV)	DOSE FLAG
--	------------	---------------------	-----------

\*

TYPE3OUT001	'RED MARR'	1.5	ACUTE
TYPE3OUT002	'LUNGS'	5.0	ACUTE
TYPE3OUT003	'EDEWBODY'	0.05	LIFETIME

Results Name - TYPE4OUT

Purpose - Edits of 360-degree average risk of a given effect at a given distance.

\* NUMBER OF DESIRED RESULTS OF THIS TYPE

\*

TYPE4NUMBER 5

\*

	RADIAL INDEX	TYPE OF EFFECT
--	--------------	----------------

\*

TYPE4OUT001	1	'ERL FAT/TOTAL'
TYPE4OUT002	2	'ERL FAT/TOTAL'
TYPE4OUT003	3	'ERL FAT/TOTAL'
TYPE4OUT004	4	'ERL FAT/TOTAL'
TYPE4OUT005	5	'ERL FAT/TOTAL'

Results Name - TYPE5OUT

Purpose - The total population dose to a given organ between two distances.

\* NUMBER OF DESIRED RESULTS OF THIS TYPE

\*

TYPE5NUMBER 3

\*

\* ORGAN I1DIS5 I2DIS5

\*

TYPE5OUT001	'EDEWBODY'	1	12		(0-10 MILES)
TYPE5OUT002	'EDEWBODY'	1	19	CCDF	(0-50 MILES)
TYPE5OUT003	'EDEWBODY'	1	26	CCDF	(0-1000 MILES)

Results Name - TYPE6OUT

Purpose - The centerline dose to an organ vs. distance by pathway.

\* NUMBER OF DESIRED RESULTS OF THIS TYPE

\*

TYPE6NUMBER 0

Results Name - TYPE7OUT

Purpose - The centerline risk of a given effect vs. distance.

\* NUMBER OF DESIRED RESULTS OF THIS TYPE

\*

TYPE7NUMBER 0

Results Name - TYPE8OUT

Purpose - The population-weighted fatality risk between two distances.

\* NUMBER OF DESIRED RESULTS OF THIS TYPE

\*

TYPE8NUMBER 2

\*

\* NAME I1DIS8 I2DIS8

\*

TYPE8OUT001	'ERL FAT/TOTAL'	1	5	CCDF	(0-EXCL ZONE + 1 MI)
TYPE8OUT002	'CAN FAT/TOTAL'	1	12	CCDF	(0-10 MILES)

## Emergency Response Scenario Number 2:

The following inputs represent changes to the base case defined above which are necessary to model the second "EARLY" cohort.

**Variable Name:** EZEANAM2  
**Purpose:** Specific description of the emergency response scenario being used.

**Source:** - NUREG-1150 MACCS 1.5.9 Peach Bottom Model.

\*\*

\* EMERGENCY RESPONSE SCENARIO NUMBER 2

\*\*

\*

EZEANAM2001 (NO EVACUATION, RELOCATION MODELS APPLY EVERYWHERE)

**Variable Name:** - WTFRAC

**Purpose:** - Weighting fraction applicable to this scenario.

**Source:** - NUREG-1150 MACCS 1.5.9 Peach Bottom Model.

EZWTFRAC001 0.05

**Variable Name:** - LASMOV

**Purpose:** - The last ring in the movement zone.

**Source:** - NUREG-1150 MACCS 1.5.9 Peach Bottom Model.

\* LAST RING IN THE MOVEMENT ZONE

\*

EZLASMOV001 0 (A ZERO TURNS OFF THE EVACUATION MODEL)

**Emergency Response Scenario Number 3:**



The following inputs represent changes to the previously defined case which are necessary to model the third "EARLY" cohort.

Variable Name - EANAM2  
Purpose - Specific description of the emergency response scenario being used.

Source - NUREG-1150 MACCS 1.5.9 Peach Bottom Model.

\*\*\*\*\*

\*\*

\* EMERGENCY RESPONSE SCENARIO NUMBER 3

\*\*\*\*\*

\*\*

\*

EZEANAM2001 'SHELTERING WITHIN 10 MILES, RELOCATION MODELS APPLY ELSEWHERE'

Variable Name - WTFRAC  
Purpose - Weighting fraction applicable to this scenario.  
Source - NUREG-1150 MACCS 1.5.9 Peach Bottom Model.

EZWTFRAC001 0.0 (THIS CASE IS NOT BEING COMBINED WITH SCENARIOS 1 AND 2)

Variable Name - LASHE2  
Purpose - The last ring of the outer shelter zone.  
Source - NUREG-1150 MACCS 1.5.9 Peach Bottom Model.

\* LAST RING OF THE OUTER SHELTER ZONE

\*

SRLASHE2001 12 (OUTER SHELTER ZONE EXTENDS FROM 0 TO 10 MILES)

Variable Name - TTOSH2  
Purpose - The time to take shelter in the outer shelter zone (sec).  
Source - NUREG-1150 MACCS 1.5.9 Peach Bottom Model. (No outer shelter zone.)

Variable Name - TTOSH1  
Purpose - The time to take shelter in the inner shelter zone (sec).  
Source - NUREG-1150 MACCS 1.5.9 Peach Bottom Model.

SRTTOSH1001 2700. (45 MINUTES TO TAKE SHELTER)

Variable Name - SHELTI  
Purpose - The shelter duration in the inner shelter zone (sec).  
Source - NUREG-1150 MACCS 1.5.9 Peach Bottom Model.

SRSHELTI001 43200. (12 HOUR SHELTER DURATION)

#### 4.0 CHRONC Input Data

Variable Name - CHNAME  
Purpose - General descriptive title describing this "CHRONC" input file.

CHCHNAME001 'CHRONC Input - Shoreham PLG-0614 Releases using PB Surrogate Site'

Variable Name - EVACST  
Purpose - The evacuation cost (dollars/person-day).  
Source - NUREG-1150 MACCS 1.5.9 Peach Bottom Model.

CHEVACST001 27.00

Variable Name - RELCST  
Purpose - The relocation cost (dollars/person-day).  
Source - NUREG-1150 MACCS 1.5.9 Peach Bottom Model.

CHRELCST001 27.00

Variable Name - TMIPND  
Purpose - The end of the intermediate phase period (seconds from accident initiation).  
Source - NUREG-1150 MACCS 1.5.9 Peach Bottom Model.

CHTMIPND001 604800. (7 DAYS, NO INTERMEDIATE PHASE)

Variable Name - TMPACT  
Purpose - The action period (projection period) from the start of the long-term phase, to the point at which the long term dose criterion is evaluated (seconds).  
Source - NUREG-1150 MACCS 1.5.9 Peach Bottom Model.

CHTMPACT001 1.58E8 (5 YEARS)

Variable Name - DSCRTI

Purpose - The dose criterion for intermediate phase relocation (sv).

Source - NUREG-1150 MACCS 1.5.9 Peach Bottom Model

CHDSCRTI001 1.0E5 (NO INTERMEDIATE PHASE RELOCATION)

Variable Name - DSCRLT

Purpose - The dose criterion for long-term relocation (sv).

Source - NUREG-1150 MACCS 1.5.9 Peach Bottom Model

CHDSCRLT001 0.04 (2 REM IN FIRST YEAR, 0.5 REM PER YEAR FOR YRS 2 - 5)

Variable Name - CRTOCR

Purpose - The critical organ name for long-term actions.

Source - The value used in the NUREG-1150 MACCS 1.5.9 Peach Bottom Model

CHCRTOCR001 'EDEWBODY'

Variable Name - LVLDEC

Purpose - The number of levels of decontamination.

Source - NUREG-1150 MACCS 1.5.9 Peach Bottom Model

CHLVLDEC001 2

Variable Name - TIMDEC

Purpose - The decontamination times corresponding to the lvldec levels of decontamination (seconds).

Source - NUREG-1150 MACCS 1.5.9 Peach Bottom Model

CHTIMDEC001 5.184E6 1.0368E7 (60, 120 DAYS)

Variable Name - DSRFCT

Purpose - The dose reduction factors corresponding to the 1v1dec levels of decontamination.

Source - NUREG-1150 MACCS 1.5.9 Peach Bottom Model.

CHDSRFCT001 3. 15.

Variable Name - CDFRM

Purpose - The cost of farm decontamination per unit area (dollars/hectare) for the various levels of decontamination.

Source - NUREG-1150 MACCS 1.5.9 Peach Bottom Model.

CHCDFRM0001 562.5 1250.

Variable Name - CDNFRM

Purpose - The cost of nonfarm decontamination per person for the various levels of decontamination (dollars/person).

Source - NUREG-1150 MACCS 1.5.9 Peach Bottom Model.

CHCDNFRM001 3000. 8000.

Variable Name - FRFDL

Purpose - The fraction of farmland decontamination cost due to labor for the various decontamination levels.

Source - NUREG-1150 MACCS 1.5.9 Peach Bottom Model.

CHFRFDL0001 .3 .35

Variable Name - FRNFDL

Purpose - The fraction of non-farm decontamination cost due to labor for the various decontamination levels.

Source - NUREG-1150 MACCS 1.5.9 Peach Bottom Model.

CHFRNFDL001 .7 .5

Variable Name - TWKFL

Purpose - The fraction of time workers in farm areas spend in  
decontamination work for the various decontamination levels.

Source - NUREG-1150 MACCS 1.5.9 Peach Bottom Model.

CHTFWK0001 .10 .33

Variable Name - TFWKNF

Purpose - The fraction of time workers in non-farm areas spend in  
decontamination work for the various decontamination levels.

Source - NUREG-1150 MACCS 1.5.9 Peach Bottom Model.

CHTFWKNF001 .33 .33

Variable Name - DLBCST

Purpose - The average cost of decontamination labor  
(dollars/man-year).

Source - NUREG-1150 MACCS 1.5.9 Peach Bottom Model.

CHDLBCST001 35000.

Variable Name - DPRATE

Purpose - The depreciation rate during interdiction period (per year).

Source - NUREG-1150 MACCS 1.5.9 Peach Bottom Model.

CHDPRATE001 .20

Variable Name - DSRATE

Purpose - The societal discount rate during interdiction period (per  
year).

Source - NUREG-1150 MACCS 1.5.9 Peach Bottom Model.

CHDSRATE001 .12

Variable Name - POPCST

Purpose - The urban population removal cost (dollars/person).

Source - NUREG-1150 MACCS 1.5.9 Peach Bottom Model.

CHPOPCST001 5000.

Variable Name - **NGWTRM**

Purpose - The number of terms in the groundshine weathering relationship.

Source - NUREG-1150 MACCS 1.5.9 Peach Bottom Model.

CHNGWTRM001 2

Variable Name - **GWCOEF**

Purpose - The groundshine weathering coefficients.

Source - NUREG-1150 MACCS 1.5.9 Peach Bottom Model.

CHGWCOEF001 0.5 0.5 (GAYLE'S EQUATION)

Variable Name - **TGWHLF**

Purpose - The half-lives corresponding to the groundshine weathering coefficients (s).

Source - NUREG-1150 MACCS 1.5.9 Peach Bottom Model.

CHTGWHLF001 1.6E7 2.8E9 (GAYLE'S EQUATION)

Variable Name - **GWCOEF**

Purpose - The number of terms in the resuspension weathering relationship.

Source - NUREG-1150 MACCS 1.5.9 Peach Bottom Model.

CHNRWTRM001 3

Variable Name - **RWCOEF**

Purpose - The resuspension concentration coefficients (/ meter).

Source - NUREG-1150 MACCS 1.5.9 Peach Bottom Model.

CHRWCOEF001 1.0E-5 1.0E-7 1.0E-9

Variable Name - TRWHLF

Purpose - The half-lives corresponding to the resuspension concentration coefficients (/ meter).

Source - NUREG-1150 MACCS 1.5.9 Peach Bottom Model.

CHTRWHLF001 1.6E7 1.6E8 1.6E9 (6 MONTHS, 5 YEARS, 50 YEARS)

Variable Name - FRACLD

Purpose - The fraction of area that is land in the region.

Source - Value is not used, since the site file is provided.

CHFRACLD001 1.0E-35 (VALUE NOT USED SINCE SITE FILE PROVIDED)

Variable Name - FRCFRM

Purpose - The fraction of land devoted to farming in the region.

Source - Value is not used, since the site file is provided.

CHFRCFRM001 1.0E-35 (VALUE NOT USED SINCE SITE FILE PROVIDED)

Variable Name - FRMPRD

Purpose - The average value of annual farm production in the region (dollars/hectare).

Source - Value is not used, since the site file is provided.

CHFRMPRD001 0. (VALUE NOT USED SINCE SITE FILE PROVIDED)

Variable Name - DPFRACT

Purpose - The fraction of farm production resulting from dairy production in the region.

Source - Value is not used, since the site file is provided.

CHDPFRCT001 0. (VALUE NOT USED SINCE SITE FILE PROVIDED)



Variable Name - VALFW

Purpose - The value of farm wealth (dollars/hectare).

Source - NUREG-1150 MACCS 1.5.9 Peach Bottom Model.

CHVALWF0001 3421. \* PEACH BOTTOM

Variable Name - FRFIM

Purpose - The fraction of farm wealth in improvements for the region.

Source - NUREG-1150 MACCS 1.5.9 Peach Bottom Model.

CHFRFIM0001 0.25 \* PEACH BOTTOM

Variable Name - FRFIM

Purpose - The non-farm wealth, property and improvements for the region (dollars/person). The value of all residential, business, and public assets which would be lost in the event of permanent interdiction of the area.

Source - NUREG-1150 MACCS 1.5.9 Peach Bottom Model.

CHVALWNF001 78000. \* PEACH BOTTOM

Variable Name - FRNFIM

Purpose - The fraction of non-farm wealth in improvements for the region.

Source - NUREG-1150 MACCS 1.5.9 Peach Bottom Model.

CHFRNFIM001 0.8

Variable Name - KSWTCH

Purpose - Detailed print option control switches.

Source - NUREG-1150 MACCS 1.5.9 Peach Bottom Model.

CHKSWTCH001 0 0 0 0 0 0 0 0 0 0 0 0 0 0 0 0

Variable Name - **NUMWPI**  
 Purpose - Number of nuclides in the water ingestion pathway model.  
 Source - NUREG-1150 MACCS 1.5.9 Peach Bottom Model.

CHNUMWPI001 4

Variable Name - **NAMWPI**  
 Purpose - Name of the nuclide used for this water ingestion pathway model.

Variable Name - **WSHFRI**  
 Purpose - The initial wash-off fraction for the specified nuclide.

Variable Name - **WSHRTA**  
 Purpose - The annual wash-off rate for the specified nuclide.

Variable Name - **WINGF**  
 Purpose - The water ingestion factor for the specified nuclide.

*	NAMWPI	WSHFRI	WSHRTA	WINGF
CHWTRIS0001	SR-89	0.01	0.004	5.0E-6
CHWTRIS0002	SR-90	0.01	0.004	5.0E-6
CHWTRIS0003	CS-134	0.005	0.001	5.0E-6
CHWTRIS0004	CS-137	0.005	0.001	5.0E-6

Variable Name - **NFICRP**  
 Purpose - Number of defined crops in the CHRONC food ingestion model.  
 Source - NUREG-1150 MACCS 1.5.9 Peach Bottom Model.

CHNFICRP001 7 (UP TO 10 ALLOWED)

Variable Name - **NAMCRP**  
 Purpose - Name of the crop category for which this set of growing season and farm fraction applies.

Variable Name - FRCTCH  
 Purpose - Fraction of the edible portion of the harvested crop that is consumed by humans.

Variable Name - FRCTCM  
 Purpose - Fraction of the edible portion of the harvested crop that is consumed by milk-producing animals.

Variable Name - FRCTCB  
 Purpose - Fraction of the edible portion of the harvested crop that is consumed by meat-producing animals.  
 Source - NUREG-1150 MACCS 1.5.9 Peach Bottom Model.

*	NAMCRP	FRCTCH	FRCTCM	FRCTCB
CHCRPTBL001	'PASTURE	' 0.0	0.1	0.9
CHCRPTBL002	'STORED FORAGE	' 0.0	0.13	0.87
CHCRPTBL003	'GRAINS	' 0.35	0.040	0.61
CHCRPTBL004	'GRN LEAFY VEGETABLES'	1.0	0.0	0.0
CHCRPTBL005	'OTHER FOOD CROPS	' 1.0	0.0	0.0
CHCRPTBL006	'LEGUMES AND SEEDS	' 0.24	0.046	0.714
CHCRPTBL007	'ROOTS AND TUBERS	' 1.0	0.0	0.0

Variable Name - NFIISO  
 Purpose - Number of nuclides defined in the CHRONC food ingestion model.  
 Source - NUREG-1150 MACCS 1.5.9 Peach Bottom Model.

CHNFIISO001 6 (UP TO 10 ALLOWED, BEWARE THAT DAUGHTER BUILDUP IS NOT TREATED)

Variable Name - NAMIPI  
 Purpose - Name of the nuclide used for this food pathway model.

Variable Name - DCYPMH

21 **Purpose** - Transfer factor that describes the processing losses and radioactive decay which occurs between the production and the consumption of milk products.

22 **Variable Name** - DCYPBH  
**Purpose** - Transfer factor that describes the processing losses and radioactive decay which occurs between the production and the consumption of meat products.

23 **Variable Name** - TFMLK  
**Purpose** - Transfer factor that describes how much of the radionuclide ingested by the animal ends up in edible milk products.

**Variable Name** - TFBF  
**Purpose** - Transfer factor that describes how much of the radionuclide ingested by the animal ends up in edible meat products.  
**Source** - NUREG-1150 MACCS 1.5.9 Peach Bottom Model

\* TRANSFER FACTORS  
 \*  $[(BQ \text{ TRANSFERRED}) /$   
 \*  $(BQ \text{ INGESTED})]$   
 \* INGESTION PROCESSING AND DECAY  
 \* NUCLIDE MILK/MAN MEAT/MAN MILK MEAT

\* Number of nuclides defined in the CHROM food ingestion  
 \* 

	NAMIPI	DCYPMH	DCYPBH	TFMLK	TFBF
CHISODEF001 SR-89	0.66	0.77	0.022	0.00022	
CHISODEF002 SR-90	1.0	1.0	0.022	0.00022	
CHISODEF003 CS-134	1.0	1.0	0.11	0.023	
CHISODEF004 CS-137	1.0	1.0	0.11	0.024	
CHISODEF005 I-131	0.28	0.18	0.13	0.0024	
CHISODEF006 I-133	0.002	0.0	0.062	0.0011	

Variable Name - TCROOT  
**Purpose** - Defines the transfer factor for the long-term transfer of radionuclides from soil to edible crops. Values are

supplied for each crop category and nuclide treated by the food pathway model.

Source - NUREG-1150 MACCS 1.5.9 Peach Bottom Model.

		GREEN	OTHER	LEGUMES	ROOTS			
		LEAFY	FOOD	AND	AND			
		VEG	CROPS	SEEDS	TUBERS			
	NUCLIDE	PASTURE	FORAGE	GRAINS				
	NAMISO	TCROOT	TCROOT	TCROOT	TCROOT			
CHTCROOT001	SR-89	4.1E-4	1.3E-3	4.3E-5	1.7E-4	8.6E-6	3.7E-4	1.1E-4
CHTCROOT002	SR-90	2.6E-2	9.0E-2	3.3E-3	1.3E-2	6.6E-4	2.8E-2	8.4E-3
CHTCROOT003	CS-134	1.3E-3	7.1E-4	3.5E-5	1.4E-5	1.1E-4	9.3E-5	5.6E-5
CHTCROOT004	CS-137	6.9E-3	1.5E-3	7.6E-5	3.0E-5	2.3E-4	2.0E-4	1.2E-4
CHTCROOT005	I-131	1.6E-4	0.0	0.0	0.0	0.0	0.0	0.0
CHTCROOT006	I-133	1.7E-6	0.0	0.0	0.0	0.0	0.0	0.0

Variable Name - DCYPCH

Purpose - Characterizes the loss due to radioactive decay between the time of harvest and the time of consumption by humans. Values are supplied for each crop category and nuclide treated by the food pathway model.

Source - NUREG-1150 MACCS 1.5.9 Peach Bottom Model.

		GREEN	OTHER	LEGUMES	ROOTS	
		LEAFY	FOOD	AND	AND	
		VEG	CROPS	SEEDS	TUBERS	
	NUCLIDE	PASTURE	FORAGE	GRAINS		
	NAMISO	DCYPCH	DCYPCH	DCYPCH	DCYPCH	
CHDCYPCH001	SR-89	0.0	0.0	0.18	0.21	0.18
CHDCYPCH002	SR-90	0.0	0.0	0.99	0.99	0.99
CHDCYPCH003	CS-134	0.0	0.0	0.84	0.85	0.84
CHDCYPCH004	CS-137	0.0	0.0	0.99	0.99	0.99
CHDCYPCH005	I-131	0.0	0.0	0.0099	0.024	0.0099
0.0099						
CHDCYPCH006	I-133	0.0	0.0	0.0	0.0	0.0

Variable Name - FPLSCH

Purpose - Crop processing and preparation retention factors for nuclides in food crops consumed by humans (fraction retained). Factors reflect loss of nuclides from foods due to processing (for example, washing of fruit, peeling of potatoes, losses during canning) and food preparation (cooking) from the time of processing of the harvested crop to the time of consumption by humans. Factors do not reflect losses due to radioactive decay. Values are supplied for each crop category and nuclide treated by the food pathway model.

Source - NUREG-1150 MACCS 1.5.9 Peach Bottom Model.

*					GREEN	OTHER	LEGUMES	ROOTS
*			STORED		LEAFY	FOOD	AND	AND
*	NUCLIDE	PASTURE	FORAGE	GRAINS	VEG	CROPS	SEEDS	TUBERS
*								
*	NAMISO	FPLSCH	FPLSCH	FPLSCH	FPLSCH	FPLSCH	FPLSCH	FPLSCH
CHFPLSCH001	SR-89	0.0	0.0	0.25	0.5	0.71	0.8	0.8
CHFPLSCH002	SR-90	0.0	0.0	0.25	0.5	0.71	0.8	0.8
CHFPLSCH003	CS-134	0.0	0.0	0.25	0.5	0.71	0.8	0.8
CHFPLSCH004	CS-137	0.0	0.0	0.25	0.5	0.71	0.8	0.8
CHFPLSCH005	I-131	0.0	0.0	0.33	0.5	0.71	0.8	0.8
CHFPLSCH006	I-133	0.0	0.0	0.33	0.5	0.71	0.8	0.8

Variable Name - DCYPCM

Purpose - Retention factors for nuclides in crops from time of harvest to time of consumption by milk-producing animals (fraction retained). Factor reflects losses due to radioactive decay. Values are supplied for each crop category and nuclide treated by the food pathway model.

Source - NUREG-1150 MACCS 1.5.9 Peach Bottom Model.

*					GREEN	OTHER	LEGUMES	ROOTS
---	--	--	--	--	-------	-------	---------	-------

*			STORED		LEAFY	FOOD	AND	AND
*	NUCLIDE	PASTURE	FORAGE	GRAINS	VEG	CROPS	SEEDS	TUBERS
*								
*	NAMISO	DCYPCB	DCYPCB	DCYPCB	DCYPCB	DCYPCB	DCYPCB	DCYPCB
CHDCYPCB001	SR-89	1.0	0.37	0.20	0.0	0.0	0.20	0.0
CHDCYPCB002	SR-90	1.0	0.99	0.99	0.0	0.0	0.99	0.0
CHDCYPCB003	CS-134	1.0	0.92	0.85	0.0	0.0	0.85	0.0
CHDCYPCB004	CS-137	1.0	0.99	0.99	0.0	0.0	0.99	0.0
CHDCYPCB005	I-131	1.0	0.063	0.032	0.0	0.0	0.032	0.0
CHDCYPCB006	I-133	1.0	0.0068	0.0034	0.0	0.0	0.0034	0.0

Variable Name - DCYPCB

Purpose - Retention factors for nuclides in crops from time of harvest to time of consumption by meat-producing animals (fraction retained). Factor reflects losses due to radioactive decay. Values are supplied for each crop category and nuclide treated by the food pathway model.

Source - NUREG-1150 MACCS 1.5.9 Peach Bottom Model.

*					GREEN	OTHER	LEGUMES	ROOTS
*			STORED		LEAFY	FOOD	AND	AND
*	NUCLIDE	PASTURE	FORAGE	GRAINS	VEG	CROPS	SEEDS	TUBERS
*								
*	NAMISO	DCYPCB	DCYPCB	DCYPCB	DCYPCB	DCYPCB	DCYPCB	DCYPCB
CHDCYPCB001	SR-89	1.0	0.37	0.20	0.0	0.0	0.20	0.0
CHDCYPCB002	SR-90	1.0	0.99	0.99	0.0	0.0	0.99	0.0
CHDCYPCB003	CS-134	1.0	0.92	0.85	0.0	0.0	0.85	0.0
CHDCYPCB004	CS-137	1.0	0.99	0.99	0.0	0.0	0.99	0.0
CHDCYPCB005	I-131	1.0	0.063	0.032	0.0	0.0	0.032	0.0
CHDCYPCB006	I-133	1.0	0.0068	0.0034	0.0	0.0	0.0034	0.0

Variable Name - NTRTRM

Purpose - Number of terms in the transfer function describing the direct deposition to crops.

Source - NUREG-1150 MACCS 1.5.9 Peach Bottom Model.

CHNTRTRM001 2

Variable Name - CTCOEF1 and CTCOEF2  
 Purpose - Coefficients in the equation for losses due to weathering from plant surfaces and during translocation from plant surfaces to interior edible portions of plants. Values are supplied for each crop category and nuclide treated by the food pathway model.  
 Source - NUREG-1150 MACCS 1.5.9 Peach Bottom Model.

					GREEN	OTHER	LEGUMES	ROOTS
					LEAFY	FOOD	AND	AND
					VEG	CROPS	SEEDS	TUBERS
* TERM 1	NUCLIDE	PASTURE	FORAGE	GRAINS				
CHCTCOEF101	SR-89	0.3	0.2	0.01	0.24	0.2	0.005	0.0006
CHCTCOEF102	SR-90	0.3	0.2	0.01	0.24	0.2	0.005	0.0006
CHCTCOEF103	CS-134	0.3	0.2	0.05	0.24	0.2	0.01	0.025
CHCTCOEF104	CS-137	0.3	0.2	0.05	0.24	0.2	0.01	0.025
CHCTCOEF105	I-131	0.3	0.2	0.0	0.24	0.2	0.0	0.0
CHCTCOEF106	I-133	0.3	0.2	0.0	0.24	0.2	0.0	0.0
* TERM 2								
CHCTCOEF201	SR-89	0.076	0.05	0.0	0.06	0.05	0.0	0.0
CHCTCOEF202	SR-90	0.076	0.05	0.0	0.06	0.05	0.0	0.0
CHCTCOEF203	CS-134	0.076	0.05	0.0	0.06	0.05	0.0	0.0
CHCTCOEF204	CS-137	0.076	0.05	0.0	0.06	0.05	0.0	0.0
CHCTCOEF205	I-131	0.076	0.05	0.0	0.06	0.05	0.0	0.0
CHCTCOEF206	I-133	0.076	0.05	0.0	0.06	0.05	0.0	0.0

Variable Name - CTHALF1 and CTHALF2  
 Purpose - Half-life values for the weathering terms of the growing crop retention model. Values are supplied for each crop category and nuclide treated by the food pathway model.  
 Source - NUREG-1150 MACCS 1.5.9 Peach Bottom Model.

\* GREEN OTHER LEGUMES ROOTS



*			STORED		LEAFY	FOOD	AND	AND
* TERM 1	NUCLIDE	PASTURE	FORAGE	GRAINS	VEG	CROPS	SEEDS	TUBERS
CHCTHALF101	SR-89	1.21E6	1.21E6	1E13	1.21E6	1.21E6	1E13	1E13
CHCTHALF102	SR-90	1.21E6	1.21E6	1E13	1.21E6	1.21E6	1E13	1E13
CHCTHALF103	CS-134	1.21E6	1.21E6	1E13	1.21E6	1.21E6	1E13	1E13
CHCTHALF104	CS-137	1.21E6	1.21E6	1E13	1.21E6	1.21E6	1E13	1E13
CHCTHALF105	I-131	1.21E6	1.21E6	1.0	1.21E6	1.21E6	1.0	1.0
CHCTHALF106	I-133	1.21E6	1.21E6	1.0	1.21E6	1.21E6	1.0	1.0
* TERM2								
CHCTHALF201	SR-89	4.32E6	4.32E6	1.0	4.32E6	4.32E6	1.0	1.0
CHCTHALF202	SR-90	4.32E6	4.32E6	1.0	4.32E6	4.32E6	1.0	1.0
CHCTHALF203	CS-134	4.32E6	4.32E6	1.0	4.32E6	4.32E6	1.0	1.0
CHCTHALF204	CS-137	4.32E6	4.32E6	1.0	4.32E6	4.32E6	1.0	1.0
CHCTHALF205	I-131	4.32E6	4.32E6	1.0	4.32E6	4.32E6	1.0	1.0
CHCTHALF206	I-133	4.32E6	4.32E6	1.0	4.32E6	4.32E6	1.0	1.0

Variable Name - **NAMCRP**

Purpose - Name of the crop category for which this set of growing season and farm fraction data applies.

Variable Name - **TGSBEG**

Purpose - Defines the start of the growing season for the named crop category in terms of the Julian date. The values supplied are not used for this analysis, since a site data file is used.

Variable Name - **TGSEND**

Purpose - Defines the end of the growing season for the named crop category in terms of the Julian date. The values supplied are not used for this analysis, since a site data file is used.

Variable Name - **FRCTFL**

Purpose - Defines the fraction of the farmland that is used for to grow the named crop category. The values supplied are not used for this analysis, since a site data file is used.

Source - NUREG-1150 MACCS 1.5.9 Peach Bottom Model.

\* IF A SITE DATA FILE IS BEING USED (AS SPECIFIED ON THE EARLY USER INPUT FILE),  
 \* THEN DATA FROM THE SITE FILE (AND NOT THE DATA BELOW) IS USED FOR THE  
 \* CALCULATION OF DOSES AND COSTS FROM THE AGRICULTURE MODEL AND THE NUMBERS  
 \* BELOW ARE IGNORED.

\*  
 \* IF A SITE DATA FILE IS NOT BEING USED, THE DATA BELOW IS USED IN ITS STEAD.

		GROWING		
		SEASON (DAYS) FARMLAND		
	CROP NAME	START	END	SHARE
	NAMCRP	TGSBEG	TGSEND	FRCTFL
CHCRPRGN001	'PASTURE	' 90.	270.	0.38
CHCRPRGN002	'STORED FORAGE	' 150.	240.	0.13
CHCRPRGN003	'GRAINS	' 150.	240.	0.23
CHCRPRGN004	'GRN LEAFY VEGETABLES'	150.	240.	0.002
CHCRPRGN005	'OTHER FOOD CROPS	' 150.	240.	0.004
CHCRPRGN006	'LEGUMES AND SEEDS	' 150.	240.	0.16
CHCRPRGN007	'ROOTS AND TUBERS	' 150.	240.	0.004

Variable Name - COUPLD

Purpose - Flag determining whether or not the food actions are coupled.

Source - NUREG-1150 MACCS 1.5.9 Peach Bottom Model.

CHCOUPLD001 .FALSE.

Variable Name - NAMIPI

Purpose - Defines the names of the ingestion model nuclides whose direct deposition protective action guides are being specified.

Variable Name - **PCSMLK**

Purpose - Defines the direct deposition protective action guides for milk and its products for the named nuclide. (Permissible surface concentration in becquerels per square meter).

Variable Name - **PCSOTH**

Purpose - Defines the direct deposition protective action guides for non-milk crops and their products for the named nuclide. (Permissible surface concentration in becquerels per square meter).

Source - NUREG-1150 MACCS 1.5.9 Peach Bottom Model.

*		MILK AND	OTHER CROPS	
*	NUCLIDE	PRODUCTS	AND PRODUCTS	
*				
*	NAMIPI	PSCMLK	PSCOTH	
CHPAGMCP001	SR-89	2.2E07	2.2E07	NEW VALUES BY J. ROLLSTIN
CHPAGMCP002	SR-90	2.4E05	2.4E05	CALCULATED JUNE 1989
CHPAGMCP003	CS-134	2.2E05	2.2E05	
CHPAGMCP004	CS-137	2.7E05	2.7E05	
CHPAGMCP005	I-131	1.3E06	8.0E06	
CHPAGMCP006	I-133	1.1E10	1.0E20	

Variable Name - **NAMIPI**

Purpose - Defines the names of the ingestion model nuclides whose direct deposition protective action guides are being specified.

Variable Name - **GCMAXR**

Purpose - Defines the protective action guides for long-term transfer to farm crops from root and other soil uptake from surface

contamination by CHRONC ingestion model nuclide (permissible surface concentration in becquerels per square meter).

Variable Name - QROOT  
 Purpose - Defines the annual depletion rate for the nuclide in the soil.  
 Source - NUREG-1150 MACCS 1.5.9 Peach Bottom Model.

	NUCLIDE	PERMISSIBLE SURFACE CONCENTRATION	ANNUAL DEPLETION RATE	
*				
*				
*				
*				
*	NAMIPI	GCMAXR	QROOT	
CHPAGLTS001	SR-89	1.8E8	4.9	NEW VALUES BY J. ROLLSTIN
CHPAGLTS002	SR-90	3.7E4	0.065	CALCULATED JUNE 1989.
CHPAGLTS003	CS-134	4.1E6	0.59	DECAY FACTORS ARE NOW BEING
CHPAGLTS004	CS-137	1.8E6	0.28	APPLIED IN THE SAME MANNER
CHPAGLTS005	I-131	1.E20	32.0	FOR THE DERIVATION OF
GCMAXR,				
CHPAGLTS006	I-133	1.E20	290.0	PSCMLK, AND PSCOTH.

Results Name - TYPE9OUT  
 Purpose - Edits the long-term population dose in a given region broken down by the 12 pathways.

\* NUMBER OF RESULTS OF THIS TYPE THAT ARE BEING REQUESTED  
 \* FOR EACH RESULT YOU REQUEST, THE CODE WILL PRODUCE A SET OF 12  
 \*

TYPE9NUMBER 2 (UP TO 10 ALLOWED)

	ORGNAM	INNER	OUTER	
*				
*				
*				
TYPE9OUT001	'EDEWBODY'	1	26	(0-1000 MILES)
TYPE9OUT002	'EDEWBODY'	1	19	(0-50 MILES)

Results Name - TYPE10OUT

Purpose - Edits the economic costs of the specific emergency and long-term actions that are taken.

\* NUMBER OF RESULTS OF THIS TYPE THAT ARE BEING REQUESTED

\* FOR EACH RESULT YOU REQUEST, THE CODE WILL PRODUCE A SET OF 12

\*

TYP10NUMBER 2 (UP TO 10 ALLOWED)

\*

\* INNER OUTER

\*

TYP10OUT001 1 26 (0-1000 MILES)

TYP10OUT002 1 19 (0-50 MILES)

Results Name - TYP11FLAG

Purpose - A flag that controls the production of the action distance results. Specifying a value of .TRUE. turns on all 8 of the action distance results, a value of .FALSE. will eliminate the action distance results from the output.

TYP11FLAG11 .TRUE.

Results Name - TYPE12OUT

Purpose - Edits the impacted area/population results in a region broken down by 6 types of impacts.

\* NUMBER OF RESULTS OF THIS TYPE THAT ARE BEING REQUESTED

\* FOR EACH RESULT YOU REQUEST, THE CODE WILL PRODUCE A SET OF 8

\*

TYP12NUMBER 2 (UP TO 10 ALLOWED)

\*

\* INNER OUTER

\*

TYP12OUT001 1 26 (0-1000 MILES)

TYP12OUT002 1 19 (0-50 MILES)

## 5.0 Auxiliary Input Files

The ATMOS module requires a site meteorological data file. The NUREG-1150 MACCS 1.5.9 Peach Bottom Model site meteorological data file was utilized.

The EARLY and CHRONC modules require two auxiliary data files, a site data file and a dose conversion file. The dose conversion file "MACCS DOSE CONVERSION FILE: MOD SER #32, 6-JUL-89, 15:59:19 SANDIA NATIONAL LABORATORIES, J. JOHNSON" was utilized. This is the most recent dosimetry file provided by SNL for MACCS 1.5. The site data file used was from the NUREG-1150 MACCS 1.5.9 Peach Bottom Model.

## 6.0 Results

The output generated from the ten cases analyzed is contained in Attachment C. This information will be used to support the quantitative analysis of the BWR Mark II improvements identified in Sections 7-10. If the impact of an improvement on the release category frequencies is established, the relative change in consequence measures for a given improvement can be determined. Comparison of the relative change in consequence measures with the cost of implementing an improvement provides a method for evaluating the usefulness of a specific improvement.

The mean values obtained for three measures of accident consequence are summarized in Table D.1 for each of the ten release categories. These include the total number of latent cancer fatalities, the total population dose within 50 miles in sieverts, and the total economic cost in dollars. Values for latent cancer fatalities and total population dose are provided assuming both 95% and 100% evacuation. The 100% evacuation values were obtained by summing the EARLY 100% evacuation cohort results with the CHRONC results. These results are also presented graphically by release category on Figures D.1 through D.3, respectively.

The total economic costs are calculated by the CHRONC module of MACCS and, as a result, the economic costs associated with different EARLY cohorts are not determined by the code. MACCS somewhat arbitrarily uses the results from the last EARLY cohort run as a basis for calculating the evacuation and relocation costs in CHRONC. This is contrary to what the user might assume, that is, that the overall EARLY results combined using the emergency response scenario weighting fractions would be used as a basis for calculating the evacuation and relocation costs in CHRONC. This distinction is not pointed out by the user's manual for MACCS 1.5. For the cases run, these costs are relatively small in comparison to the total economic costs and do not impact the results reported in Table D.1.

Dr. S. Acharya, NRC, has pointed out that the numbers of early health effects obtained using the Peach Bottom site may be lower than for other Mark

II sites. This effect is due primarily to the above average evacuation speeds for the Peach Bottom site compared to other reactor sites in the region. This would reduce the number of early health effects below the average expected for the region for a given release. For this reason early health effects will not be reported for the analysis.

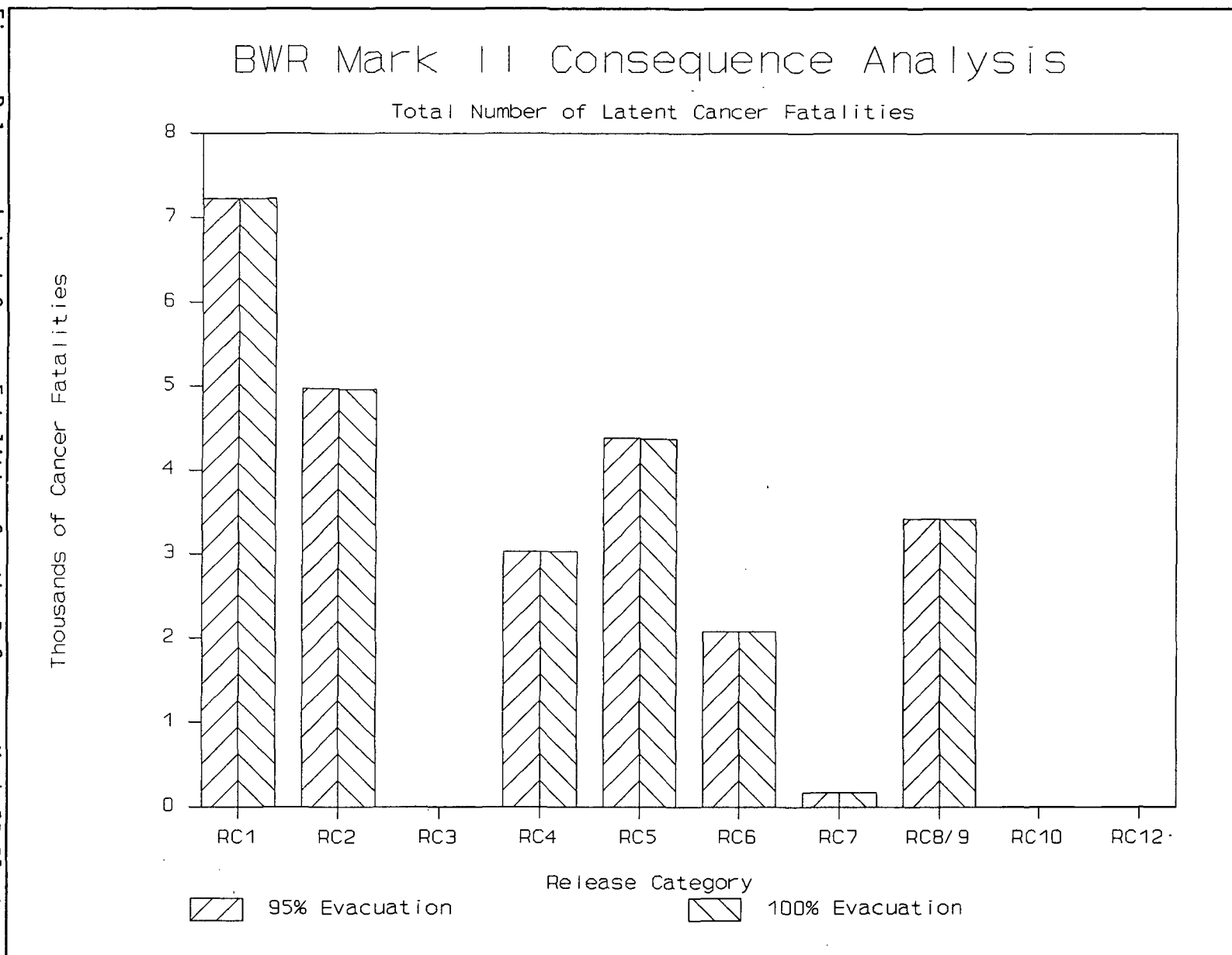
Table D.1 Summary of Results of Consequence Analysis Using MACCS 1.5.9

Release Category	Mean Total Number of Cancer Fatalities		Mean Total Population Dose Within 50 Miles (sv)		Mean Total Economic Cost (\$)
	95% Evac.	100% Evac.	95% Evac.	100% Evac.	
RC1	7.23E+03	7.23E+03	5.95E+04	6.67E+04	4.81E+10
RC2	4.97E+03	4.97E+03	4.27E+04	4.77E+04	2.87E+10
RC3	7.67E+00	7.67E+00	1.86E+02	1.94E+02	1.13E+06
RC4	3.03E+03	3.03E+03	3.58E+04	3.88E+04	5.77E+09
RC5	4.38E+03	4.38E+03	3.94E+04	4.38E+04	2.57E+10
RC6	2.08E+03	2.08E+03	2.75E+04	2.96E+04	2.99E+09
RC7	1.77E+02	1.77E+02	3.87E+03	4.05E+03	3.48E+07
RC8/9	3.42E+03	3.42E+03	3.18E+04	3.52E+04	1.22E+10
RC10	3.97E+00	3.97E+00	7.81E+01	8.21E+01	1.13E+06
RC12	4.31E+00	4.31E+00	1.24E+02	1.28E+02	1.52E+06



Figure D.1

Latent Cancer Fatalities for the Reference Mark II Plant



# BWR Mark II Consequence Analysis

Total Population Dose Within 50 Miles

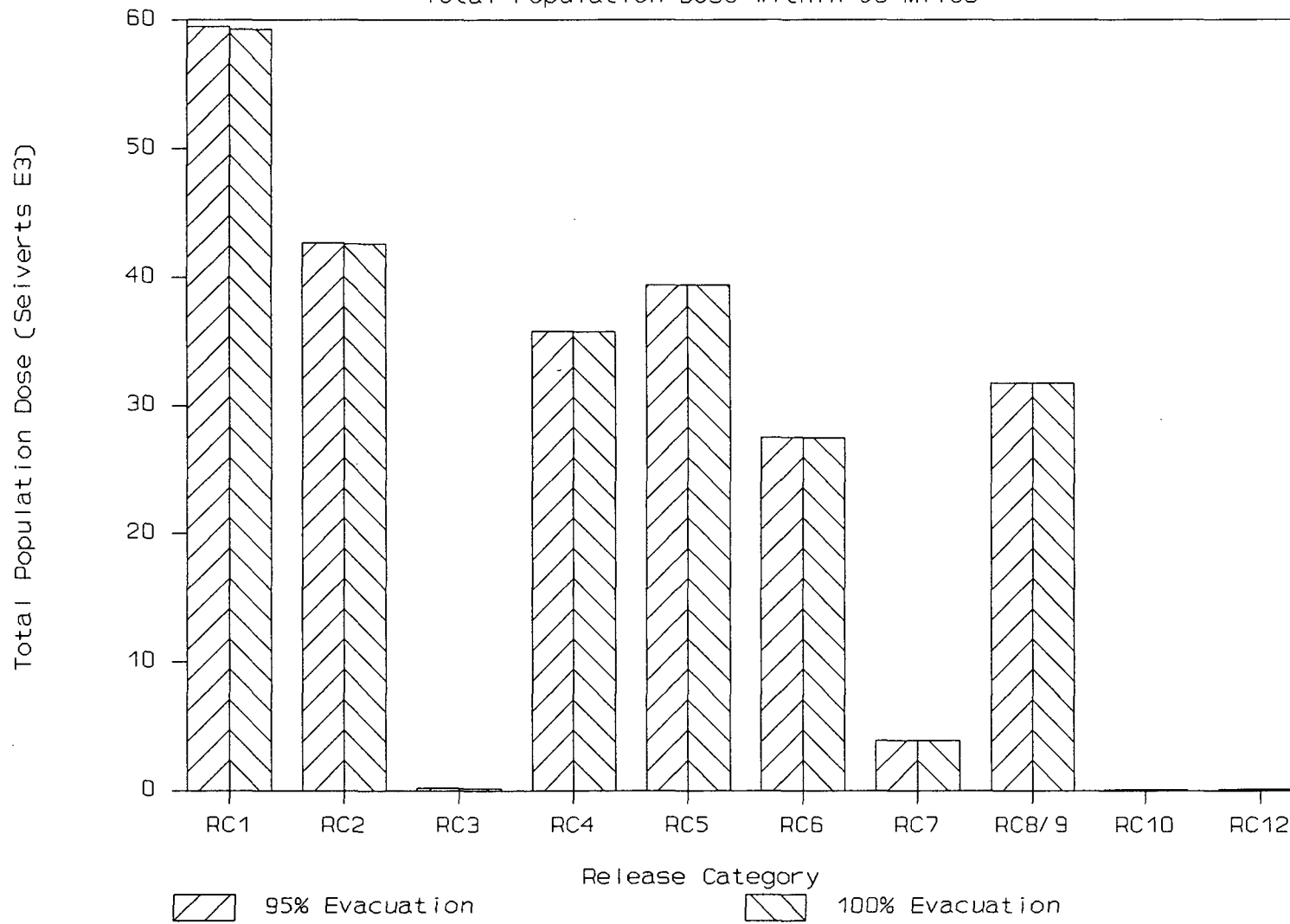


Figure D.2 50-Mile Population Dose for the Reference Mark II Plant

# BWR Mark II Consequence Analysis

Total Economic Costs

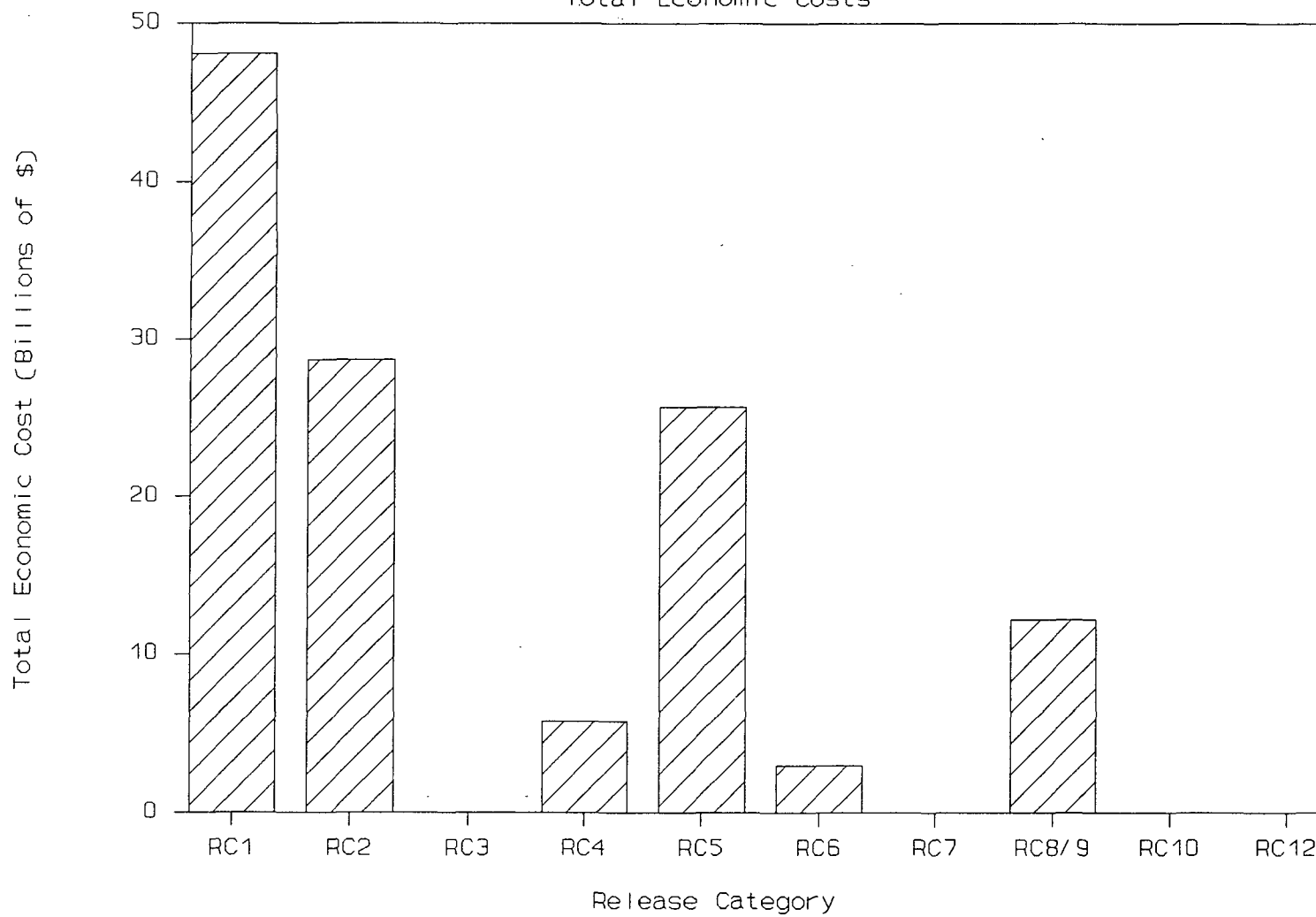


Figure D.3 Economic Costs for the Reference Mark II Plant

## Appendix D.1

### Documentation of PC Version of MACCS 1.5.9

MACCS 1.5.9 is composed of a single FORTRAN-77 program. This appendix lists the coding modifications required to compile and run this program on a PC. These modifications consist of changes in system-dependent subroutine calls and the addition of a file handle processor. These modifications are not of a nature that would affect the calculational results of the code. The program was compiled using the Lahey F77/EM32 compiler version 1.01 and executed under the A. I. Architects OS/386 operating system on an IBM PS/2 Model 70. An Intel 80387 math coprocessor and a minimum of 3.32 Mb of extended memory are required to execute the program. The machine accuracy and calculational precision of this machine are comparable to that of the VAX computer used by SNL for MACCS 1.5 development.

The following modifications were made to the original version of MACCS 1.5.9 obtained from SNL (these modifications were made by K. R. Jones and the old cards are retained as comment cards):

TO TRANSFORM MACCS9\_A.FOR INTO PCMAX9\_A.FOR ...

\*\*\* CHANGE 592 IN MACCS9\_A.FOR TO [592,593] IN PCMAX9\_A.FOR \*\*\*  
 < DATA REVNAM /'VERSION 1.5.9, 7/25/89, D. CHANIN'/

-----  
 >CKRJ DATA REVNAM /'VERSION 1.5.9, 7/25/89, D. CHANIN'/  
 > DATA REVNAM /'INEL PC VERSION 1.5.9, 9/5/89, K. JONES'/

\*\*\* CHANGE 710 IN MACCS9\_A.FOR TO [710,711] IN PCMAX9\_A.FOR \*\*\*  
 < MACHIN = 'VAX/VMS'

-----  
 >C\*KRJ MACHIN = 'VAX/VMS'  
 > MACHIN = 'IBM-PC/DOS4.0'

\*KRJ

\*\*\* APPEND AFTER 713 IN MACCS9\_A.FOR \*\*\*

>CKRJ  
 >CKRJ SET UP FILE HANDLES  
 >CKRJ  
 > CALL IOFILES(5,6)  
 >CKRJ

\*KRJ

```

*** CHANGE 721 IN MACCS9_A.FOR TO [727,728] IN PCMAX9_A.FOR ***
<     SUBROUTINE MXXCPU (CPUTIM)

```

```

-----
>CKRJ  SUBROUTINE MXXCPU (CPUTIM)
>CKRJ  SUBROUTINE REPLACED WITH PC VERSION, SEE IOFILES.FOR

```

```

*** CHANGE [725,728] IN MACCS9_A.FOR TO [732,735] IN PCMAX9_A.FOR ***
<     CHARACTER *80  MACHIN
<     COMMON /MACHIN/ MACHIN
<
<     DATA ICPUTC / 2 /

```

```

-----
>CKRJ  CHARACTER *80  MACHIN
>CKRJ  COMMON /MACHIN/ MACHIN
>CKRJ
>CKRJ  DATA ICPUTC / 2 /

```

```

*** CHANGE 732 IN MACCS9_A.FOR TO 739 IN PCMAX9_A.FOR ***
<     DATA FIRST / 0.0 /

```

```

-----
>CKRJ  DATA FIRST / 0.0 /

```

```

*** CHANGE [736,741] IN MACCS9_A.FOR TO [743,748] IN PCMAX9_A.FOR ***
<     IF (MACHIN .NE. 'VAX/VMS') CALL ABORT ('MXXCPU')
<
<     IF (FIRST .EQ. 0.) THEN
<         FIRST = 1.
<         CALL LIB$INIT_TIMER
<     ENDIF

```

```

-----
>CKRJ  IF (MACHIN .NE. 'VAX/VMS') CALL ABORT ('MXXCPU')
>CKRJ
>CKRJ  IF (FIRST .EQ. 0.) THEN
>CKRJ      FIRST = 1.
>CKRJ      CALL LIB$INIT_TIMER
>CKRJ  ENDIF

```

```

*** CHANGE [745,750] IN MACCS9_A.FOR TO [752,759] IN PCMAX9_A.FOR ***
<     CALL LIB$STAT_TIMER (ICPUTC,IECPUI)
<
<     CPUTIM = 0.01 * FLOAT (IECPUI)
<
<     RETURN
<     END

```

```

-----
>CKRJ  CALL LIB$STAT_TIMER (ICPUTC,IECPUI)
>CKRJ

```

```

>CKRJ  CPUTIM = 0.01 * FLOAT (IECPUI)
>CKRJ
>CKRJ  CALL CPUSEC(CPUTIM)
>CKRJ
>CKRJ  RETURN
>CKRJ  END

*** CHANGE 761 IN MACCS9 A.FOR TO [770,771] IN PCMAX9_A.FOR ***
<      IF (MACHIN .EQ. 'VAX/VMS' ) THEN

-----
>CKRJ  IF (MACHIN .EQ. 'VAX/VMS' ) THEN
>      IF (MACHIN .EQ. 'IBM-PC/DOS4.0' ) THEN                                *KRJ

*** CHANGE [780,781] IN MACCS9_A.FOR TO [790,793] IN PCMAX9_A.FOR ***
<
<      IF ( MACHIN .EQ. 'VAX/VMS' ) THEN

-----
>      DATA MONTH /'JAN','FEB','MAR','APR','MAY','JUN',
>      $           'JUL','AUG','SEP','OCT','NOV','DEC'/
>
>CKRJ  IF ( MACHIN .EQ. 'VAX/VMS' ) THEN                                *KRJ
                                                                *KRJ

*** CHANGE 785 IN MACCS9 A.FOR TO [797,806] IN PCMAX9_A.FOR ***
<      CALL DATE (CHAR9)

-----
>CKRJ  CALL DATE (CHAR9)
>CKRJ  ENDIF
>      IF ( MACHIN .EQ. 'IBM-PC/DOS4.0' ) THEN
>C
>C  FORM OF THE TEXT STRING RETURNED IN CHAR9 IS '11-01-88'
>C
>      CALL DATE (TODAY)
>      READ(TODAY,'(I2)') IMONTH
>      CHAR9 = TODAY(4:5)///'-'/MONTH(IMONTH)///'-'/TODAY(7:8)
>
                                                                *KRJ
                                                                *KRJ
                                                                *KRJ

```

The following code was added as a replacement for the system-dependent subroutine MXXCPU, which returns the current CPU time in seconds.

```

SUBROUTINE MXXCPU(SECONDS)
SAVE
CHARACTER*8  STARTDAY,TODAY
DATA IFIRST /0/
IF(IFIRST.EQ.0) THEN
  CALL TIMER(I100STRT)
  CALL DATE(STARTDAY)
  READ(STARTDAY,'(I2,1X,I2,1X,I2)') IM,ID,IY
  IY = IY + 1900

```

```

        JULSTART = JULDAY(IM, ID, IY)
        IFIRST = 1
        SECONDS = 0.0
ELSE
    CALL TIMER(I100NOW)
    CALL DATE(TODAY)
    READ(TODAY, '(I2,1X,I2,1X,I2)') IM, ID, IY
    IY = IY + 1900
    JULNOW = JULDAY(IM, ID, IY)
    IFIRST = 1
    SECONDS = FLOAT(JULNOW-JULSTART)*86400.
+          + FLOAT(I100NOW-I100STRT)/100.
END IF
RETURN
END
FUNCTION JULDAY(MM, ID, IYYY)
PARAMETER (IGREG=15+31*(10+12*1582))
IF (IYYY.EQ.0) PAUSE 'There is no Year Zero.'
IF (IYYY.LT.0) IYYY=IYYY+1
IF (MM.GT.2) THEN
    JY=IYYY
    JM=MM+1
ELSE
    JY=IYYY-1
    JM=MM+13
ENDIF
JULDAY=INT(365.25*JY)+INT(30.6001*JM)+ID+1720995
IF (ID+31*(MM+12*IYYY).GE.IGREG) THEN
    JA=INT(0.01*JY)
    JULDAY=JULDAY+2-JA+INT(0.25*JA)
ENDIF
RETURN
END

```

The subroutine IOFILES was linked to MACCS 1.5.9 to establish file handles based on user input from JCL-type statements placed before the input file. This allows the user to specify file names (including the DOS path), file status, file access, file form, and carriage control file attributes for each FORTRAN unit. This subroutine also prints a banner page and file handle summary on the output, which contains the date and start time to uniquely identify the run. A "/"\* card terminates the file specification list and program input may follow. The subroutine requires two arguments, which correspond to the primary input and output FORTRAN unit numbers for the program, respectively. The input file name containing the file specifications is read from the command line. The format for specification of file handles is as follows:

```

*****
* Comments can be entered by placing a '*' in column 1 and will be      *
* echoed to the output file.                                           *
*                                                                      *
* An example file specification format is shown below. Only the UNIT *
* number and file name are required input. Columns 73 to 80 are      *
* reserved for comments, a line ending in a comma is continued on    *
* the following line.                                                 *
*****
*
FILEnn='D:\path\filename', STATUS='status' , ACCESS='access',
      FORM='form', CARRIAGE CONTROL='carriage'
*
/* end of JCL card
program input may follow ...

```

Where:      nn      is the FORTRAN Unit number to be opened. Must be preceded by "FILE" in columns 1 to 4. Possible range of values is 01 to 99.

D:\path\filename    is the DOS Drive, Path and Filename. DOS devices CON,LPT1,LPT2,LPT3,PRN,COM1,COM2, or NUL may also be used.

status          is the open status of the file. Valid options include: 'NEW', 'OLD', 'UNKNOWN' or 'SCRATCH' corresponding to the FORTRAN77 standard. The default value is 'UNKNOWN'.

access          is the access method for the file. Valid options are 'SEQUENTIAL' and 'DIRECT' with 'SEQUENTIAL' being the default value.

form            indicates the file format and has two possible options: 'FORMATTED' and 'UNFORMATTED'.

carriage        indicates whether the first character from each sequentially formatted output record will be used as FORTRAN printer carriage control characters. Possible options are 'FORTRAN' and 'LIST'. The default values are 'LIST' for disk files and 'FORTRAN' for DOS devices.

A sample case was executed using the PC version of MACCS 1.5.9 and the results were compared with results provided by SNL from the same case run on a



VAX computer. The slight differences between these results are due to round-off error and lie within the calculational precision of the machines.

#### REFERENCES

- D-1. MELCOR Accident Consequence Code System, NUREG/CR-4691, MACCS Version 1.5 User's Manual, draft version last revised September 21, 1988.
- D-2. Pickard, Lowe, and Garrick, Inc., Core Melt Accident Dose-Versus-Distance Probability Distributions. 100% Power Operations, Shoreham Nuclear Power Station, prepared for Long Island Lighting Company, February 1988.



NRC FORM 335 (2-89) NRCM 1102, 3201, 3202		U.S. NUCLEAR REGULATORY COMMISSION	
<b>BIBLIOGRAPHIC DATA SHEET</b> <i>(See instructions on the reverse)</i>		1. REPORT NUMBER <i>(Assigned by NRC. Add Vol., Supp., Rev., and Addendum Numbers, if any.)</i>  <b>NUREG/CR-5528 EGG-2593</b>	
2. TITLE AND SUBTITLE  <b>An Assessment of BWR Mark II Containment Challenges, Failure Modes, and Potential Improvements in Performance</b>		3. DATE REPORT PUBLISHED MONTH   YEAR <b>July   1990</b>	
		4. FIN OR GRANT NUMBER <b>A6885</b>	
5. AUTHOR(S)  <b>Dana L. Kelly, Ken R. Jones, R. Jack Dallman, K. C. Wagner</b>		6. TYPE OF REPORT  <b>Technical</b>	
		7. PERIOD COVERED <i>(Inclusive Dates)</i>	
8. PERFORMING ORGANIZATION - NAME AND ADDRESS <i>(If NRC, provide Division, Office or Region, U.S. Nuclear Regulatory Commission, and mailing address; if contractor, provide name and mailing address.)</i>  <b>Idaho National Engineering Laboratory EG&amp;G Idaho, Inc. P.O. Box 1625 Idaho Falls, Idaho 83415</b>			
9. SPONSORING ORGANIZATION - NAME AND ADDRESS <i>(If NRC, type "Same as above"; if contractor, provide NRC Division, Office or Region, U.S. Nuclear Regulatory Commission, and mailing address.)</i>  <b>Division of Safety Issue Resolution Office of Nuclear Regulatory Research U. S. Regulatory Commission Washington, D.C. 20555</b>			
10. SUPPLEMENTARY NOTES			
11. ABSTRACT <i>(200 words or less)</i>  <p>             This report assesses challenges to BWR Mark II containment integrity that could potentially arise from severe accidents. Also assessed are some potential improvements that could prevent core damage or containment failure, or could mitigate the consequences of such failure by reducing the release of fission products to the environment. These challenges and improvements are analyzed via a limited quantitative risk/benefit analysis of a generic BWR/4 reactor with a Mark II containment. Point estimate frequencies of the dominant core damage sequences are obtained and simple containment event trees are constructed to evaluate the response of the containment to these severe accident sequences. The resulting containment release modes are then binned into source term release categories, which provide inputs to the consequence analysis. The output of the consequence analysis is used to construct an overall base case risk profile. Potential improvements and sensitivities are evaluated by modifying the event tree split fractions, thus generating a revised risk profile. Several important sensitivity cases are examined in order to evaluate the impact of phenomenological uncertainties on the final results.           </p>			
12. KEY WORDS/DESCRIPTORS <i>(List words or phrases that will assist researchers in locating the report.)</i>  <b>BWR Mark II containment integrity</b>		13. AVAILABILITY STATEMENT <b>Unlimited</b>	
		14. SECURITY CLASSIFICATION <i>(This Page)</i> <b>Unclassified</b> <i>(This Report)</i> <b>Unclassified</b>	
		15. NUMBER OF PAGES	
		16. PRICE	









**UNITED STATES  
NUCLEAR REGULATORY COMMISSION  
WASHINGTON, D.C. 20555**

**OFFICIAL BUSINESS  
PENALTY FOR PRIVATE USE, \$300**

SPECIAL FOURTH-CLASS RATE  
POSTAGE & FEES PAID  
USNRC  
PERMIT No. G-67